Forschungszentrum Jülich
in der Helmholtz-Gemeinschaft

Institut für Sicherheitsforschung und Reaktortechnik

Valuation of the Safety Concept of the Combined Nuclear/Chemical Complex for Hydrogen Production with HTTR

Karl Verfondern, Tetsuo Nishihara

Jül-4135

Valuation of the Safety Concept of the Combined Nuclear/Chemical Complex for Hydrogen Production with HTTR

Karl Verfondern, Tetsuo Nishihara

Berichte des Forschungszentrums Jülich ; 4135
ISSN 0944-2952
Institut für Sicherheitsforschung und Reaktortechnik Jül-4135

Zu beziehen durch: Forschungszentrum Jülich GmbH · Zentralbibliothek
D-52425 Jülich · Bundesrepublik Deutschland
☎ 02461 61-5220 · Telefax: 02461 61-6103 · e-mail: zb-publikation@fz-juelich.de

Valuation of the Safety Concept of the Combined Nuclear/Chemical Complex for Hydrogen Production with HTTR

by

Karl Verfondern, Tetsuo Nishihara*

*Department of Advanced Nuclear Heat Technology, JAERI, Oarai, Ibaraki-ken, JAPAN

Abstract

The High-Temperature Engineering Test Reactor (HTTR) in Oarai, Japan, will be worldwide the first plant to demonstrate the production of hydrogen by applying the steam reforming process and using nuclear process heat as primary energy. Particular safety aspects for such a combined nuclear/chemical complex have to be investigated to further detail. One of these special aspects is the fire and explosion hazard associated with the presence of flammable gases including a large LNG storage tank in close vicinity to the reactor building. A special focus is laid upon the conceivable development of a detonation pressure wave and its damaging effect on the reactor building. A literature study has shown that methane is a comparatively slow reacting gas and that a methane vapor cloud in the open atmosphere or partially obstructed areas is highly unlikely to result in a detonation if inadvertently released and ignited. Various theoretical assessments and experimental studies, which have been conducted in the past and which are of significance for the HTTR-steam reforming system, include the spreading and combustion behavior of cryogenic liquids and flammable gas mixtures providing the basis of a comprehensive safety analysis of the combined nuclear/chemical facility.

Bewertung des Sicherheitskonzepts für die kombinierte nuklear/chemische Anlage zur Wasserstoffproduktion mit dem HTTR

von

Karl Verfondern, Tetsuo Nishihara*

*Department of Advanced Nuclear Heat Technology, JAERI, Oarai, Ibaraki-ken, JAPAN

Kurzfassung

Der “High-Temperature Engineering Test Reactor” (HTTR) in Oarai, Japan, soll die weltweit erste Anlage zur Produktion von Wasserstoff werden, bei der auf der Basis des Wasserdampf-Reformierungsprozesses nukleare Prozesswärme als Primärenergie eingesetzt wird. Die sich daraus ergebenden speziellen Sicherheitsaspekte für eine solche kombinierte nuklear/ chemische Anlage müssen näher untersucht werden. Einer dieser besonderen Aspekte ist die Gefahr eines Feuers oder einer Explosion, die mit der Anwesenheit entzündbarer Gase sowie des großen LNG Speichertanks in unmittelbarer Nähe des Reaktorgebäudes verbunden ist. Ein besonderer Schwerpunkt bildet die denkbare Ausbildung einer Detonations-Druckwelle, die das Reaktorgebäude beschädigen könnte. Eine Literaturstudie hat gezeigt, dass Methan ein vergleichsweise langsam reagierendes Gas ist und dass im Falle einer unfallbedingten Freisetzung und Zündung es äußerst unwahrscheinlich ist, dass eine Methan-Gaswolke in freier Atmosphäre oder in teilweise bebauter Umgebung sich zu einer Detonation entwickeln kann. Verschiedene theoretische Abschätzungen sowie experimentelle Studien aus der Vergangenheit, die von Bedeutung für den Komplex aus HTTR und Wasserdampf-Reformierung sind, beinhalten das Ausbreitungs- und Verbrennungsverhalten kryogener Flüssigkeiten und zündfähiger Gasgemische, die eine Basis für eine umfassende Sicherheitsanalyse einer derartigen kombinierten nuklear/chemischen Anlage darstellen.

TABLE OF CONTENTS

LIST OF ACRONYMS

ACS	Auxiliary Cooling System (HTTR)
AD	Arbeitsgemeinschaft Druckbehälter – Working Group Pressure Vessel (Germany)
AEC	Atomic Energy Commission (USA)
AGA	American Gas Association (USA)
AHX	Auxiliary Heat Exchanger (HTTR)
AOO	Anticipated Operational Occurrences (HTTR)
AVR	Arbeitsgemeinschaft Versuchs-Reaktor (Germany)
BAM	Bundesanstalt für Materialforschung und -prüfung – Federal Institute for Materials Research and Testing (Germany)
BLEVE	Boiling Liquid Expansion Vapor Cloud Explosion
BMI	Bundesministerium des Innern – Federal Ministry of the Interior (Germany)
BR	Blockage Ratio
CHP	Combined Heat and Power
CJ	Chapman - Jouguet
CV	Containment Vessel (HTTR)
DBA	Design Basis Accident
DDT	Deflagration-to-Detonation Transition
DLF	Dynamic Load Factor
DOE	Department of Energy (USA)
efpd	Equivalent Full Power Days
FIMA	Fissions per Metal Atom
FZJ	Forschungszentrum Jülich – Research Center Jülich
FZK	Forschungszentrum Karlsruhe – Research Center Karlsruhe
GRS	Gesellschaft für Anlagen- und Reaktorsicherheit – Society for Plant and Nuclear Reactor Safety (Germany)
HDR	Heißdampfreaktor – Hot Steam Reactor
HT	High-Temperature
HTGR	High-Temperature Gas-Cooled Reactor
HTTR	High Temperature Engineering Test Reactor
IAEA	International Atomic Energy Agency
IHX	Intermediate Heat Exchanger (HTTR)

INSC	International Nuclear Societies Council
IS	Iodine-Sulfur
JAERI	Japan Atomic Energy Research Institute
JMTR	Japan Material Test Reactor
LFG	Liquid Flammable Gas
LFL	Lower Flammability Limit
LNG	Liquefied Natural Gas
LOX	Liquid Oxygen
LPG	Liquefied Petroleum Gas
LWR	Light Water Reactor
MCS	Main Cooling System (HTTR)
MESG	Maximum Experimental Safe Gap
METI	Ministry of Economy, Trade and Industry (Japan)
MITI	Ministry of International Trade and Industry (Japan)
NEA	Nuclear Energy Agency (OECD)
NFPA	National Fire Protection Association (USA)
NPP	Nuclear Power Plant
OECD	Organization for Economic Cooperation and Development
PAFC	Phosphoric Acid Fuel Cell
PBMR	Pebble Bed Modular Reactor (South Africa)
PGC	Primary Gas Circulator (HTTR)
PHPS	Primary Helium Purification System (HTTR)
PNP	Prototype Nuclear Process Heat (Germany)
PSA	Probabilistic Safety Assessment
PWC	Pressurized Water Cooler (HTTR)
PWR	Pressurized Water Reactor
RLM	Refrigerated Liquid Methane
RPT	Rapid Phase Transition
RPV	Reactor Pressure Vessel (HTTR)
RSK	Reaktorsicherheitskommission – Reactor Safety Commission (Germany)
SG	Steam Generator (HTTR)
SH	Super Heater (HTTR)
SHPS	Secondary Helium Purification System (HTTR)
SNG	Synthetic Natural Gas

SR	Steam Reformer (HTTR)
STP	Standard Temperature Pressure
SWACER	Shock Wave Amplification by Coherent Energy Release
THTR	Thorium-Hochtemperaturreaktor – Thorium High Temperature Reactor (Germany)
TNO	Organization for Applied Scientific Research and Development (The Netherlands)
TNT	Trinitrotoluene
TRB	Technische Regeln zur Druckbehälterverordnung - Druckbehälter – Technical Rules for the Pressure Vessel Ordinance - Pressure Vessel (Germany)
TRG	Technische Regeln Druckgase – Technical Rules Pressurized Gases (Germany)
TRR	Technische Regeln zur Druckbehälterverordnung - Rohrleitungen – Technical Rules for the Pressure Vessel Ordinance - Piping (Germany)
UNEP	United Nations Environment Programme
UVCE	Unconfined Vapor Cloud Explosion
VCS	Vessel Cooling System (HTTR)
vpm	Volume Parts per Million
WGSI	Westcoast Gas Services Inc.

1. INTRODUCTION

As a result of the worldwide increasing consumption of energy due to an increasing population and rising life standards in the less industrialized countries, the world faces the problem of depleting energy resources and the impairing impact of the present energy consumption pattern on the global climate as well as on man and environment. At present, 90 % of the total primary energy demand are covered by fossil fuels. Their combustion is connected with the release of huge amounts of CO_2, one of the most relevant greenhouse gases. A response to the global warming issue are enhanced efforts to obtain a clean and sustainable, however, economic and safe energy technology.

Measures that need to be taken now are

- the extension of lifetime of the fossil resources by saving energy and making its consumption more efficient, and
- the gradual transition away from fossil energies to a CO_2 emission free energy structure.

Hydrogen appears to be one of the promising candidates, which help achieving the goal of an environmentally benign energy system. Hydrogen is clean, storable, and transportable. And with the fuel cell, a device is available that, in combination with hydrogen, allows for an efficient energy conversion at a time when energy is needed.

The production of hydrogen as a secondary energy carrier requires a substantial amount of primary energy, which should definitely be non-fossil in the long term. Besides hydro power, nuclear energy is the only significant non-fossil energy resource. It is able to provide heat and/or electricity offering the advantages of a large resource base, the absence of most air emissions, and a saving of the existing fossil resources.

Among the different types of nuclear power plants (NPP), the high-temperature gas-cooled reactor (HTGR) may play an eminent role in future. Apart from its inherent safety features, the coolant outlet temperature at a high level of around 1000 °C allows for an energy production with a high efficiency. The unique potential of HTGRs is given in the Combined Heat and Power (CHP) operation mode, where the hot helium coolant can directly be routed to high-temperature (HT) process heat components to be combined with most H_2 production methods such as steam reforming, oil recovery, coal gasification, electrolysis, thermo-chemical cycles. Furthermore, the high-temperature high-pressure level on the secondary side allows a whole variety of process steam applications. These features can be used for the production of storable and transportable secondary energy carriers, thus being able of serving both heat market and traffic sector.

Several countries such as China, Germany, Japan, Russia and the USA have carried out specific HTGR design studies associated with the production of hydrogen and methanol, both of which are considered key energy carriers of the future. Particular efforts have been done in Germany and Japan by conducting or preparing a comprehensive research program including out-of-pile tests and components tests to study nuclear process heat applications.

In Japan, the New Sunshine Program (R&D Program on Energy and Environmental Technologies) was started in April 1993, with focus on the development of hydrogen

production and utilization technologies supported by the Ministry of International Trade and Industry, MITI, (now: Ministry of Economy, Trade and Industry, METI). Within this program, the Japan Atomic Energy Research Institute (JAERI) has been investigating the HTGR system for process heat production. A first important milestone has been achieved with the construction and completion of the High Temperature Engineering Test Reactor (HTTR), in Oarai. JAERI is now on the way to develop and realize in the second step a first-of-its-kind nuclear hydrogen production system by combining the HTTR with a respective process heat utilization system.

The purpose of this report is three-fold:

- Description of the H_2 production system by steam reforming with the HTTR;
- Examination of the safety aspects of a combined nuclear/chemical system;
- Summary of the status of knowledge on vapor cloud explosions.

The report starts with a detailed presentation of the combined HTTR/steam reforming facility (HTTR/SR) (chapter 2) and the identification of major items that may cause severe hazards under accidental conditions (chapter 3). These two chapters try to touch the most important items which will have to be elaborated in more detail in a safety report. Chapter 4 is devoted to a description of the status of knowledge in the field of accidental release of flammable gases or cryogenic liquids with a major focus on natural gas (methane). It is completed in chapter 5 with a summary on the acquired knowledge and experience from accidents in the past and from both experimental and theoretical studies whose results might be of interest to the HTTR and the steam reforming process. The report ends with the conclusions in chapter 6.

2. DESCRIPTION OF THE HTTR/SR

2.1. General

2.1.1. PURPOSE AND MAIN ACTIVITIES

The combined system of HTTR and natural gas steam reforming facility, HTTR/SR, will be the first establishment in the world, which is able to produce hydrogen in a steam reforming process based on nuclear process heat as primary energy input. The system is designed to generate hydrogen at a rate of approx. 4000 Nm^3/h.

The combination of the HTTR with a heat utilization system represents a significant upgrading of HTGR technologies by demonstrating one of its most pertinent features, which is the provision of HT process heat. The consideration of HTGR heat utilization technologies is at the same time connected with the research, development, and demonstration of innovative and basic technologies, e.g., nuclear water splitting processes for hydrogen production.

The HTTR/SR system has two major goals:

- demonstration of nuclear hydrogen production at a high performance level,
- demonstration of the high safety level of this system during operation.

In order to achieve these goals, it needs to be demonstrated that particularly all components which are unique to this system, work as expected. They include the intermediate heat exchanger to decouple nuclear heat from the primary circuit, and the steam reformer, where the heat is transferred to the process side. The nuclear hydrogen production process should have an efficiency as to be in the range of competitiveness with conventional, fossil-fired facilities.

Furthermore it is necessary to prove that the selected safety concept of the whole system is appropriate to ensure safety for man and environment under any normal or abnormal conditions to the highest possible level. These activities will focus in particular on the prevention of the transition of radioactivity from the nuclear to the process side and also on the hazard of an accidental explosion or fire on the chemical side and its impact on the nuclear containment.

Prior to the first connection of the HTTR to the steam reforming system, a comprehensive out-of-pile test program will be conducted to confirm controllability, safety, and performance of the key components for both the operation of the nuclear reactor and the hydrogen production system.

2.1.2. HISTORY AND DEVELOPMENT OF ACTIVITIES

2.1.2.1. High-Temperature Engineering Test Reactor

In 1987, the Japanese Atomic Energy Commission has initiated a “Long-Term Program for Research Development and Utilization of Nuclear Energy”, which included the decision for the construction of the High Temperature Engineering Test Reactor, HTTR. Its construction eventually started in March 1991. All major components were completed and installed by the end of 1994. Following to various functional tests, fuel loading started with the first criticality

being achieved in 1998. A program of commissioning tests was conducted afterwards comprising the stepwise increase of the power, testing of the single and simultaneous operation modes. The performance at a coolant outlet temperature of 850 °C at full rated power of 30 MW was confirmed in 2001. With the successful conduction of all commissioning and safety demonstration tests, the construction of the HTTR has been formally completed, the operation permit for the HTTR was granted in March 2002. In April 2004, HTTR operation at a coolant outlet temperature of 950 °C at full rated power was successfully demonstrated.

2.1.2.2. Development of Heat Utilization Activities

JAERI has been investigating since more than 30 years the potential of the HTGR as an adequate system to provide nuclear process heat for a whole variety of applications in different industries. With the construction of the HTTR at the Oarai Research Establishment, an important milestone has been achieved.

2.1.2.3. R&D Work for the Hydrogen Production System

Parallel to the HTTR activities, JAERI has been studying the possibility of hydrogen and methanol production technologies with the HTTR since 1990. Among different candidate processes, particular focus was laid upon the methane steam reforming process, which has several advantages:

(1) Steam reforming of natural gas (methane) or naphtha is a mature and widely applied technology in the chemical industries and represents at present the most economical production method for hydrogen.

(2) Technical solutions demonstrated by coupling the steam reforming system to the HTTR will contribute to other nuclear-heated hydrogen production systems.

(3) The provision of nuclear process heat as a substitute for conventional firing means a significant saving of fossil resources and thus a reduction in greenhouse gas emissions. In this way, it facilitates the transition from fossil fuels to future hydrogen energy systems.

(4) The key components of this system, such as the helium-heated steam reformer, have been developed and tested under “nuclear conditions” already in several countries in the past.

JAERI developed the framework of the HTTR steam reforming system in a preliminary phase between 1990 and 1995. The conceptual design of this system has been carried out subsequently. In 1997, the Ministry of Education, Culture, Sports, Science and Technology (MEXT) of Japan entrusted JAERI with the development of the HTTR hydrogen production system comprising design and safety studies, construction of an out-of-pile test stand, component tests and materials investigation. The mock-up facility was constructed in 2001 and is being operated since.

Another H_2 production method selected for further consideration to be coupled to a nuclear heat source is a water-splitting process based on the sulfur-iodine (S/I) thermo-chemical cycle, for which JAERI has initiated basic studies. A third candidate process, H_2 production by HT

electrolysis was abandoned for a while, but seems to be revived as a candidate process for the VHTR project since recently.

An HTTR Utilization Research Committee was founded in 1993 to promote innovative basic research. It has selected several projects in the fields of materials development, radiation chemistry, fusion research, or high-temperature in-core instrumentation, which are checked at present for their scientific and technical feasibility and effectiveness in future irradiation experiments in the HTTR.

2.1.2.4. Future Activities for Process Heat Applications

Future activities at JAERI will concentrate on the final achievement of power operation of the HTTR and the acquisition of operational data. With insertion of the 2nd fuel loading into the HTTR core after nominal 660 efpd (or estimated four years of operation), the demonstration of nuclear heat application systems will be starting focusing on the steam reforming process with the completion and operation of the out-of-pile facility in connection with the component tests (see chapters 4.5.1. and 4.5.2.). A parallel activity is the further investigation of the IS thermo-chemical cycle with the erection of a bench-scale and later pilot-scale test facility. A longer-term goal is the development of a conceptual design for a commercial H_2-HTGR connected with a hydrogen production system (time target: 2020) [Ogawa 2003].

2.1.3. MAIN HAZARDS FROM ACTIVITIES

Both the nuclear energy production process and the chemical process of steam reforming of natural gas are, separately considered, since long widely applied technologies in the world. Hazards associated with the processes have been dealt with in detail resulting in a comprehensive system of codes and standards, which is directed towards a reduction of the risk of hazards to a minimum.

There are, however, a few new aspects in the combined HTTR/SR system:

- There is not much experience with HTGR in the world compared with other types of nuclear reactors. But the HTGR system is in general considered to be on a high safety level.
- The development and testing of novel components is required to combine the nuclear with the chemical system.
- Due to the immediate vicinity of the nuclear and chemical systems, a new category of hazards evolves with potential effects from one system to the other.

In a nuclear hydrogen production system, the link between the chemical and nuclear system is given via the secondary helium circuit, thus enabling, in case of respective pipeline ruptures, feed/product gases to accumulate inside the nuclear containment jeopardizing the nuclear primary circuit in case of an explosion. The product gas will be a mixture of H_2, CO, CO_2, residual H_2O, and still unreformed methane which may form flammable compositions under certain conditions. The impact from outside to an HTGR for process heat applications is given by the possible formation and explosion of a flammable gas cloud in the open atmosphere. The accident conditions may arise from leakages in the chemical complex including the main

components steam reformer and storage tanks for LNG or hydrogen.

2.2. Location

The Oarai Research Establishment is approximately 100 km north of the Tokyo metropolitan area and located near the Pacific Ocean, about 5 km away from the center of Oarai, a town of approximately 20,000 inhabitants. The site of the Research Establishment is about 1.7 km long and 1.5 km wide. The HTTR plant is located on the Oarai Research Establishment site as is shown in Fig. 2-1. The HTTR plant area is 200 m x 300 m in size. The shortest distance between the HTTR reactor core and the site boundary is about 280 m in southwest direction.

Besides the HTTR, two more nuclear reactors have already been established on the site of the Oarai Research Establishment. One is the Japan Materials Testing Reactor (JMTR), a 50 MW(th) light-water cooled and moderated reactor, located approximately 400 m north of the HTTR. The other is an experimental liquid metal fast breeder reactor "JOYO" with 130 MW(th), approximately 650 m east of the HTTR.

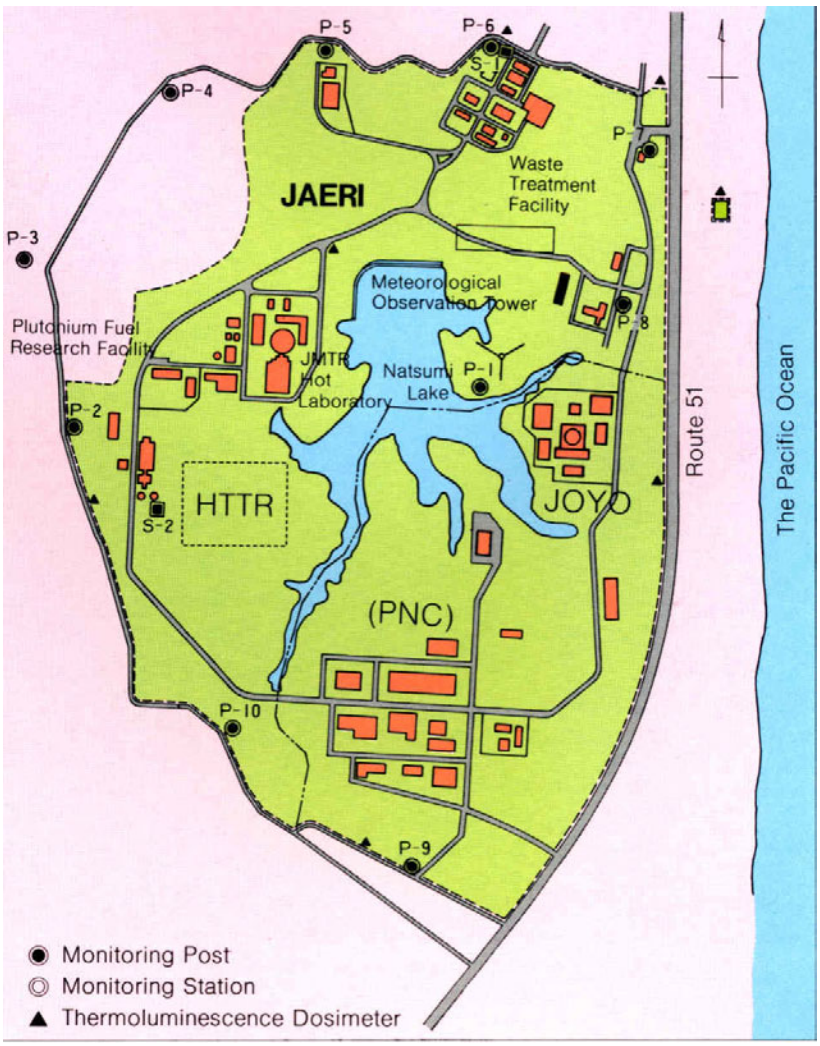

Fig. 2-1: Location of Oarai Research Establishment

The HTTR reactor has been erected on a sand layer (Ishizaki layer) formed during the Quaternary era. Its adequacy was verified by drilling surveys and shallow reflection seismic surveys that the supporting ground is horizontally formed with continuity of strength and stiffness. It could be recognized from seismic surveys that the supporting ground at the site has the seismic safety equivalent to base rock, which is usually required for important buildings and structures according to the Japanese "Guidelines for Aseismic Design of Nuclear Power Plants".

2.3. Layout of the HTTR/SR

2.3.1. HTTR

The HTTR plant with a thermal power of 30 MW is composed of a reactor building, a spent fuel storage building, a machinery building, cooling towers, an exhaust stack, warehouses, an HT process heat utilization system and others (see Fig. 2-2). The reactor building is covering a ground area of 48 m x 50 m; it is with two floors above ground and three under ground as shown in Fig. 2-3. North of the reactor building, there is the exhaust stack of 80 m in height, through which the air ventilated from the reactor building is released to the atmosphere. The heat utilization system to be attached later will be constructed south of the reactor building.

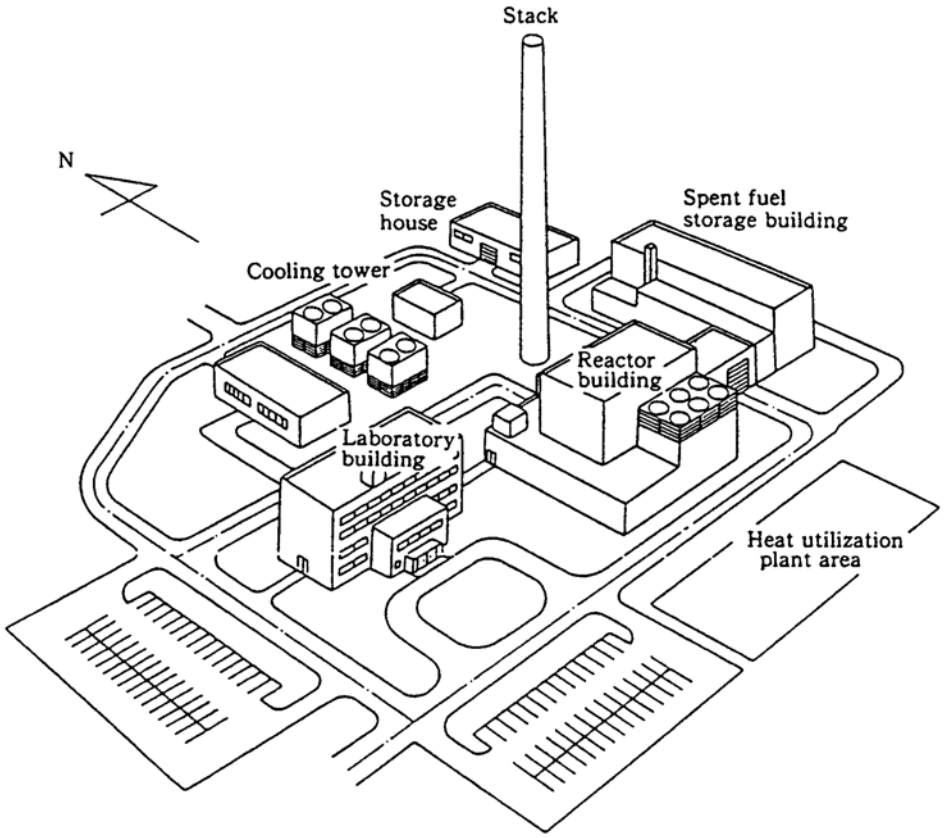

Fig. 2-2: Overall arrangement of the HTTR facility

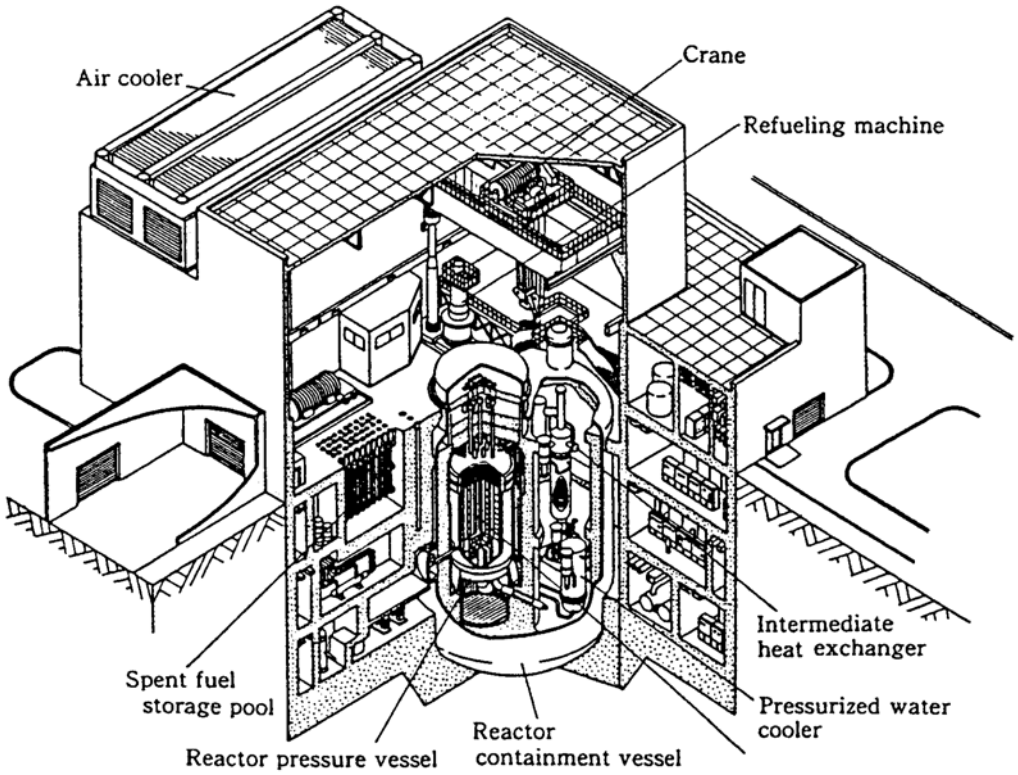

Fig. 2-3: Cutaway view of the HTTR reactor

Nominal lifetime of the permanent structural components in the HTTR plant is based on 20 years with a load factor of 60 % of full power operation. The design of the HTTR is described in full detail in [Saito 1994]. The major design specifications are summarized in Table 2-1.

Table 2-1: Main characteristics of the HTTR

Thermal power	30 MW
Fuel Fuel element type	Low-enriched UO_2 Prismatic block
Primary coolant Inlet / outlet temperature Pressure	Helium gas 395 / 850 and 950 °C 4 MPa
Pressure vessel	Steel
Cooling systems	Main cooling system Auxiliary cooling system Vessel cooling system
Heat removal system	Pressurized water cooler Intermediate heat exchanger
Containment vessel	Steel
Plant lifetime	20 yr

2.3.1.1. Reactor Components

Reactor Containment Vessel (CV)

A steel reactor containment vessel (CV) is installed in the center of the reactor building enclosing the Reactor Pressure Vessel (RPV) and the Primary Cooling System (PCS). A refueling hatch is attached to the CV above the RPV at the level of an operating floor of the first floor as well as a maintenance hatch. With 2800 m^3 of free volume, the CV is comparatively small. The main functions of the CV in the HTTR are:

(1) to contain all fission products in case of an accident and to withstand all temperature and pressure transients;

(2) to limit the ingress of air, which reacts with the core graphite, in case of a primary pipe rupture accident.

Major specifications of the CV design are given in Table 2-2.

Table 2-2: Design specifications of the reactor containment vessel

Material	Carbon steel
Size Inner diameter Height Wall thickness Top head closure thickness Refueling hatch diameter Maintenance hatch diameter Free volume	 18.5 m 30 m 30 mm 38 mm 8.5 m 2.4 m 2800 m^3
Pressure during reactor operation Maximum allowable pressure	Atmospheric pressure 0.49 MPa
Temperature during reactor operation Maximum allowable temperature	Room temperature 150 °C
Leakage rate	0.1 % of free volume / day at room temperature 0.25 % of free volume / day for depressurized reactor

The so-called Service Area is the space surrounding the CV. Under the condition of an accident, the pressure inside of the service area is kept slightly below atmospheric pressure using an emergency air purification system to remove any air-borne radioactivity. Filters in the emergency air purification system remove iodine at an efficiency of > 95 % and metallic fission products at an efficiency of > 99 % for 0.7 μm particles.

Reactor Pressure Vessel (RPV)

The RPV contains the core, the graphite reflector blocks, the core support structure, and the core restraint mechanism (Fig. 2-4). It is composed of a vertical cylinder with hemispherical top and bottom head closures, and 31 standpipes for control rods, irradiation devices, and instrumentation. The top head closure is bolted to a flange of the vessel cylinder. The RPV is supported by the vessel skirt outside the bottom head closure, stabilizers, and a standpipe support beam.

The thermal shield consisting of layers of metallic, heat-reflecting plates, is attached to the inner surface of the top head closure to prevent the closure from overheating during a depressurization accident. Design specifications of the RPV are given in Table 2-3.

Table 2-3: Design specifications of the reactor pressure vessel

Material	2.25Cr-1Mo low alloy NT steel
Size Inner diameter Height Wall thickness Top head closure thickness	 5.5 m 13.2 m 120 mm 160 mm
Operating pressure Design pressure	4.0 MPa 4.81 MPa
Maximum operating temperature Design temperature Maximum accident temperature	400 °C 440 °C 530 °C

Reactor Internals

The reactor internals consist of graphitic and metallic core support structures and shielding blocks as is also shown in Fig. 2-4. The graphitic core support structures are composed of permanent reflector blocks, hot plenum blocks, support posts, and core bottom structures. The metallic core support structures include the support plates, a support grid, the core restraint mechanism supporting the active core, and replaceable reflector blocks.

The permanent reflector surrounding the replaceable reflector is composed of large polygonal graphite blocks, which are fixed by key elements and the core restraint mechanism.

Through a primary helium piping system, the reactor coolant enters the RPV at the bottom from the primary cooling system, and then flows up through an annulus between the RPV and reactor internals.

The permanent reflector and the hot plenum blocks are fabricated from grade PGX graphite, a medium-to-fine grained, molded structural graphite. In the hot plenum block assembly, the reactor coolant is collected and flows into the hot gas duct inserted into a core bottom block. It is connected to the primary helium piping system in the main cooling system.

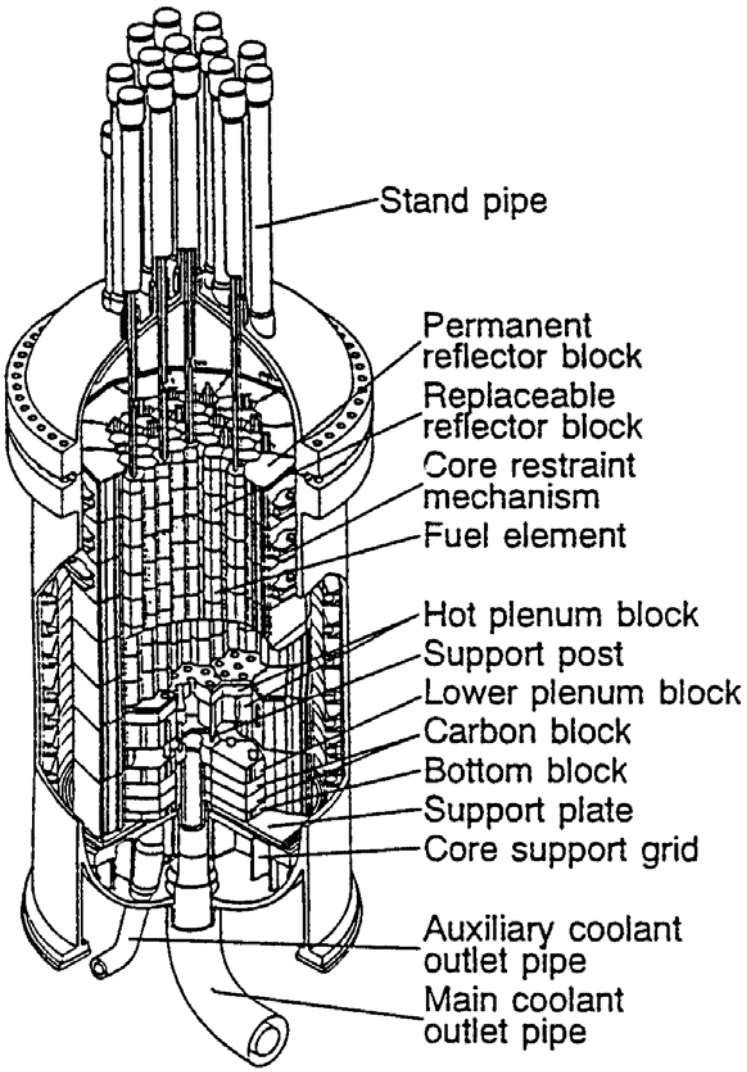

Fig. 2-4: Structure of reactor internals

Control System

Reactivity is controlled through control rods, which are inserted into the active core and the replaceable reflector columns. A reserve shutdown system is provided as a backup shutdown system in form of pellets inserted into the third channel in each control rod guide column. Neutron absorber pellets are made of B_4C/C, sheathed with a cylindrical clad of Alloy 800H.

During a scram, the temperature of the sheathing reaches approximately 900 °C. To prevent the control rod sheathing from thermal damage, at first, nine pairs of control rods are inserted into the replaceable reflector column holes. The remaining seven pairs are inserted into the active core column holes after the core is cooled down and the coolant outlet temperature is decreased below 750 °C.

Helium Purification System

The purification system for the primary helium is located in the service area surrounding the containment vessel. It is composed of a charcoal trap, two copper oxide fixed beds, two molecular sieve beds, and two cold charcoal traps. The throughput of the system is 200 kg/h of primary helium to keep impurity concentrations less than upper limits whose values are given in Table 2-4. The system allows a cleansing of 10 % of the total primary helium inventory per hour. In particular, it is designed to have the hydrogen concentration limited to < 3 ppm (corresponding to < 12 Pa partial pressure), which is an important issue with respect to the permeation effect of H_2 from the process gas side in the steam reformer to the primary circuit.

Table 2-4: Upper limits of impurities in the HTTR primary circuit in [vol ppm]

H_2O	CO_2	H_2	CO	CH_4	N_2	O_2
0.2	0.6	3.0	3.0	0.5	0.2	0.02

There is another purification system for the secondary helium which has a smaller capacity because of the expected lower impurity level; it is designed to have a throughput of 10 kg/h.

2.3.1.2. Reactor Core

The reactor core itself is located within the pressure vessel of the HTTR. It is composed of in total 61 columns of nine vertically stacked blocks each. The upper two and lower two layers form the top and bottom graphite reflector.

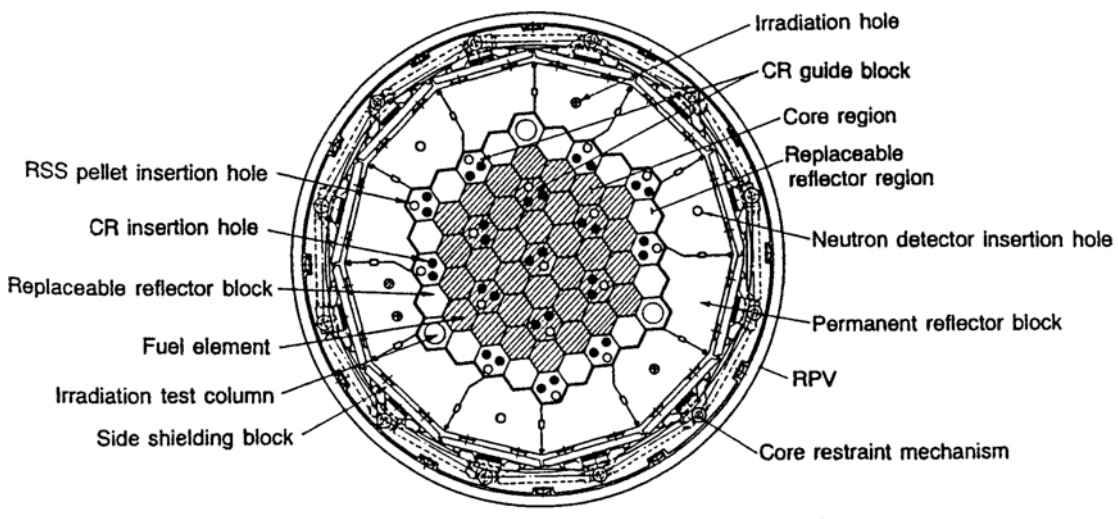

Fig. 2-5: Horizontal core structure

The active core dimensions are 2.9 m in height and 2.3 m in equivalent diameter. It is composed of 150 pin-in-block type fuel assemblies (hexagonal graphite blocks) which are arranged in 30 columns of five vertically stacked blocks each. Seven columns to guide control rods also

located in the active core. The dimensions of the active core are 2.9 m of total height and 2.3 m of equivalent diameter. The active core is surrounded by additional nine control rod guide columns, 12 replaceable reflector columns plus three columns for irradiation testing. Permanent side reflector blocks are tightened by the core restraint mechanism. In Fig. 2-5, the arrangement of the HTTR core structure is presented exhibiting the different kinds of core columns employed. The radial zoning of the active core columns into four categories is distinguished by the degree of U-235 enrichment of the fuel.

2.3.1.3. Cooling Systems

The reactor cooling system is composed of a main cooling system (MCS), an auxiliary cooling system (ACS) and two reactor vessel cooling systems (VCS). The flow sheet of the reactor cooling system in the HTTR is shown in Fig. 2-6.

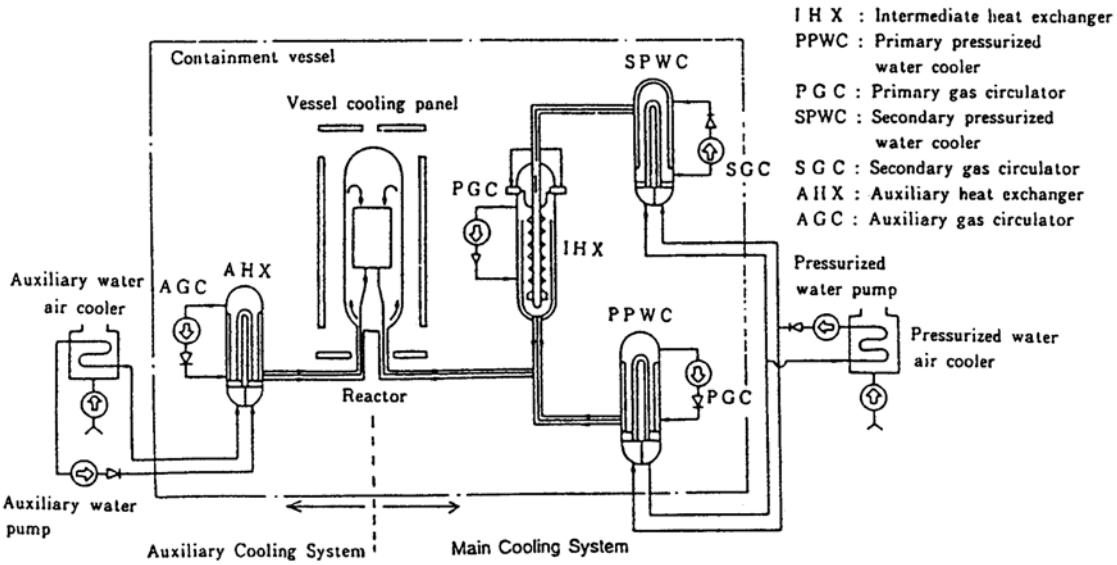

Fig. 2-6: Flow sheet of the reactor cooling system

Main Cooling System

The MCS removes the heat energy from the reactor core during the normal operation. Its major components are the intermediate heat exchanger (IHX), the primary pressurized water cooler (PWC), the secondary PWC and the pressurized water air cooler. The primary coolant circuit contains the primary helium gas and has four high-speed primary gas circulators (PGC). It consists of two parallel circuits outside the reactor pressure vessel. One circuit has the IHX and one PGC; the other circuit has the primary PWC and three PGC. After a reactor scram, the gas circulators of the MCS stop to prevent core and heat exchanger tubes from over-cooling. The major design specifications of the PWC are summarized in Table 2-5.

The MCS can thus be operated in two modes: (i) "single load operation" and (ii) "simultaneous load operation". During the single load operation, the primary PWC is operated to remove the

total reactor heat of 30 MW. In the simultaneous load operation, the primary PWC removes 20 MW and the IHX removes 10 MW; the secondary PWC removes the heat from the IHX. Switching between these two loop modes is done manually in the shut-down state of the reactor. The heat is discharged from the primary PWC, which is a vertical U-tube heat exchanger, via air coolers into the atmosphere as the final heat sink. In the IHX, the heat is transferred to the secondary helium circuit, before it is discharged by the secondary PWC via the same air coolers into the atmosphere as well.

Table 2-5: Design specifications of the primary PWC

Material	
Shell	2.25Cr-1Mo steel
Tube	SUS 321 TB
Size	
Outer shell diameter	2.1 m
Shell height	7.1 m
Outer tube diameter	25.4 m
Tube wall thickness	2.6 mm
Number of tubes	136
Heat capacity	
single mode	30 MW
simultaneous mode	20 MW
Primary helium	
inlet temperature	850 °C (950 °C at HT operation)
outlet temperature	395 °C
flow rate single mode	45 t/h (37 t/h at HT operation)
flow rate simultaneous mode	30 t/h (24 t/h at HT operation)
Pressurized water	
inlet temperature	150 °C
outlet temperature	190 °C
flow rate	
single mode	640 t/h (630 t/h at HT operation)
simultaneous mode	420 t/h

During normal operation, the pressure of the secondary helium is controlled to be always 0.1 MPa higher than that of the primary helium at the IHX heat transfer tubes. Reasons are to reduce the pressure load on the tubes and to protect in case of an accidental leak the transition of radioactivity into the secondary helium. The pressure on the water side is always fixed at 3.5 MPa, meaning that a large amount of water would not penetrate into the core in case of a primary PWC tube rupture accident.

A major problem to be solved was the possible burnout effect of the PWC due to the large temperature difference of approximately 850 °C between the primary helium and the pressurized water. Using Hastelloy XR as baffle plate material and reducing the helium flow in the high-temperature region to keep the heat flux at the heat exchanging tubes less than $1.2 * 10^{-5}$ W/(m^2 K) are expected to prevent a burnout.

Hot Gas Duct

The primary concentric hot gas duct is used to transfer helium at high temperature (850/950 °C) from the core to the IHX and/or the primary PWC, and helium at low temperature (400 °C) back to the core. It consists of the outer pressure tube (outer diameter: 860 mm; wall thickness: 42 mm) and the inner tube (outer diameter: 660 mm; wall thickness: 15 mm), which contains on its inside a 90 mm insulation and a Hastelloy XR liner. The liner forms a boundary for the hot helium gas and reinforces the ceramic fiber insulation, which minimizes heat loss to the outside and keeps the inner tube temperature lower than its specified limit.

Air Cooler

The air cooler consists of heat transfer tubes which have fins and fans transferring heat from the primary and secondary PWC to the atmosphere. It has a cooling capacity of 30 MW with an air flow rate of 2600 t/h.

Auxiliary Cooling System

The ACS consists of the auxiliary heat exchanger (AHX), two auxiliary helium circulators and the air cooler. During normal operation, a small helium flow rate of 200 kg/h passes through the AHX to the primary helium purification system for the purpose of removing impurities contained in the reactor coolant. In case of an emergency shutdown with the reactor coolant pressure boundary remaining intact, the ACS is automatically operated by the two auxiliary PGC to cool down the core, where the decay heat is transferred via an auxiliary heat exchanger to an auxiliary water system. The ACS has a heat transfer capacity of approximately 3.5 MW. It is backed up by an emergency power supply.

Vessel Cooling System

The VCS is part of the HTTR safety equipment. Therefore it consists of two independent complete sets, which are backed up by emergency power supply. The VCS is employed to remove the decay heat in the case of accidents with a loss of forced convection, i.e., when the ACS is not available. It is, however, also operated during normal operation removing heat of less than 0.6 MW to keep the temperature of the biological concrete shield of the reactor at a temperature below 50 °C.

The VCS consists of water-cooled panels surrounding the RPV and two cooling water systems with each being capable alone of controlling the temperatures of core and RPV within safe limits. The heat removal rate from the RPV to the VCS is designed to be 0.6 MW or less during the normal operation so as to effectively transfer the reactor heat to the MCS. Also under accident conditions, it is 0.3 MW or more for decay heat removal from the core.

Intermediate heat exchanger

The IHX is a vertical helically coiled counter flow type heat exchanger as shown in Fig. 2-7. The primary helium enters the IHX through the inner pipe of the primary concentric hot gas

duct attached to the bottom of the IHX. It flows upwards outside the tubes transferring the nuclear heat of 10 MW to the secondary helium cooling system and flows back through the annular space between the inner and outer shells. The secondary helium flows downwards inside the heat transfer tubes and flows upwards in the central hot gas pipe through the hot header.

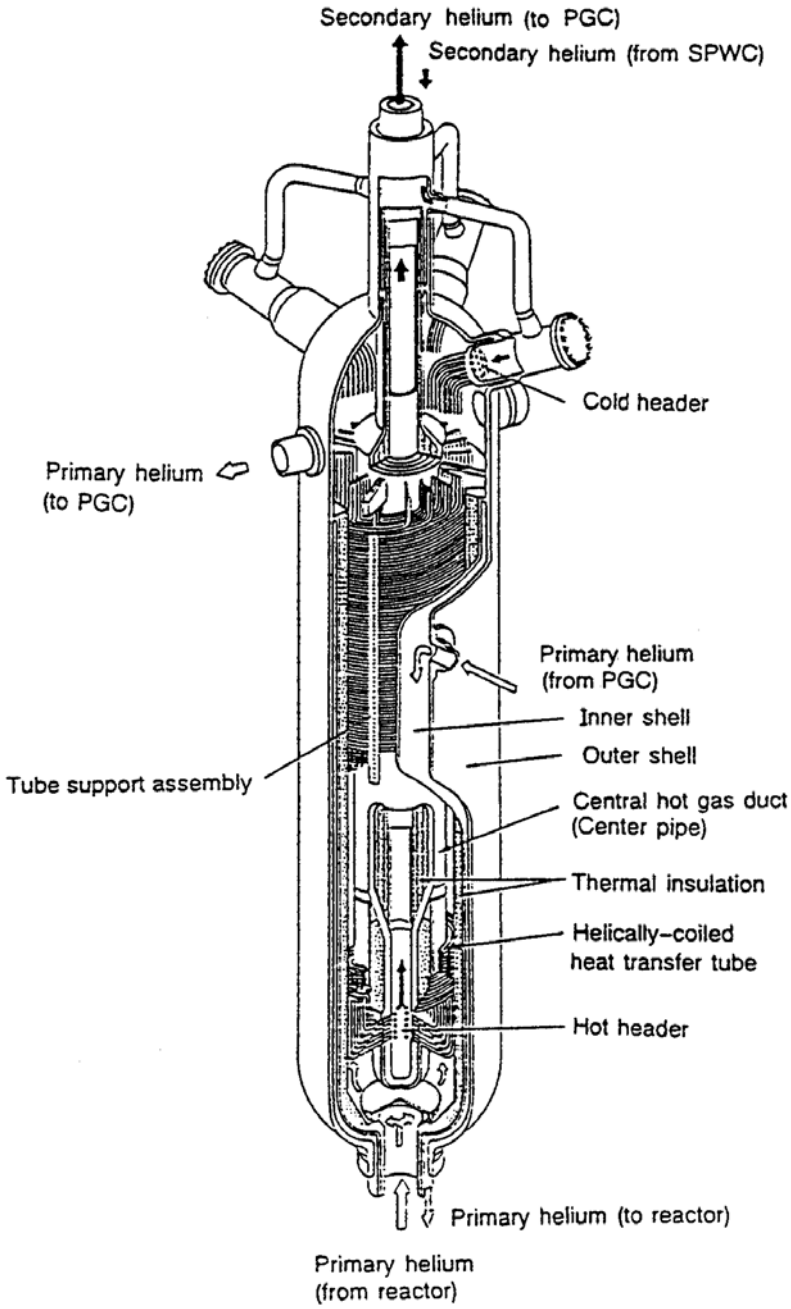

Fig. 2-7: He-He intermediate heat exchanger

A double-walled shell with a thermal insulation attached on the inside surface of the inner shell provides reliable separation of heat-resisting and pressure-retaining functions. Cold helium flowing through the annulus brings uniform temperature distribution throughout the outer shell, which has a pressure-retaining function. Insulation inside and outside the central hot gas pipe

keeps the heat transfer low to obtain a high efficiency.

To minimize constraints of axial and radial thermal expansions of the helically coiled heat transfer tubes, a floating hot header combined with the central hot gas duct and passing through the central space inside the helix bundle, is adopted. A tube support allows free thermal expansion of a helix in radial direction. Table 2-6 shows the major design specifications of the IHX.

Table 2-6: Design specifications of the He-He Intermediate Heat Exchanger

Type	Counter-current and helically wound tube type of shell-and-tube heat exchanger
Heat capacity	9.94 MW
Material Shell Tube Thermal insulation	 2.25Cr-1Mo steel Hastelloy XR Kaowool 1400SHA
Size Inner / outer shell diameter Shell height [m] Outer tube diameter Tube wall thickness Number of tubes	 1.35 / 2.0 m 11 m 31.8 mm 3.5 mm 96
Heat capacity	10 MW
Maximum temperature Shell Tube	 430 °C 955 °C
Maximum pressure Shell Tube (differential pressure)	 4.81 MPa 0.29 MPa
Primary helium inlet temperature outlet temperature design pressure drop flow rate	 950 °C 389 °C 9.2 kPa 12.2 t/h
Secondary helium inlet temperature outlet temperature design pressure drop flow rate	 158 °C 905 °C 50.2 kPa 9.07 t/h

2.3.2. STEAM REFORMING SYSTEM

2.3.2.1. Layout

A flow diagram of the hydrogen production system and its connection to the HTTR is given in Fig. 2-8. A layout of how the whole system might look like in future is shown in Fig. 2-9. The picture does not include the LNG storage tank, which will be located in a safe distance away from the nuclear and chemical plants.

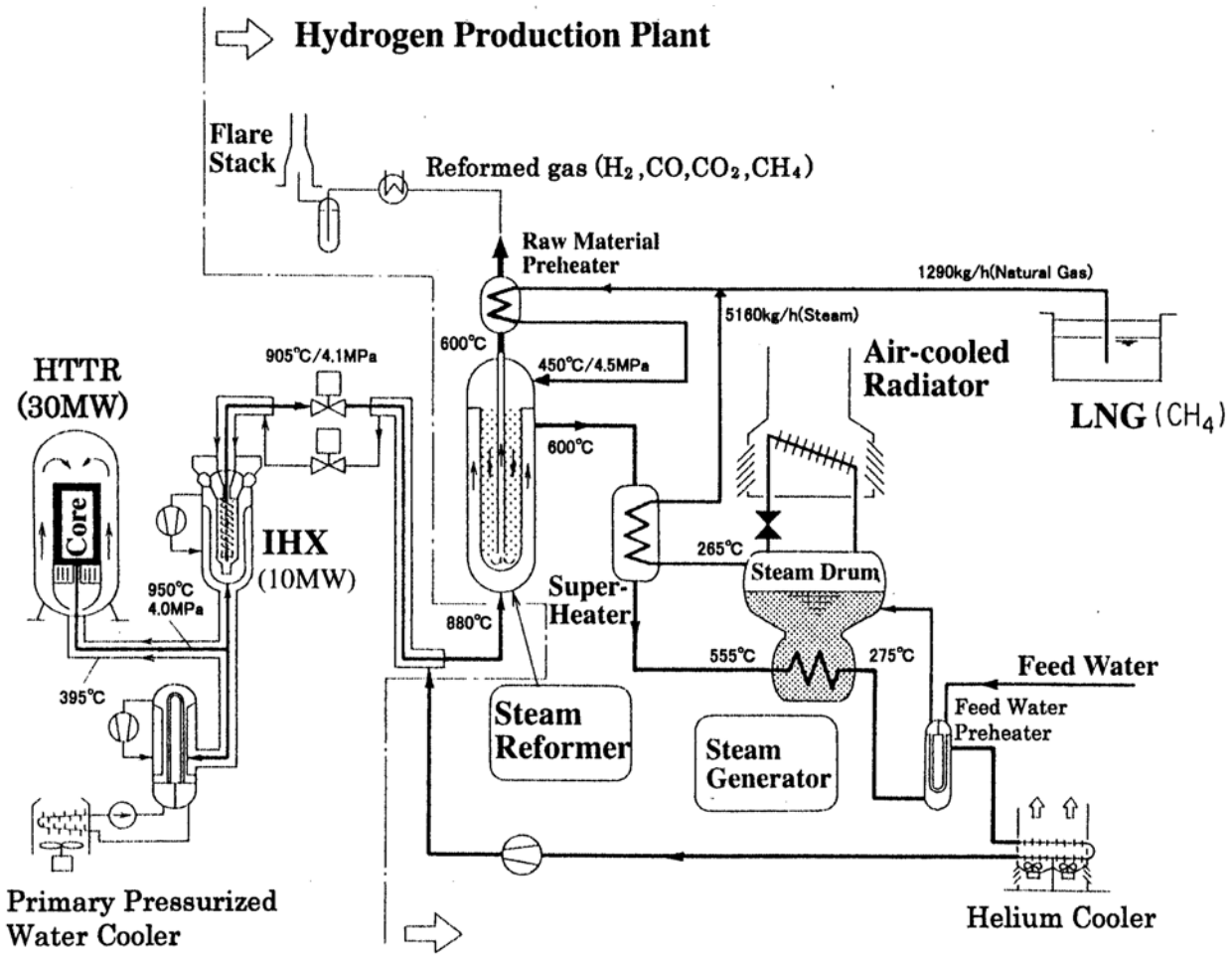

Fig. 2-8: HTTR plant with heat utilization system

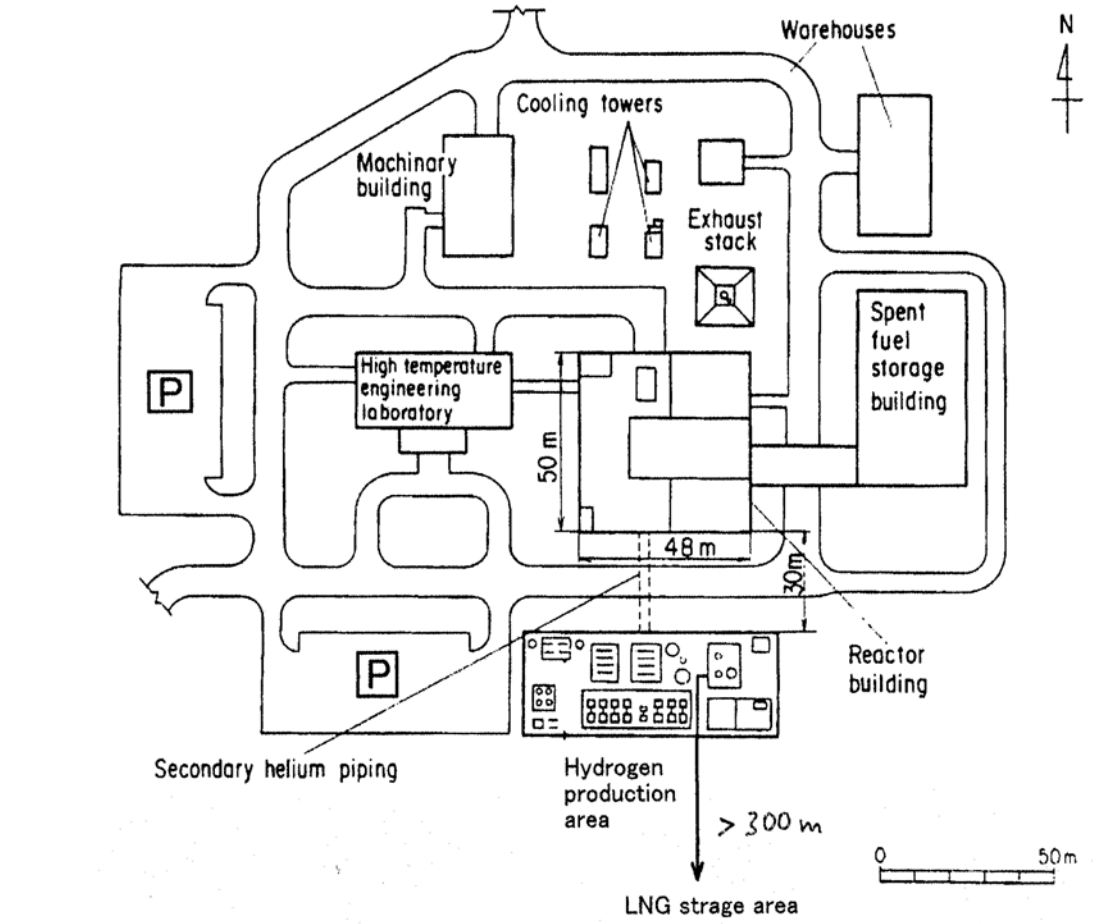

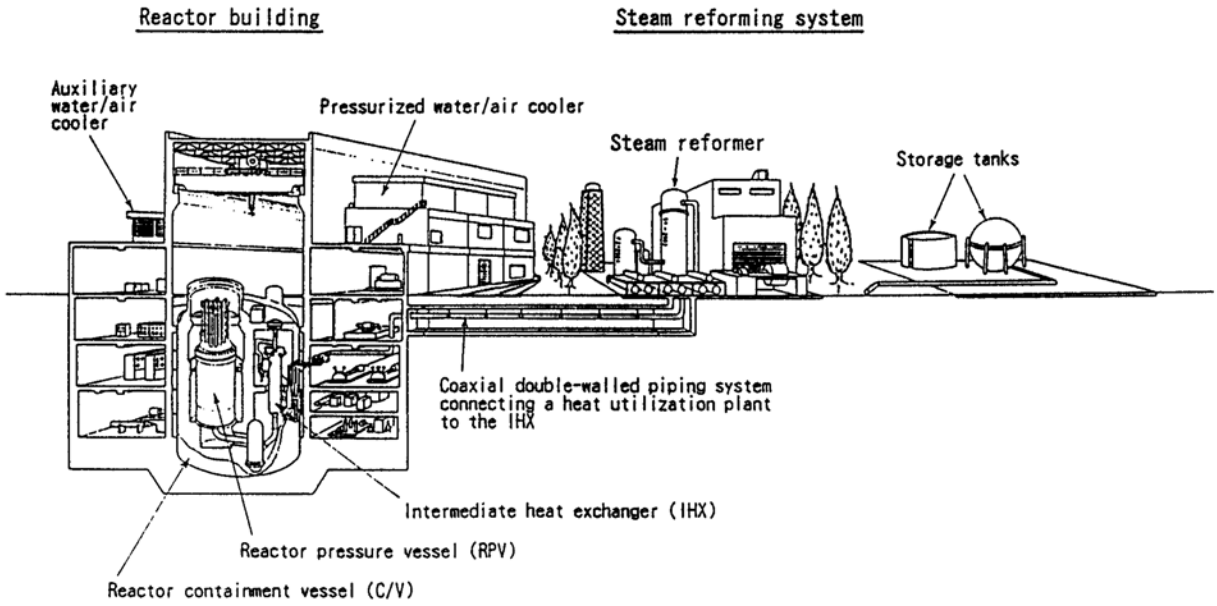

Fig. 2-9: Cutaway view of the combined HTTR/SR system

The requirements for a system with safe operation and high hydrogen production efficiency has initiated engineering design work on key components for the nuclear steam reforming process:

(1) A new concept steam reformer heated by helium gas from the nuclear reactor has been designed to achieve high hydrogen production performance and competitiveness to an economical, fossil-fired hydrogen production plant.

(2) A natural convection type of steam generator has been selected to achieve sufficient system controllability accommodating a large difference in thermal dynamics between the nuclear reactor and the steam reformer.

(3) An air-cooled radiator is connected to the steam generator to operate as a final heat sink during normal and anticipated operational occurrence condition.

The HTTR steam reforming system can provide about 4200 Nm^3/h of hydrogen production using a Ni-based catalyst with 10 MW of thermal energy. A heat utilization ratio (defined as the ratio of output hydrogen energy to total input thermal energy) of 73 % is expected. This value is competitive to the conventional system, where the heat utilization ratio is about 80 %.

2.3.2.2. Steam Reformer

In comparison to a conventional steam reformer, the employment of a nuclear steam reformer requires certain changes, since operational conditions of a nuclear reactor are not that flexible as a fossil-fueled furnace. Also safety requirements are much more stringent than for a fossil-fueled system. It is therefore desired to achieve highest effectiveness in utilizing the nuclear process heat in the whole production process system.

Design

A large H_2 production rate is achieved, if the process feed gas rate and the conversion rate are high. The feed gas rate depends on the amount of heat input into process gas and the temperature of process gas. The conversion rate depends on temperature and pressure of the process gas.

In the HTTR, the thermal energy of 10 MW is transferred via the IHX to the secondary helium gas which is pressurized up to 4.2 MPa in order to prevent the accidental release of fission products from the core to the environment and to assure the structural integrity of the IHX heat exchanger tubes against creep damage. The HTTR can provide high-temperature helium gas of 905 °C at the outlet of the IHX and of 880 °C at the inlet of the steam reformer.

Helium flows outside the catalyst tubes transferring heat by forced convection flow (in contrast to heat radiation in the conventional design). The catalyst tubes contain packings of Ni/Al_2O_3 reforming catalysts, through which the process feed gases (natural gas, steam) are routed. The catalyst tube wall thickness is 13 mm meeting the requirements on design limits for pressure-retaining components.

The design specifications of the steam reformer are summarized in Table 2-7.

Table 2-7: Design specifications of the steam reformer

Nuclear heat input	3.6 MW (plus 1.3 MW from product gases)
Material Tubes Catalyst	 Hastelloy XR Ni/Al_2O_3
Size Shell diameter Shell height	 1.19 m 14 m
Catalyst tube Outer tube diameter wall thickness length Inner tube diameter wall thickness length Number of tubes	Bayonet type, concentric double-walled tube 153.8 mm 13 mm 7.9 m 60.5 mm 3.9 mm not decided yet 37
Secondary helium inlet temperature outlet temperature pressure flow rate	 880 °C 585 °C 4.1 MPa 9070 kg/h
Heat transfer rate at outer surface	1700 $W/(m^2 K)$
Process feed gas inlet temperature outlet temperature pressure raw gas flow rate raw gas conversion	 450 °C 580 °C (max.: 800 °C at catalyst zone outlet) 4.5 MPa 1400 kg/h 64.2 %
Steam-methane ratio	3.5
Hydrogen production rate	4240 Nm^3/h

Furthermore the reforming process requires a thermal heat input of 4.8 MW. In order to generate feed steam by the thermal energy of secondary helium gas, the helium gas temperature at the outlet of the steam reformer is required to be about 600 °C, so that only thermal energy of 3.6 MW is supplied to the steam reformer from helium gas. This high-pressure and low-temperature condition is a disadvantage for the steam reforming reactions.

Improved Concept

A new heat exchanger type concept of steam reformer is required to enhance the hydrogen production rate. It should allow

(1) an increased heat input into the process gas by employment of orifice baffles;

(2) an increased reaction temperature of the process gas at the outlet of the catalyst zone;

(3) an optimizing reforming gas composition to enhance the reforming rate.

Table 2-8: Comparison between nuclear and conventional design

Parameter	Steam reformer		
	Fossil-heated	**Helium-heated for HTTR/SR**	**Helium-heated improved design**
Process gas pressure [MPa]	1 - 3	> 4	4.5
Maximum temperature of process gas [^{o}C]	850 - 950	≤ 750	800
Maximum heat flux to catalyst zone [kW/m^2]	50 - 80	10 - 20	40
Heat transfer	radiation	forced convection	
Efficiency [%]	80 - 85	50	78
CO_2 emission [t/h] (Basis: 10 MW)	3	0	

The aim of reaching a heat flux density closer to that of the conventional method (see Table 2-8) can be achieved by employing a helium-heated counter flow heat exchanger. Helium under pressure shows excellent heat transfer properties.

JAERI has adopted a bayonet type of catalyst tube, a concentric, double-walled tube which can use both the outside and inside gas flow for heating up the process gas. The thermal energy input into the process gas increases from 3.6 to 4.9 MW.

Assuming an infinitely long catalyst tube, the process gas temperature approaches that of the helium gas. But in general, a catalyst tube length limit of approximately 10 m is mandated from the viewpoint of seismic design. It is necessary to enhance the heat transfer rate in order to design for an adequate steam reformer size. There are several means for enhancement of the heat transfer such as baffles, double tubes, fins, and others. JAERI has performed an analytical comparison of the heat transfer rate and selected a double tube with a radially finned catalyst tube, for which the thermal radiation rate is more than 1800 W/(m^2 K).

Excessive steam is supplied to the steam reformer so as to react sufficiently and to prevent carbon deposition. In the HTTR steam reforming system, a steam to carbon ratio of 3.5 has been selected. If a high performance catalyst can be used at low cost, the steam-carbon ratio could be decreased to utilize steam for electric generation.

The proposed steam reformer is shown in Figure 2-10. These improvements are applicable not

only to HTGR steam reforming system but also to other HTGR hydrogen production systems. This is because a heat exchanger type of endothermic chemical reactor is an essential technology for the production of hydrogen through the use of nuclear heat.

The effective consumption of the nuclear process heat input of 10 MW can be seen from the following Table 2-9 [Hada 1994]:

Table 2-9: Consumption of 10 MW nuclear heat input

Heat loss	0.5 MW
Air cooler	0.7 MW
Feed water preheater	0.8 MW
Reboiler	2.7 MW
LNG preheater	0.2 MW
Superheater	1.0 MW
Process gas heater	0.5 MW
Steam reformer	3.8 MW
Σ	10.2 MW

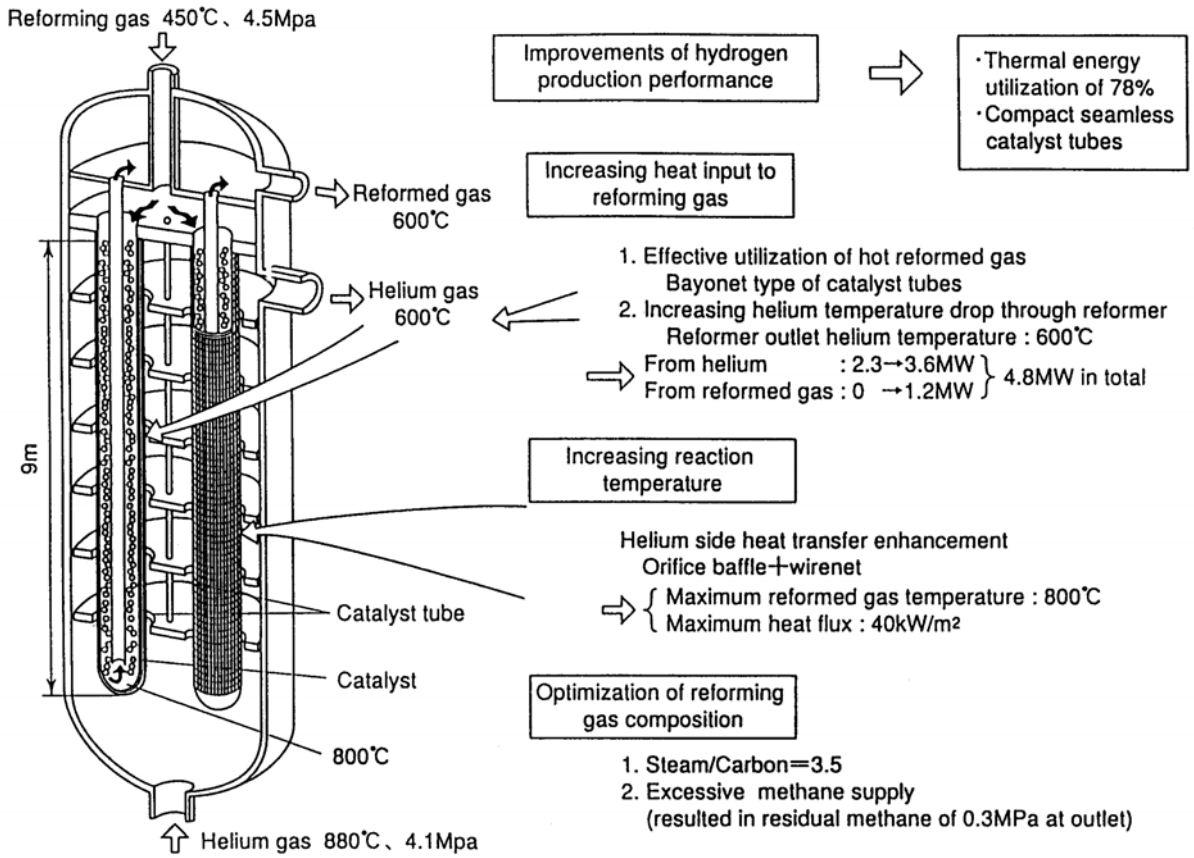

Fig. 2-10: New concept of He-heated steam reformer

2.3.2.3. Steam Generator

As shown in the figure of the HTTR steam reforming system layout, the steam generator is installed downstream of the reformer and has the task to produce steam for the steam reforming reaction according to the desired steam-methane ratio of > 3.5. A schematic of the steam generator is shown in Fig. 2-11; design specifications are listed in Table 2-10.

Table 2-10: Design specifications of the steam generator

Heat capacity	8.12 MW
Maximum temperature Shell Tube	 300 °C 400 °C
Maximum pressure Shell Tube	 5.5 MPa 5.0 MPa
Primary helium (tube) inlet temperature outlet temperature flow rate	 555 °C 275 °C 9070 kg/h
Secondary water/steam (shell) inlet temperature outlet temperature flow rate	 190 °C 265 °C 6677 kg/h

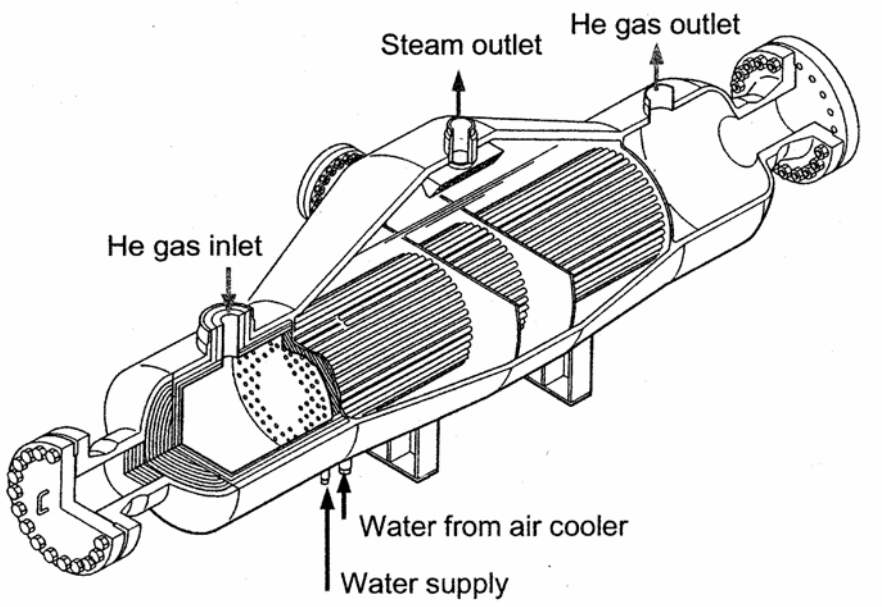

Fig. 2-11: HTTR steam generator

The second major feature of the HTTR steam generator is its potential property to stabilize the temperature of the contained water returning to the IHX under constant pressure conditions. A passive cooling system using the steam generator with radiator is proposed to enable continuous normal operation.

If thermal disturbances occur due to some malfunction in the steam reforming system, the steam generator acts as a thermal absorber. Helium temperature at the steam generator outlet can be kept constant at the saturation temperature of steam by controlling the pressure in the steam generator.

The advantage of the steam generator is utilized to prevent a reactor scram due to a malfunction or accident within the steam reforming system. Consequently, the secondary helium loop with steam generator can function as a mitigation system as mentioned above.

2.3.2.4. HT Isolation Valve

Fig. 2-12 shows a design of the high temperature isolation valve, which is still under development with focus on mitigation of thermal deformations. Testing in a mock-up facility is planned.

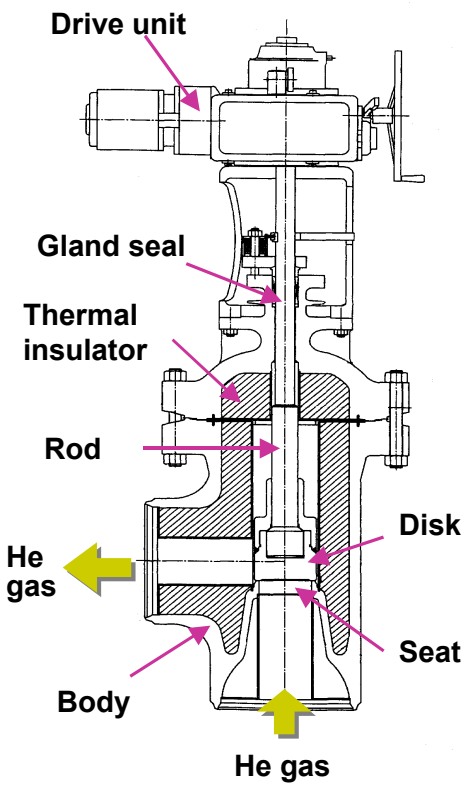

Fig. 2-12: High temperature isolation valve

2.3.2.5. Methane Gas Supply System

The area containing the pressurized methane gas supply system will be located approximately 300 - 500 m away from the nuclear reactor building. The supply system includes, apart from the underground LNG storage tank with a capacity of 400 m^3, the main components LNG vaporizer, surge tanks, desulphurizer, and transport lines to the steam reformer. The steam reformer itself will be erected in a distance of approximately 30 m away from the reactor building.

The figure for the feed gas flow of 1290 kg/h of natural gas translates into a volume flow for LNG of about 3 m^3/h. This would correspond – under steady-state conditions – to the consumption of a tank truck load (assumed: 30 m^3) every 10 hours or the emptying of the LNG storage tank (with 400 m^3) within 5.5 days.

2.4. Operation

2.4.1. HTTR

2.4.1.1. Basic Features of Operation

The HTTR generates a thermal power of 30 MW at an average power density of 2.5 MW/m^3. Two operational modes are possible, the single load operation and the simultaneous load operation, using either the cooling circuit with the PWC only or the cooling circuit with the IHX and PWC components. The nominal irradiation period of the first core fuel of the HTTR is 660 equivalent full power days (efpd). Although the final HTTR operation plan has not decided yet, one way of operation has been investigated in detail based on the so-called "standard HTTR operation plan" [Saito 1994]. In this option, the reactor is in the "rated operation" mode during the periods of 0 - 220 efpd and 330 - 660 efpd, and in the "high-temperature operation" mode during the period of 220 - 330 efpd. With respect to process heat utilization, i.e., the simultaneous load, HT test operation is the relevant operational mode.

2.4.1.2. Operating Conditions

Primary Helium Cooling System

During the normal operation of the HTTR, the helium coolant enters the core from the top with a nominal temperature of 395 °C and flows downward through the annular gap (3.5 mm) between fuel rods and bore holes of the fuel assemblies. The average outlet coolant temperature is 850 °C at rated operation and 950 °C at HT test operation. The minimum effective coolant mass flow rate is 88 % of the total flow rate which is 12.4 kg/s at rated operation and 10.2 kg/s at HT test operation. Adequate mass flow is maintained by controlling the speed of the PGC. The helium temperature is primarily controlled by the reactor power output, not by the coolant flow rate. Thus the gas outlet temperature generally goes linear with the power output. In the simultaneous load operation, two thirds of the primary helium enter the primary PWC, while the remaining part of the coolant passes through the IHX. The primary helium pressure is kept at 4.04 MPa at the inlet of the RPV and it is 3.9 MPa at the reactor outlet. The design limit is fixed at 4.7 MPa.

The nominal maximum fuel temperature during normal operation with a coolant outlet temperature of 950 °C is 1290 °C. The respective figure during the "rated operation", i.e., for the lower coolant outlet temperature, is 1150 °C. Taking an uncertainty range (hot spot factor) into account, the result is a maximum fuel temperature of 1360 °C at rated operation and 1492 °C at HT test operation. The average core fuel burnup at the end of its lifetime is 22 GWd/t; the maximum value is 31.5 GWd/t remaining below the design limit of 33 GWd/t. The maximum burnup will be expected in the 2^{nd} layer of the active core. The averaged fast neutron fluence at the end of its lifetime to which the fuel is exposed, is $1.3*10^{25}$ m^{-2}. Maximum fast neutron fluence will also appear in the 2^{nd} layer of the active core.

Secondary Helium Cooling System

The secondary helium temperature is strongly dependent upon the operating conditions of the pressurized water cooling system. Under nominal conditions, the secondary helium is heated up to 870 °C. The heated helium is cooled to 237 °C by the secondary PWC. If the heat utilization system is connected to the HTTR, the flow rate of secondary helium is reduced to increase the outlet helium temperature at the IHX to 905 °C.

During normal operating, the helium pressure in the secondary circuit is always kept at a pressure 0.074 MPa higher than the primary helium pressure. The pressure control is achieved by the secondary helium storage and supply system via the secondary helium purification system.

Pressurized Water Cooling System

At rated power operation, the pressurized water temperature increases to 40 °C by passing through the primary and secondary PWC. After mixing, the water enters the air cooler which is mounted on the roof of the reactor building. As the atmospheric temperature varies, the water flow rate through the air cooler is adjusted to maintain a heat-transferring rate of 30 MW with a flow rate control valve at the inlet of the air cooler. The atmospheric temperature may range between around 30 °C in summer time and around -15 °C in winter time. Since the total flow rate is required to be maintained at 618 t/h, a bypass line is provided to the remainder at the air cooler. The water pressure is kept at constant 3.5 MPa. The water pressure control is achieved by a supply or discharge of nitrogen gas to the pressurizer.

2.4.1.3. Procedures for Safe Operation

An essential feature of HTGRs is the role of the coated fuel particle acting as a tiny containment serving the principal barrier against radionuclide release under operational and accident condition. For a safe operation of the HTTR, among other measures, the continuous and reliable measurement of the coolant activity is required to allow for an evaluation of the fuel performance and for the radiological assessment of the plant during normal operation conditions. It is at the same time a judgment on the quality of the fuel in the core including a check against the specification limits guaranteed by the manufacturer. In addition, the (stationary) coolant activity represents the starting release level during any abnormal event with a total loss of coolant.

Apart from the fuel coating, further barriers against fission product release into the environment are the RPV and the CV representing a double containment concept, and finally the reactor building.

The service area is maintained at a slightly negative pressure to the atmosphere by an air conditioning system during both normal operation and accident condition. The barriers of the CV and the service area in the reactor building drastically reduce the off-site radiation dose in such an accident as a primary pipe rupture accident.

Safety Requirements

Strict operational limits and conditions are specified to ensure the safe operation of the plant during normal operation as well as during anticipated operational occurrences (AOO) or accidents. The most essential and important safety design criteria for the HTTR are listed in Table 2-11.

Table 2-11: Safety design criteria for normal operation and accidents in the HTTR

Maximum values	Normal operation	Accidents
Fuel temperature [°C]	1495	1600
Temperature of reactor vessel [°C]	395	550
Pressure of reactor coolant [MPa]	4.05	5.75
Temperature of IHX heat transfer tube [°C]	955	1000

The maximum fuel temperature of 1495 °C in normal operation condition is set to meet the allowable design fuel temperature of 1600 °C at severest AOO of quasi-steady overpower operation.

Dimensions of the reactor coolant pressure boundary structures have been specified primarily based on design temperature, design pressure and other associated mechanical loads. These design parameter values include allowances of control system error, system configuration effects and measurement inaccuracies. Service pressure limits stipulated can meet the design requirements in AOO and accidents as follows.

(1) In case of an AOO, the pressure shall be less than 1.1 times the design pressure or the maximum pressure in service.

(2) In case of accidents, the pressure shall be less than 1.2 times the design pressure except for the IHX heat transfer tubes and central hot gas duct.

The IHX structure forming the boundary between primary and secondary helium shall withstand a creep buckling load as the result of an accidental pipe rupture within the secondary helium piping system. This accident is considered the severest to these structures.

Maximum allowable change rates for the reactor coolant temperature under normal operation depend upon the temperatures of the reactor coolant and the metal structures in contact with the coolant. An acceptable stress is limited to the lower level at higher temperatures due to creep

damage on the structures. Based on a parametric analysis on the structural integrity of the IHX hot header and reducer, the maximum allowable change rate for the coolant temperature is limited to 15 °C/h at temperatures ≥ 650 °C.

2.4.2. STEAM REFORMING SYSTEM

2.4.2.1. Basic Features of Steam Reforming Operation

Steam Reforming Process

Steam reforming is the endothermal catalytic conversion of lighter hydrocarbons, e.g., methane or naphtha, by means of steam. This process on a larger scale is usually operated at temperatures of 750 - 900 °C and pressures of 2 - 3 MPa according to the relations

$$C_nH_m + n\ H_2O = (n+m/2)\ H_2 + n\ CO \text{ (endothermal)}$$

$$CH_4 + H_2O = 3\ H_2 + CO \quad - 206 \text{ kJ/mol}$$

$$CH_4 + 2\ H_2O = 4\ H_2 + CO_2 \quad - 165 \text{ kJ/mol}$$

In order to increase the output of hydrogen and to avoid carbon deposition due to the Boudouard reaction, the carbon monoxide is catalytically converted in the exothermal water-gas shift reaction with steam according to

$$CO + H_2O = H_2 + CO_2 \quad + 41 \text{ kJ/mol}$$

For this reaction, excess steam of generally around 300 % is injected to shift the equilibrium towards more CO_2. The yield is a reformer gas composed of H_2, CO, CO_2 plus residual steam and unreformed methane. The quantitative composition is depending on the operating conditions which are being chosen according to the desired synthesis gas applications, e.g., as feedstock in the chemical industries.

A decreasing temperature or increasing pressure lowers the concentration of hydrogen in the equilibrium mixture. Partial pressure conditions of the process gas components for the catalyst zone inside the reformer tubes are given in Table 2-12 [Hada 1994].

Table 2-12: Partial pressure distribution for product gases in the catalyst zone

Gas component	**Partial Pressure [MPa] in catalyst zone**	
	Inlet	**Outlet**
CH_4	0.82	0.28
H_2O	3.42	1.95
H_2	0.13	1.72
CO	0.03	0.27

The gas mixture is purified by passing through special adsorber beds to obtain pure hydrogen. To use the residual methane in the product gas, it may be recycled as feedstock gas.

2.4.2.2. Operating Conditions

Steam Reforming with the HTTR

The process parameters of the HTTR steam reforming system such as temperature, pressure, and flow rate, were shown already in Table 2-7. Although the temperature of secondary helium at outlet of the IHX is 905 °C, it becomes 880 °C at the inlet of steam reformer due to the heat loss from hot gas duct between the IHX and the steam reformer.

The helium flows into the steam reformer at the bottom and then flows upwards outside the catalyst tubes, squeezed by multiple plates of orifice baffles. Finally the helium, which is cooled down to 585 °C, exits and flows to a superheater.

The process feed gas mixture of natural gas and steam, after preheated to 450 °C at a pressure of 4.5 MPa enters the steam reformer at the top and then flows downwards in an annular flow between the walls of outer and inner tube through the catalyst bed, where the methane and other lighter hydrocarbons together with steam are reformed. The reformed gas having reached a maximum temperature of 830 °C, flows then upwards inside the inner tubes transferring at the same time heat to the feed gas and eventually leaving the steam reformer at a temperature of 580 °C and a pressure of 4.1 MPa.

In the HTTR steam reforming system, a steam/methane ratio of 3.5 has been selected. The required steam is about 5160 kg/h at rated conditions so that the thermal energy necessary to generate steam is 3.1 MW. The thermal energy of the product gas at outlet of the steam reformer is only 1.9 MW. Therefore, a steam generator is necessary on the secondary helium loop in order to supply this large amount of thermal energy. The superheater and the steam generator are installed downstream of the steam reformer to generate feed steam for the steam reformer. The required helium temperature at the inlet of the IHX is 160 °C, requiring the addition of a feed water preheater and a helium cooler. In the future HTGR heat application system, the outlet helium gas of steam generator will be returned to the IHX directly.

Startup Operation

The heat demand is drastically increasing when the endothermal chemical reactions start the reforming process. On the nuclear side, the helium temperature is “conventionally” increasing linearly with power output. Because of this mismatch between heat demand and heat supply during startup, an additional heat exchanger component, a so-called heat load controller, with a capacity of 2.8 MW is integrated into the steam reforming system. The controlling is achieved by adjusting the helium flow rate. Fig. 2-13 shows the relationship between nuclear power and helium temperatures during the startup phase [Hada 1994].

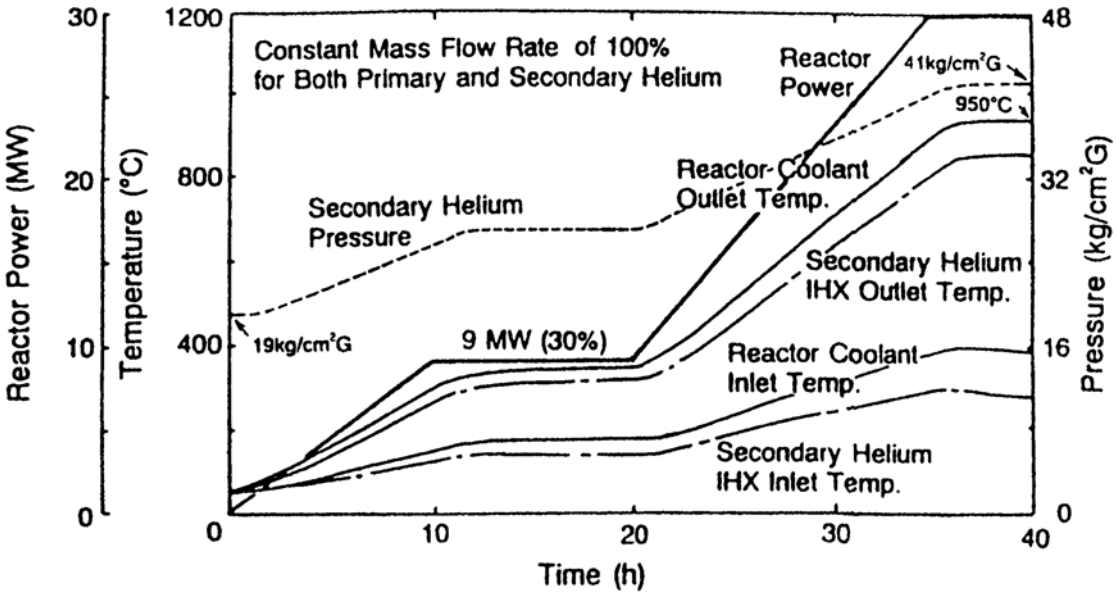

Fig. 2-13: Nuclear power and helium temperature during the startup phase

Safety Requirements

A safety-related issue is the operability of the production process system during a nuclear reactor scram. According to the actual safety regulations, the ultimate heat sink of an NPP is limited to water and/or air, and cannot be electricity or chemical energy as the result of a conversion process. Therefore the production process system is not designed to take over safety functions for the nuclear system; these are exclusively left to the reactor cooling system.

In case of a reactor scram, the power output falls immediately to such a low level that the reactor safely shuts down and remains in a subcritical state. Concerning the steam reforming system, the abrupt cut in heat input is usually followed by an instantaneous disconnection of the feedstock supply and filling of the steam reforming loop with nitrogen to prevent carbon deposition on the catalyst. Also the large heat capacity of the catalyst allows for a reduced rate of temperature decrease [Hada 1994].

Feed Stock and Product Gas Quantities of the HTTR/SR

The flow rate of natural gas as a feed gas is 1290 kg/h and the flow rate of steam is 5160 kg/h at the inlet of the steam reformer. The temperature of the product gas is about 600 °C. This gas is cooled down by the water cooler and separated into steam and dry gas compositions including hydrogen, carbon oxide, carbon dioxide and residual methane in the separator. The pressure and maximum temperature of the process feed gas are 4.5 MPa and 830 °C so that the conversion ratio from methane to hydrogen is expected to be 68 %. As a result, 32 % of methane will remain in the product gas. In the conceptual design of the HTTR/SR, this residual methane is burned in the flare stack together with the other combustible gases.

Steam Generator for Stable Controllability

The operating procedures for startup and shutdown are similar, but reversed. Before startup, nitrogen is supplied at a pressure of 2.2 MPa. The HTTR is then started. When the secondary helium gas is heated to above 500 °C and the steam generator is controlled at the rated pressure of 5.0 MPa, steam is gradually supplied to the system and nitrogen is released into the environment with this steam by switching the flow line. With the steam flow rate constant at rated conditions and the helium gas temperature at the inlet of the steam reformer increased to 700 °C, methane feed gas is supplied to the system. Even during low startup system operation, a stepwise increase in the feed flow rate by 10 % (as it is difficult to control the feed gas at low flow rate levels), results in a stable helium gas temperature level at the inlet of IHX due to the influence of the steam generator. After 60 h, the helium gas temperature reaches 950 °C and the entire system can be operated automatically.

2.5. Flammable Substances

2.5.1. METHANE

2.5.1.1. Physical Properties

Methane (CH_4) is in its gaseous state colorless, odorless, non-toxic, non-acid, and in principle physiologically not dangerous. If inadvertently released it can cause asphyxiation by displacing oxygen in the workplace atmosphere. From the environmental point of view, methane is considered after CO_2 the most relevant greenhouse gas; still it does not have a significant impact to the local environment if accidentally discharged.

Methane gas under normal conditions is lighter than the ambient air and thus tends to rise upon release and mixes with the air by diffusion. Because of its moderate buoyancy and its much smaller diffusion velocity compared with hydrogen, methane is slower in being dispersed down to non-flammable concentrations such that despite its low value for the upper flammability limit the life time of a flammable methane gas cloud is comparatively long.

Liquid methane (LCH_4) vaporizes at 112 K and forms a heavier-than-air vapor tending to layer and settle near the ground. The methane gas temperature has then to increase by approx. 50 degrees, until it becomes positively buoyant in the ambient air. This means that after larger spills of LCH_4, the cold methane gas can form flammable mixtures with air over considerable distances, before it has risen, diffused, and dispersed to non-dangerous concentrations. LCH_4 also requires much more heat per unit volume from the ambient air than hydrogen to vaporize (296 versus 32 MJ/m^3 of liquid).

The vaporization of LCH_4 and heating up to ambient temperatures results in an increase of volume by a factor of 649 and thus in a significant change of the local atmosphere. The spillage of LCH_4 carries an enhanced hazard of asphyxiation because of its rapid vaporization velocity. Particularly in confined areas, it can lead to a reduction of the oxygen concentration down to lethal values. Further physiological hazards are given by cryogenic burning of tissue upon contact with the cold liquid directly or with respectively cold surfaces.

At cryogenic temperatures, changing strength characteristics of container materials are observed; they may become brittle and may fracture under stress.

The storage of methane at very high pressures requires strong storage tanks. The impact on safety issues is given by the fact that in case of inadvertent opening of valves or loosening of fittings, the high pressure gas may create a fire hazard and also metal parts or fragments may be ejected at high speed.

Furthermore the rapid expansion of the methane gas from a high pressure container will result in a significant cooling effect resulting in a vapor cloud of very cold and dense gas. Conventional practice has been to assume that any leak of CNG will rise immediately due to the fact that methane at normal temperatures is lighter than air. Consequently, safety design practices have been focused on ceiling ventilation and detection of methane vapors. In fact, it is highly likely that any significant leakage from storage tanks and transfer lines will migrate down and fill in low lying areas as it is moved about by any wind or circulatory effects. Ultimately, the methane will warm up and rise (assuming a flammable mixture has not come into contact with an ignition source),but it is extremely difficult to estimate the time involved and the configuration of the flammable methane/air mixture during that time period.

2.5.1.2. Chemical Properties

Methane is a highly flammable gas and is violently reactive with oxidizers or halogens. In mixtures with air, it is explosive within the concentration range 4.4 - 16.5 vol% (or 29 - 110 g/m^3, respectively) with the maximum released energy at the stoichiometric mixture of 9.4 vol%. The lower flammability limit, which is the more relevant figure in most accident scenarios (small leakage rates), is in the same range as for hydrogen. The LFL is a function of temperature. It is 7.7 % at the boiling point (112 K) and 2.3 % at 723 K. For methane, the following expression (Burgess-Wheeler law) applies for the temperature range of -155 ^oC to +25 ^oC [Zabetakis 1967]:

$$\text{LFL}\,[\%] = 5.0 - 0.0039\,(T\,[^oC] - 25)$$

The LFL of methane is also increased with lowering the initial mixture temperature. It is approximately 20 %, if the temperature is reduced from ambient by 150 K.

The upper flammability limit is raised to 60 vol% in mixtures with oxygen. A flammability diagram for the system methane-oxygen-nitrogen at atmospheric pressure and 26 °C is given in Fig. 3-18 [Zabetakis 1967]. The range of flammable mixtures is enveloped with the thick lines. Mixture compositions are shifted along the straight lines. Also the special case of air is given in the diagram in Fig. 2-14 indicating the portion of flammable mixtures with methane where it is intersecting the flammability range.

Certain effects are also given with change of the pressure or the addition of an inert gas. Increasing pressure widens the flammability range. The addition of, e.g., CO_2 or N_2 narrows the range until a suppression of flammability is reached at added fractions of 38 % of N_2 or 24 % of CO_2 in the methane-air mixture.

CH_4 burns in a bluish flame to carbon dioxide and water:

$$CH_4 + 2\,O_2 \rightarrow CO_2 + 2\,H_2O - 979.6\ \text{kJ/mol}$$

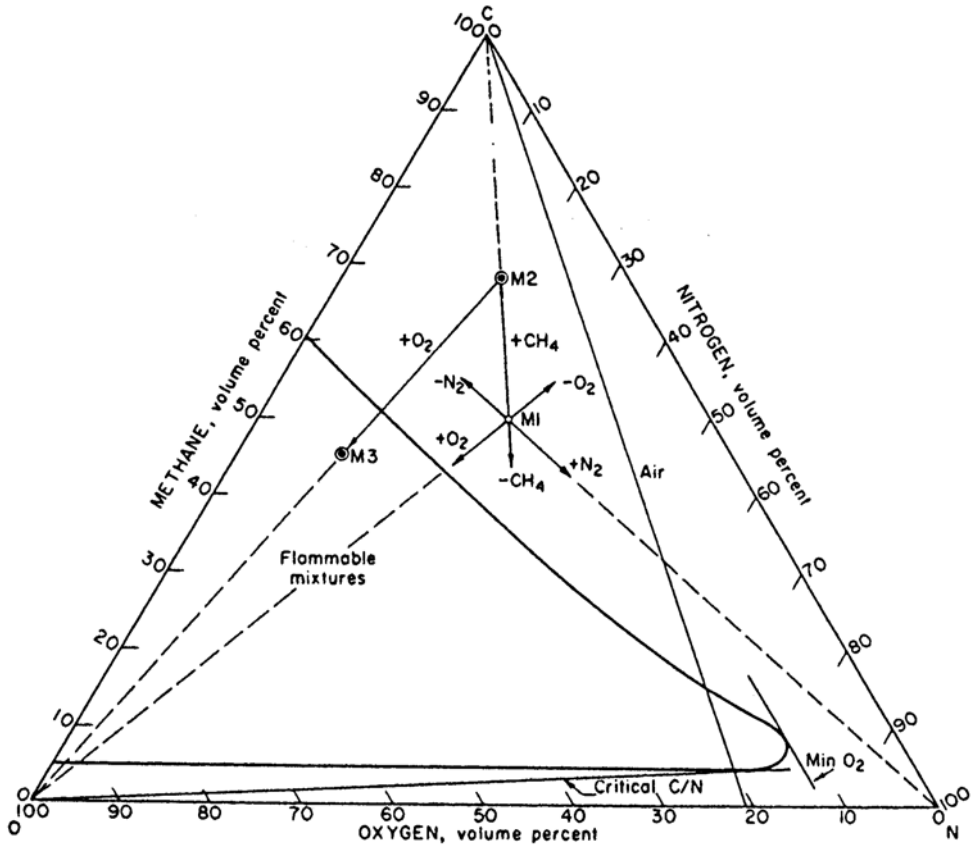

Fig. 2-14: Flammability diagram for methane-oxygen-nitrogen mixtures

The autoignition temperature is 813 K. The minimum energy required to ignite a methane-air mixture is with 0.29 mJ very low and most easily reached by common sources of ignition (spark, open flame, static electricity from human body). Furthermore, the minimum ignition energy will decrease with increasing temperatures, pressures, or higher oxygen contents. No flash point (the temperature at which the vapor pressure is such as to reach the LFL concentration in air) nor a fire point (lowest temperature, at which a substance in the open air would continue burning once ignited) are given for methane.

If a free methane gas cloud is evolving after an inadvertent release, the fraction of its thermal energy contents is expected to be not higher than 10 %.

Methane is thermally decomposed at temperatures above 1373 K. At least a fraction of 12 vol% of oxygen is required in a mixture with methane to keep a flame spreading going. The maximum burning velocity in a methane-air mixture at ambient conditions is 0.36 m/s, being about a factor of 9 smaller than for hydrogen; it increases in pure oxygen to 3.9 m/s. The transition from a deflagration to a detonation is thus less easily obtained. Also with respect to the smaller detonation range, the expected probability of a methane detonation is less than for the detonation of a hydrogen-air mixture. Flame speeds in stoichiometric mixtures exhibit strong fluctuations in the range between 400 - 800 m/s.

The quenching distance, i.e., the largest diameter of a tube, through which flame propagation is still suppressed, is 2.16 mm for methane in air compared to only 0.5 mm for hydrogen. Quenching distances are reduced with increasing oxygen contents. Another parameter

experimentally determined is the maximum experimental safe gap (MESG), i.e., the maximum width of a (25 mm long) gap, through which (in ten tries) the flame of an explosion inside a container does not pass to a fluid mixture outside. This value is smaller than the quenching distance because of the increased pressure inside the container due to the ongoing combustion process.

The methane flame at a temperature as high as 2148 K (stoichiometric mixture) causes a much stronger thermal radiation compared with hydrogen due to a less effective absorption by the water vapor in the ambient air and due to the contributions by soot and CO_2 to the emission. This means in principle the demand for larger safety distances compared to hydrogen. The overpressures resulting from deflagrations of equivalent quantities are significantly weaker for methane than for hydrogen.

With respect to gas mixtures, it was shown experimentally that a hydrogen-methane mixture with 10 % H_2 is as reactive as propane, and 40 % of H_2 are needed to make the mixture as reactive as ethylene [Puttock 1995].

In Table 2-13, the safety-relevant characteristic data of methane are listed.

2.5.1.3. Natural Gas

Natural gas is a mixture of gases comprising primarily methane with small amounts of heavier hydrocarbons (ethane, propane, butane, etc.) plus marginal amounts of N_2, O_2, CO_2, H_2S, He, or H_2O with varying shares. The typical range of methane fractions in pipeline natural gas is from 80 to 95 % resulting in considerable variation in its general physical properties. The higher hydrocarbons are in practice the most dangerous substances for a given quantity, because they are able to explode violently in the unconfined condition. The marginal constituents CO_2 and H_2S in connection with the water can have a corrosive effect on the tank material which is increased with pressure.

Natural gas is colorless, tasteless, and relatively non-toxic. The autoignition temperature varies with fuel composition, 450 - 500 °C, and is always lower than for pure methane. The range of flammability for natural gas mixtures with air is somewhat narrowed to 5 - 15 %. The energy required to ignite a natural gas/air mixture is in the range of 0.15 - 0.30 mJ

2.5.1.4. LNG

Liquefied natural gas (LNG) is usually purified during the production process to a desired methane content of > 95 % including the removal of all corrosive constituents. LNG suppliers are even able to provide a highly purified form of LNG known as Refrigerated Liquid Methane (RLM) with a 99 % fraction of methane. The advantages of LNG are the smaller volume and its storability at lower pressures compared to the compressed form. A drawback is its handling at cryogenic temperatures. Another drawback is that LNG cannot be odorized and thus is not detectable in case of small leakages. Therefore it requires intensive monitoring and control.

Table 2-13: Physical and chemical parameters of methane, hydrogen, and carbon monoxide with relevance to safety (from various sources)

Parameter	Methane	Hydrogen	Carbon Monoxide
Molecular weight [g/mol]	16.043	2.01594	28.01
Stoichiometric fraction in air [vol%]	9.48	29.53	29.53
Boiling point [K]	111.632	20.268	81.7
Melting point [K]	90.7	13.8	74.2
Density of liquid @ boiling point [kg/m^3]	422.5	70.78	788.6
Density of gas @ boiling point [kg/m^3]	1.82	1.338	4.355
Density @ STP [1)] [kg/m^3]	0.71740	0.08990	1.25
Expansion ratio liquid/ambient	649	845	700
Diffusion coefficient @ STP[1)][m^2/s]	$0.16*10^{-4}$	$0.61*10^{-4}$	
Diffusion velocity [m/s]	< 0.0051	< 0.02	
Buoyant velocity [m/s]	0.8 - 6	1.2 - 9	
Heat of vaporization [kJ/kg]	509.9	445.6	215.2
Vaporization index [K cm^3/J] [2)]	0.87	8.9	
Flammability limits in air [vol%]	5.3 - 15.0 [3) 6)]	4.0 - 75.0 [6)]	12.5 – 74.2
Detonability limits in air [vol%]	6.3 - 13.5	18.3 - 59.0 [4)]	-
Minimum ignition energy [mJ]	0.29	0.019	
Auto-ignition temperature in air [K]	903 - 1493 (810)	793 - 1023 (833)	878
Flash point [K]	-	-	-
Gross heat of combustion [kJ/mol] @ 15 °C	891.5	286.1	282.9
Net heat of combustion [kJ/mol] @ 15 °C	803.3	241.7	282.9
Laminar burning velocity in air [m/s]	0.37 - 0.45	2.65 - 3.25	0.33
Flame front velocity [m/s]	3.2	18.6	0.52
Quenching distance [mm]	2.03	0.64	-
Maximum experimental safe gap [mm]	1.2	0.08	
Adiabatic flame temperature [K]	2148	2318	2370
Detonation velocity [m/s]	1390 - 1640	1480 - 2150	-
CJ velocity [m/s]	1801	1968	-
CJ detonation pressure ratio	17.2	15.6	-
Energy release [MJ/kg mixture]	2.31	2.82	
Detonation cell size [mm]	250 - 310	15	-
Critical tube diameter [m]	-	0.2	
Detonation initiation energy [g tetryl]	22,000 [5)]	1.1	-
Critical explosion diameter [m]	4.0	0.16	
TNT equivalent [g TNT/g]	11.1	26.5	

1) STP (Standard temperature and pressure): 273 K, 101325 Pa.

2) Indicates the relative ease of a substance to vaporize.

3) Other authors give a range of 4.4 - 16.5 vol%. It is 5 - 61 vol% in oxygen.

4) Valid for weak ignition. For a high-energy igniter, a range of 11.6 - 74.9 is given in [Stamps 1991].

5) According to prediction in [Bull 1976] (see also chapter 5.2.2.)

6) LFL are valid for upward propagation of flame. For downward propagation, LFL values are 5.9 vol% for methane and 5.3 vol% for hydrogen.

Constant vaporization of LNG results in a so-called ‘ageing’ or ‘weathering’ effect. The methane in the fuel will boil off before some of the other hydrocarbon components such as propane and butane. Therefore, if LNG is stored over an extensive period of time without withdrawal and replenishment, the methane content will continuously decrease and the actual physical characteristics of the fuel will change to some extent. If the methane fraction drops below 40 %, it turns into an explosive mixture leading to a vapor explosion upon contact with water. This hazard, however, can be almost excluded, since more than 90 % of the initial volume would have to be boiled off until the explosive condition is reached.

Even with highly insulated tanks, there will always be a continuous build up of internal pressure and a need to eventually use the fuel vapor or safely vent it to the atmosphere. When transferring LNG, considerable care has to be taken to cool down the transfer lines in order to avoid excessive amounts of vapor from being formed.

Another consideration is that under low temperatures, many materials undergo changes in their strength characteristics making them potentially unsafe for their intended use. Materials such as carbon steel lose ductility at low temperature, and materials such as rubber and some plastics have a drastically reduced ductility and impact strength.

An explosion of an LNG container is a highly unlikely event that is possible only if the pressure relief equipment or system fails completely or if there is some combination of an unusually high vaporization rate (due to loss of insulation) and some obstruction of the venting and pressure relief system preventing adequate vapor flow from the inner pressure vessel with a resultant pressure build up. If the pressure builds up to the point where the vessel bursts, the resulting explosion is known as a BLEVE (boiling liquid expanding vapor explosion) with the container pieces propelled outward at a very high velocity. This is a highly unlikely event due to the extensive requirements for pressure relief including pressure relief valves and burst discs that are built into the design codes. No report in the literature is known of any BLEVE occurring with LNG.

In the event that the LNG vessel is ruptured in a transport accident and the LNG is spilled, there will be a high probability of a fire because a flammable natural gas vapor/air mixture will be formed immediately in the vicinity of the LNG pool. In an accident situation, there is a high likelihood of ignition sources due to either electrical sparking, hot surface, or possibly a fuel fire created from the tanker truck engine fuel or other vehicles involved in the accident. The vapor cloud from an LNG pool will be denser than the ambient air; therefore, it will tend to flow along the ground surface, dispersed by any prevailing winds.

When spilled along the ground or any other warm surface, LNG boils quickly and vaporizes. A high volume spill will cause a pool of LNG to accumulate and the boiling rate will decrease from an initial high value to a low value as the ground under the pool cools. The heat release rate from an LNG pool fire will be approximately 60% greater than that of a gasoline pool fire of equivalent size.

A safety hazard connected with LNG is the potential exposure of personnel to cryogenic temperatures. Workers can receive cryogenic burns from direct body contact with cryogenic liquids, metals, and cold gas. Exposure to LNG or direct contact with metal at cryogenic temperatures can damage skin tissue more rapidly than when exposed to vapor. It is also possible for personnel to move away from the cold gas before injury.

The risk of cryogenic burns through accidental exposure can be reduced by the use of appropriate protective clothing. Depending upon the risk of exposure, this protection can range from loose fitting fire resistant gloves and full face shields to special extra protection multi-layer clothing.

Another unusual hazard associated with aged LNG will arise in the unlikely event that there is a large spill of LNG onto a body of water. This could occur in an accident situation involving an LNG transport vehicle container rupture and spill into an adjacent water body. The hazard is known as a rapid-phase transition (RPT) – in this case a rapid transformation from the liquid phase to vapor. If significant vaporization occurs in a short time period, the process can, and usually does, resemble an explosion.

The RPT "explosion" phenomenon for LNG on water has been observed in a number of situations and has been studied extensively in both laboratory and large scale tests. The temperature of the water and the actual composition of the LNG are important factors in determining whether an RPT will take place. It should also be noted that RPTs have been obtained for pure liquefied propane with water temperature in the range of 55 °C.

2.5.1.5. Gas Mixtures

With respect to gas mixtures, it was shown experimentally that a hydrogen-methane mixture with 10 % H_2 is as reactive as propane, and 40 % of H_2 are needed to make the mixture as reactive as ethylene [Puttock 1995].

2.5.1.6. Methane in the HTTR/SR System

The 400 m^3 of LNG or 169 t of methane (to make it simple) take in its gaseous state under normal conditions of temperature and pressure a volume of $2.5*10^5$ m^3 or in a stoichiometric mixture with air a volume of $2.7*10^6$ m^3. This volume is equivalent to a spherical gas cloud with 170 m diameter or a hemispherical gas cloud with 212 m diameter. The total quantity of methane carries the explosion potential of 1859 tons of TNT.

2.5.2. HYDROGEN

Hydrogen (H_2) has been applied since long time in the chemical industries in various kinds of processes. Comprehensive operating experience in handling hydrogen has been gathered, also with respect to safety aspects.

2.5.2.1. Physical Properties

Hydrogen in its gaseous state is colorless, odorless, tasteless, non-toxic, non-acid, and in principle physiologically not dangerous. The energy density of hydrogen is very high so that 1 kg of hydrogen contains approximately 2.5 times more energy than 1 kg of natural gas. One of its most important characteristics is its low density, which makes it necessary for any practical applications to either compress the hydrogen or liquefy it. It is positively buoyant above a temperature of 22 K, i.e., over (almost) the whole temperature range of its gaseous state. Due to

its high diffusivity, it rapidly mixes with the ambient air upon release. Corresponding diffusion rates of H_2 in air are larger by about a factor of 4 compared to those of air in air. This is a positive safety effect in unconfined areas, but can cause a hazardous situation in (partially) confined spaces, where the H_2 can accumulate, e.g., underneath a roof.

Because of its small molecular weight and its low viscosity, H_2 can cause a problem with respect to leakages. Diffusion in small amount is even possible through intact materials, in particular organic materials. This holds for both gaseous and liquid state. Leakage rates are by a factor of 50 higher than for water and by a factor of 10 compared to nitrogen. At elevated temperatures and pressures, hydrogen attacks mild steels severely, causing decarburization and embrittlement. This is a serious concern in any situation involving storage or transfer of hydrogen gas under pressure. Proper material selection, e.g., special alloy steels, and technology is available to prevent embrittlement.

Hydrogen coexists in two different forms, ortho and para hydrogen, whose partition is dependent on the temperature. Normal hydrogen at room temperature is 75 % ortho and 25 % para. In the lower temperature range < 80 K, para H_2 is the more stable form. At 20 K, the thermal equilibrium concentrations are 99.825 % para and 0.175 % ortho. The rate of equilibrium between ortho and para states is slow in the gas phase. The proton spin state has to flip from 1 to 0, which is intrinsically triggered by the collision between two ortho molecules. The intrinsic rate of conversion is 0.0114 h^{-1}. The transition takes place over a longer period (about 3 - 4 days), until a new equilibrium state is reached. However, magnetic impurities and also small oxygen concentrations are able to catalyze ortho-para conversions raising the rate by several orders of magnitude (very good: $Fe(OH)_3$) to the order of hours. The presence of a radiation field results in the generation of free hydrogen atoms and ions, which act as catalysts also before recombining. The recombination on the other hand produces excess ortho hydrogen. There will be therefore a balance between recombination and all catalytic processes with the latter assumed to be dominant.

The heat liberated during the ortho-para conversion at 20 K is huge with 670 kJ/kg compared to a figure of 446 kJ/kg for the latent heat of vaporization at the same temperature. This represents a safety issue requiring a design of the hydrogen loop which is able to remove the heat of conversion in a safe manner.

Hydrogen also exhibits a positive Thompson-Joule effect at temperatures > 200 K. It means that the temperature increases upon a decrease in the pressure which may lead to ignition. For example, the temperature change is 6 degrees, if a sudden depressurization from 20 MPa to ambient pressure takes place. The chance of a spontaneous ignition just by that effect is small, however, an explosion is likely to occur because of electrostatic charging of dust particles during the depressurization.

2.5.2.2. Chemical Properties

In connection with oxygen, hydrogen is highly flammable over a wide range of concentrations. As a fuel it represents a clean, environmentally benign energy source with a high energy content. It burns in a non-luminous hot flame to water vapor liberating the chemically bound energy as heat. A stoichiometric H_2-air mixture contains 29.5 vol% of hydrogen. The flammability range is between 4 and 75 vol% of concentration in air and up to 95 vol% in oxygen. The LFL

decreases with higher temperatures, e.g., 7.7 % at the boiling point and 2.3 vol% at 723 K. In most accident situations, the LFL is the pertinent parameter.

The potential for an explosion or detonation of a flammable hydrogen-air mixture is very high. The auto-ignition temperature of 858 K is relatively high, but can be lowered by catalytic surfaces. The minimum ignition energy is with 0.02 mJ very low, much lower than for hydrocarbon-air mixtures. A weak spark or the electrostatic discharge by a person would suffice for an ignition; this is, however, no different from other burnable gases. The minimum ignition energy is even decreasing with increasing temperature, pressure, or oxygen contents.

The thermal radiation emitted from a H_2 flame is very low due to absorption by ambient water vapor ($\varepsilon = 0.1$) unlike other gases. Therefore, despite its high flame temperature (max. 2403 K), the burning hazard is comparatively small. The major problem is given in the non-visibility even in a dark room (unless impurities in the air are present), and therefore difficult to recognize and localize. Hydrogen has no flash point.

The combustion product of hydrogen is water vapor:

$$H_2 + 0.5\ O_2 \rightarrow H_2O - 292.5\ kJ/mol$$

It is known from the experience that a hydrogen-air gas cloud evolving from the inadvertent release of H_2 upon the failure of a storage tank or a pipeline liberates only a small portion of its thermal energy contents in case of an explosion, which is in the range between 0.1 and 10 %, in most cases < 1 %.

The explosion of an H_2-air mixture cloud results in the formation of a pressure wave, which is different dependent on the combustion mode. In the deflagration of a free H_2-air gas cloud, the maximum overpressure is in the order of 10 kPa. An overpressure of 7 kPa is still deemed not dangerous; at 7 kPa, people would fall down to the ground; at 35 kPa, damage of ear drums is expected; 240 kPa is considered a threshold value above which fatalities must be taken into account.

The maximum burning velocity of H_2 in air at ambient conditions is 3.2 m/s, which increases to 11.75 m/s in pure oxygen. Compared to other hydrocarbon fuel-air mixtures, it is highest for hydrogen because of its fast chemical kinetics and high diffusivity. This comparatively high value results in a greater chance for a transition from deflagration to detonation (DDT). The detonability range is usually given to be 18 - 59 vol% of H_2 concentration, however, the range was found to be depending on the system size. In the Russian detonation test facility RUT, the largest of its kind, a lower detonability limit of as low as 12.5 vol% has been observed. The detonation velocity reaches values in the range of 2000 m/s; in pure oxygen, it is up to 3500 m/s.

The critical tube diameter is the minimum diameter required for a detonation wave to emerge from a tube and become a detonation in an unconfined cloud. It is a measure of minimum dimensions of an unconfined detonable cloud and is usually in the range of 10 - 30 detonation cell widths. The detonation initiation energy is the minimum energy necessary to initiate a spherical detonation wave; the energy content of tetryl corresponds to 4.3 MJ/kg.

The safety-relevant characteristic data of hydrogen are also summarized in Table 2-13.

2.5.2.3. Basic Considerations on Hydrogen Systems Safety

Primary goal is the safe use of hydrogen and the control of the risks associated with its use. Inherent in all hydrogen designs are:

1. Considerations for the conditions in which the system is operated;
2. Failsafe operation, that accounts for the potential modes of failure;
3. Long-term plans which cover the operational life of the system.

Primary hazards associated with hydrogen systems are combustion, pressure, low temperature, hydrogen embrittlement, exposure.

Quantities greater than 7.500 m^3 under standard conditions are usually located outside or in specially designed structures. Storage vessels that contain liquid hydrogen use special insulation or vacuum jacketing. Vacuum must be maintained with vacuum pumps.

The most common mechanical components for controlling the flow of hydrogen are valves, check valves, and regulators. These may be manual or remotely controlled using electric or pneumatic actuators, which must be ex-proof designed. Check valves are used to prevent unwanted back flow. Regulators control the system pressure. Controls also include fluid sensors such as pressure gauges, flow meters, liquid level indicators, and the control system.

Vessels and piping that confine or potentially may confine hydrogen should be protected against over-pressurization with a pressure relief system. The relief system typically uses relief valves and rupture disks to direct overly pressurized hydrogen to the vent system. Rupture disks are usually used in parallel with relief valves as a failsafe path for over-pressurization. Outside the hydrogen containing system, the control system may monitor for gas or fire. Hydrogen detectors are typically placed above a likely leak point, where hydrogen may accumulate, and at the intake of ventilation ducts. Infrared cameras can image heat over a wide field of view. Ultraviolet detection is used to specifically detect hydrogen flame.

Hydrogen systems may use catalytic converters and getters to remove unwanted or excess hydrogen. Filters may be used to remove impurities from hydrogen in the system

In a risk assessment, a systematic approach is made to identify risk factors and potential hazards, to determine frequencies of abnormal event scenarios, to quantify consequences as well as to evaluate mitigation measures to control or minimize the risk. Risk management measures are, e.g.,

- efficient leak / fire detection, isolation and shutdown systems;
- efficient natural ventilation;
- safety valves and ventilation to safe locations;
- grounding;
- safety distances, fire walls.

2.5.3. PROCESS GASES

2.5.3.1. Carbon Monoxide

Carbon monoxide is a colorless, tasteless, odorless, but highly toxic and flammable gas and requires special precautions in handling and storage. Its toxicity in humans and animals is caused by the extraordinary affinity for haemoglobin (210-240 times greater than that of oxygen), which is responsible for the O_2 transport in blood. If inhaled for a sufficient period of time, it results in unconsciousness and death at higher levels. An atmosphere containing 0.2 % of CO is lethal after about 2 hours. It is a chemical asphyxiant with a recommended threshold limit of 0.01 % in air.

CO is not corrosive and not an irritant; it is rapidly oxidized to form CO_2. CO is slightly lighter than air at ambient conditions. CO is an unwanted byproduct of all oxygen-undersaturated combustion processes involving carbon.

A pure (dry) CO-air mixture does not burn at STP, but at presence of small amounts of H_2O or H_2, it can significantly enhance the rate of CO oxidation reactions. CO burns in air with a non-luminous bluish flame. The flammability range is 12.5 - 74 vol% in air and 15 - 94 vol% in oxygen; it widens with increasing temperatures. A CO mixture with air does not detonate. In a mixture with oxygen, the detonation range is 38 - 90 vol%. The maximum detonation velocity in oxygen is around 2800 m/s. At high pressures, CO reacts with steel to produce small quantities of iron carbonyl.

In Table 2-13, the safety-relevant characteristic data of carbon monoxide are summarized.

2.5.3.2. Carbon Dioxide

Carbon dioxide is an inert, colorless, odorless gas. It is non-toxic at physiological concentrations, turns to become narcotic above 5 %, results in unconsciousness at levels of 7 - 10 % after a few minutes; the recommended threshold limit for an 8-hour day is 0.5 %. CO_2 is universally present in fires. It is also present at an approx. 5 % concentration in exhaled air. CO_2 is heavier than air and therefore tends to flows into low-lying areas.

2.5.3.3. Process Gas Mixtures

Information on flammability ranges of mixtures of CO, water gas, inert gas (He, H_2, H_2O) and air as a function of pressure and temperature as well as the maximum allowable fuel content and the maximum inert gas content has been gained from experiments within the PNP safety program. Flame extinguishing effect was observed to be in the order H_2O > He > N_2. The mixture relation according to the Le Chatelier Rule

$$1/L_{mixture} = \Sigma (y_i/L_i)$$

where y_i is the volume fraction and L_i the flammability limit of fuel i

was found to be in good agreement with experimental data and can therefore be used for calculating flammability ranges of any mixture [Kumar 2000]. The effect of an addition of H_2O on the flammability limits has not been verified so far, but it will presumably not be significantly different from CO_2 or N_2. The influence of graphite dust on the flammability range

still needs to be examined.

The addition of CO to an H_2-air mixture increases the detonation sensitivity of the mixture. The lean limit of H_2 decreases, if CO concentration increases. The addition of 1.2 vol% CO to an H_2-air mixture means a reduction of the LFL from 4 to 3.6 vol%; the addition of 6 % CO requires only 2 % H_2 to become flammable. A mixture of CO and H_2 will have a flammability limit lower than that of either fuel [Kumar 2000].

Not much information is available on the autoignition behavior of CO-H_2 mixtures. The autoignition temperature of CO drastically decreases with the addition of small amounts of H_2 or moisture. Also on burning velocities, only little data have been gained for both H_2-CO and H_2-CO-steam mixtures in air [Kumar 2000].

Extensive measurements of laminar flame front velocities of H_2-CH_4 mixtures have been conducted at the University of Erlangen [Uni.Erlangen 1981]. Some results for hydrogen, methane and different mixtures of these fuels are summarized in Fig. 2-15. Flame spreading in process gas mixtures considered was discovered to be depending on the location of ignition. For homogeneous CO-air mixtures, flammability limits and maximum pressures were independent of the location of ignition.

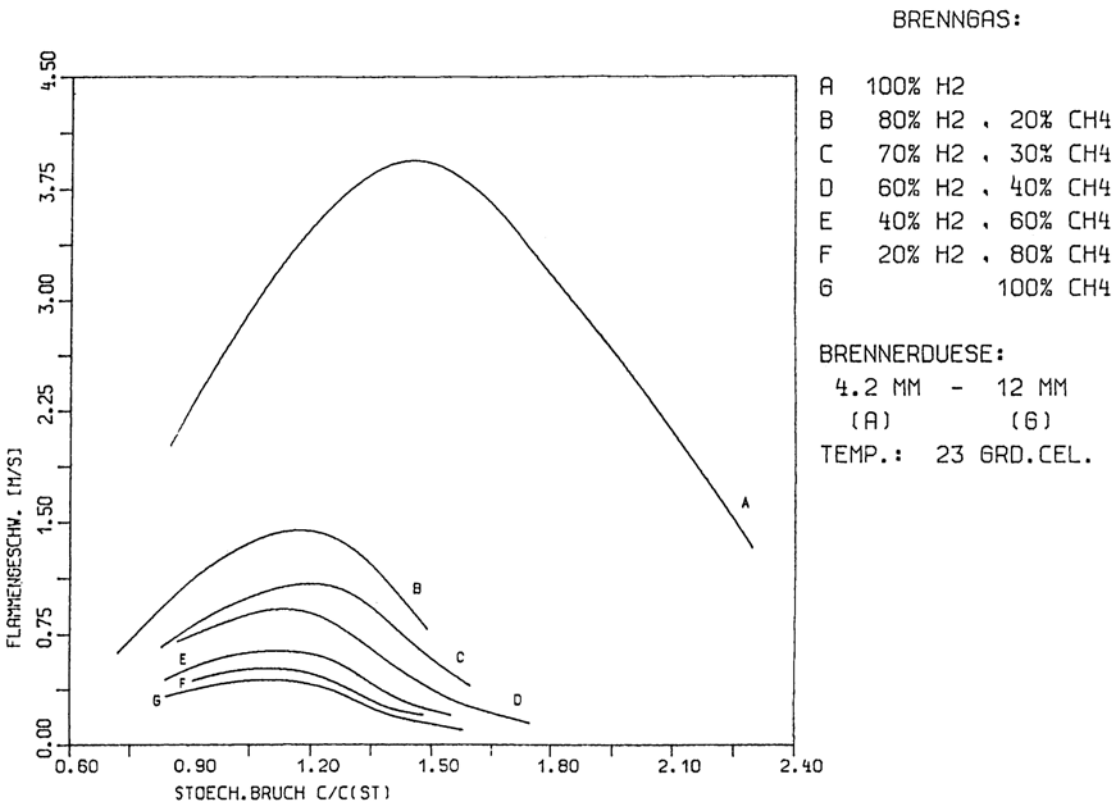

Fig. 2-15: Flame front velocities for hydrogen-methane mixtures

In case of accidents, the process gases are mostly light and hot and tend to rise immediately and do not form free explosive gas clouds. However, increase turbulence. Various inert components in the gas mixture strongly reduce the chance of an ignition or reduce flame speed and overpressure.

Process gas mixtures of coal gasification plants are usually composed of the fuel components CH_4, CO, H_2, C_2H_6, and the inert gas components CO_2, N_2, and water vapor under certain pressure and temperature conditions.

An undesired reaction within the reforming process is the decomposition of carbon monoxide with the formation of carbon

$$2\,CO \rightarrow C + CO_2$$

which is enhanced with decreasing temperatures.

2.5.3.4. HTTR/SR System

The thermal equilibrium composition of the product gas mixture can be calculated from the thermal dynamics. It is strongly dependent on the process parameters temperature, pressure, and steam-methane ratio. An example composition is given in Fig. 2-16 as a function of the process temperature for a H_2O over CH_4 ratio of 2 and a typical process heat HTGR system pressure of 4 MPa. The result shows a complete methane conversion with maximum hydrogen output at process temperatures beyond 1150 °C [Boltendahl 1980].

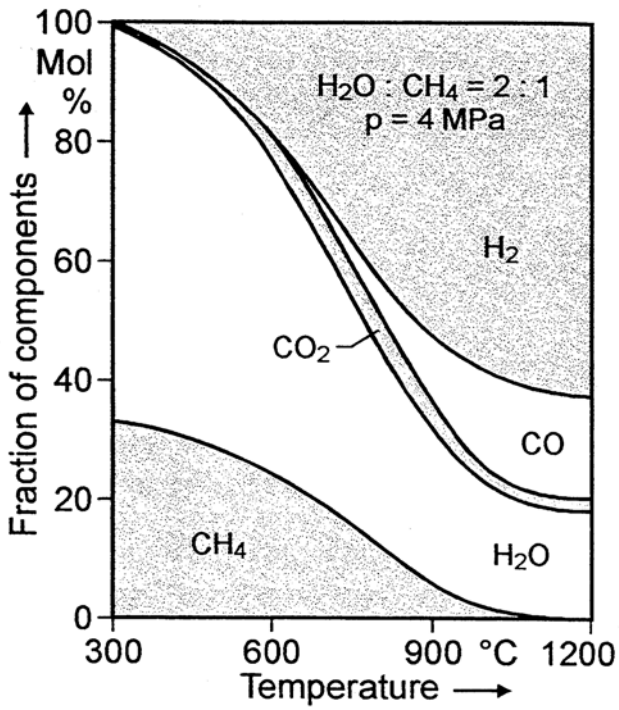

Fig. 2-16: Calculated equilibrium process gas as a function of the temperature

3. STATUS OF KNOWLEDGE ON THE BEHAVIOR OF LIQUEFIED GASES UNDER ACCIDENT CONDITIONS

Liquefied Natural Gas (LNG) has become one of the most important energy carriers that are being commercially provided worldwide since several decades. With increasing transportation of LNG to the customer countries, both in number of shipments and in quantity of cargo of a ship, a major concern was seen in the increased probability of an accidental release representing a significant societal risk. LNG is usually carried in ship tanks of 75,000 - 125,000 m^3 capacity. In the early 1970s, comprehensive efforts have started to investigate the safety and risk of large-scale transportation of liquefied gases both in terms of experimental work and in terms of simulation tools development.

3.1. Phenomenology of Flammable Gas Release and Combustion Behavior

Many different situations are conceivable, which can give rise to the emission of a flammable substance and which have great influence on the evolution of a vapor cloud. It can be released as a liquid or a gas or a two-phase mixture. The component, from which the substance is released, may be a tank, a pump, a valve, pipe work or other equipment. The orifice, through which it is leaking, can vary over different shapes and sizes. The leaking fluid can flow into different geometries. And finally it is the thermodynamic conditions of the fluid, which determine its release behavior.

3.1.1. SPILL OF LIQUEFIED GAS

Liquefied gases are characterized by a boiling point well below the ambient temperature. If released from a pressure vessel, the pressure relief from system to atmospheric pressure results in spontaneous (flash) vaporization of a certain fraction of the liquid. Depending on leak location and thermodynamic state of the cryogen (pressure expelling the cryogen through the leak is equal to the saturation vapor pressure), a two-phase flow will develop, significantly reducing the mass released. It is connected with the formation of aerosols, which vaporize in the air without touching the ground. Conditions and configuration of the source determine features such as release height, initial plume distribution, dimensions of evolving vapor cloud, cloud composition, or energy balance. A safety problem in connection with a cryogenic spill is the development of a local atmosphere, which is depleted of oxygen.

3.1.1.1. Pool Spreading and Vaporization

The release as a liquefied gas usually results in the accumulation and formation of a liquid pool on the ground, which expands, depending on the volume spilled and the release rate, radially away from the releasing point. The pool also immediately starts to vaporize due to the heat input from the ground, the ambient atmosphere (wind, insolation from the sun), and in case of a burning pool, radiation heat from the flame. For gases liquefied at very low temperatures such as LH_2 or LNG, heat transfer from the ground by conduction is dominant. Cooling of the ground

results in a decrease of the heat input. For a constant spill rate, this will lead to a gradually increasing pool size. A growing pool surface area implies an enhanced vaporization rate. After an initial phase, a state is reached which is characterized by the incoming mass to equal the vaporized mass. A cutoff of the mass input eventually results in a breakup of the pool from the central release point creating an inner pool front. The ring-shaped pool then recedes from both sides until it has completely died away.

An additional significant influence on the pool spreading and vaporization behavior is given, if the pool propagation is limited due to obstruction or, e.g., the walls of an impoundment area. The smaller surface area results in a reduced vapor production rate.

The respective shares of heat input from outside into the pool are depending on the cryogen considered. Table 3-1 lists the data for the cryogens LH_2, LN_2, and LNG assuming a pool of 1 m^2 on a water surface and a wind speed of 5 m/s [Dienhart 1995].

Table 3-1: Sources of heat input into a vaporizing cryogenic liquid pool

Heat input by	**Heat source [kW/m^2]**		
	LH_2	**LN_2**	**LNG**
Atmospheric Convection	0.8	1.8	1.1
Radiation from flame	12	-	100 - 200
Radiation from ambient	1.6	1.6	1.6
Conduction from ground	100	25	9.2

As can be seen from the table, the most dominant heat source is heat transport from the ground. For a burning pool, also the radiation heat from the flame provides a significant contribution. This is particularly true for the burning LNG pool due to a much larger emissivity resulting from the soot formation.

If the cryogen is spilled on a liquid ground, e.g., a water surface, additional phenomena can occur such as a certain penetration of the ground by the cryogen reducing the effective pool height or ice formation. Also so-called rapid phase transitions (RPT) could be observed, which are “physical” vapor explosions resulting from a spontaneous and violent phase change of the fragmented liquid gas at such a high rate that shock waves may be formed. Although the energy release is small compared with a chemical explosion, it was observed for LNG that RPT were able to cause some damage to test facilities.

The vaporization behavior is principally different for solid and liquid grounds. On liquid grounds, the vaporization rate remains approximately constant due to natural convection processes initiated in the liquid, whereas on solid grounds, the rate decreases due to cooling of the ground. The general relationship between the mass vaporization rate per unit area of surface, m, and the time from initial contact, t, is given by:

$$m = B * \Delta T * t^{-1/2}$$

where ΔT is the difference between initial temperature of the ground and the boiling point of the

cryogen. B is a factor comprising the effective thermal properties of the surface, e.g., the impoundment area of a storage tank. Some examples for B values are 0.6 [kg/(m^2 s$^{1/2}$ K)] for soil, 0.58 for standard concrete, 0.14 for light-weight concrete, 0.07 for super-insulating concrete. The maximum vaporization rate on concrete is 0.5 kg/(m^2 s) which is reduced to about 3 % of its value after 20 min [Moorhouse 1988].

For a concrete ground, the following expressions for mass vaporization rates were suggested in [Jenkins 1983]:

for dry concrete:	$m = 0.4 * t^{-0.56}$
for wet concrete:	$m = 1.0 * t^{-0.67}$

showing also the approximate $t^{-1/2}$ dependence. The different behavior on dry and wet concrete can be traced back to different properties of ice and water, the reduced surface area due to immediate sealing of the pores in the concrete by ice, and the release of the solidification enthalpy.

3.1.1.2. Pool Burning

For a burning gas cloud above a ground pool or tank, heat transport from the burning cloud to the pool is given by conduction, convection, and radiation, which enhances the vaporization rate and the pool regression rate, respectively. The regression rate is depending on the pool radius. For small radii, when heat transport by conduction is dominant, the regression rate decreases with increasing radius. For large radii, heat radiation becomes dominant resulting in increasing regression rates for increasing radius. The regression rate v of a pool burning in air under wind-free conditions is given in [Zabetakis 1967]:

$$v = v_o * (1 - \exp(-k*d))$$

where d is the pool diameter and v_o is the regression rate for an indefinite pool, k the opacity coefficient (0.6 - 0.9 ft^{-1} (0.18 - 0.27 m^{-1}) for hydrocarbons) with $v_o = 0.0076\ h_c/h_v$ [cm/min] and h_c as the net heat of combustion and h_v as the sensible heat of vaporization.

Empirical burning rates have been measured for various flammable liquids. Examples are:

LPG:	0.1	kg/(m^2 s)
Gasoline:	0.06	kg/(m^2 s);
Methanol:	0.03	kg/(m^2 s).

The burning rate can be controlled by using adequate dikes and insulation.

LNG pool fires, especially at presence of wind, were observed to be dynamic and non-homogeneous with a somewhat cyclically changing flame height. Since methane is preferably vaporized, the flame is increasingly getting “dirty” (more soot), when more heavier hydrocarbons are burnt. Effects of wind on the flame length are complex. Wind tilts the flame expanding the flame base area and also changing the distribution of radiant heat flux hitting the pool [Battelle 1973].

The extinction of pool fires can generally be done by cooling with water and/or by blanketing with foam. For contained fires, foam is preferable means. Any fire fighting agent is good to extinguish smaller LNG fires. Water was long been considered the prime agent suitable for

controlling LNG; beyond a certain size, however, the quantities of water required turn out to be impracticable. Here it is foam and dry chemicals that appear more appropriate.

3.1.2. EVOLUTION OF FLAMMABLE VAPOR CLOUD

The processes of release and subsequent distribution of a gas are strongly dependent on its thermodynamic state during storage. Pressurized gases form a free jet or will be flash-released, if there is a complete failure of the storage vessel. For cryogenic storage, the substance will be released - depending on the leak location - as a liquid, which starts to vaporize immediately, or as saturated vapor. Parameters of concern are the expansion of a flammable vapor cloud, the height that it could attain, the time until it becomes sufficiently diluted, and the total quantity of fuel in the cloud.

The spreading and dispersion behavior of a gas is strongly dependent on the density difference to the ambient air. In case of the release of a heavier-than-air gas, there is only a poor and slow mixing with air, such that only a part of the gas cloud is within the flammability range; the cloud must be picked up by the ambient flow before it can be carried downstream and diluted. If the source rate is larger than the removal rate, a vapor blanket can accumulate on the ground until a certain size is reached with steady-state conditions.

The initial phase after release of a heavy gas is characterized by a slumping of the gas cloud under gravitation with a behavior similar to a liquid. It shows a spreading behavior which is – at least in the initial phase – independent of the wind direction. It forms a shallow pancake-shaped plume with great resistance to vertical dispersion. The spreading of the heavy gas is further influenced by factors such as surface area, type of ground, thermal effects from the interaction with the ambient atmosphere, which can either enhance or dampen turbulence by buoyancy. Air entrainment from the upper surface and the edges due to atmospheric turbulence eventually results in dilution to effectively neutral density. Top entrainment for heavy gases is significantly smaller than for neutral gases.

Methane at its boiling point (111 K) is heavier than air; small quantities of LNG released tend to rise after a few pool diameters. In contrast, the release of a large amount of LNG within a short period of time will be bound to the ground for a longer time because of only gradual air entrainment from the outside into the vapor cloud. The cold natural gas is thus able to disturb the wind and turbulence profiles in the lower atmospheric boundary layer particularly at low wind speeds diverging around the cold cloud. Under strong wind conditions, the concentrations on the ground are lower than in the air.

Cold gas causes the moisture in the air to condense and make the vapor cloud visible. The presence of droplets, either liquefied gas resulting from the release process or water from the moisture, result in vaporization and condensation processes with removal of heat from or addition of heat to the gas. Low moisture content thus means a larger lifetime of a heavier-than-air gas cloud. LNG clouds remain usually visible beyond the lower flammability limit; the visible edge and the LFL coincide, if the humidity in the ambient air is 50 %.

At presence of obstruction or congestion, downwind distances have been observed to be much reduced compared to open land due to turbulence generation, which leads to a faster dilution. Barriers, however, are less effective at higher wind speeds and for very large spills.

3.1.3. COMBUSTION OF FLAMMABLE VAPOR CLOUD

A fuel-air mixture with either fuel concentrations outside the flammability limits or no ignition source present will dilute and eventually fade away. In an industrial environment, numerous kinds of potential ignition sources are present such as flames, direct heat, hot surfaces, sparks, or static electricity. The most dangerous constellation is the evolution of a premixed state and central ignition. The flame front will propagate through the explosive region at various velocities. The flame speed determines the release rate of combustion energy and the blast wave, which transports the energy into the neighborhood. The combustion process is called an explosion, if it takes place as a spontaneous, exothermal oxidation reaction connected with a strong pressure and temperature increase. The temperature increase and, to a lesser extend, the higher specific volumes of the combustion products generate expansion forces in addition to the buoyancy.

3.1.3.1. Flash Fire

Heat addition to the stored liquid gas causes pressure increase in the storage container (tank, pipe, pump, etc.). Continuous addition could lead to catastrophic failure (BLEVE). Expanding rates are even higher, if the liquid is supersaturated in energy, a situation, which is generally beyond the venting capabilities of relief valves.

If the ignition occurs at an early stage, the result will be a flash fire, where the vapor cloud burns, but does not explode. A diffusive flame develops with a burning rate depending on the air entrainment. Spherical spreading of the flame front takes place in small volumes without any significant flame acceleration. In most cases, the accidental release and ignition of a hydrocarbon-air mixture is expected to start with a slow laminar flame (3 - 4 m/s), concomitant overpressures will be negligible. The fire hazard is then mainly given by thermal radiation or by direct flame impingement damage. One significant hazard to humans is given by a sudden depletion of oxygen.

The type of combustion mostly encountered for unconfined clouds is the fireball. It has been observed to occur from BLEVEs or jet releases. BLEVE is a combination of fire and explosion, exhibiting a sudden and violent release of energy almost exclusively as an intense radiant heat emission. In a fire ball, there is hardly any mixing between fuel and air. The combustion takes place in rich mixtures in a diffusion flame from outside to the inside, connected with the formation of considerable quantities of carbon.

A BLEVE occurs when a pressure vessel with liquid is heated, until the wall loses its strength and ruptures. If the tank contains a flammable material, this may form a vapor cloud upon release and even give rise to a second explosion. In connection with a cryogenic liquid, a rising burning cloud after release and ignition was seen only, when the cryogen was spilled on water, where rapid phase transitions occurred resulting in a largely increased vaporization rate. Although spectacular, BLEVEs do usually not coincide with the generation of a strong pressure wave. Its primary hazard is the heat radiation from the fire ball; other hazards are vessel fragments and overpressure.

3.1.3.2. Unconfined Vapor Cloud Explosion

If the ignition is delayed, a large potentially flammable fuel-air cloud will develop, in which mixing with air has already taken place. Any inhomogeneities in the cloud or disturbances of the flame symmetry, which are always present, make significant flame acceleration possible. This effect is enhanced by obstruction, which creates a higher level of turbulence in the cloud. The combustion will be called an explosion, if the energy is released over a sufficiently short time in a sufficiently small volume, in order to be able to generate a pressure wave.

Fires of combustible vapors will usually develop very quickly. The consequences of a vapor cloud explosion are sensitive to a whole variety of parameters such as type of fuel, size and fuel concentration of the vapor cloud, degree of initial turbulence, location and strength of the ignition source, degree of obstruction, presence of explosion vent areas, mitigation schemes. Depending on flame speed and degree of congestion, a more or less strong pressure wave is generated, which can carry away an up to 60 % fraction of the total combustion energy of the flammable part of the vapor cloud. Flame speed and overpressure tend to increase with increasing scale of the configuration due to increased available time for the development of instabilities and by the effect of self-confinement in larger volumes.

The burning velocity is also an important parameter in terms of flashback, i.e., the effect that a flame travels back to the source, in particular, if the velocity of the leaking gas is small. The travel distance of a cloud is unlikely to be very long in industrial or urban areas.

3.1.3.3. Deflagration

An unconfined vapor cloud explosion (UVCE) belongs to the most serious hazards in the process industries. The most common mode of combustion of a vapor cloud is the deflagration where the flame travels typically at subsonic speed < 1000 m/s. The propagation mechanism is diffusion of the combustion products into the unburnt gas. Overpressures reach values between 0.1 and several 100 kPa. However, the cloud must be very large, if a damaging wave is to be expected. In a very rough classification given in [Baker 1983], a lower limit of 100 kg of fuel under weak ignition conditions is mentioned for methane.

In a deflagration, the combustion process is determined by the flame front velocity, which is typical for the fuel considered. In a spherical flame spreading (see Fig. 3-1), the flame front is pushed forward like a permeable spherical piston building up a stagnation pressure. The increased pressure propagates at sonic speed into the unburnt mixture and further into the neighborhood. When the flame front has reached the cloud boundary, the piston stops. The pressure amplitude is determined by the flame front velocity. The total duration is dependent on the cloud extension.

3.1.3.4. Detonation

In contrast, the detonation is a combustion flame traveling at supersonic speeds in the order of 2000 m/s. The flame front proceeds by shock wave compression of the unburnt gas. The combustion process is completed without any expansion of the gas cloud. Peak overpressures in the near field are typically in the range of 1.5 - 2 MPa.

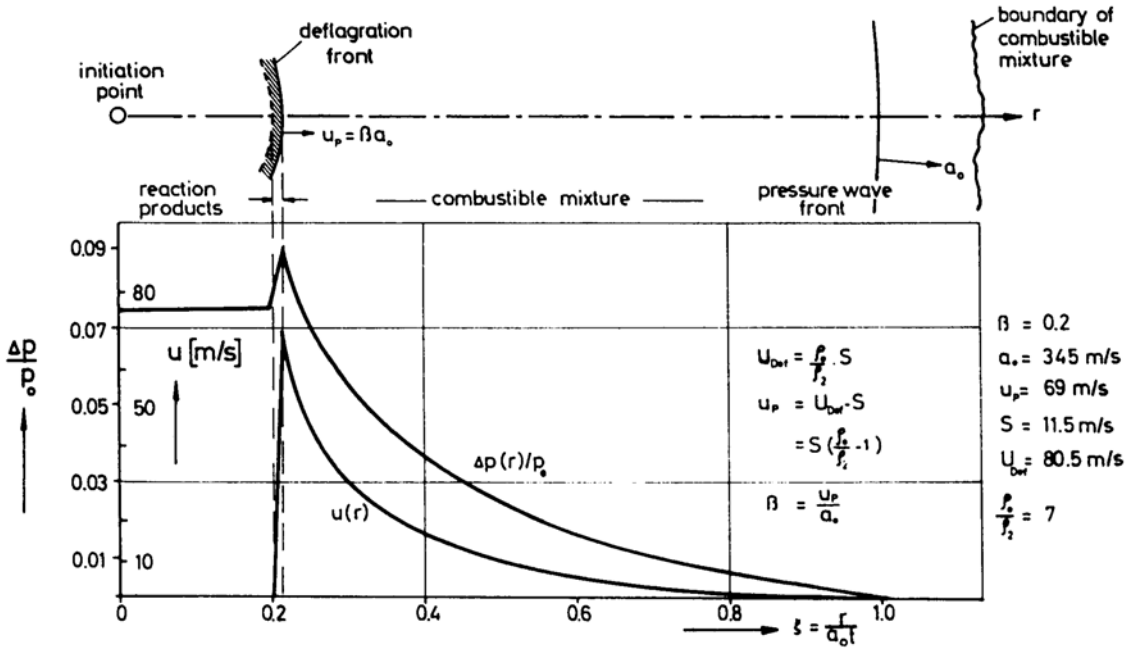

Fig. 3-1: Overpressure and flow velocity distribution for a spherical detonation wave

According to the Chapman-Jouguet (CJ) theory, detonation represents a discontinuity with infinite reaction rate. Detonation velocity and pressure can be calculated from equilibrium chemistry as a function of the gas mixture only. Respective data for hydrogen and methane are given in chapter 2.5.

The direct initiation of a detonation by an explosive is also possible, but very unlikely in a typical industrial area, because the large ignition energies required are usually not available. Experimental results with different fuels including methane are depicted in Fig. 3-2 [Moen 1993].

The transfer of a detonation wave into adjacent mixtures is possible and has been observed for planar clouds, whereas in spherical clouds, fast deflagrations are more likely to occur.

Although not a common occurrence for hydrocarbon-air mixtures under unconfined conditions, detonations cannot be ignored in safety and risk analyses. Processes inside the detonation front are extremely complex involving multi-dimensional shock interactions in an intensive turbulent reacting medium. Still, the simple CJ model prediction of velocity and overpressure is quite close to what is being observed. However, it is not capable of determining the dynamic detonation parameters such as detonability limits, initial energy or critical tube diameter. No theory exists so far that provides estimates of these parameters.

The size of the detonation cell is a measure of the reactivity; the smaller the cell, the more reactive is the mixture (Fig. 3-3). It serves to some extent as an indicator for DDT and can be measured experimentally. Methane with a cell size measured of approx. 330 mm is the least sensitive of the common fuels.

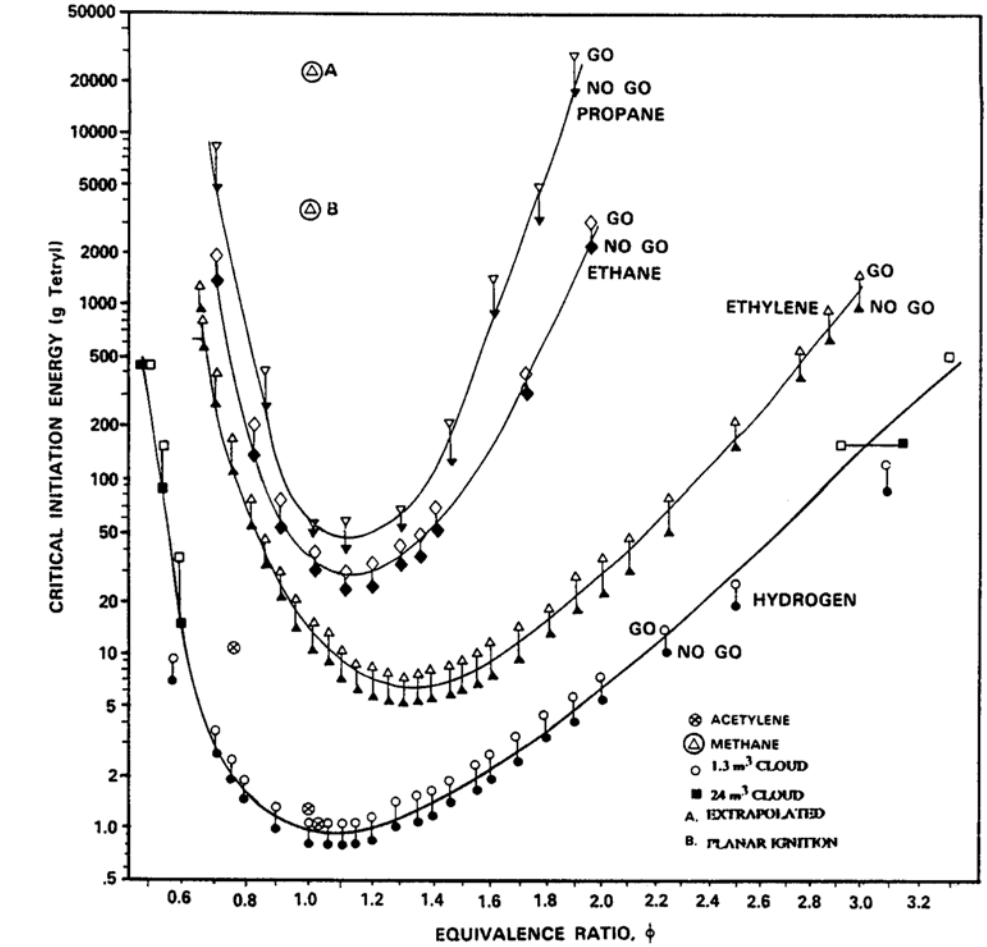

Fig. 3-2: Critical initiation energy for selected fuel-air mixtures

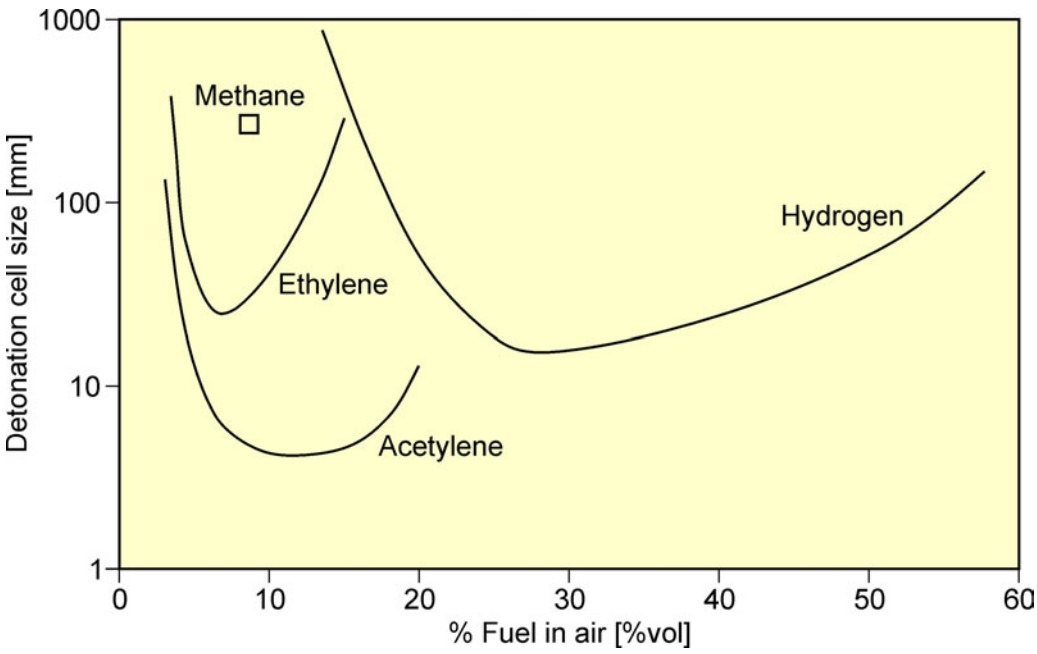

Fig. 3-3: Detonation cell size as a function of fuel-air concentrations

It was in the late 1970s, when the usefulness of measurements of the detonation cell size, λ, was well acknowledged. First step was the finding of a correlation between cell size and critical tube diameter (d=13*λ). This empirical law was the basis to develop a simple surface energy model which allows the derivation of a critical initiation charge weight for various hydrocarbon-air mixtures in pretty good agreement with experimental data.

3.1.3.5. Deflagration-to-Detonation Transition

In partially confined areas which are more typical for a chemical plant, the potential for a transition from deflagration to detonation (DDT) is less than in heavily confined areas. DDT critically depends on the degree of confinement, obstacle configuration, ignition source, initial turbulence and fuel-air mixture [Boni 1977]. In an industrial area with process equipment providing some sort of obstruction, the flame speed may accelerate to several 100 m/s. Flame acceleration is caused by the turbulent flow field, which is generated ahead of the flame front increasing the effective flame area and thus the burning rates (fast deflagration). Under certain conditions, this positive feedback mechanism on flame acceleration can lead to the transition to a detonation (DDT), causing blast damage at a considerable distance outside the vapor cloud. Flame speeds at the onset of a detonation are found to be in the order of 800 m/s.

The DDT is initiated by a local explosion (hot spot) creating a shock wave which is then amplified by some effective mechanism, until autoignition of the area in front of the reaction zone occurs. SWACER, “Shock Wave Amplification by Coherent Energy Release”, appears to be the most viable mechanism for DDT, based on the stimulated release of the chemical energy, which goes synchronous with the shock wave [Chan 1991].

Acceleration Factors

Parameters known to be important for the possible transition to a detonation in an open-air vapor cloud are the fuel gas concentration, atmospheric conditions, flame velocity in the cloud, obstruction, strength of the ignition source. Turbulence plays a central role in all stages of the transition from deflagration to detonation. Flame acceleration results from an increased level of turbulence ahead of the flame. For a complete description of the turbulent flow behavior, important factors are the intensity of turbulence and the scale of turbulence with the intensity to have the more significant influence on flame propagation.

There is a number of more or less turbulent enhancing mechanisms, which might have an effect on the combustion process in a vapor cloud in an industrial area, such as:

- Atmospheric turbulence has a certain influence on the flame speed, but is unlikely to reach levels, where pressure damage will occur.
- Heat radiation transport by dust results in a preheating in isolated dust pockets, which may lead to auto-ignition due to the fact that heat radiation is much faster than the flame speed. It would be a concern in large vapor clouds containing large dust pockets with high dust concentration.
- Local explosions behind the flame front are, e.g., given by the delayed explosion of

gas pockets which, however, must be strong and take place at the “right” moment. They are thus not very likely.

- A flame front interacting with partial obstruction or repeated obstacles results in a high degree of turbulence. Combined with the large temperature change in the vicinity of the combustion front due to the liberated chemical energy, a displacement flow in the ambient mixture is created, whose velocity is in the same order as the propagating flame. Due to the resulting velocity gradients, the flame front will be stretched and folded leading to increasing burning rates (positive feedback).
- A jet ignition seems to be the most effective acceleration mechanism for generating high explosion pressures. A jet of hot products resulting from a confined combustion and relieved through an opening represents a strong ignition source that can lead to increased overpressures in an unconfined cloud and even may result in a detonation.
- Acceleration due to turbulent boundary layer along surface
- Raleigh-Taylor instabilities (pressure wave – flame interaction) result from disturbances at the boundary layer between two fluids of different densities.
- Buoyancy acceleration of the flame may occur above some critical cloud size.
- Acceleration by re-entrant corners or dead ends
- Propagation into confined spaces

The time scale for acceleration must be small compared to the hydrodynamic processes, which relieve the pressure increase. At flame speeds beyond 300 m/s, an additional contribution to the acceleration process is given by a pre-compression of the unburnt gas by the front pressure wave. Upper limit for the flame front velocity is given, when the counteracting effects of an enhanced mixture process and the temperature decrease due to the mixing are in equilibrium.

In tubes, pipes, and confined channels, high flame speeds and pressures are reached within less than four diameters, also for methane-air mixtures. This holds also for an area covered by a roof serving possibly as strong ignition source for external clouds.

The qualitative process of flame acceleration is fairly well understood. On a quantitative basis, however, a-priori predictions of turbulent flame speeds and overpressures are not possible. Main problem is the prediction of the transient turbulent flow field structure ahead of the flame front and of the combustion processes.

Turbulent Burning Velocity

In a free gas cloud, many mechanisms of supporting a detonation do not exist. No gas-oxygen mixture, only mixtures with air can arise; no confinement will prevent outward flow of the combustion products; and no detonative ignition source is usually available. The only possible mechanism might exist in form of a flame front acceleration due to enhanced turbulence. The turbulent flame speed can be described by the relation [Koch 1975]

$$u_{turb} = \varepsilon * f_T * u_{lam}$$

where ε is a factor describing the expansion, $\varepsilon = T_2/T_1$ with T_1 as temperature of the reactants, T_2 as the temperature of the combustion products, f_T an empirical turbulence factor in the order

of 2 - 7. An estimation of the flame speed in hydrocarbon-air mixtures results in a product of ranges

$$u_{turb} = (0.3 \text{ to } 0.8) * (5 \text{ to } 8) * (2 \text{ to } 7) = 3 \text{ to } 44.8 \text{ m/s}$$

At very high turbulence levels, quenching causes a decrease of the turbulent combustion velocity.

Regimes of Combustion

The different regimes of premixed combustion, which are passed during the transition from deflagration to a detonation, can be visualized in so-called Schlieren pictures. Fig. 3-4 shows the respective Schlieren contours for the example of hydrogen-air mixtures demonstrating the complicated interplay between hydrodynamics flow and chemistry.

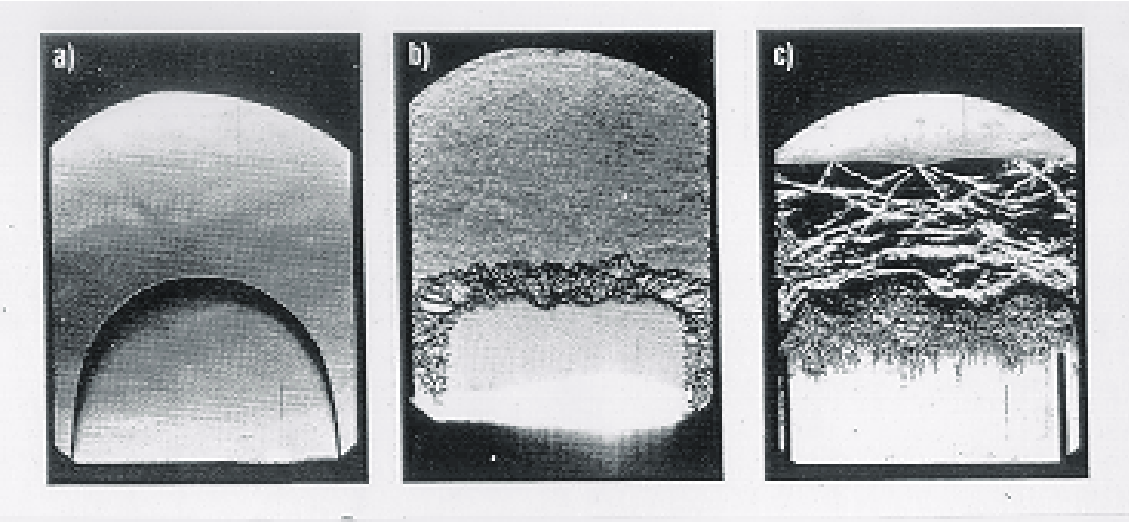

Fig. 3-4: Schlieren pictures of a laminar deflagration (a), turbulent deflagration (b), and quasi-detonation (c)

By varying the H_2 content in the gas mixture, also the combustion modes changes: (i) with lean concentrations of 9 - 10 vol% H_2 in air, slow or laminar burning velocities < 200 m/s are observed, where the unburnt and burnt gases are separated by a smooth thin flame front; (ii) with H_2 concentrations around 12 %, fast turbulent flames can be seen characterized by pockets of unburnt and burnt gas surrounding each other and increasing the flame front surface and thus the burning rate; (iii) at H_2 concentrations > 15 % the combustion will take place as a quasi-detonation which is an even faster turbulent combustion (> 2000 m/s, creating a pressure wave that increases the temperature in the unburnt gas beyond its ignition point.

The dark areas in Fig. 3-4 indicate high density gradients. Fig. 3-4a depicts a laminar flame, in which unburnt and burnt gas are separated by a smooth, very thin flame front. The flame surface travels with a constant velocity up to the top. The continuity of the combustion is maintained by diffusion of heat and radicals. Fig. 3-4b shows a typical fast turbulent flame. Instead of a smooth flame surface, pockets of unburned and burned gas are surrounded by the

respective other medium. The heat and mass transport are governed by turbulence, not by molecular diffusion.

An even faster combustion form, a so-called quasi-detonation, can be seen in Fig. 3-4c. The movement of the flame front is extremely fast, so that the associated shock wave causes a temperature rise in the unburned gas in front of the flame beyond its ignition temperature within microseconds. The pressure waves were created by the rapid expansion of the burnt and compressed gas during the combustion.

The three combustion regimes described above can also be identified in a velocity-distance diagram (see Fig. 3-5) [Breitung 2000]. Lean H_2 concentrations (9 - 10 vol% H_2 in air) lead to a subsonic flame (v < 200 m/s) with almost no flame acceleration. This regime can be regarded as an intermediate state of the situations displayed in Figure 3-4a and b. An increase of the H_2 concentration (12 % H_2 in air) entails, after an initial acceleration phase a fast turbulent combustion, comparable to the one depicted in Fig. 3-4b. The maximum flame speed is close to the sound velocity in the burned gas (shoked flow). By further increasing the H_2 concentration (15 % H_2 in air), again after an acceleration phase, the flame speed reaches the level of a quasi-detonation (comparable to Fig. 3-4c). Mixtures with even higher H_2 concentrations (> 20 % H_2 in air) develop into a stable detonation with a velocity close to the theoretical CJ speed.

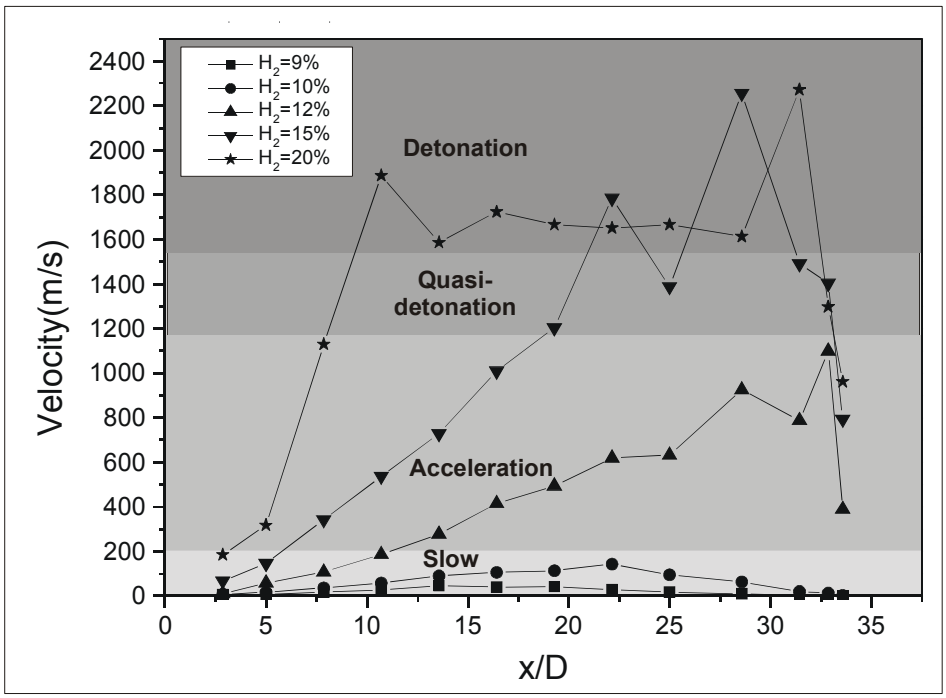

Fig. 3-5: V-x diagram of FZK tube experiments with various H2-air mixtures (BR=45%)

3.1.3.6. Real Gas Cloud

Much more realistic is a gas cloud showing a non-premixed, inhomogeneous concentration distribution, air entrainment at the boundaries, and if evolving from a liquefied gas, with stratification. Deviations from the ideal situation are able to either enhance or to attenuate the pressure buildup. Non-stoichiometry as well as ignition at the cloud edge will certainly have a

damping effect on the pressure buildup. However, the flat long-stretched cloud may experience multi-point ignition and more turbulence-generating terrain roughness or obstacles in the flow path, both effects of which lead to an enhancement of the pressure buildup.

The ignition itself is essentially a stochastic process depending on the ignition source seeing a flammable gas pocket. On the other hand, a high degree of initial turbulence in the gas cloud is created under conditions of high-pressure leakage as is probable in chemical plants. If pressurized gas is released, it is likely to burn in form of a rising and expanding fire ball. This seems unlikely for a flat vapor cloud arising from an LNG spill.

The realistic shape of a heavy gas cloud would be of a pancake form (or even cigar-shaped) covering an area, which is larger than that of a hemispherical cloud with the same explosive inventory. The flame spreading in such a cloud is spherically until it reaches the upper cloud edge; then it continues in horizontal direction. The pressure is decreasing immediately behind the flame front because of the upward expansion of the combustion products. Peak overpressures outside the cloud at a given distance from the center are somewhat higher for a flat cloud, but the pulse duration of the blast wave would be shorter, such that the impulse in approximately the same [Geiger 1980].

The Figs. 3-6 and 3-7 give a comparison of the detonation/deflagration of an ideal, hemispherical and a real, pancake-shaped gas cloud. The detonation front moves until the edge of the cloud without attenuation, whereby most of its combustion energy is consumed in generating the blast wave; it decays rapidly beyond the cloud edge. The high-pressure area is much longer in the real-cloud detonation; both overpressure and positive-phase impulse are considerably higher than in spherical-cloud detonations. In case of a deflagration, the high pressure will again cover a wider area compared with a hemispherical cloud, but outside the cloud limits it will decay more rapidly due to the narrow zone, to which the pressure is restricted when traveling with the flame front [Geiger 1982].

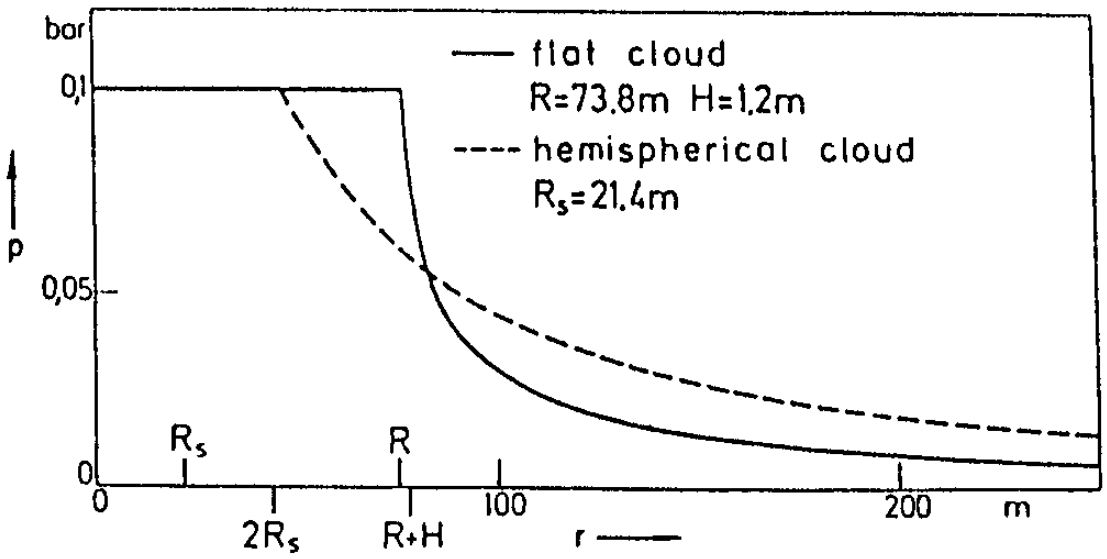

Fig. 3-6: Deflagration pressure profile in a hemispherical and in a flat gas cloud

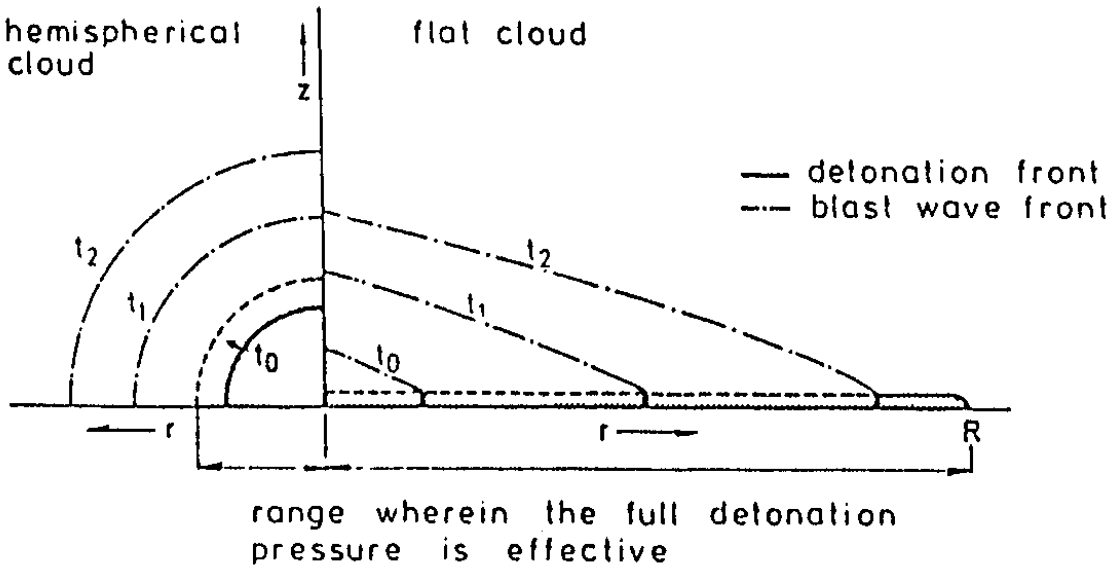

Fig. 3-7: : Detonation pressure profile in a hemispherical and in a flat gas cloud

A confined explosion usually occurs in a relatively small volume or small pockets of flammable gases within larger volumes. The explosive effect is created, when a boundary fails under the developing pressure.

The explosive combustion of an unconfined hydrogen-air mixture liberates only a fraction of 0.1 - 10 % of its thermal energy content, in most cases less than 1 %. Depending on the combustion mode (deflagration/detonation), the explosion is connected with a more or less destructive pressure shock wave. The overpressure to be expected in the deflagration of an unconfined hydrogen-air vapor cloud is in the order of 10 kPa.

3.1.3.7. Heat Radiation

Most of the heat transfer from a fire is by convection and by thermal radiation. Typically 75 % of the heat emanates by convection with the hot combustion products spreading upwards. However, the principal hazard is represented by the radiation, which does not go preferentially upwards and crosses open spaces. Fire potentially results in damaging nearby objects directly or by the thermal radiation. Radiation preheating of materials may result in a rapid extension of the burning along interior surfaces ("flash-over"). Some examples of critical data are listed in Table 3-2.

The fraction of the combustion energy, which is released as radiation, is being given as 17 - 25 % for hydrogen-air combustion and 23 - 33 % for methane-air flames.

The simplest method for calculating thermal radiation is the "Point Source Method":

$$D = 0.28 * (F * W * Cv / K)^{1/2}$$

where D [m]: distance from flame center to point with radiation K;
F: fraction of heat radiated, e.g., 0.15 for H_2, CO, NH_3 or 0.3 for hydrocarbons;

K [kW m^{-2}]: allowable radiation level;
W [kg s^{-1}]: burning rate;
Cv [kJ kg^{-1}]: calorific value of the fuel.

Limitation of this method is given by the assumption that all radiation comes from the flame center point.

Table 3-2: Critical heat radiation for human and goods [Böke 1995]

Object	**Time period [s]**	**Heat radiation [kW/m²]**
Maximum radiation strength for skin	any	< 1.7
Dolor tolerable	< 20 < 13	4 5
Burn 1st grade	> 8 > 3	6.4 10.4
Burn 2nd grade	> 10 > 16	10.5 16
Blister formation	10 - 12	10.5
Lethal	> 40	10
Sensitive buildings		1 - 2
Public roads		4.5
Factory building		8 - 12.6
Uncooled storage tank		10
Instantaneous ignition of wood		16 - 25
Cooled storage tank		37.8
Autoignition of wood fiber sheets		52

3.1.3.8. Blast Wave

A great portion of the explosion energy is usually carried by the developing blast wave which is uniformly distributed in all directions. This effect is strongest at ground level (hemispherical) explosions where the respective yield ratio can be twice as high as for a spherical explosion. The blast wave resulting from an UVCE usually consumes a fraction of 1 - 10 % of the heat of combustion theoretically available.

In a deflagration, the volume expansion of the gas acts like a piston displacing the unburnt gas. In contrast, the detonation generates a compression wave characterized by a distinct pressure spike and a subsequent almost exponential decrease to values even lower than atmospheric pressure (molecular collapse). In the long-distance range, the pressure wave for both

deflagration and detonation is decaying with 1/r. The different pressure functions for the two combustion modes are shown in Fig. 3-8.

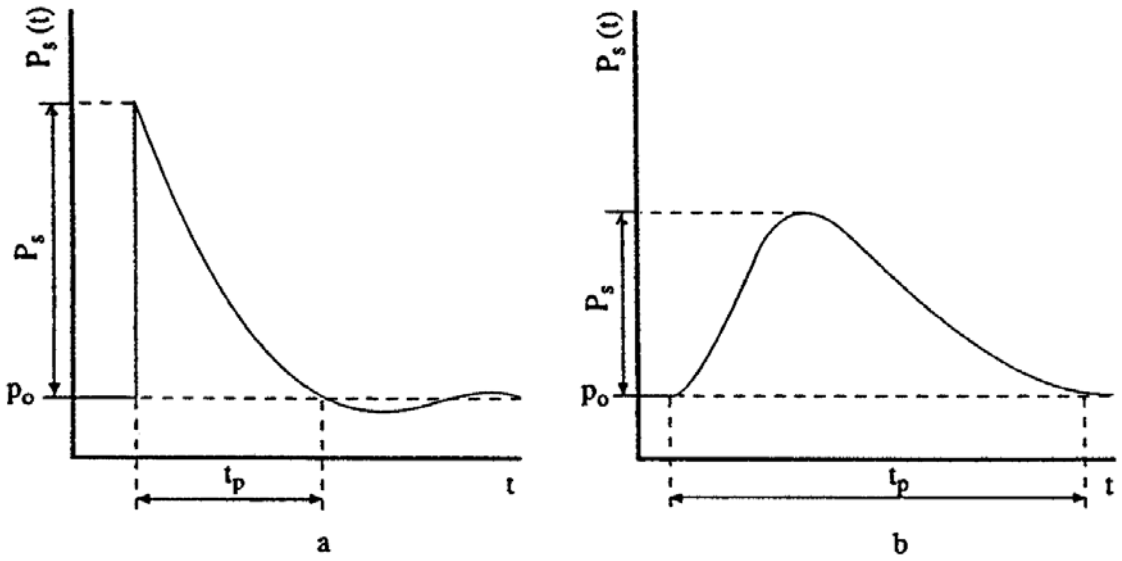

Fig. 3-8: Characteristic shape of pressure-time function for a detonation shock wave (left) and a deflagration pressure wave (right)

Deflagration and detonation differ in peak overpressure, in the duration of the impulse, in the steepness of the wave front, and in the decrease of overpressure with propagation distance. The deflagration pressure wave is characterized by a slow increase of pressure and fluid velocity in the region preceding the flame front.

The pressure buildup depends on the flame propagation and the degree of confinement. Particularly hazardous configurations are those, which are heavily confined like tubes, pipes, or channels, where – if long enough – even in insensitive methane-air mixtures, high flame speeds and pressures can be reached. The maximum possible value in a closed vessel for a hydrocarbon-air mixture is 0.8 MPa, for a hydrocarbon-oxygen mixture 1.6 MPa. In pipes with no obstacles, the transition distance increases with increasing diameter (example: 8 m for propane-air mixture in a 50 mm diameter pipe) [Moen 1993]. There must be a high effective burning velocity reaching the order of 100 m/s to produce significant blast overpressures of 10 kPa. Pressures are generally lower in a spherical propagation of the gas mixture (unconfined) than in a planar propagation. The pressure behind the flame front is decaying away from the flame, since wave energy dissipates.

A very simple way of modeling blast effects is the TNT Equivalent method derived from the decay of shock waves from nuclear explosions in the atmosphere. It is deemed overestimating near-field and underestimating far-field effects. A more suitable approach is the Multi-Energy method developed by TNO. It suggests that damaging explosion can occur only, when flame acceleration takes place within a plant structure. Special “blast charts” have been developed from gas-air explosions (Fig. 3-9) showing the relationship between a “scaled blast overpressure” (= ratio of blast overpressure over ambient overpressure) and a “scaled distance” [Mercx 2000].

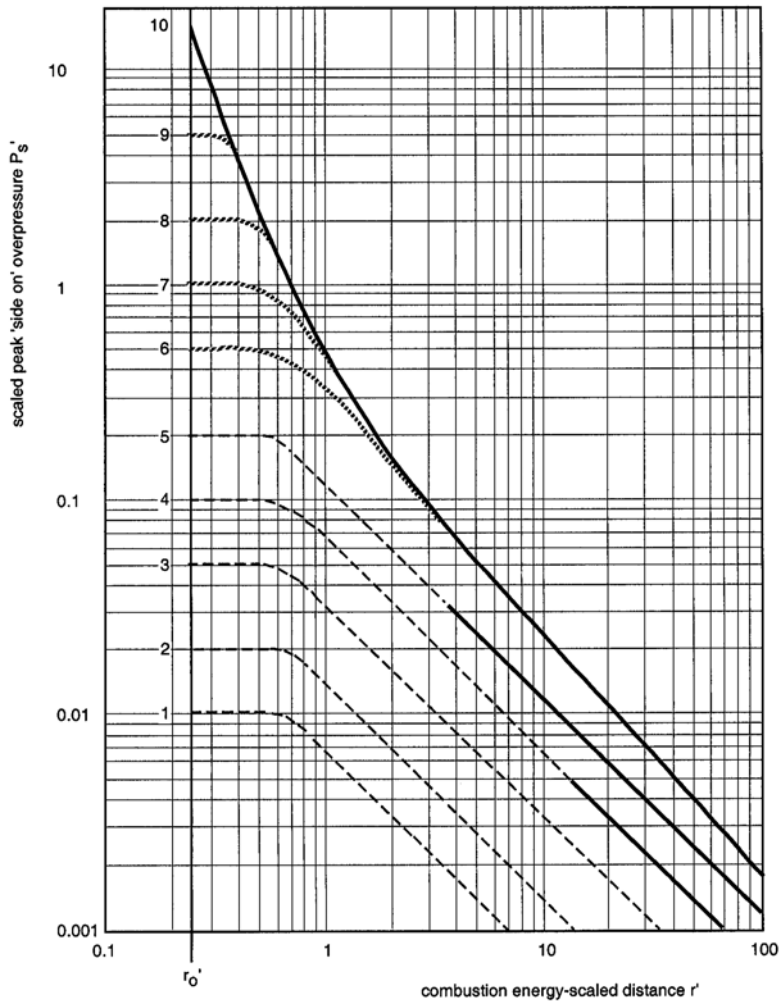

Fig. 3-9: TNO for blast overpressure according to the Multi-Energy method

3.2. Structure Response to Explosions

3.2.1. INTERACTION OF BLAST WAVE WITH STRUCTURE

The effects from an explosion, which have an impact on structures, are pressure changes (blast wave) and air movement ("explosion wind") as well as thermal radiation and flying missiles. Pressure-time characteristics of an unconfined gas cloud deflagration are different from an explosive, because it exhibits a finite rise time to the maximum overpressure, where the flame front velocity as a decisive parameter leads to a decoupling of pressure wave and impact time period.

The pressure load exerted upon a structure has to act for a certain period before damage can occur. Pressure waves result from relatively slow explosions, e.g., a deflagration of unconfined vapor clouds. In contrast, shock waves develop after very short explosion processes like detonations. The blast parameters are dependent on the distance between structure and blast center (see Fig. 3-10).

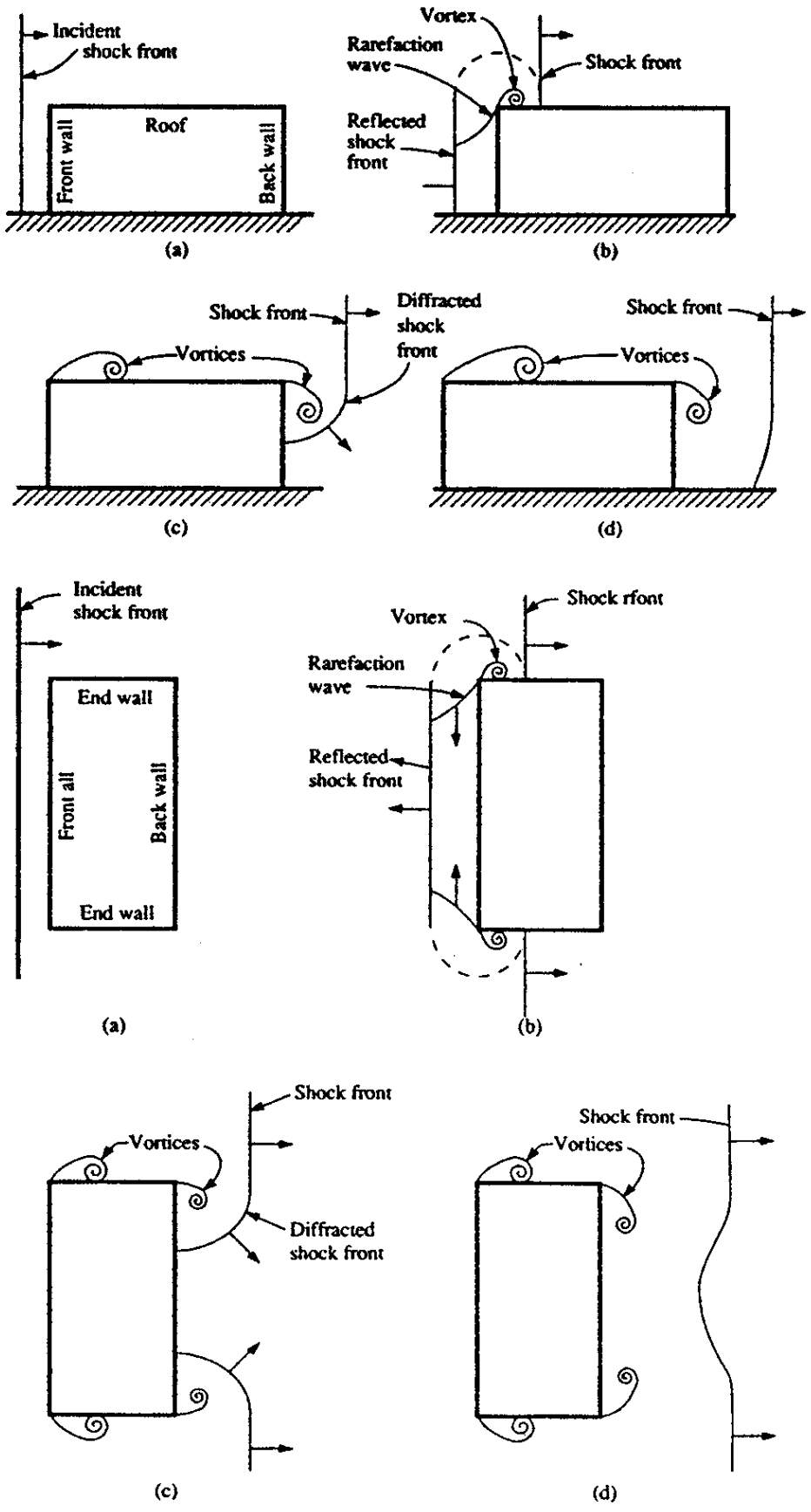

Fig. 3-10: Blast parameters as a function of distance

In a partially obstructed area, an explosion will create a mixture of reflected pressure waves and deflected air flows, which give a more or less complex load upon a building. The more complex the structure, the more difficult is the prediction of the critical conditions for mechanical failure for a given load history.

The dynamic interaction of a blast wave with the structure depends on the pressure-time history, i.e., rise time and duration of positive phase and peak pressure or the impulse (which is the time integral of the pressure). It is distinguished between the initial "diffraction loading" and the subsequent "drag loading". Diffraction loading is given by forces resulting from direct and reflected pressures during the initial phase. The reflection of the pressure wave at the front side determines the maximum load. The flow around the obstacle determines the further pressure development at the front and at the back side. The net horizontal loading is that on the front minus that on the back face. The reflection coefficient, i.e., the ratio between reflected and incident overpressure, depends on the incident angle and the blast wave type (pressure or shock wave). For a pressure wave, this coefficient can have a value up to about 3 depending on the incident angle; for a shock wave, it can be 2 - 5 and under certain conditions up to 8 (and even higher for explosives).

After the diffraction phase is completed, the structure is subjected to a "stagnation pressure". The distance of the incident wave when interacting with the structure, causes major pressure differences developing from the edges of the structure. Resulting from this rarefaction wave, pressures decrease. During this so-called drag phase, strong transient winds with flow velocities of several 100 m/s are effective. Drag forces would particularly have an impact on smaller structures such as pipe work. Loading duration during vapor cloud explosions may be long enough to be comparable with the time required for the dynamic response time of the structure. In case of large structures, the rarefaction from the edges is insignificant.

3.2.2. STRUCTURAL RESPONSE

Forces acting on a structure will lead to a deformation to an extend which depends on the material properties and structure composition. For a static load, i.e., a constant or slowly changing load, it will be in equilibrium with the internal forces resulting in a deformation of the structure. For a dynamic load, i.e., a fast load transient, however, a "dynamic" contribution from inertia forces will add to the equilibrium, which can show positive or negative acceleration, i.e., mass and stiffness of the structure will play a major role. The load from a gas explosion is considered a dynamic load due to its short overpressure duration, which is typically in the range of 100 - 200 ms.

A structure can be schematically represented by a system of masses coupled with springs or dampers. If linear-elastic or non-linear-elastic forces are acting, displacements of the masses become zero again, when the load disappears. In case of plastic or elasto-plastic behavior, displacement is zero or very small, until the maximum load is reached. Under a static load, the structure will then fail; under dynamic load, it may retain a residual displacement. In general, structures must be designed to react elastically under typical loads like wind; plastic displacement must be limited to abnormal load conditions. The maximum displacement depends on load duration, t_D, and the natural frequency of the structure, T. For low t_D/T ratios, the displacement is smaller than for static loads. For large t_D/T ratios, the displacement can be

larger than under static load conditions. Other important parameters are the static strength and the ductility. Load schemes are distinguished between a step function for a long-duration pressure wave and an impulse load for a short-impact shock wave.

The analytical procedure is usually simplified by introducing a so-called dynamic load factor (DLF), which is defined as the ratio of maximum dynamic displacement over static displacement. It transforms a dynamic peak load into a static load with the same effect on the structure. The DLF is dependent on the dynamic load time and the natural frequencies of the structure. For long explosion times and in case of an idealized triangle-shaped shock wave load, the DLF approaches its boundary limit of 2.

Detonations tend to excite the high natural frequencies of a building, whereas deflagrations are more effective for the lower frequencies. It appears to be technically more difficult to design a building against both explosion modes rather than only one.

3.2.3. DAMAGE

An empirical and very global approach of determining the strength of structures is to relate overpressures to the degree of observed damage. The relationship between pressure and damage, which is derived from TNT explosions, cannot satisfactorily be transferred to vapor cloud explosions. The pressure decay from a TNT explosion is much faster than from a vapor cloud explosion. The high impulse and the suction effect due to the below-atmospheric pressure phase will certainly result in a different damage pattern. Thus damage criteria such as those derived by Schardin from TNT explosions are not directly applicable.

In the past, many pressure criteria have been defined related to various structures and specific components, however, varying over a large uncertainty range. A rough classification is given in Table 3-3.

Table 3-3: Damage classification

Zone	Damage level	Overpressure of incident blast wave [kPa]
A	Total destruction	> 83
B	Heavy damage	> 35
C	Moderate damage	> 17
D	Minor damage	> 3.5

Damage levels can also be visualized in pressure-impulse diagrams. An example is given in Fig. 3-11 showing the experimental results for the observed damage in per cent, after different types of houses were exposed to a certain explosion (pressure/impulse) load [TNO 1992]. Important for the damage effect of a short-term load (= shock wave) is only the impulse, whereas it is the maximum overpressure for that of the longer-term load (= pressure wave). The solid lines in the figure indicate the lower boundaries for light damages, for severe damages, and for collapsing structures of the houses investigated. This will be different for other types of structures. Similar PI diagrams have also been derived for impacts on humans.

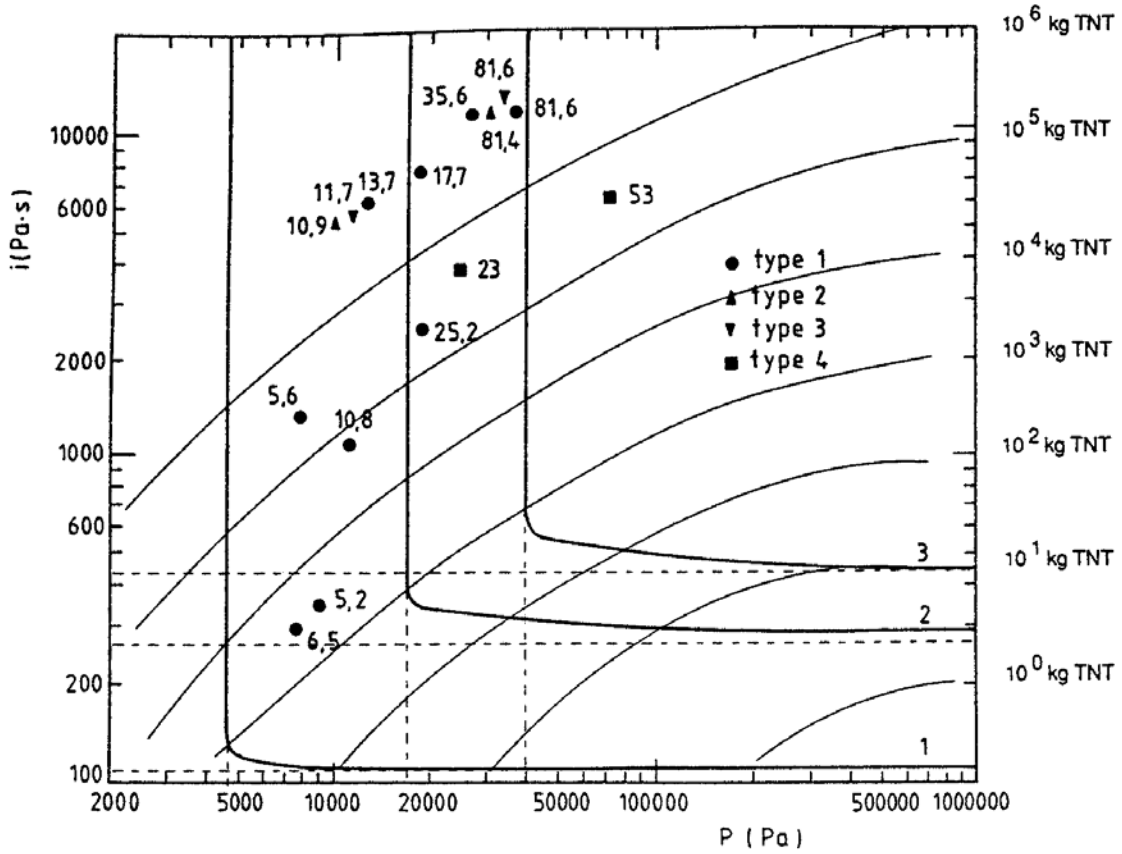

Fig. 3-11: Pressure-impulse diagram with experimental damage values for different types of houses

For the assessment of the probability to obtain a certain level of damage, so-called probit functions have been introduced and suitable damage criteria have been defined. For industrial installations, [TNO 1992] provides the following limits to be met for the control building:

Pressure wave:	walls:	30 kPa	
	roof:	20 kPa	for 100 ms
Shock wave:	walls:	300 kPa	
	roof:	200 kPa	for 15 ms

A comparison between detonations of explosives and blast waves resulting from nuclear weapon explosions, characterized by quasi-static pressure due to a longer impulse time shows that, assuming the same damage, the detonation pressure or the pressure resistance of an object is much higher than the resistance against a blast wave from the nuclear tests [Pförtner 1975]. The pressure resistance behavior of a building under detonative dynamic and quasi-static loading derived from numerous detonative explosion studies can be summarized in an empirical equation for the quasi-static reference overpressure of the building p_{st}:

$$p_{st} = 0.15 * p_r^{2/3},$$

where p_r is the perpendicularly reflected overpressure or the pressure resistance of the building subjected to a detonation. If the TNT equivalent, as has been derived from the damage of some of the severe accidents is interpreted as the incident pressure wave which appeared to be in the

order of 70 kPa, is interpreted as a pressure wave resulting from a deflagration, the respective quasi-static pressure would be much smaller:

$$p_{st} = 22 \text{ kPa}.$$

The figure given in the BMI guideline of 30 kPa corresponding to a flame velocity of 26 m/s, thus translates into a pressure resistance of 283 kPa corresponding to an incident shock wave overpressure of 0.1 MPa [Pförtner 1977].

Structural dynamic calculations have been conducted with a computer model developed at the Battelle Institute in Frankfurt. Fig. 3-12 shows the results for a deflagrative pressure wave intercepting a rectangular-shaped building. Static and dynamic loads are simulated by step functions [PNP 1981].

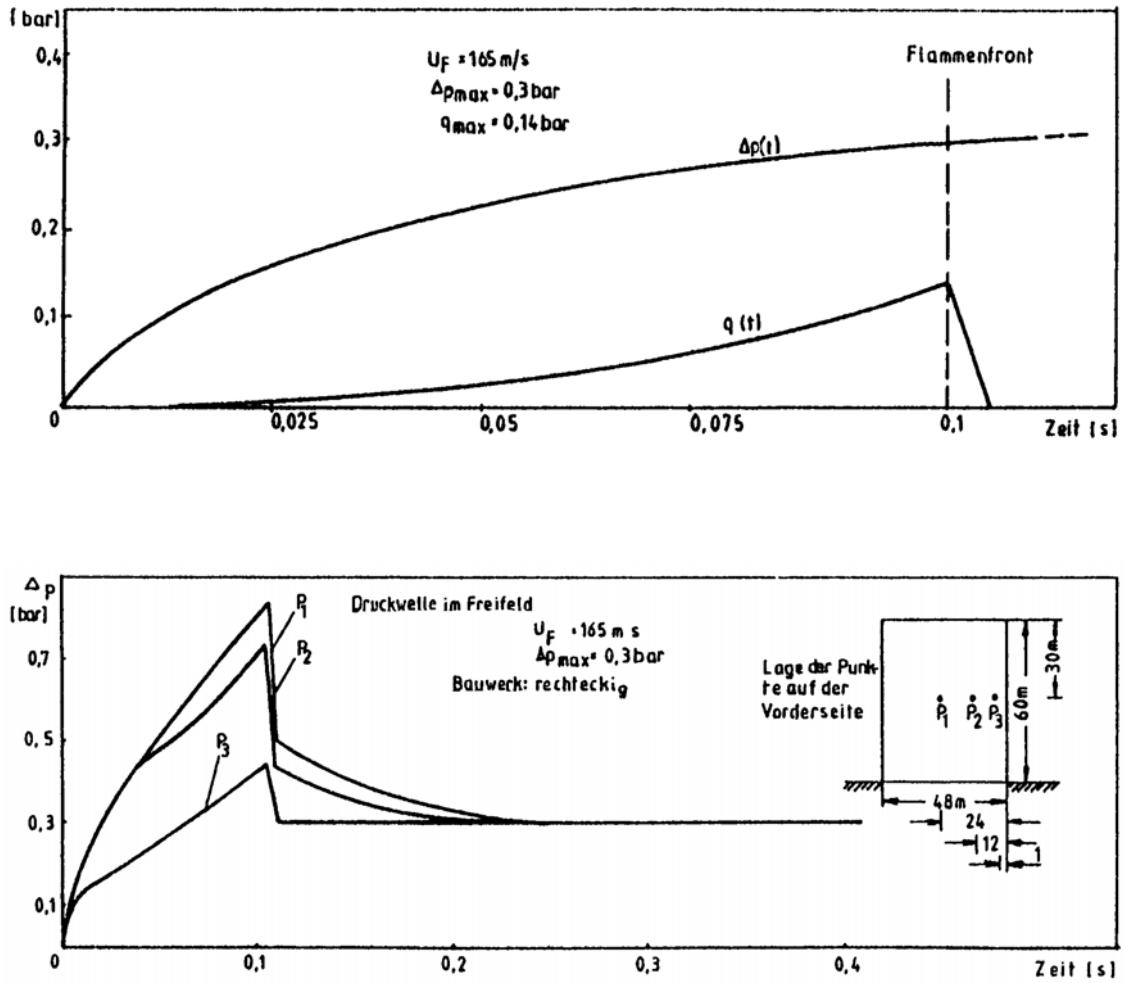

Fig. 3-12: Deflagrative pressure wave intercepting a rectangular structure

4. HAZARD IDENTIFICATION AND RISK ASSESSMENT

4.1. Experience

4.1.1. HIGH-TEMPERATURE GAS-COOLED REACTORS

Graphite-moderated, gas-cooled reactors (GCR) are in operation since 1956 with units sizes of up to 670 MW(e). They have accumulated so far more than 600 operation years. The final stage of the GCR development is represented by the high-temperature gas-cooled reactor, HTGR, characterized by a high coolant outlet temperature in the range of 750 - 950 °C, which has the potential for HT process heat applications. A comprehensive outline of the historical development of GCR in the world is given in [IAEA 1984].

Direct experience with HTGR plants has been gathered in the countries United Kingdom, Germany, the USA, Japan, and China. A total of seven units has been constructed as given in the following Table 4-1. The HTGR, however, has not reached up to now a commercial state. South Africa may become the next HTGR country being on the verge of starting to construct the first in a series of 11 commercial units of the modular type, PBMR, for electricity production.

Table 4-1: High-temperature gas-cooled reactor experience in the world

HTGR	Thermal power [MW(th)]	First criticality	Out of operation
Dragon (Winfrith, UK)	20	1964	1975
AVR (Jülich, Germany)	46	1968	1989
Peach Bottom (USA)	115	1967	1974
THTR (Hamm, Germany)	756	1983	1988
Fort St. Vrain (USA)	842	1974	1988
HTTR (OARAI, Japan)	30	1999	-
HTR-10 (Beijing, PR China)	10	2000	-

4.1.2. STEAM REFORMING SYSTEMS

Steam reforming is a technically mature and worldwide well-established technology practiced on an industrial scale. Today's reformer plant capacities vary in size between typically 100 Nm^3/h up to 140,000 Nm^3/h. Although small-scale steam reformers are commercially available today, only a few small units have been constructed. Suitability on a small scale makes them beneficial for integration into a fuel cell power systems, in particular for mobile applications. Large-scale reformers could be used for H_2 supply to stationary fuel cell applications at the 100 MW scale. Recent reformer improvement developments have focused on high efficiency, good load-changing capability, and low cost by using cheaper materials and production methods.

4.1.3. LNG REFERENCE PLANTS

The construction and operation of large-scale LNG facilities including liquefaction and storage has become worldwide a well-established, economic, and safe technology. About 250 LNG facilities are being operated at present comprising baseload liquefaction plants, peak-shaving (liquefaction – storage – regasification) plants, receiving terminals and fuel stations. In addition, approx. 130 LNG tank ships are traveling the oceans trading the energy carrier LNG as a major commodity. Current safety standards are the result of the experience gathered over many decades. Storage tanks for LNG of various kinds and over a wide range of sizes from vehicle tanks of 0.2 m^3 to stationary storage tanks up to 200,000 m^3 of liquid are now state-of-the-art with a safe record over many years.

There is also experience in the construction of underground LNG storage tanks with Japan to have completed the world's first of this kind. The world largest LNG underground tank with a capacity of 200,000 m^3 is being constructed by Kawasaki Heavy Industries for Tokyo Gas Company at Ogishima; it has a diameter of 72 m. The first underground tank in Japan was constructed in 1970.

4.2. Identification of Hazard Sources and of Events Threatening Safe Operation

Safety items can be categorized into several classes. The items associated with the accidental release of a large amount of radioactive materials and core damage from thermal turbulence are categorized into the class with the largest hazards. In relation to these items, the system must be designed with high reliability and redundancy to avoid the loss of safety functions. On the other hand, the items associated with continuous normal operation are categorized into the class with lowest hazards, for which such a high level of reliability and redundancy is not required.

The steam reforming system connected to the HTTR will not be designed as a nuclear grade system. Therefore, particular safety items others than the "conventional" safety features will not be provided in the steam reforming system, as will be described below.

4.2.1. NUCLEAR STEAM REFORMING

There are three areas of concern associated with the connection of a steam reforming system to the HTTR:

- Steam reforming system is the final cooling system of the HTTR;
- Large amounts of flammable substances are used in the steam reforming system;
- The products hydrogen (and methanol) will probably be handled outside the nuclear plant in the future.

Potential hazardous events in connection with the steam reforming system are

- Tritium transportation from the core to the product hydrogen and methanol;
- Thermal turbulence induced by problems in the steam reforming system;
- Fire and explosion of flammable mixtures with the process gases.

4.2.1.1. Tritium Transportation

Tritium is produced in the core during normal operation as a ternary fission product and by activation reactions of lithium and boron in the graphite components and control rods. In addition, the helium coolant is a significant tritium source in the HTGR. The tritium produced in a fission process will be retained within the fuel particles, which have an intact coating; only a small fraction originating from fuel particles with a broken coating or from uranium contamination of the core graphite is expected to escape into the coolant. On the other hand, tritium produced in the graphite can rapidly diffuse through the graphite components into the coolant. Most impurities including tritium in the coolant are removed by the helium purification systems provided in the primary (PHPS) and secondary (SHPS) cooling system. There is, however, a small amount of tritium that can be transported to the process side by permeation through the heat exchanger tubes into the products hydrogen or methanol. Flow pathes of the tritium ("HT") and hydrogen ("H_2") are shown in Fig. 4-1.

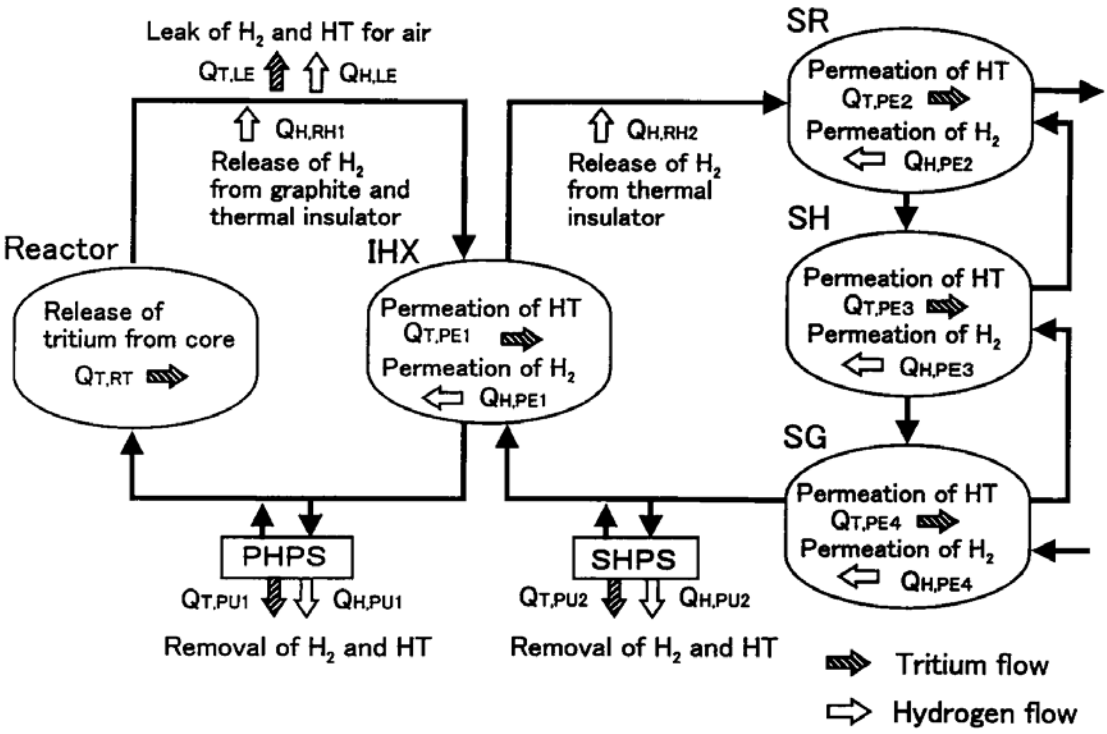

Fig. 4-1: Tritium ("HT") and hydrogen balance in HTGR H_2 production system

In order to be usable as a normal commodity, the product gas of the nuclear steam reforming process must have a tritium concentration below the allowable limits specified by the legislation. Therefore, one safety requirement is to correspondingly reduce tritium penetration into the products. In this case, the required safety items are not directly related to the reactor safety and thus can be classified into the lowest safety level.

There are two approaches to reduce the tritium concentration in the products; one is removing tritium from the coolant and the other one is protecting against permeation through the heat exchanger tube walls. The first approach is only partially effective, since in the HTTR, the

purification systems are installed in the bypass loop and their flow rates are selected based on the concentrations of other impurities.

Tritium permeation rates depend on the tube surface conditions. The tritium permeability is high for clean tube surfaces; it decreases, if an oxide layer or another effective coating covers the surface. Under steam reforming conditions, an oxide layer will rapidly develop on the tube surface. Preliminary calculations have been performed to determine tritium concentration at steady state for the HTTR steam reforming system. Results are shown in Table 4-2.

Table 4-2: Tritium permeation for steady-state operation of the HTTR

Calculation condition				Tritium concentration in product gas hydrogen [Bq/g]
Tube surface		Purification rate [kg/h]	Hydrogen release	
IHX	SR, SH, SG			
Clean	Clean	200	No	89.5
Clean	Oxidized	200	No	20.5
Coated	Oxidized	200	No	8.9
Defect	Oxidized	200	No	12.0
Coated	Oxidized	400	No	5.3
Clean	Oxidized	800	No	8.5
Coated	Oxidized	200	Yes	6.8

In this calculation, the tritium permeability of the IHX is reduced to 1/10 and that of the reformer to 1/100 of that under clean conditions due to the oxide layer on the tube surface developed during operation. These results show that the combination of the self-grown oxide layer effect and a reasonable flow rate through the helium purification systems are sufficiently effective to restrict the tritium concentration in the product gas to an acceptable level.

JAERI tests on hydrogen isotopes permeation are described in more detail in chapter 4.5.2. The treatment of the tritium problem in the German PNP project is explained in chapter 5.4.1.

4.2.1.2. Release of Radioactivity due to Leakage in Heat Exchanger

Another possible path for a transition of radionuclides into the product gas is by leakage in the heat exchangers. A leakage of radioactivity from the primary to the secondary circuit requires a pressure drop from the primary towards the secondary loop, in contrast to the plant's condition during normal operation. However, as long as the heat exchangers remain intact, even under conservative assumptions, the expected radioactivity on the secondary side remains small compared with the tritium concentration by permeation [PNP 1981].

A measure to prevent a major risk is the installation of gas supervising systems to trigger the disconnection of the product gas lines from the grid.

4.2.1.3. Thermal Turbulence in the Steam Reforming System

A system with an endothermal chemical reactor connected to an HTGR exhibits thermal dynamics, which differ significantly from those of the HTGR itself. In the HTGR core, the nuclear heat is transferred to the cooling gas and as a result reactor power and helium temperature have a linear relationship. On the other hand, in the chemical reactor, in which endothermal reactions take place, the heat input necessary to cause the reaction tremendously increases with increasing reaction temperature due to the Arrhenius type temperature dependence of the reaction rate. The development of a new control technology is required in order to balance the difference in the thermal dynamics between the nuclear and chemical reactor. The selected design and arrangement of the steam generator is expected to fulfill this control function (see chapter 2.3.2.).

A higher probability of malfunction or failure is expected on the process side rather than on the power generation side. Safety measures are required to mitigate potential disturbances resulting from a malfunction or failure in the hydrogen production system to allow for a continuous reactor operation without reactor scram.

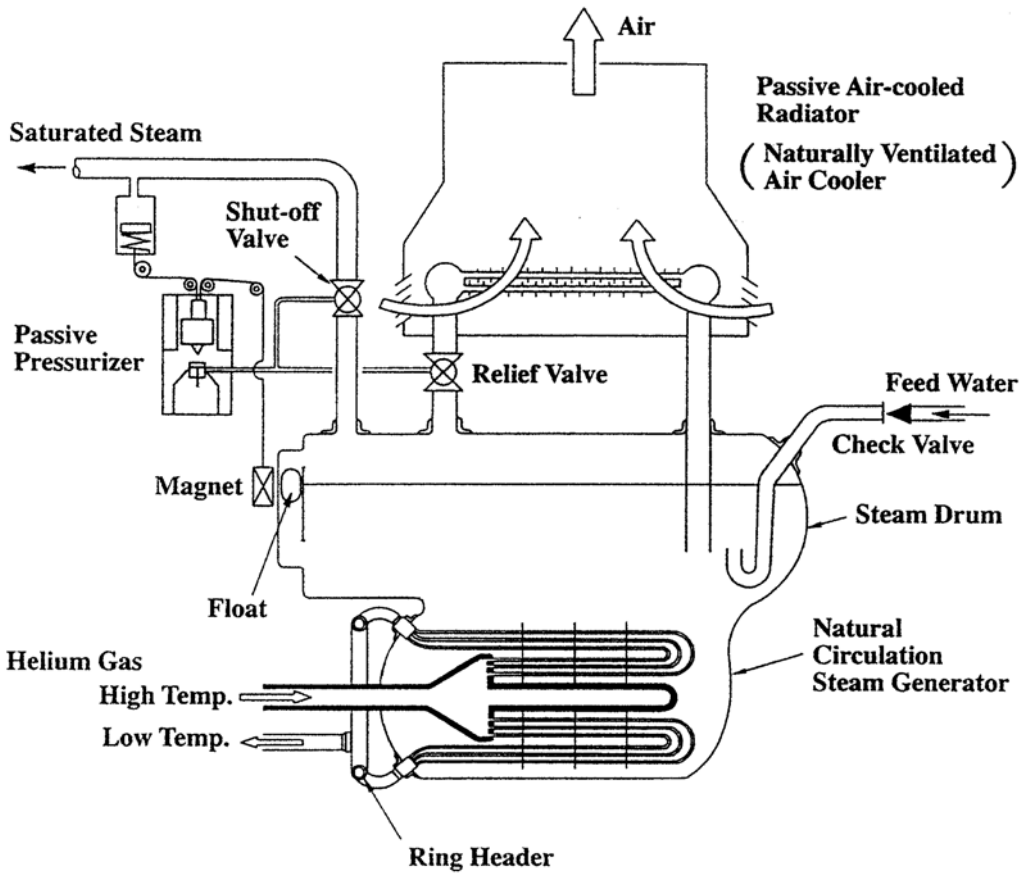

Fig. 4-2: Innovative helium cooling system

If the methane supply system is shut down due to a loss of electric power or a malfunction of the control system, the helium gas temperature at the steam reformer outlet will increase. The steam generator installed downstream of the steam reformer in the secondary loop, can cool down the hot helium gas to the saturation temperature of the steam, thus providing a stable

controllability for any disturbance at the steam reformer due to the large heat sink capacity and preventing a reactor scram. However, if the feed water supply is interrupted, the steam generator cannot continue to operate. It is therefore proposed to re-use the generated steam as feed water after condensation in the radiator. The conceptual geometry of this cooling system is shown in Fig. 4-2.

In order to prevent a reactor scram due to a loss of feed water, the hot helium gas is cooled by the steam generator and the generated steam from the steam generator flows into a natural ventilation type radiator connected to the steam generator. The condensed water is then supplied to the steam generator as feed water. The steam generator can keep its water contents for normal operation. The total heat capacity is about 8.8 MW representing the heat capacity of both the steam reformer, the super heater and the steam generator. Furthermore, if a pressure drop is detected in the cooling system due to pipe failure or valve malfunction, and the water level in the steam generator is low due to interruption of the feed water flow, the valve in the steam line closes, while that in the radiator steam supply line opens passively through an automatic air supply system. Generated steam is supplied to the natural convection type radiator and is cooled down. Condensed water is recycled to the steam generator as feed water. This system does not require electric power nor feed water.

The steam reforming system is a ternary cooling system. A change of the flow rate of either the feed gas or the water to the steam reformer induces a thermal disturbance of the helium outlet temperature on the reformer due to the change of the amount of heat input for the reforming reaction. If the temperature of the helium returning to the IHX exceeds the allowable limit, the reactor will scram.

Static calculations of the cooling ability of the steam generator have been carried out showing that a reduction of the feed gas changes the outlet temperature of the reformer correspondingly. But the steam generator mitigates the temperature variation within 5 °C. The continuous cooling of the hot helium gas by the steam generator allows the HTTR steam reforming system to continue at normal operation. The result of a transient analysis is shown in Fig. 4-3 for a stepwise decrease in process gas flow rate by 20 %. It indicates that an increased heat input to the steam generator due to increasing helium inlet temperature only results in an increase in steam quality at saturation temperature due to boiling, but not in an increase of the steam temperature.

The function of the ternary cooling system is to remove heat from the core during normal operation. Since the reliability required for this system is not particularly high, problems may occur more often during operation lifetime.

The safety design of the nuclear plant is based on the defense-in-depth concept. Therefore in case of a reactor scram, the propagation of thermal turbulences should be stopped in the secondary loop. The safety requirement for this event is to limit the secondary helium temperature variation within ±15 °C at the inlet of the IHX to prevent a reactor scram.

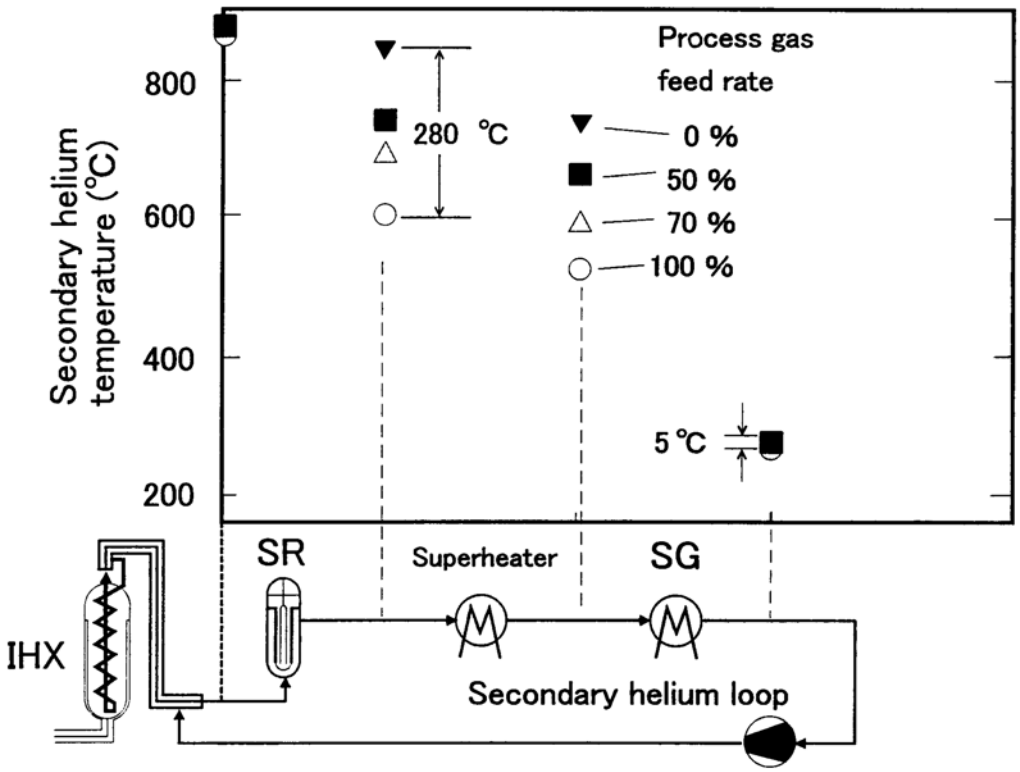

Fig. 4-3: Transient analysis for variation in the process gas flow rate

4.2.2. EXPLOSION HAZARDS

Fire and explosion hazards resulting from the leakage of flammable materials such as methane and hydrogen should be considered because they have the potential of causing significant damage to safety components. Therefore these components should be designed against fire and explosion according to the highest safety level.

General safety requirements against fire and explosion hazards have been established already in the IAEA SAFETY SERIES, according to which the amount of flammable materials in the plant and in the vicinity of the plant should be reduced to a minimum possible as a precaution measure. This concept, however, cannot be applied to the HTTR steam reforming system. Since the HTTR containment building does not have the capacity to withstand severe radiation heat and blast overpressure, it is necessary to minimize the risk of a huge fire or explosion event. One possibility is the separation between the accident source and the HTTR, which may be given by a safety distance or a fire-proof separation wall.

4.2.2.1. Release of Flammable Gases into the Containment Building

Fire and explosion events inside the reactor building may cause severe damage to nuclear safety systems. It is therefore required that the possibility of a flammable gas leak inside the reactor building should be low enough to avoid any fire and/or explosion at this location. The potential sequence of flammable gas ingress into the reactor building is the simultaneous failure of the secondary helium pipe and the reformer tube (Fig. 4-4). The only cause of the simultaneous

failure of these components is conceived to be an earthquake. Therefore they are designed for a high seismic safety level.

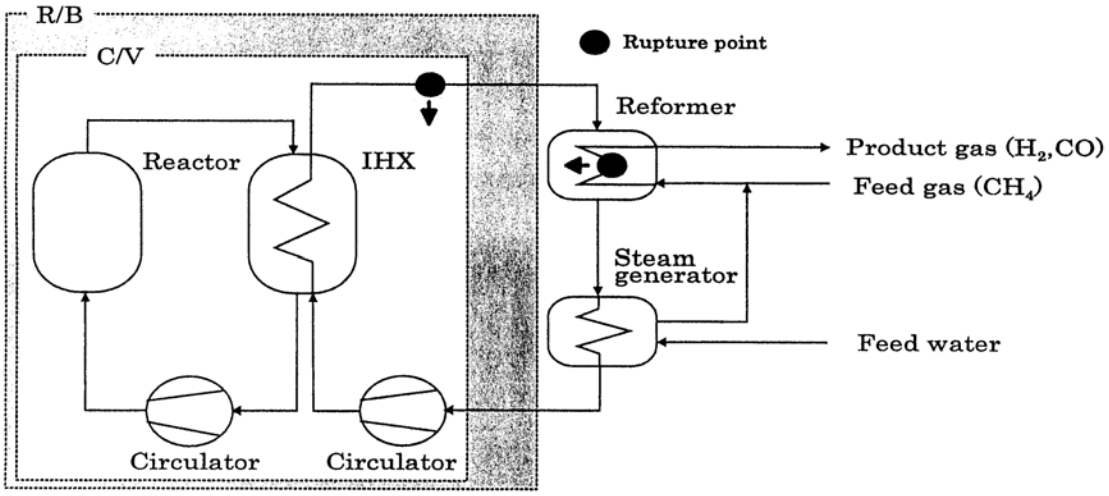

Fig. 4-4: Ingress of flammable gases into the reactor containment

Since the steam reforming system will be designed as a non-nuclear facility, it is basically not equipped with additional safety systems. In case of an explosion event in the vicinity of the reactor building, the thermal load and blast overpressure may be strong enough to cause some damage to the containment. Therefore, it is required to prevent significant leakage of flammable gases in the vicinity of the reactor building. A double tube has been adopted in the HTTR steam reforming system to prevent leakage of flammable gas. Emergency shut-off valves are also provided to isolate the failure location of the pipe and, thereby, limiting the amount of leakage.

4.2.2.2. Release of Flammable Gases outside the Containment Building

The danger of possible detonations or deflagrations of explosive gas clouds, which were released from tank ships or trucks or nearby chemical plants and which might travel towards a reactor building, has been subject of substantial theoretical and experimental investigation (see chapter 5.2). This kind of threat is strongly dependent on the local environment and the future development plans for that area. Individual characteristics of the site and also the layout of reactor buildings will be relevant. Considerable basic aspects would be to avoid large flat surfaces, the surround the reactor building with auxiliary equipment buildings, to use underground construction for important connecting conduits.

Storage Tank

In case of an event far from the reactor building (Fig. 4-5), a safety distance can be selected to mitigate the effects of thermal load from fire and blast overpressure from explosion. Comparing these effects, the explosion pressure wave causes a greater damage than the fire itself. The explosion event is taken into account to estimate adequate safety distances.

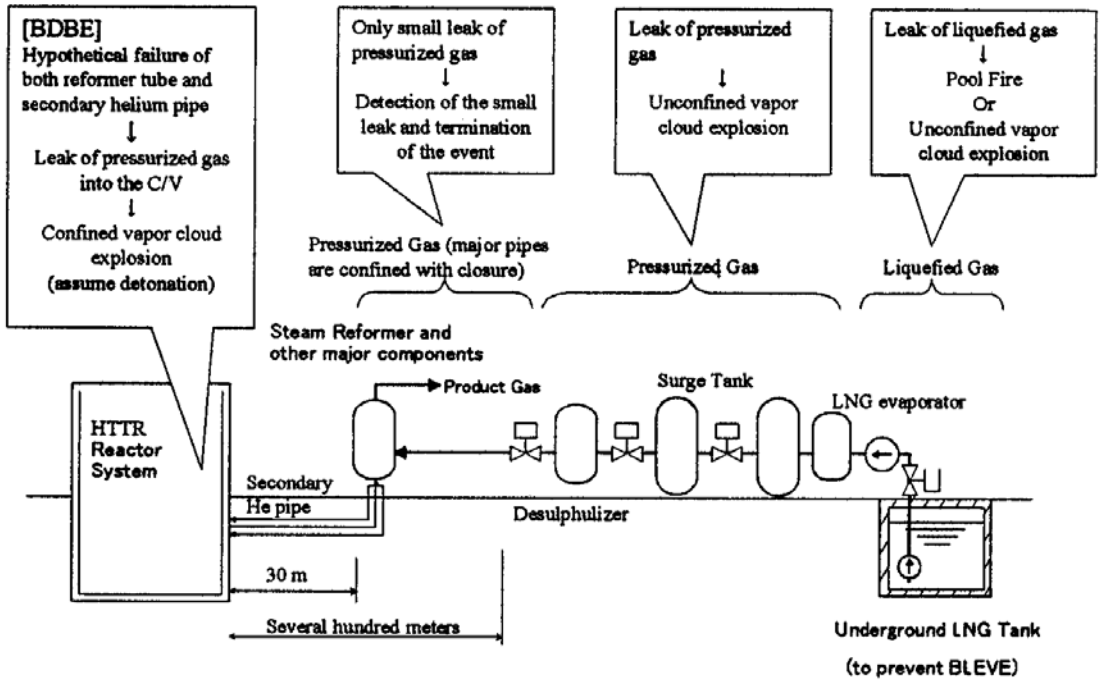

Fig. 4-5: Possible effects of fire/explosion accidents outside the reactor containment

Refueling by Truck

The frequency of accidents with involvement of trucks carrying hazardous substances is approximately the same as for trucks with other usual cargo. However, their significant damage potential is revealed in accidents with the release and spreading in the environment. According to a conservative estimation valid for Germany, the event frequency is two tank truck accidents per year with potential of a large damage (in the order of 100 million German Marks) [Gwehenberger 1999].

4.3. Safety and Risk Assessment

4.3.1. RISK METHODS IN THE REGULATION OF NUCLEAR POWER

The original regulatory process in most countries appears to be largely based upon deterministic criteria where the intent was to ensure safety with multiple layers of defense-in-depth. Design basis accidents (DBA) were defined and safety systems incorporated into the design to respond to these accidents.

As a result of the accidents at Three Mile Island and Chernobyl, most countries have taken additional steps to control the risk from core damage accidents. In some countries, risk methods have been incorporated into the regulatory process either by rules or by providing regulatory guidance. In some cases, this has resulted in plant modifications or changes in procedures. High-level quantitative safety goals, which define an acceptable level of safety have also been established in some countries. All of these goals have a probabilistic basis and in some cases involve deterministic considerations.

Most countries adhere to the IAEA Level-1 PSA guidelines. Many countries maintain their own expertise to produce and review PSA, although there are common interests in particular areas such as collaboration on data exchange, criteria and standards. Severe accident studies (probabilistic and deterministic) are being performed in all countries even though they are not required in most countries by the regulations. For most countries the studies are used to identify potential design improvements and as a basis for developing severe accident management (AM) strategies. Most countries also believe that external events and all operating modes should be considered. Extended PSA models including external events and internal fires require validation and refined physical modeling for key phenomena. Data bases for fire safety analysis need to be improved.

For future reactors, most countries are requiring the consideration of severe accidents in the design process and a PSA is usually required. Some countries also require design features to address specific severe accident phenomena. Methodology is under development for the quantification of the reliability and failure modes of programmed systems including the problem of software reliability [INSC 1998, OECD-NEA 2001].

Several computer codes exist for the simulation of fire growth and spreading, dispersion, and fire/water spray interaction. Further efforts are needed in refined modeling of certain phenomena such as heat release or flame spreading in cables and equipment. Also fire data bases need to be improved. An IAEA fire safety project assembles fire experience and produces guidelines for fire hazard analysis and inspection of fire protection and fire fighting techniques [OECD-NEA 2001].

4.3.2. SAFETY PRINCIPLES IN THE CHEMICAL INDUSTRIES

Since the first comprehensive risk study, WASH-1400, in the nuclear area in 1975, numerous safety and risk assessments have been conducted, particularly in the chemical and petrochemical industries, among them the classical studies on Canvey Island (UK) [Canvey 1978] and Rijnmond (near Rotterdam, The Netherlands) [Rijnmond 1982], in which for a whole region all industrial establishments with relevant hazardous potential were included.

Despite the many lessons learned from fire and gas explosion accidents, additional measures can be taken to further reduce the risk of severe consequences: safety management, safety and risk analysis. The safety and risk analysis of a system includes hazard identification, accident scenario development and frequency estimation within the probabilistic part as well as the simulation of accident situations and the evaluation of the consequences within the deterministic part.

4.3.2.1. Safety Principle against Hazards from Cryogenic Spills

Leakage and spillage are the most typical causes for a fire to occur in an industrial process plant following the failure of a system component. The basic principle to avoid the spillage of a cryogenic liquid is to pay proper attention to operating procedures and maintenance schedules. A particularly important role plays the instrumentation. Gas detectors and temperature sensors would be able to identify a release of LNG. Storage tanks would be normally equipped with multi-level sensing devices to be maintained either regularly or permanently during any transfer

operation. Multi-tier alarm systems would be linked to an automatic isolation of the tank fill line. Exposed sections of pipe work could be protected physically by respective housings or by use of double-integrity pipes.

Furthermore specific items need to be protected against contact with the cryogen to avoid rapid cooling, shrinkage and transition to the brittle state at low temperatures. This could be given by preparing preferred leak paths to channel the liquid from around potential leak locations to safe areas. Other measures may be shields between source and target.

Condensation of an unwanted substance can present a hazard in work with cryogenic systems. Mechanical hazards may arise from

- Plugging of pressure relief valves or pipes;
- embrittlement;
- stresses due to thermal contraction;
- erosion of valve or gasket material.

4.3.2.2. Defense-in-Depth Principle for Explosion Protection

Integrated explosion protection means that protection measures are taken in a graduated order:

(A) Primary Explosion Protection: Prevent formation of explosive atmospheres

- Substitution of burnable by unburnable substances;
- Inerting (Systems with LNG shutoff valves can be equipped such that in case of a leakage through the valve, nitrogen would into the system rather than LNG out.);
- Different kinds of venting through flare stacks, technical venting;
- Purging;
- Gas detection devices;
- Protection against leakage by period retesting and recertification;
- Purging the substances from the system before cooling;
- Keeping system pressure above ambient pressure, if possible;
- Thermal insulation;
- Keeping all air out of the system or area;
- Storage of liquids in closed containers or systems.

(B) Secondary Explosion Protection: Exclude ignition sources

- Identify all ignition sources and define the requirements for either zone;
- Use inert gas in the atmosphere instead of air.

Fire protection extinguishing and suppression efforts include shutting fuel supplies to the location.

(C) Tertiary Explosion Protection: Mitigate consequences of an explosion

- Design to sustain maximum overpressure;
- Relief into non-dangerous areas outside (rupture disk);
- Explosion suppression, introduction of extinguishing substances;
- Precluding air from entering the environment;
- Cooling the liquid to stop evaporation.

In environments prone to explosions, explosion suppression systems are installed instead of or in complement with automatic sprinklers and explosion testing.

The need of explosion protection, in particular in the modern chemical industries, requires adequate tools for a reliable assessment of the consequences of explosive hazards. A result of this philosophy was, e.g., the design of a 30 kPa pressure-resistant central control station, which is now standard installation in the chemical industries in most industrialized countries.

4.3.2.3. Safety Distances

A safety distance is the required distance between the location of a gas leakage and the object to be protected which takes account of the evolving flammable atmosphere as well as of the pressure and heat wave resulting from a possible ignition. The distance can be fixed according to physically defined criteria, e.g., the dose of thermal radiation or the peak overpressure, to have reach a certain threshold value. A minimum safety distance is desirable for economic purposes.

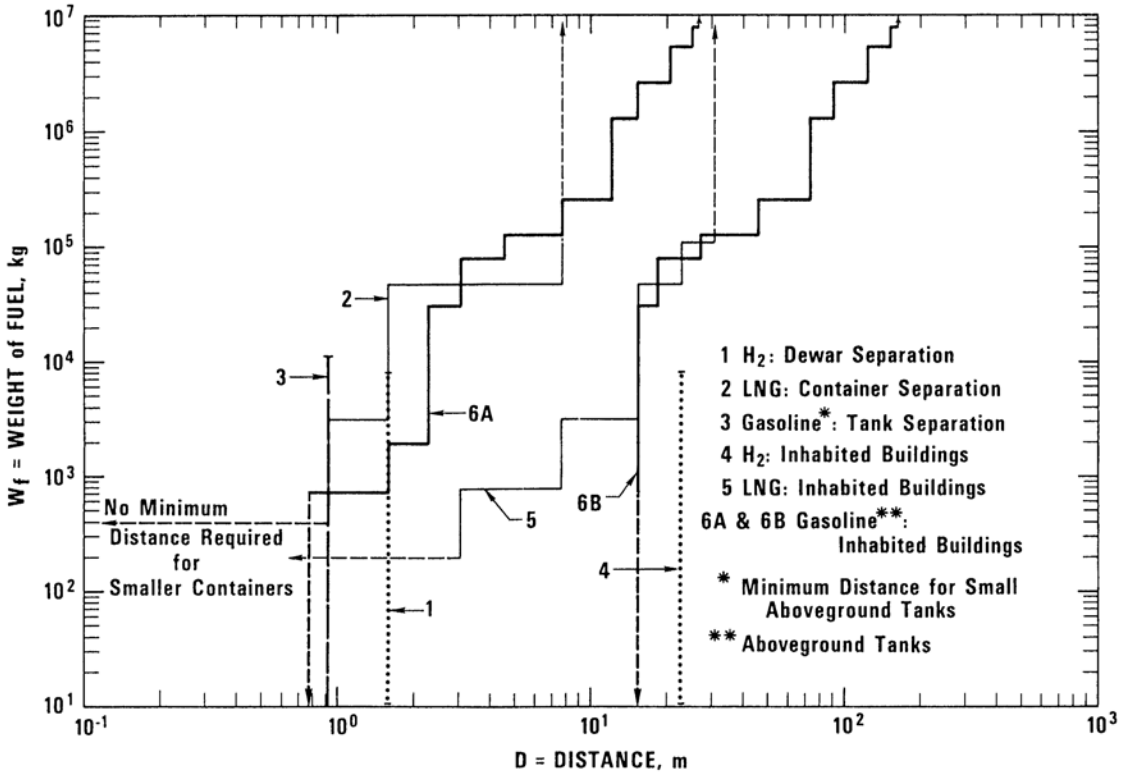

Fig. 4-6: Industrial storage standards for H_2, LNG, and gasoline

A basic prerequisite is the knowledge of the source term which is dependent on leak size and thermal dynamic conditions of the leaking substance. A problem is given by non-quantifiable leakages, e.g., from cracks in welding seams Quantity-distance relationships are usually different for people and equipment and they are different for experimental and storage areas. Industrial storage standards for hydrogen, LNG, and gasoline are given in Fig. 4-6 [Hord 1978].

Safety zones around storage tanks for liquefied gases according to the German law are shown in Fig. 4-7 for both above-ground and underground tank arrangement [Westfalen-Gas 2001].

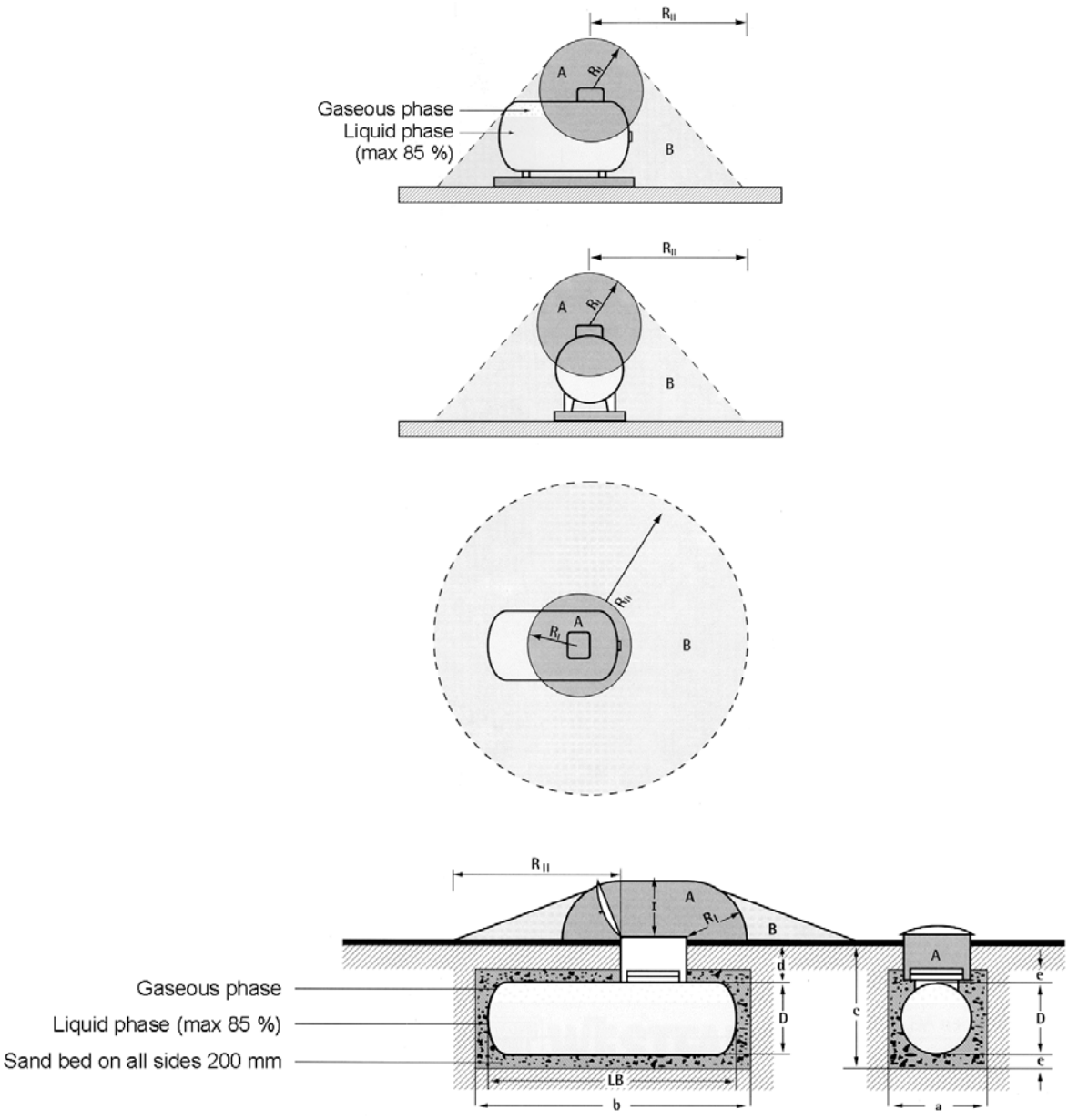

Fig. 4-7: Schematic of safety zone arrangement for above-ground (top) and underground (bottom) storage tanks for liquefied gas. No ignition sources are allowed in zones A and B. Entering and passing through is prohibited in zone A during operation, in zones A and B during the filling process. R_I = 1 m; R_{II} = 3 m.

A formula for the safety distance is generally acknowledged to have the form

$$R = k * M^{1/3}$$

where R is the safety distance in m and M the mass of the flammable substance in kg. The relation may be modified by damping parameters, if some sort of protective measure is applied, e.g., wall or earth coverage. The k-factor depends on the building to be protected (from German recommendations: 2.5 - 8 for working building, 22 for residential building, 200 for no damage) and on the type of substance.

The detonation of a mass M results in a maximum overpressure of 30 kPa in a distance of r according to the above equation for a k-factor of 8.

4.3.2.4. Fire Protection

Since a major fire in an NPP might result in an uncontrolled release of radioactive material or threaten the safe shutdown and cooling of the reactor, a comprehensive fire protection program must be planned in close cooperation with fire technical experts and the public fire authority. The program should include:

- the assessment of the direct danger of fire damage and the consequences through contamination of the environment or through damage by corrosion or smoke;
- the establishment of preventive measures with the aim of minimizing the fire loading, preventing a fire outbreak, localizing the damage, limiting the fire spread;
- the preparation of fire fighting equipment and the measures to be taken upon an outbreak of fire.

A fundamental principle in the field of fire protection is that of compartmentation, i.e., the subdivision of the plant into single fire areas in order to avoid the spreading of the fire. Respective floors, walls, ceilings should have a minimum fire resistance of three hours or more, if required by national practice.

Furthermore plants should be designed such that the fire loading is insignificant, particularly in areas containing reactor safety equipment, e.g., control room. This can be achieved by reducing the amount of combustible materials and maintaining it at a minimum level, by a wise selection of building materials, and by designing systems for storing, controlling and, in case of a leakage, draining combustibles.

For early fire detection and effective fire fighting, each fire area should be covered with a fire detection and alarm system specifically engineered for fire risks in that area. Fire water supply systems should be designed to ensure an adequate supply of water in any conceivable situation.

4.3.3. PRINCIPAL HAZARDS ASSOCIATED WITH LNG STORAGE

4.3.3.1. LNG Storage Tank

Principal Design

A key component is the storage tank, since it usually contains the largest quantity of a hazardous material separate from the process. A major part of losses in the industry is given by

losses through fire in storage. Storage is pertinent to plant siting and layout. The segregation of process plant and storage reduces the risk of losing both installations in case of an accident.

A typical LNG tank is designed (see Fig. 4-8) as a double-walled tank. The outer tank is in the form of a prestressed concrete containment and serves as protection of the inner tank against impacts from outside as well as of the neighborhood, if the inner tank fails. The inner tank is made of steel, 8% Ni steel is appropriate for cryogens. The sheet thickness decreases reaching a minimum at the top. A thermal insulation is between inner and outer tank to minimize heat transfer. It consists of a perlite filling and a multilayer foam glass liner system attached to the inner surface of the outer tank. Elastic matting serves to take up the tank movement caused by thermal contraction. Heating in the base slab serves to avoid a freezing of the ground. Properly designed base isolators, on which the tank is placed, allow for largely reduced stresses, e.g., those imposed following an earthquake.

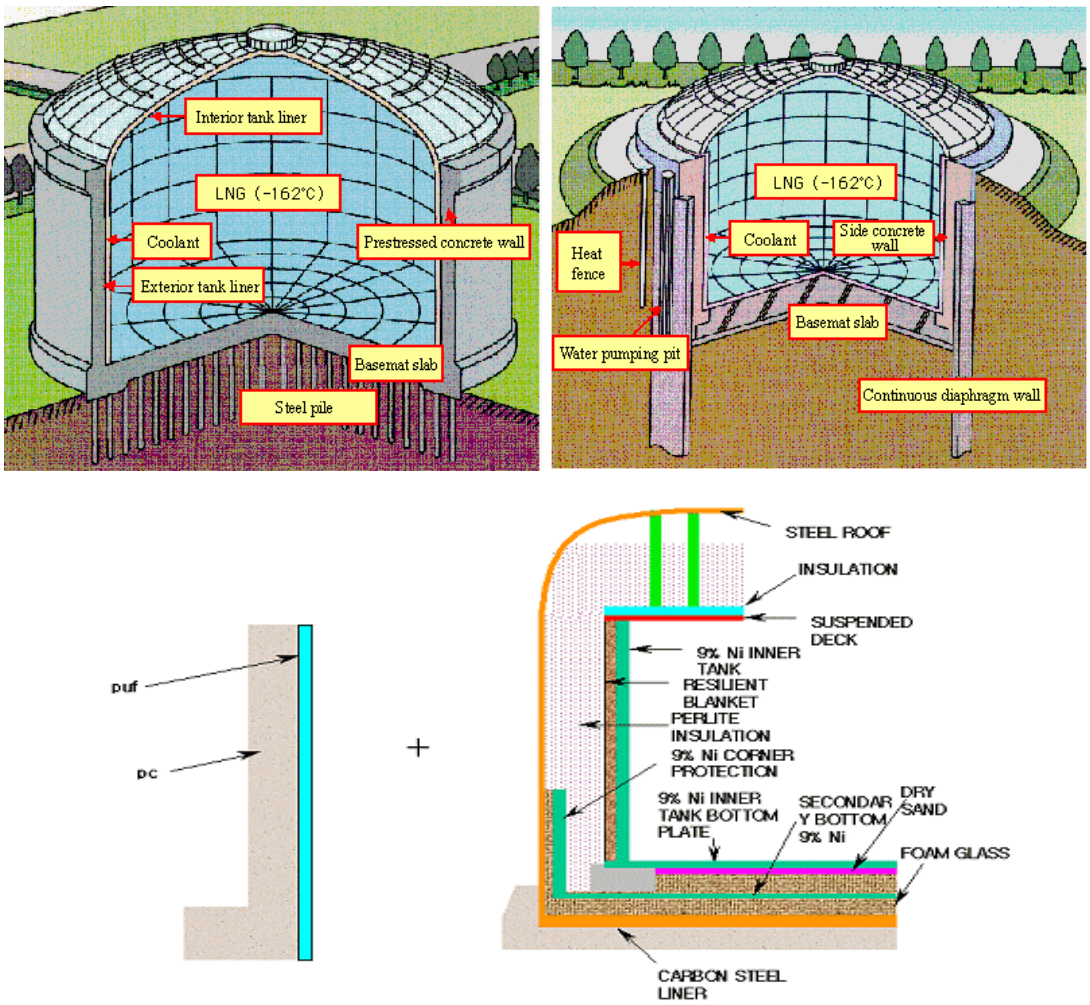

Fig. 4-8: LNG storage tank schematics

Pressurized LFG storage tanks > 100 m^3 are designed to withstand outside temperatures of 40 °C of a hot summer day. The design pressure should be greater or equal 110 % of the maximum operating pressure or 100 % plus 0.1 MPa. Maximum and minimum design

temperatures are determined by the loss of strength of the storage walls at the higher end and by loss of ductility (embrittlement) at the lower end. A relief valve should be designed as to handle abnormal operating conditions such as overfilling; it should open at a pressure less or equal the design pressure and allow a relief such that the pressure does not rise beyond 110 % of the design pressure. The relief discharge should be preferably into a closed system.

Therefore a strong focus has been laid upon the proper design of a respective storage facility. The tank to hold a cryogenic liquid requires an effective insulation to minimize the amount of heat to penetrate the tank from outside and reduce unavoidable boil-off losses.

Underground LNG tanks

The utilization of small underground LNG tanks has some significant advantages, but also raises some technical questions:

- Reduced installation time;
- Shorter piping meaning smaller risk of accident;
- Compactness, meaning smaller site area (smaller footprint);
- No impoundment system required;
- No risk to the tank from fire, protected against thermal radiation;
- Vapor dispersion and heat radiation zones can be reduced;
- Installation in more densely populated areas possible;
- Lower requirements to venting rate of safety relief valve;
- Corrosion from outside;
- Freezing of soil;
- Very long cool-down time and attendant high boiloff loss, if not internally insulated.

Comparing the risks between earth-covered and aboveground storage tanks, it is estimated that the risk in accidents with aboveground storage tanks is significantly greater in larger ranges > 30 m, whereas in the near range, both risks are at about the same level.

Storage facilities constitute a much greater potential fire hazard than the process units. Therefore, a sufficient separation should make sure that vapor escaping from the storage site is not ignited at the process site.

Fig. 4-9 describes incidental/accidental situations typically considered for propane storage tanks, certainly not significantly different from LNG storage tanks including temperature load cases (upper row in the figure). The dynamic load cases (lower row) describe the conditions for an earthquake, a gas cloud explosion, and the (vertical) zip effect of a tank rupture. In the latter case, the liquid is expected to be released into the gap between inner and outer tank, developing two waves creating locally a six times higher dynamic pressure pulse, when clashing together on the opposite side of the crack, than the hydrostatic pressure. In total, as many as 70 single effects on a storage tank have to be considered [Holzmann 1986].

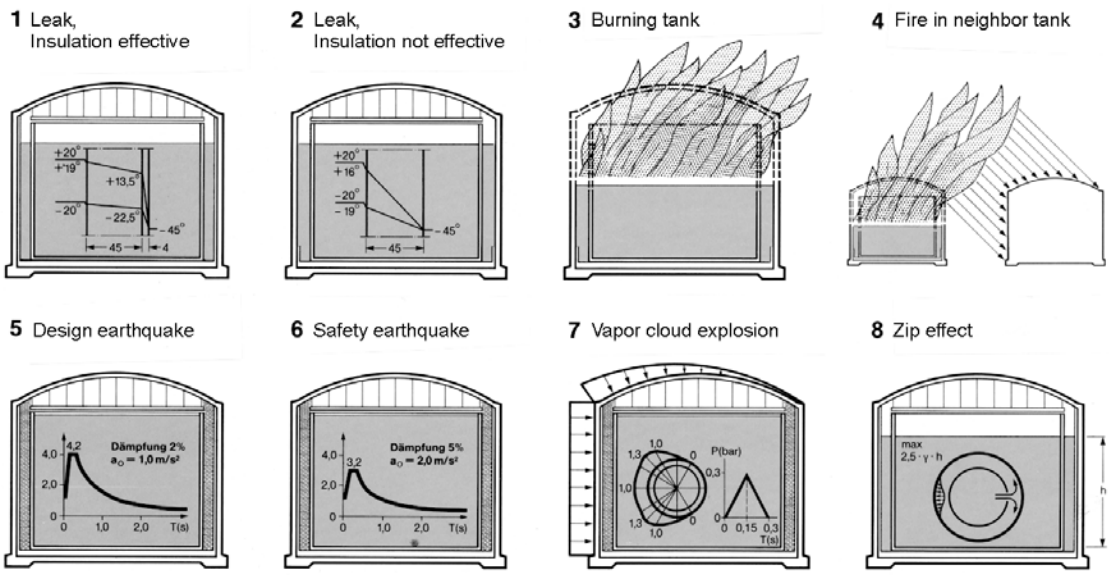

Fig. 4-9: Safety concept for storage tanks, assumption of special load cases

4.3.3.2. LNG Tank Rollover

The so-called "rollover" is a well known phenomenon that may occur in an LNG storage tank and be a concern because of increased vapor production rates. It describes the effect of stratification due to heat input in the bottom portion of the tank contents, which rises to the surface at a temperature that can be higher than its thermodynamic equilibrium point and eventually liberating a larger quantity of vapor resulting in an abnormal pressure increase and possibly a venting through the safety relief valves. A stratification of the LNG in the tank can also occur, if LNG is loaded into a tank with some residual liquid, which may have different densities, or if the refillings of LNG are from different sources with different compositions. During long storage periods, the aging effect of LNG, by which the methane tends to boiloff first compared to the heavier components of the natural gas, also results in stratification. The more homogeneous the liquid, the lower is the probability of a rollover.

4.3.3.3. Release Behavior

If the pressure in an LNG tank is kept constant, i.e., the vapor boiloff being removed, the temperature also remains constant (auto-refrigeration); if the boiloff is not removed, both temperature and pressure will rise.

If there is heat input in a confined volume of a cryogen, the pressure will rise. The container will eventually rupture, if no or not sufficient gas can be vented from the system. Therefore a safe and reliable relief system must be provided. At closed valve, the heat input from the outside initiates a thermal stratification, which makes the pressurization process somewhat faster than in the case of thermal equilibrium. However, the relative heat transfer into the tank is lower, the

larger the tank and the better the surface-to-volume ratio and the insulation. The speed of pressurization also depends on the boiling temperature of the cryogen. The lower the boiling point, the stronger is the driving force for heat input.

Thermal expansion of the cryogen also results in a pressure increase. Thermal expansion coefficients are higher for cryogens with lower boiling point. Therefore overfilling must be avoided.

Undesired events caused by either human error or component failure or external impact can occur during steady-state operation or during the loading/unloading process such as

- Leakage or rupture of the pressure vessel;
- Leakage or rupture of transfer lines;
- Overfilling;
- Vessel failure due to impact from outside;
- BLEVE.

According to the type of event and according to the state, in which the fluid can be stored in different states, it may exhibit a different physical release behavior, if accidentally released:

- Volatile liquid at ambient conditions showing slow evaporation;
- Flashing liquefied gas under pressure showing immediate large flashoff and slower evaporation of any residue; considered as the most serious case;
- Semi-refrigerated liquefied gas under pressure and at low temperature showing initial flash-off and violent evaporation);
- Refrigerated liquefied gas at low temperature and atmospheric pressure (initial flash-off, relatively slow evaporation);
- Gas under pressure (large physical energy release).

Reasons could be the failure of pump packing, valve packing, gaskets or the rupture of liquid gas transfer lines.

4.3.3.4. Accident Sequences

As a result of the different types of storage, several accident scenarios are conceivable for a storage tank to release its contents into the environment:

- Formation of a pool on the ground and vaporization of the liquid;
- Release of a jet stream of liquid or gas or a mixture through a small opening in a pressurized system;
- Catastrophic failure of the tank resulting from high internal pressure with the explosive-like release of the whole content.

Line rupture may result in a jet fire or an UVCE. Fire protection of storage serves the purpose to minimize hazards to personnel and loss as well as prevent a spreading of initial fire. For atmospheric storage, stationary or mobile water or foam spray systems are employed. In

refrigerated storage, it has to be considered that heating and vaporization is much more rapid. Initial protection is given by fire proof insulation to obtain a fire resistance of at least two hours.

The scale of fire/explosion on a storage tank can be very large. Fires can occur in the vapor phase of the tank or outside, when an escaping vapor cloud ignites. Causes for fires are often given due to malfunctions in the operation procedure such as overfilling, failure of instrumentation, or operator error.

Spillage into the impoundment area may form a vapor cloud that ignites and flashes back. Subsequent failures can occur once a fire is established; for example, pipework fails within approx. 15 min if exposed to fire.

4.3.3.5. Mitigation Measures

If liquefied gases are handled, plant layout should provide sufficient spacing for a vapor cloud to disperse before it can reach ignition sources and a possible explosion of the storage contents to pose a fire risk to the adjoining plant. Estimation of downwind distance as a function of atmospheric conditions and source strength.

In general, storage tanks for refrigerated liquids require an impoundment area to retain the liquid in case of a leakage, unlike substances stored in a pressurized or refrigerated state.

Separation distances for LFG are generally greater than for petroleum products. The ICI code lists recommended distances distinguishing between Class A/B liquids and LFG. Alternative approaches based on the heat (direct flame, radiation) from a burning liquid and the ignition of a vapor escape are mentioned in the code, but they are not used for distance determination.

Main safety goal is the prevention of damage to the inner container. Mitigation measures to reduce the risk of a tank loss are

- Generous spacing between tanks;
- Minimum pipework and ancillary equipment;
- Properly designed pressure relief;
- Pump installation outside bunds;
- Water spray system;
- Availability of sufficient quantity of water/foam;
- Separated bunds;
- Prevention of overfilling;
- Bachup instrumentation.

A well established LFG storage tank design comprises the assessment of the consequences of potential accident scenarios. They should be based on estimated transient release rates or design spill rates as a function of pressure, orifice, detection time, disconnection time including certain safety margins.

4.3.3.6. Safety Features

Safety in storage is a matter of both operation and maintenance and of design. Numerous codes and standards are applicable to storage. Following the defense-in-depth principle, measures should be taken in terms of

(A) Minimization of Spillage

- Reduction of storage quantity to a minimum;
- Reduction of number of connections below top liquid level to the lowest possible;
- Design of vessel and pipework according to appropriate calculation methods, materials selection and fabrication processes;
- Employment of high-level measurement and control instrumentation;
- Selection of ground with good load-bearing characteristics;
- Protection against external damage.

(B) Control of Spillage

- Provision of gas detectors;
- Safe dilution of evolving vapor cloud;
- Selection of siting with regard to prevailing wind;
- Selection of ground contours such that collection of liquid or heavy gas in a depression should not be possible;
- Employment of dispersion walls to divert large vapor flows to safer areas;
- Utilization of fire walls to provide protection against flame and heat radiation.

(C) Control of Fire

- Leakage to be drained away to an impoundment area where it can be safely burnt;
- Provision of fire-proof insulation and support;
- Provision of water cooling;
- Provision of appropriate fire fighting equipment;
- Siting of storage between process plant and terminals.

4.3.4. PRINCIPAL HAZARDS ASSOCIATED WITH LNG TANK TRUCK OPERATION

The transfer of LNG from a tank truck to a storage tank is a complex procedure and involves active participation of both truck driver and storage operator. After the truck is choked and the engine is switched off, a grounding cable is attached to the truck to ground any electrostatic discharge. A flexible liquid transfer hose is attached to the truck and purged with LNG to remove all air. The storage vessel liquid fill line and then the trailer's main liquid valve will be opened. The pressure in the trailer tank is controlled via a pressure building line where LNG is vaporized and returned to the tank to maintain a pressure differential of at least 100 kPa between trailer tank and storage vessel.

Typical safety features are remote-controlled, redundant liquid valves, storage vessel alarms in case of overfilling, long drain lines for safety-directing vented LNG vapor. Also the trailer liquid valves are interlocked with the truck brake system to prevent transfer, before the truck is properly secured. Another hazard is given by the continuous cycling of the fuel transfer equipment between cryogenic and ambient temperatures causing additional thermal stresses on equipment and sealing which could result in decreased reliability overtime.

A high potential of accidents is given during the refilling process from a tank truck to the storage tank. Here flexible hoses can be fitted with automatic disconnecting and isolating devices to protect against inadvertent movements of the truck (see Fig. 4-10).

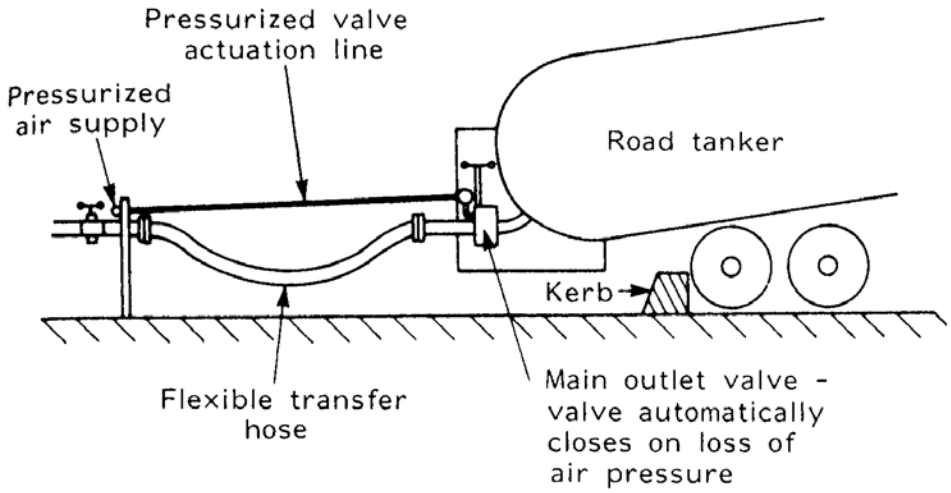

Fig. 4-10: Hose failure protection system for tank truck

Undesired occurrences during loading/unloading or operation of LNG tank trucks are:

- Wrong connection of loading arms;
- Wrong degassing of connection pieces;
- Leakage or rupture of filling line;
- Overfilling;
- Departure of tank truck during loading/unloading process;
- Crash of tank truck during transportation.

4.3.5. ACCIDENT STATISTICS ON HANDLING LIQUEFIED GASES IN GERMANY

An evaluation of accident reports involving liquefied gases for the decade 1977 - 1986 has been made by the Federal Institute for Materials Testing and Research (BAM) comprising 178 documented accidents. The analysis with respect to the type of facility shows a strong accumulation of accidents on the consumer side, in particular for pressure bottles and small storage tanks, but also not to be neglected accidents with tank trucks during transport or filling processes. A distribution according to the accident causes and consequences reveals a concentration on human and construction errors. In more than 90 % of the accidents, there was a gas release with subsequent ignition and fire/explosion observed in 80 % of the cases. A summary of this evaluation is given in Table 4-3 [Droste 1990].

Table 4-3: Causes and consequences of accidents with liquefied gas in Germany in the period 1977 - 1986

Cause of Accident	Frequency [% of 178]
Mechanical impact	10.1
Thermal impact	8.4
Corrosion (metals)	5.6
Ageing (plastic)	2.2
Gasket failure	2.2
Technical (construction) error	9.5
Fabrication error	20.8
Mal-operation	30.3
Sabotage	2.2
Others	2.2
Unknown	20.8
Consequence of Accident	**Frequency [% of 178]**
None	5.1
Continuous gas release, no ignition	14.6
Continuous gas release, ignition, fire	24.7
Continuous gas release, ignition, explosion	42.1
Instantaneous gas release, no ignition	-
BLEVE	6.2
Building collapse	13.5
Unknown	1.1

4.4. Evaluation of Consequences of Major Accidents

4.4.1. ANALYTICAL STUDIES ON THE BEHAVIOR OF CRYOGENS

4.4.1.1. Calculation Model LAuV for Cryogenic Pool Spreading and Vaporization

The state-of-the-art calculation model, LAuV, has been developed at FZJ, which allows the description of the transient behavior of the cryogenic pool and its vaporization. It addresses the relevant physical phenomena in both instantaneous and continuous (at a constant or transient rate) type releases onto either solid or liquid ground. A system of non-linear differential equations that allows for description of pool height and velocity as a function of time and location is given by the so-called "shallow-layer" equations based on the conservation of mass and momentum. Heat conduction from the ground is deemed the dominant heat source for vaporizing the cryogen, other heat fluxes are neglected. The friction force is chosen considering distinct contributions from laminar and from turbulent flux.

The code was validated against cryogen (LNG, LH_2) spill tests from the literature and against own experiments with the release of liquid hydrogen. The post-calculations have shown a good agreement between the computer simulations and the experimental data. These validation calculations demonstrated the code's ability to realistically simulate the initial phase of an accidental release of a cryogenic liquid and to provide an adequate source term for the subsequent analysis steps for dispersion and combustion of the flammable gas cloud.

4.4.1.2. Comparison of LNG Spill Experiment with Computer Models

One of the experiments conducted by British Gas with the release of LNG has been used in [Dienhart 1995] to compare the measurements with the prediction by respective computer models, which have been developed to simulate such accidental cryogen spill events, the British code GASP and the German code LAuV [Dienhart 1995].

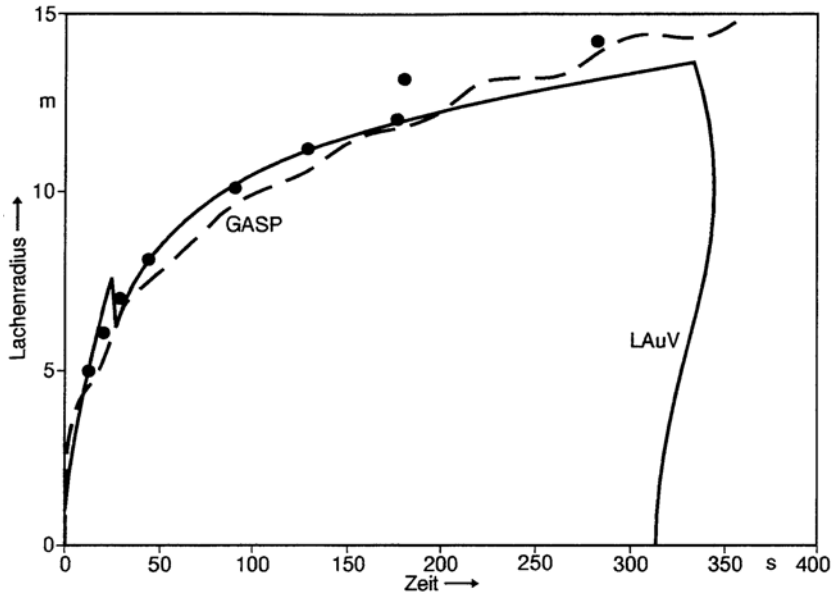

Fig. 4-11: Comparison between LNG spill experiment on dry concrete and calculations with the German LAuV code and the British GASP code

The boundary conditions of the test considered were dry concrete as ground, a spill time of 300 s, and a released quantity of 2.5 m^3 of LNG corresponding to a gradually decreasing release rate between 47 and 37 l/s. Measurements and calculational results given in Fig. 4-11 show the maximum radius of the LNG pool develops to approx. 13 m. About 10 s after spill termination, t = 310 s, the pool is predicted to break up from the central spill point, forming a ring-shaped pool, which recedes from both inside and outside, until at t = 350 s, it has completely died away. The measurements refer to the outer pool radius, no experimental information is available for the inner radius. The experimental data are in pretty good agreement with the model calculations.

4.4.1.3. Prediction of LNG Release Behavior from a Larger Storage Tank

Within the joint German/Russian "Cryoplane" project, the feasibility of a cryogenic propulsion system with LH_2 and LNG as fuel for an aircraft is being investigated since 1990. The hydrogen version of an Airbus A310-300 as the baseline aircraft is designed to be equipped with four large fuel tanks containing a total quantity of 240 m^3 (2 x 80 plus 2 x 40 m^3). The corresponding LNG version would have a total storage capacity of 90.5 m^3 (30.2 m^3 for one large tank) of LNG based on the assumption of identical energy content.

In a theoretical study on the accidental spillage of the LNG from the storage tanks, the pool spreading and vaporization behavior was investigated [Dienhart 1995]. The predicted LNG behavior is shown in Fig. 4-12 for the instantaneous release of 90.5 m^3 and 30.2 m^3, compared with the continuous release of 30.2 m^3 at a constant rate over 40 s.

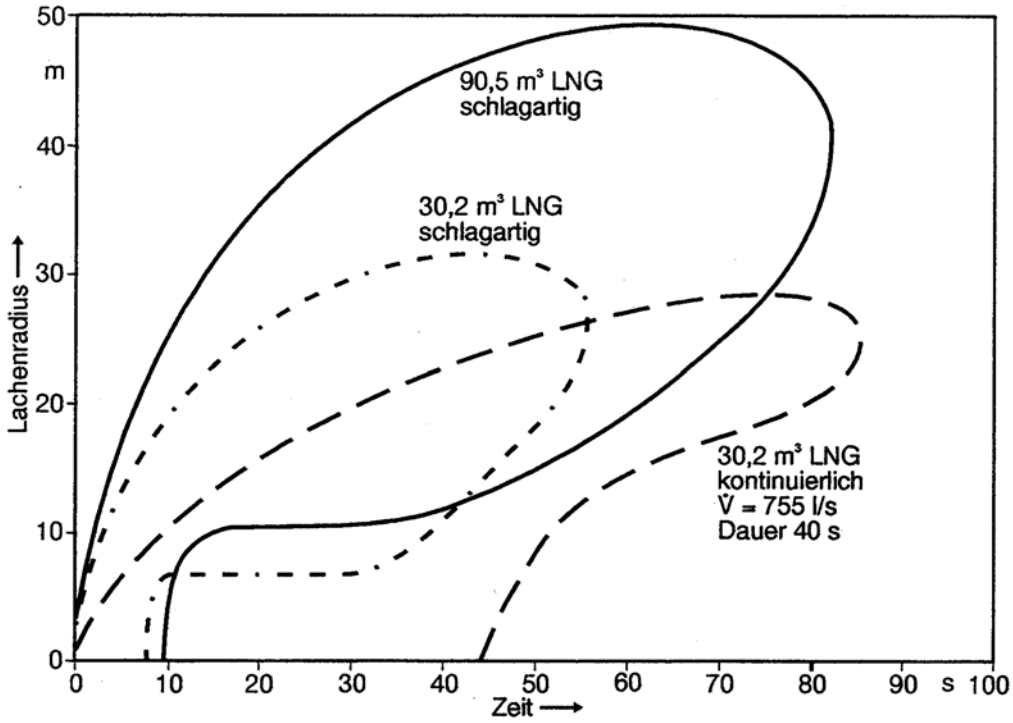

Fig. 4-12: Prediction of LNG accidental release from an aircraft tank

In case of the instantaneous release, an early breakup of the pool at the central spill point takes place after 7 s and 9 s, respectively. The outwards spreading LNG ring pool reaches a maximum radius of 32 m after 40 s and 50 m after 60 s for the 90.5 m^3 spill. The total life times of these pools are 56 s and 82 s, respectively. The continuous release of LNG at a rate of 755 l/s develops a slower growing pool, which breaks up 5 s after spill termination at t = 45 s and reaches at t = 75 s a maximum pool radius of 28 m, only slightly smaller than in the instantaneous case; however, its life time is expected to be 85 s and thus 30 s larger than for an instantaneous spill.

4.4.1.4. Comparison of Cryogen Spills from a Tank Truck

Another predictive study with the FZJ code LAuV has been conducted, in which the behavior of cryogenic liquids, LH_2, LN_2, LOX, LNG, was compared to demonstrate the differences in the spreading behavior. The case assumed is the complete release of a tank truck load of 40 m^3, either instantaneously or continuously at a rate of 1 m^3/s on solid ground (macadam). The results of maximum pool radius, vaporization time, and maximum vaporization rates are summarized in Table 4-4. The pool radius as a function of time elapsed after release of all four liquefied gases is given in Fig. 4-13 and Table 4-4 for the case of a continuous release over 40 s (top), and for the case of an instantaneous release (bottom).

Table 4-4: Predicted pool radius, vaporization time, and vaporization rate after a 40m^3 instantaneous / continuous spill on solid ground

Cryogen	**LH_2**	**LN_2**	**LOX**	**LNG**
Instantaneous release of 40 m^3				
Maximum pool radius [m]	20	32	38	38
Vaporization time [s]	13	48	63	65
Maximum vaporization rate [m^3/s]	4.0	1.2	0.9	0.8
Maximum vaporization rate [kg/s]	280	970	910	340
Continuous release of 40 m^3 at a constant rate, spill time 40 s				
Maximum pool radius [m]	12	26	37	33
Vaporization time [s]	45	84	55	94
Maximum vaporization rate [m^3/s]	1.0	0.6	1.0	0.5
Maximum vaporization rate [kg/s]	70	480	1140	220

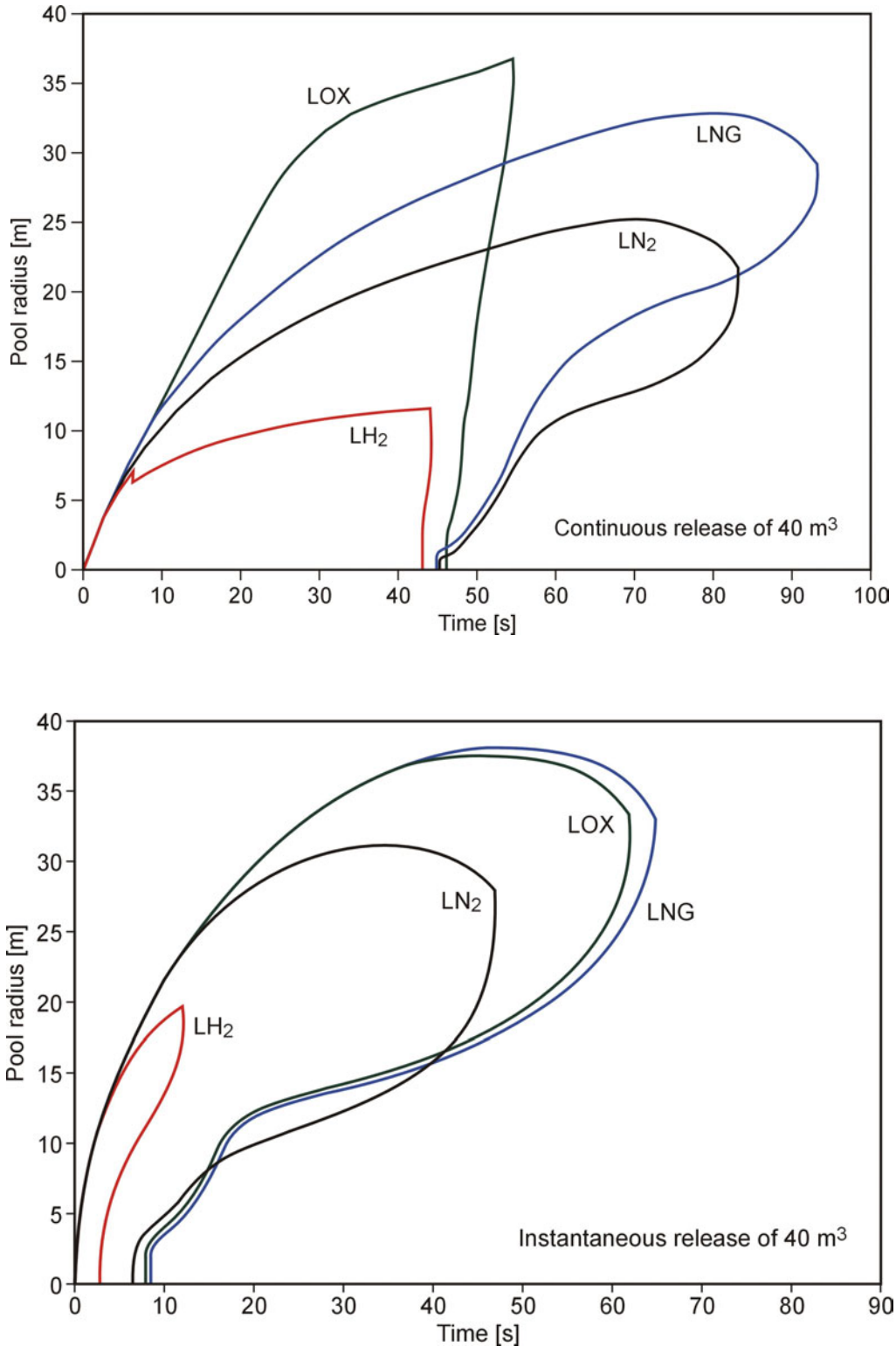

Fig. 4-13: LauV prediction of the spreading behavior of an LH_2, LN_2, LNG, and LOX pool, respectively, after a 40 m³ spill onto solid ground (macadam)
(top) continuous release, (bottom) instantaneous release

A remarkable difference is the small size and the short lifetime of the LH_2 pool compared to the other cryogenic liquids due to their higher densities causing a larger gravitational force. With a maximum radius of about 20 m after the instantaneous spill, the LH_2 pool covers a surface are which is by a factor of 4 smaller than the respective LOX and LNG pools, and vaporizes within 13 s while the corresponding periods of time for LOX and LNG are larger by a factor of 5. LN_2 takes a somewhat intermediate position corresponding to the lower latent heat of vaporization per m³ liquid compared to LNG and LOX. In the continuous case, LOX with the largest density develops by far the largest pool and thus exhibits a maximum vaporization rate even similar to LH_2. The liquid pool with the largest lifetime is again LNG.

4.4.2. EXPERIMENTAL AND ANALYTICAL STUDIES ON EXPLOSION HAZARDS WITH PROCESS GASES

4.4.2.1. Prediction of Combustion Behavior of H_2-CO-He Mixtures in Hypothetical AVR Water Ingress Accident Scenario

For the German small-size HTGR in Jülich, AVR, the hazardous potential of a H_2-CO-He-air mixture, which might develop in a conceivable water ingress accident from the corrosive reaction between steam and hot fuel element graphite, was analyzed [Wischnewski 1971]. Ignition experiments in a 120 l combustion chamber with gas mixtures of different H_2+CO concentrations have shown that mixtures with up to 22 % fuel concentration were not flammable at temperatures up to 120 °C. The fuel concentration estimated to occur during this accident scenario was 8 vol%.

4.4.2.2. FZK Detonation Experiments with H_2-CO Mixtures with Air

At the Research Center Karlsruhe (FZK), an experimental program has been started in the 12 m Hydrogen Combustion Test Tube Facility to investigate the combustion behavior of H_2-CO-air mixtures and to quantify the influence of CO concentration on the combustion process of the H_2-CO-air mixtures under different conditions [Breitung 2000]. FZK experiments performed so far concentrated on the turbulent combustion in fully confined, partially obstructed geometry. To this end the tube was equipped with an array of obstacles of a blockage ratio (BR) 45 % and a distance of 0.5 m. Mixture composition and initial pressure are the parameters the test series.

H_2-CO-air mixture experiments have been performed with 11 % and 18 % fuel gas concentration, the results are presented in the v-x diagrams as given in Fig. 4-14. Replacing half of the H_2 by CO (5.5 % H_2 + 5.5 % CO = 11 % fuel gas) (Fig. 4-14 top) results in a subsonic flame (< 200 m/s), without any acceleration, in contrast to the combustion of pure hydrogen in air, which reaches after an acceleration phase the regime of a choked flame (500 - 700 m/s flame speed). Some influence of the initial pressure can also be observed. An increase of the initial pressure (0.05, 0.1, 0.2 MPa) leads to a decrease of the flame speed and finally results in an unstable flame propagation due to local flame quenching near the end of the tube.

Analogous experiments with 18 % fuel gas concentration reveal a different picture in the v-x diagram (Fig. 4-14 bottom). The combustion of pure H_2 causes a rapid flame acceleration up to the quasi-detonation regime, while more moderate and longer lasting acceleration up to detonation speed is the outcome of the experiments with 9 % H_2 and 9 % CO. The influence of

a initial pressure rise (0.05, 0.1, 0.2 MPa) is noticeable only at the beginning of the experiment through a faster acceleration of the flame front with increasing pressure.

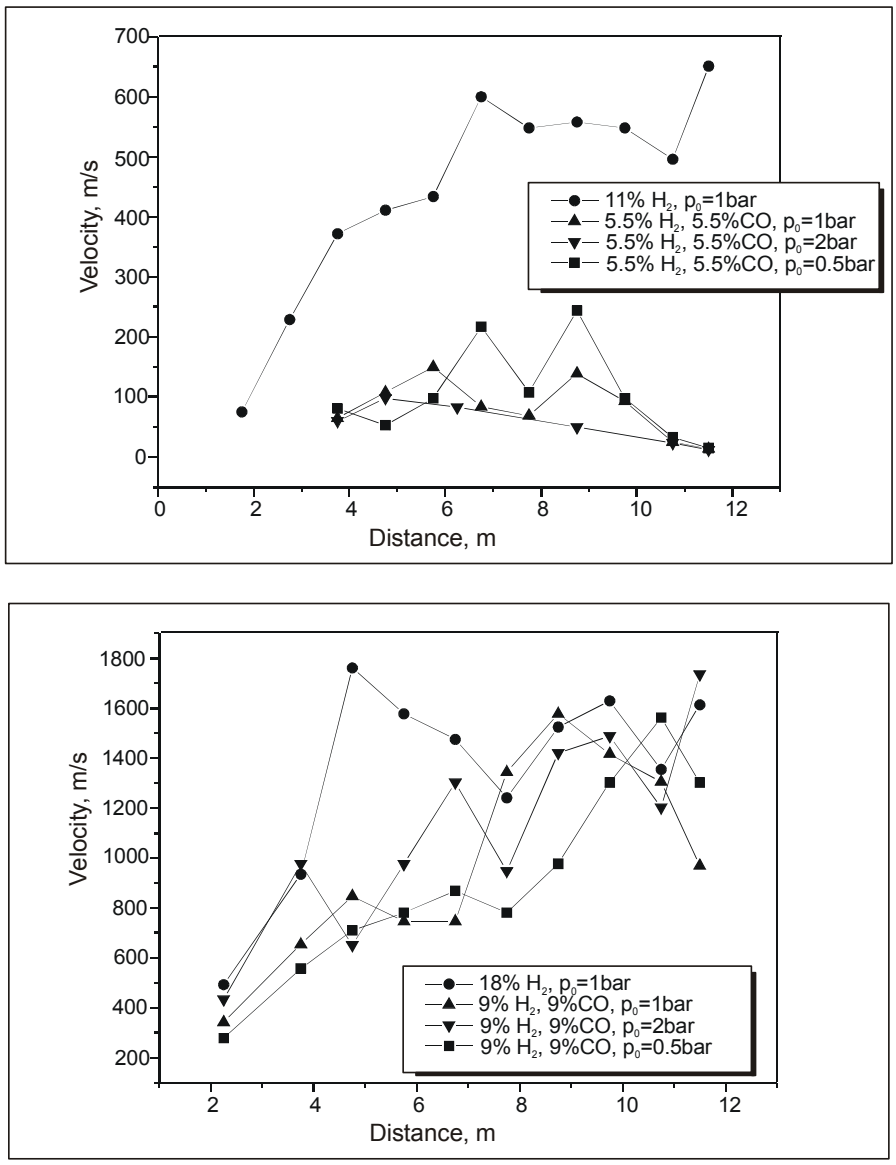

Fig. 4-14: Flame velocity vs. detonation tube length with 11 % (top) and 18 % (bottom) fuel (H_2 + CO) gas

The results obtained so far clearly demonstrate a damping effect of CO on the turbulent combustion speed of H_2-CO-air mixtures when compared to turbulent combustion in pure H_2-air mixtures. This effect, is probably caused by the relatively long induction and reaction time of the complicated oxidation mechanism of CO. This process requires as an initiating component OH-radicals, which have to be provided in a sufficient amount by the H_2 oxidation. The resulting time delay between hydrogen and CO oxidation could be detected in the H_2-CO-air experiments with the installed photodiodes, which showed two spatially separated flame zones moving along the tube.

With respect to safety analysis, the mitigation effect of CO additions on the observed flame speed and the resulting pressure loads should be taken into account. Treating CO simply as H_2 in the analysis would lead to more than conservative load estimates.

4.5. Hazard Prevention, Control, and Mitigation Measures for the HTTR/SR System

4.5.1. OUT-OF-PILE TESTING

4.5.1.1. Design of Test Facility

Prior to the connection of the steam reforming system to the HTTR, the process will be tested in out-of-pile experiments under simulated nuclear conditions [Miyamoto 1998]. The objective of these tests is the verification of

- the performance of the HT components steam reformer, steam generator, and isolation valves including the hydrogen productivity;
- the technology for operation and control;
- the absorbing effect of the steam generator for thermal disturbances;
- the durability and leak tightness of the HT isolation valve.

For this purpose, a 1:30 downscaled mock-up facility has been constructed. A flow scheme of the out-of-pile test facility is shown in Fig. 4-15. A comparison of the design specifications of this out-of-pile experiment with the HTTR steam reforming system is given in Table 4-5.

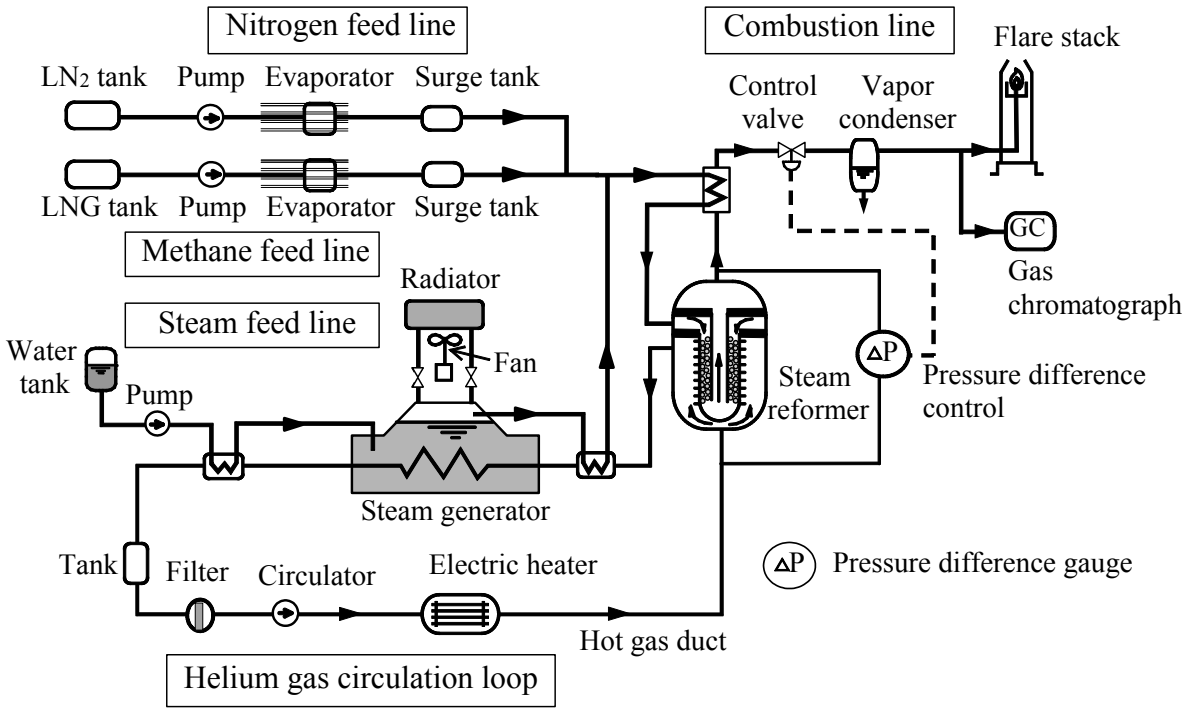

Fig. 4-15: Out-of-pile steam reforming test facility

Table 4-5: Comparison of operation parameters of the steam reforming systems for the HTTR and in the out-of-pile test facility [Ohashi 2004]

Parameter	Steam reforming system	
	Out-of-pile facility	**HTTR**
Heat source [MW]	0.42	10
Pressure process gas [MPa] secondary helium [MPa]	 4.5 4.1	 4.5 4.1
Inlet/outlet temperature of steam reformer process gas [°C] secondary helium [°C]	 450 / 600 880 / 650	 450 / 580 880 / 585
Secondary helium flow rate [kg/h]	327.6	9070
Natural gas input [kg/h]	43.2	1400
Steam-methane ratio	2.5 - 4	3.5
Hydrogen output [Nm^3/h]	120	4240
Material of reaction tube	Alloy 800 H	Hastelloy XR

The test facility simulates the process downstream from the IHX. It consists of a helium circuit representing the secondary helium loop, and feed lines for steam and methane. In addition, a nitrogen line is needed to control the pressure difference between helium and process gas. A combustion line is used to flare the generated hydrogen.

The nuclear heat source is simulated by a 420 kW electrical heater to provide helium gas of 880 °C at the steam reformer inlet. The process gas pressure is controlled by a control valve installed downstream the steam reformer, monitoring the pressure difference between helium and process gases. The steam reformer consists of three bayonet-type reforming tubes made of Alloy 800 H and containing the catalyst at a length of approx. 3.5 m. Disc-type fins with 2 mm in height, 1 mm in width, and 3 mm in pitch are arranged around the catalyst tube in order to enlarge the heat-transferring area by a factor of 2.3 compared to a smooth surface, and to increase the heat transfer coefficient of the helium gas to a value of 2150 W/(m^2 K).

The steam generator of a kettle type is composed of 27 heat exchanger tubes allowing a thermal power transfer from the helium to the water of 135 kW at rated condition and 251 kW under the condition of a loss of chemical reaction. An HT isolation valve of an angle type is installed in the HT section at the helium pipe work.

4.5.1.2. Out-of-Pile Test Program

The test program planned to run over four years has been starting in 2002. It comprises normal startup/shutdown tests to investigate temperature and pressure fluctuations and its controllability as a function of the steam-methane ratio, in order to optimize feed flow of methane and steam according to temperature and pressure of the helium gas. In a system controllability test, potential thermodynamic disturbances at the pressure boundary between helium and methane are examined by the stepwise change of the methane and steam flow rates, in order to optimize the control system for the pressure difference.

Furthermore safety-related tests to examine malfunctions and accidental sequences in the process gas line including emergency shutdown. The goal is that in case of an accident in the process line, the HTTR should be shutdown by the normal operation procedure rather than by a reactor scram. In such a case, the heat of the helium is to be removed via the steam generator, which limits the temperature fluctuations in the helium.

4.5.1.3. First Test Results

Performance tests have been conducted between October 2001 and February 2002 to check the ability of hydrogen production and controllability of the experimental facility. The test of the system controllability was made to investigate the transient behavior of the gas flows in case of a loss of chemical reaction, i.e., the disconnection from the methane feed flow (see Fig. 4-16) [Ohashi 2004].

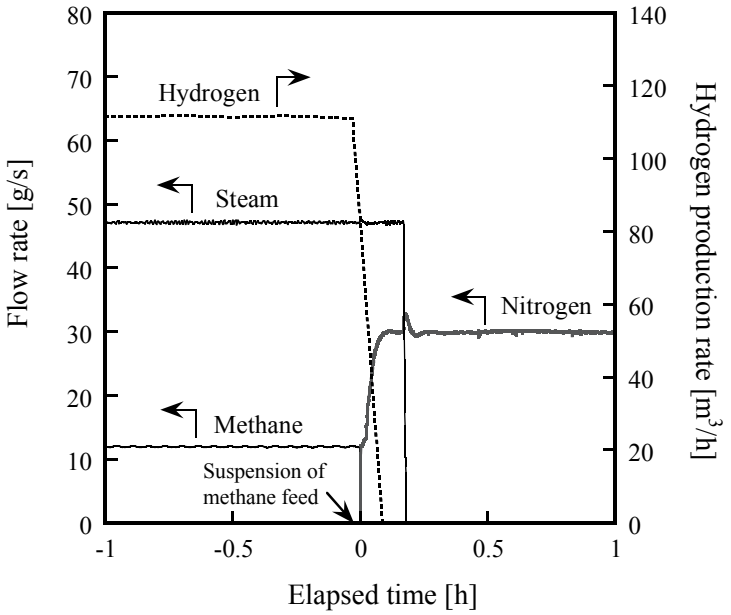

Fig. 4-16: Flow rates of methane, steam, nitrogen, and production rate of hydrogen during the system controllability test

Nominal flow rates were 12 g/s of methane and 47 g/s of steam, when – at time 0 – methane feed, and thus hydrogen production, was shut off. The helium temperature at the SR outlet increased from 611 °C and stabilized at around 800 °C after 1.3 h. At the same time, the temperature at the inlet was raised from 531 to 762 °C. Helium temperatures at the steam generator outlet were observed to fluctuate not more than within the range of -5.5 to +4.0 K, which is within the specified range of –10 to +10 K required for HTTR/SR operation (see Fig. 4-17).

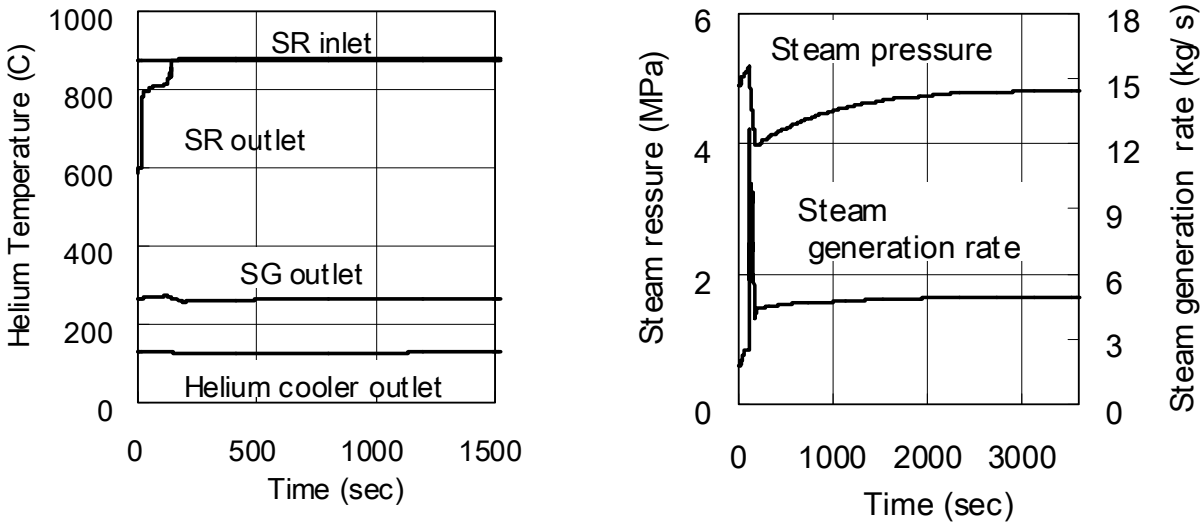

Fig. 4-17: Helium temperature (left) and steam pressure (right) during the system controllability test

4.5.2. COMPONENT TESTING

In the component tests, two major aspects, which are of safety relevance, will be investigated, the hydrogen/tritium permeation and corrosion from process gases with the goals to establish respective safety-related technology and to use acquired data for code validation. [Miyamoto 1998].

4.5.2.1. Hydrogen Isotopes Permeation Tests

The tritium produced, e.g., as fission product in the active core and flowing with the primary helium is not completely removed from the circuit in the coolant purification system. Remaining tritium can permeate through the tube walls of the IHX into the secondary helium circuit, and from there eventually through the tube walls of the steam reformer into the product gas causing a radiation hazard to the customer. In the opposite direction, hydrogen produced on the process side can permeate through the tube walls into the primary circuit causing corrosion reaction with the graphite structures.

The aim of the diffusion tests, in which the isotope deuterium is used instead of tritium, is the derivation of permeation coefficients with focus on the low partial pressure range < 10 Pa and the influence of oxide layers on the tube surfaces.

Results have been acquired in a small-scale apparatus using test pipes made of the HT alloys Hastelloy-X and Hastelloy-XR, the designated materials for IHX heat exchanger tubes and SR pipes. Test tube dimensions were 1000 mm in length, 31.8 mm outer diameter, and 3.5 mm wall thickness. Test conditions were tube temperatures of 600-850 °C and H_2 partial pressures of 0.1-4 kPa (or vol%) in helium gas. Flow rate was 0.1 Nl/min of the mixture gas. Some results are shown in Fig. 4-18. The test series also confirmed the phenomenon of oxide layer formation, which reduces the permeation rates [Takeda 1999].

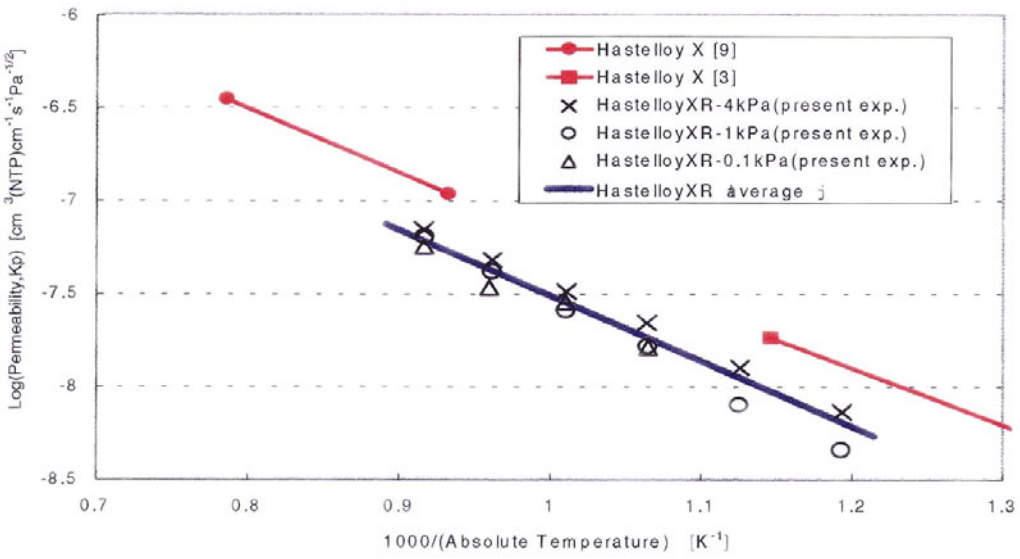

Fig. 4-18: Hydrogen permeability of Hastelloy-XR and Hastelloy-X

In another experimental series, the effect of counter-permeation of deuterium (to simulate tritium) and hydrogen was investigated. The test tube here consisted of Inconel 600 with an inner diameter of 7 mm and a thickness of 1.2 mm. Mixtures of argon with hydrogen and deuterium, respectively, were flown at constant rate and constant pressure through the test pipe and the outer so-called measurement tube (inner diameter: 50 mm). With deuterium flowing inside and hydrogen outside the test tube, it was found that for low partial pressures of deuterium < 100 Pa, its permeation rate to the outside is decreasing, if the hydrogen partial pressure is > 10 kPa. This is due to the fact that the amount of dissolved H atoms are saturated on the surface. In the HTTR/SR, H_2 partial pressures will be about 2.3 MPa, therefore a comparatively low amount of tritium is expected to be transferred from the primary circuit to the hydrogen production system [Takeda 2004].

The reduction of permeability at the presence of an oxide film layer was again confirmed, the observed factor of 100-1000 enhancing with time. The ratio of hydrogen over deuterium permeability was measured to be 1.32 at 670 °C; it decreases with increasing temperatures.

4.5.2.2. Corrosion Tests

The main goal of these tests is the investigation of the corrosion effect of the process gases CH_4, CO, H_2O, or H_2 on the tube material Hastelloy XR which is a nickel-base, helium corrosion and heat resistant super alloy, under HTTR/SR typical operating conditions. In particular, the metal dusting and oxidation as well as the strength reduction resulting from H_2 embrittlement will be examined. Respective metallographic as well as strength and creep test methods for temperatures up to 900 °C are presently under development. The corrosion resistance of Hastelloy-XR in high temperature helium was found to be much better than that of Hastelloy-X.

4.5.3. SAFETY CONCEPT OF HTTR/SR AGAINST FIRE AND EXPLOSION

The proposed basic safety design concept is to provide some safety barriers between the HTTR and the steam reforming system so as to prevent the anticipated operational occurrences for anticipated design basis events related to the steam reforming system. Design basis events related to the HTTR reactor system have already been considered. It is therefore important to discuss additional anticipated design basis events that could originate due to the connection of the steam reforming system with the HTTR. Additional safety design requirements and corresponding countermeasures for the hydrogen production system are given in Table 4-6 for the different operational conditions of the HTTR.

The hydrogen production plant is designed according to the same level of safety as requested in the domestic regulations for conventional chemical plants without any additional safety features. It obeys the defense-in-depth principle with its graduated steps of prevention of occurrence, prevention of propagation, and mitigation of consequences (see also Fig. 4-19):

- Prevent leakage and ignition;
- Prevent inflow into nuclear building;
- Detect leakage and disconnect natural gas feed line;
- Define safe distance.

Table 4-6: Safety design requirements for the HTTR hydrogen production system

Operational condition	Event	Safety requirement	Countermeasure
Normal operation	Tritium transport from core to product gas H_2	Reduction of tritium radiation level in product gas	Restriction of permeation through tube walls Removal of tritium in the coolant by purification system
Anticipated operational occurrence	Thermal turbulence	Prevention of thermal turbulence to propagate to primary He loop	Mitigation of vibration of secondary helium temperature by steam generator installed downstream
Accident	Fire/explosion from leakage of flammable gases	Prevention of leakage inside and in the vicinity of reactor building	Upgrade design category of helium piping and reforming tubes Double-walled tubes Inerting of the compartment
		Mitigation of accident consequences	Safety distance

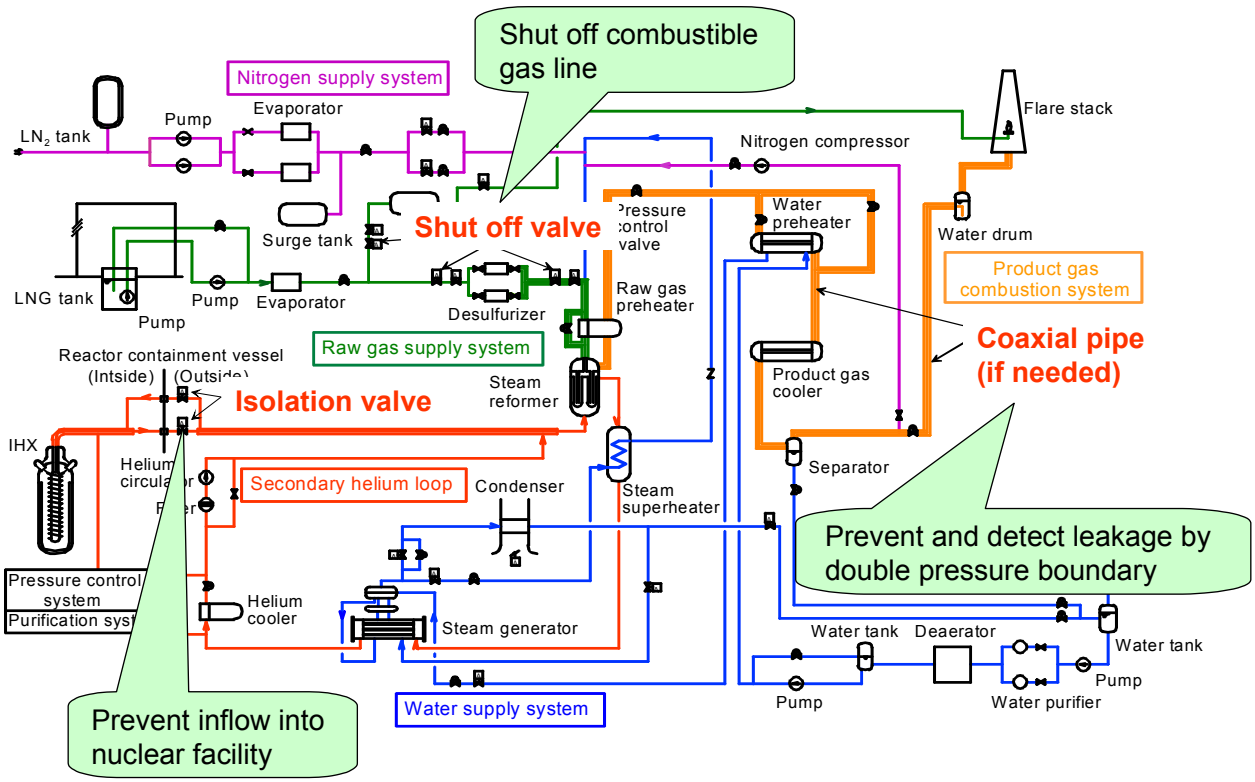

Fig. 4-19 Measures in HTTR/SR system against fire and explosion

Adequate measures for occurrence of an event or its propagation are provided: pressure resistance design, combustible gas leak detection system, fire extinguishing system, emergency shutoff system. Appears to represent no hazard to the nuclear system in cases of small or medium incidents. In terms of mitigation, safety distance and alternatively an explosion- / fire-proof wall to allow shorter distances are considered (Fig. 4-20).

Explosions inside the nuclear containment resulting from the ingress and ignition of combustible gases may have a severe impact on safety-related systems of the reactor. To minimize explosion hazard inside, helium piping and chemical reactor should be designed according to the highest level of reliability and designed against extreme design earthquake. Furthermore, a combination of the CV isolation valve installed in the helium piping and the emergency shutoff valve in the process feed line is planned.

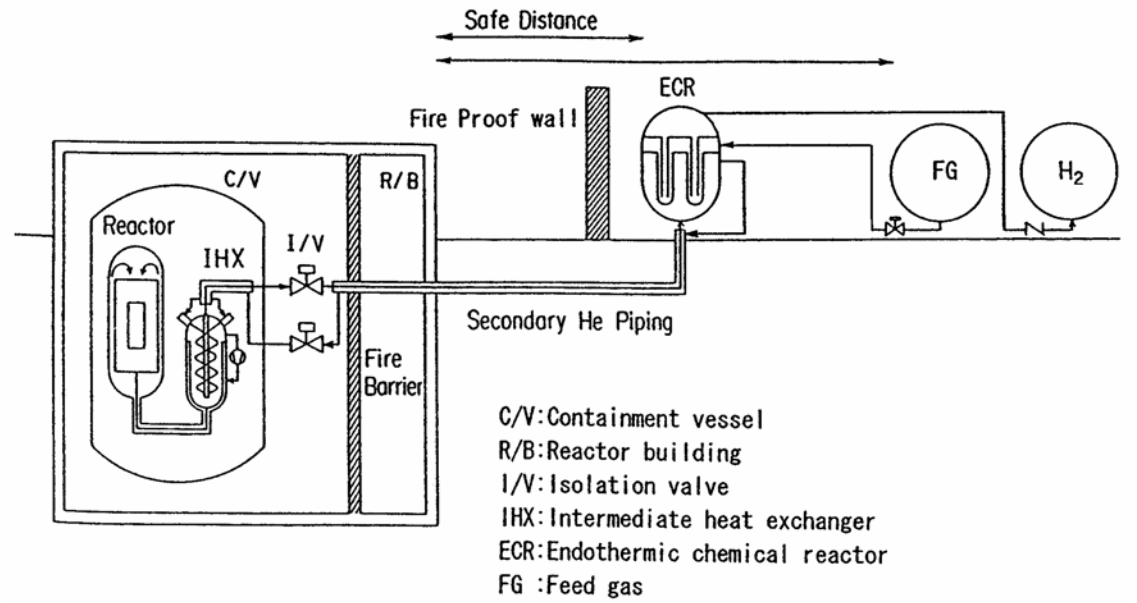

Fig. 4-20: HTTR safety design concept against fire and explosion

Concerning the concrete of the building, it is expected to exhibit no significant change of its mechanical properties over 24 hours at 175 °C, design to not exceed a wall-averaged limit of 175 °C from radiation heat, in order to maintain the structural strength of the concrete.

Overpressure of the incidental blast wave is limited to 10 kPa (USA: 7 kPa, Germany: 30 kPa) to ensure no failure of the reinforced concrete and the steel frame components.

4.6. Safety Distance for the HTTR/SR System

4.6.1. FORMATION OF A METHANE VAPOR CLOUD

Assuming a cylindrically shaped tank with a 10 m diameter basis, the full LNG load will have a height of approximately 5 m. Furthermore assuming that the liquid cannot spill outside the tank, a "spill" scenario would be represented by an open tank, i.e., pool size be equivalent to the tank basis of 78.5 m^2.

Because of the almost atmospheric pressure of the LNG tank, there will be in case of a tank failure, no or hardly any explosion-like spreading of the tank contents. The LNG will mainly vaporize according to the heat supply from the ambient. The amount of flash-vaporizing liquid can be estimated according to the relation

$$M_{rel} = (c_p * (T_i - T_s)) / h_v * M_{liquid}$$

where c_p: specific heat between T_i and T_s
h_v: vaporization heat
T_i: initial temperature before accident, equilibrium temperature at bursting pressure
T_s: Boiling temperature at atmospheric pressure

According to the IAEA recommended cryogenic pool vaporization rates, 10 % of the liquid flash-vaporizes, while for the remainder, the rates are set at 10 mm during the first minute and 0.5 mm/min afterwards [IAEA 1981]. This approach translates into a flash release of 40 m^3, followed by a continuous release of 0.8 m^3 of LNG to vaporize during the first minute or 5.5 kg/s of methane and half of this rate afterwards. The full LNG tank would be completely vaporized after about 900 min or 15 hours. This is an extremely long time in terms of a dispersion process in the open atmosphere, meaning that it appears impossible to have all methane available involved in a vapor cloud explosion.

4.6.2. SAFETY DISTANCE ACCORDING TO THE GERMAN BMI GUIDELINE

The guideline on the "Protection of Nuclear Power Stations from Shock Waves Arising from Chemical Explosions", drafted by the German Federal Ministry of the Interior (BMI) in 1976 [BMI 1976] has defined for nuclear power plants a k-factor of 8 in the safety distance relation (see chapter 4.3.2.), with the mass L released to be unsaturated hydrocarbons or compressed gas assuming a premixed stoichiometric mixture of hemispherical shape and central ignition. If the flammable mass is a pressurized liquid, k is reduced to 6.3 (or 50 % of the mass). For cryogenic liquids or hydrocarbons under standard conditions, k is 3.7 $m/kg^{1/3}$ (or 10 % of the mass).

Applying the k-factor 3.7 to the 400 m^3 LNG tank of the HTTR/SR according to the German BMI guideline, the result is a required safety distance of 205 m (see dashed line in Fig. 4-21). Such a safety distance would actually be fulfilled, if the planned distance between reactor building and the LNG tank of at least 300 m be realized.

What is not considered here is the flammable content of the steam reformer which is sited in the immediate vicinity of the reactor building and, thus, not in compliance with the BMI guideline, which requires a minimum safety distance of 100 m. This distance would be needed for an

explosive mass (TNT) of 1953 kg or, related to a liquefied gas, of 19,530 kg of LNG which corresponds to 46 m^3 of LNG. The guideline is valid for NPP of present design; it is explicitly mentioned that "no statement can be given at present concerning its application to future nuclear process heat plants". It is supposed to be a concomitant effort with the development of nuclear process heat plants to solve the problem of external vapor cloud explosions.

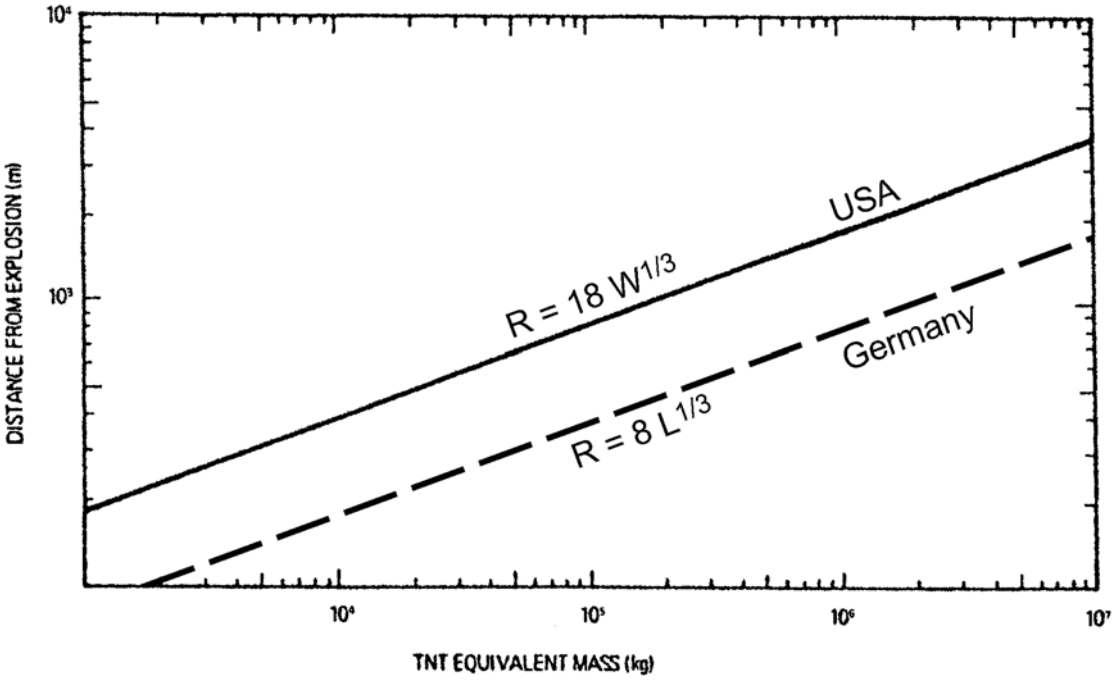

Fig. 4-21: Safety distance as a function of the quantity of released liquefied gas according to the BMI guideline and the US regulatory guide 1.91

4.6.3. SAFETY DISTANCE ACCORDING TO THE US REGULATORY GUIDE 1.91

In the USA, it is judged according to the US-AEC Regulatory Guide 1.91 that structures, systems, and components important to safety and designed for high wind loads are also capable of withstanding pressure peaks of at least 7 kPa resulting from explosions. No additional measures need to be taken, if the equation

$$R = 18 * W^{1/3}$$

is met, where R is the safety distance [m] from an exploding charge and W is the mass of TNT (equivalent) [kg] of the exploding material (see solid line in Fig. 4-21).

For the LNG storage tank of the HTTR/SR system, the 400 m^3 of LNG correspond to a mass of 169 tons of LNG, and this to a TNT equivalent of 1859 tons which then translate into a safety distance of as long as 2.2 km.

This approach appears to be unrealistic for the HTTR/SR system considering the fact that much larger stationary LNG tanks up to 200,000 m^3 ($\rightarrow R \approx 18$ km) have been established worldwide. Aspects not taken into account here are the different explosive characters of a liquefied gas and

a TNT explosive, the possibility of additional options offered by the 1.91 guideline, and finally the extreme unlikeliness of the total tank content to "explode" rather than assuming less conservative "design spills".

4.6.4. APPLICATION OF THE TNO MULTI-ENERGY METHOD

Concerning the hazard of a methane vapor cloud explosion in the open atmosphere, JAERI has conducted an assessment of a safety distance between the potential release point in the methane gas supply area and the nuclear reactor building. The calculations were based upon the procedures as recommended in the TNO Yellow Book [TNO 1980]. An atmospheric dispersion model with the Pasquill equation was taken to estimate the distance, until the methane has diluted below the LFL. The so-called Multi-Energy method was used to estimate the distance required to decay the blast wave pressure down to a level that the reactor building is designed to withstand (Fig. 4-22).

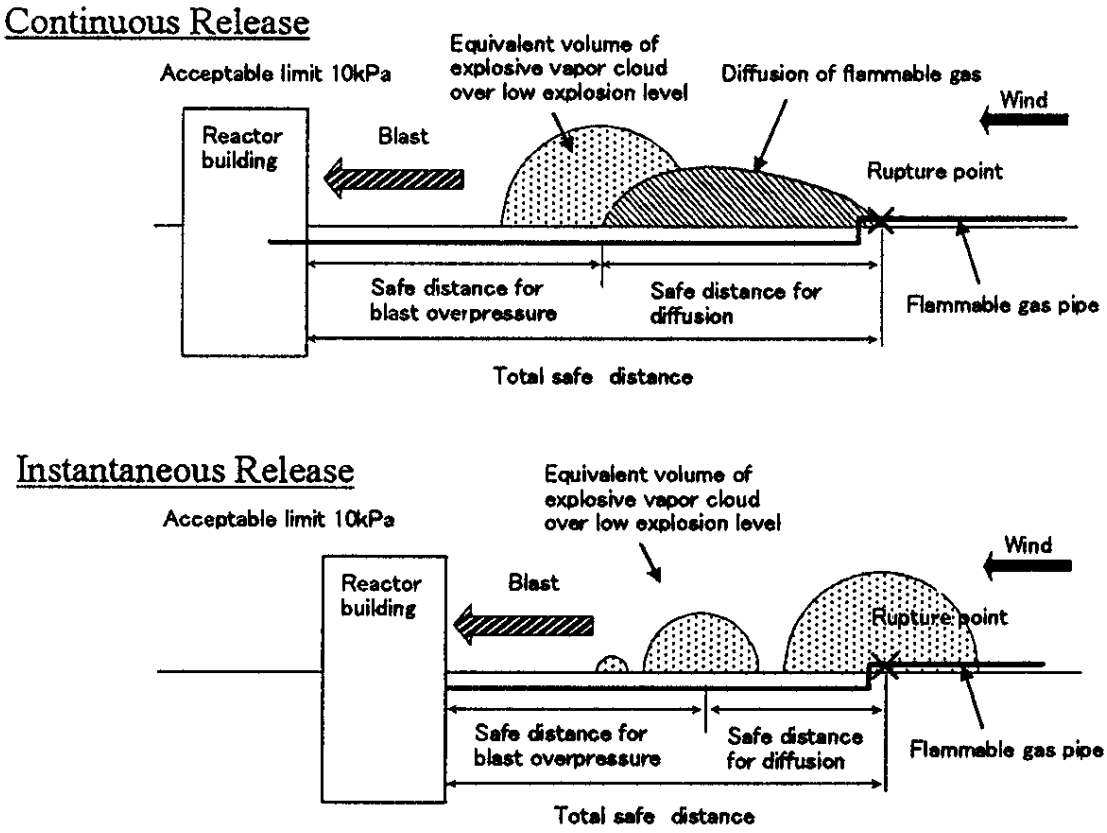

Fig. 4-22: JAERI estimation methods of safety distance against explosion

For the dispersion calculations, pertinent parameters to influence the concentration distribution are the release mode (continuous/instantaneous), the atmospheric stability class, and wind velocity.

The vapor cloud contains an equivalent volume amount of explosive vapor over the low explosion level in the spread fuel-air charge. It is assumed that the equivalent vapor cloud of

fuel-air charge is a stoichiometric composition and heat of combustion is $3.5*10^6$ J/m^3. The distance needed to meet the allowable overpressure is obtained by reading from the blast charts (see Fig. 3-9 in chapter 3.1).

The preliminary estimation of safe distance is carried out against vapor cloud explosion in the HTTR steam reforming system. With respect to release conditions, a continuous release and an instantaneous release are both considered within this estimation. A wind velocity of 1m/s and a stability condition of "most stable" are assumed as conservative estimations. If the amount of leakage can be restricted to below 100 kg, the required safe distance is only 200 m.

4.6.5. APPLICATION OF THE P2A COPUTER CODE SYSTEM

The computer code system P2A has been developed at JAERI to analyze fire and explosion accidents for the HTTR/SR system [Inaba 2002]. It consists of the commercially available programs PHOENICS for leakage, pool fire, and atmospheric dispersion simulation, AutoReaGas for deflagration and blast wave effects, and AUTODYN for detonation and impact on structures. The three single codes are coupled by interface programs. Calculations have been made considering a leakage of LNG from the storage tank or a pipeline with subsequent large-scale pool fire changing the local atmospheric wind flow pattern, or the formation of a methane vapor cloud, its ignition and explosion with a pressure wave hitting the HTTR building.

Assuming a leak position at 200 m distance from the reactor building and a leakage rate of 34 kg/s over 44 s (corresponding to a total volume released of about 3.5 m^3 of LNG) did not show a spreading of the vapor cloud towards the reactor building at significant concentrations. The cloud volume within the flammability limits was estimated to be around 2300 m³ after 69 s. The ignition of the cloud near the leak position resulted in a maximum overpressure of 0.3 kPa, which decayed to a level as low as 0.01 kPa in front of the reactor building [Inaba 2002].

5. EXPERIENCE WITH COMBUSTION AND EXPLOSION OF FLAMMABLE GAS CLOUDS

5.1. Accidental Occurrences

Numerous accidents have occurred in the past with the combustion or explosion of a flammable vapor cloud, the majority in the chemical process industries. According to UNEP statistics, about 180 severe industrial accidents occurred worldwide between 1970 and 1990. These accidents were mainly caused by fires, explosions, or collision during transport, and killed about 8000 people, injured more than 20,000, and led to evacuations involving hundreds of thousands of people.

Among the largest losses in the hydrocarbon process industries, vapor cloud explosions represent a significant portion and accounting for an even higher share in terms of the financial loss they have caused. Fig. 5-1 summarizes the type of accident for the 100 largest losses in the hydrocarbon process industries between 1957 and 1986.

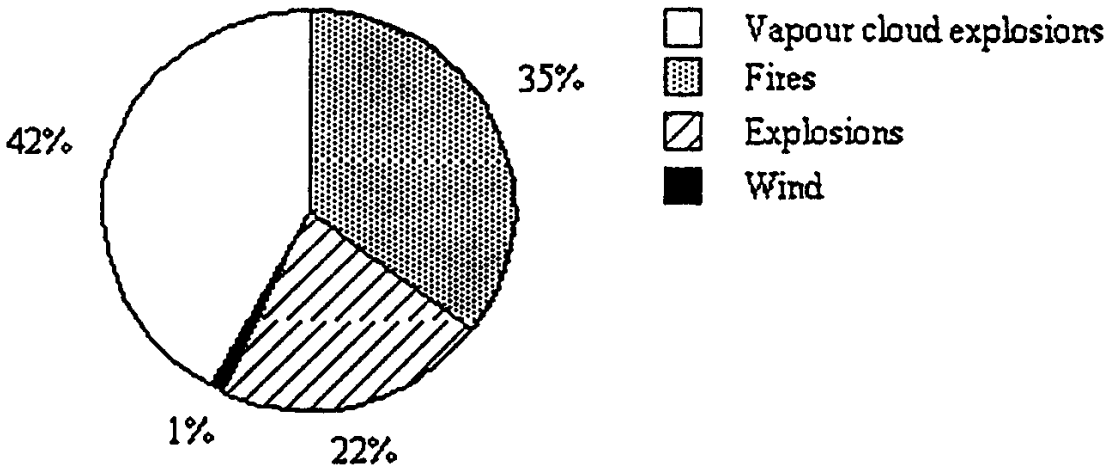

Fig. 5-1: Type of loss for the 100 largest losses in the hydrocarbon industry between 1957 and 1986

In the following, various accidental occurrences are listed to give an idea about the variety of causes and consequences that one can encounter at the presence of flammable gas mixtures. They all have more or less contributed to a subsequent modification, improvement, extension of the existing set of codes and standards, which provides the basis for a safe handling of flammable hazardous substances. A more extended list is given in [Gugan 1978].

1937 The spectacular disaster at Lakehurst with the 'Hindenburg', the largest airship ever built has set a sudden end to this type of transportation system. The airship (Zeppelin) filled with 200,000 Nm^3 of hydrogen caught fire during the docking procedure. The cause for this fire accident, however, was not the hydrogen itself, it was the outside protective paint, which was later found to be a highly flammable substance and in the

case of the Hindenburg, caught fire during a thunderstorm.

1944 An LNG liquefaction, storage and regasification plant at Cleveland was involved in a severe accident, when a new larger storage tank of 4500 m^3 capacity failed shortly after the installation. Approx. 2000 m^3 of LNG were spilled. The LNG penetrated a sewer system, where it eventually ignited. This accident claiming the life of 213 people, stopped virtually all LNG activities for a long time.

1964 In a test for a rocket nozzle, the Los Alamos National Laboratory at Jackass Flat has conducted an intentional venting of 1000 kg of hydrogen within 30 s, when unintentionally a spontaneous ignition occurred. The burning gas cloud of approx. 9 m diameter and 45 m height contained about 9 kg of H_2. The flame speed reached about 35 m/s, the overpressure an estimated 3.5 kPa at buildings in a distance of about 60 m.

1965 At the Escambia Chemical Corporation in Florida, USA, the failure of a valve has led to the discharge of hydrogen and carbon monoxide through a 25 mm diameter opening at a pressure of 35 MPa. The estimated quantity released of 70 - 140 kg ignited after 10 - 20 s causing damage within a distance of 240 m.

1966 In Raunheim, Germany, LNG was accidentally released from a vent at high level forming a low lying dispersion which ignited, after about 500 kg had been released. Blast damage was considered not particularly severe. Extensive glass breakage occurred up to a distance of 400 m.

1966 The explosion at Feyzin, France, was one of several accidents where a BLEVE has occurred. A spherical propane tank with a 1200 m^3 capacity leaked; the leakage ignited and engulfed the tank in a fire, which exploded after 1.5 h. No blast effects were reported.

1970 In the Port Hudson accident in the USA, the release and explosion of 15,000 m^3 or 29 t of propane occurred after rupture of an underground pipeline. The vapor cloud collected in an approx. 500 m long and 3 - 6 m high plume and then, about 13 min after the rupture, hit a “strong” ignition source. The damage indicated that the unconfined vapor cloud explosion had developed to a detonation.

1970 In Blair, Nebraska, USA, an ammonium aerosol vapor cloud was accidentally released by overfilling a storage tank, developing a fog of 3 - 10 m thickness and almost 3 km length, which contained 160 t of NH_3. Due to inversion weather conditions, the cloud had a life time as long as half a day.

1970 Gas explosion at a subway construction site in Osaka, Japan

1971 An LNG “rollover” incident occurred in the harbor of La Spezia, Italy, 18 hours after refilling a storage tank, following the sudden mixing of two LNG layers of different densities. The different densities resulted from the fact that the LNG ship was unloaded not until one month after arrival with the LNG having had much time for “ageing”.

1972 In the East St. Louis accident in the USA, a rail tank car filled with propylene was accidentally punctured while moving, spilling the liquid over a distance of 500 m, before the car finally stopped. The vapor cloud eventually encountered an ignition source after 8 - 10 min some distance away from the car causing a severe explosion.

1973 A construction accident occurred at Staten Island in an LNG peak-shaving plant, when the roof of a storage tank collapsed. During liner repair works, the liner and then

the thick, so-called self-extinguishing polyurethane foam insulation inside the tank were accidentally ignited. Increase in temperature and pressure was so fast that the concrete dome of the tank was lifted and then collapsed down. The ignition was made possible by the use of non-explosion-proof equipment. The term "self-extinguishing" never meant "non-combustible", however, it was misleading and later deleted from the fire engineering vocabulary.

1973 A flash fire with natural gas liquids occurred at Austin with the vapor cloud traveling approx. 800 m before it ignited after about 15 min.

1974 In the accident at Flixborough, a quantity of approximately 36 t of cyclohexane at a pressure of 0.85 MPa and a temperature of 155 ^{o}C was released after the failure of a poorly installed, temporary connecting pipe. The fuel flash-vaporized and developed a vapor cloud throughout the plant area. A "weak" ignition occurred presumably at a furnace, before flame acceleration took place producing a blast wave with an estimated overpressure of 0.1 MPa at the center. The accident demonstrated the potential of devastation of an unconfined vapor cloud explosion in an industrial environment with impact to the public in the surrounding area. It had prompted systematic investigation to understand cause and development of the phenomena responsible for such a destruction as well as a significant revision and improvement of the actual legislation.

1974 One of the largest hydrocarbon spills accidentally took place in Griffith, Indiana, where a pipe connected to a 36,000 m^3 underground storage tank of liquid butane opened and released in a vertically upwards directed jet over seven hours before the gas cloud exploded. The flame traveled back to the source and torched without producing a damaging blast wave.

1975 The explosion accident in Beek, The Netherlands, occurred in a naphtha cracker plant, where ca. 5.5 tons of propylene were released, when a level controller failed. After a delayed ignition of the vapor cloud at a furnace 46 m away, the initially laminar flame was accelerated, presumably due to a high level of turbulence created near the exit of a lane-type structure. The TNT equivalent was estimated to be 2.2 t developing an overpressure of approx. 0.1 MPa. Six of the 14 people killed were working in the control room building.

1978 In Taragona, Spain, a tank truck carrying liquid gas (propylene) overturned and exploded on a campground claiming the life of 215 people.

1979 The Cove Point LNG terminal in Maryland, USA, experienced an unexpected explosion. LNG was leaking through an inadequately tightened LNG pump electrical penetration seal, vaporized, passed through a 60 m underground electrical conduit, and entered an electrical substation where it finally ignited. Codes and standards, which all were met at the time of the accident, were changed afterwards with particular consideration of equipment and systems downstream of pump seals.

1983 In Bontang, Indonesia, an LNG explosion occurred, when a heat exchanger failed due to overpressurization. It was caused by an inadvertently closed valve on a blowdown line, to which all relief systems were connected.

1984 A severe explosion accident occurred in the tank depot of a chemical plant in San Juan Ixhuatepec near Mexico City, where an LPG leakage caught fire and BLEVE'ed the tank. Four storage tanks with each containing 1500 m^3 of LPG and several smaller tanks caused massive fireballs. The cost in terms of human loss was tragically high

due to the fact that residential areas approached to a distance as short as 130 m.

1988 On the offshore rig Piper Alpha, 167 people were killed, when the platform was engulfed in a series of fires and explosions. The accident was initiated by a leakage of light oil forming a gas cloud which ignited when the personnel restarted a pump. A pressure relief valve had been removed before from the relief line and replaced by a blank flange, which was not leak-tight. The personnel was not informed about the changes.

1989 In the Ural mountains, LPG was leaking from a pipeline along the Trans-Siberian railway. The vapor cloud exploded, when two passenger trains were passing the location.

1992 When a new LNG bus was prepared for its operation, a mechanic was repairing a natural gas fuel system leak. Although forbidden, the bus was in a normal bus repair bay and not outdoors. When a gas detector inside the bus sounded an alarm, the mechanic bypassed the alarm to start the bus to move it outside. When the bus was started, a flammable methane-air mixture that had accumulated in the interior of the bus, ignited. The resulting explosion blew out all windows and roof hatches.

1976 Finally, another accident should be mentioned here, although it does not quite fit the above list of accidents. A dense vapor cloud of dioxin ("TCDD") evolved from a chemical plant in Seveso, Italy. This poisonous and carcinogenic substance, lethal to humans in microgram doses, was released in the order of kilograms contaminating about 30 km^2 of land and vegetation and exposing some 37,000 people to a high toxic level. Poor emergency planning exacerbated poor prevention planning. The accident had prompted European legislation activities resulting in the so-called Seveso.

The analysis of explosions and respective damage observed indicates that in most cases, there was too less damage for a stable detonation and too large damage for an undisturbed deflagration.

5.2. Experimental Investigations of the Release and Combustion Behavior of Flammable Gases

5.2.1. EXPERIMENTS WITH THE FORMATION, VAPORIZATION, AND COMBUSTION OF LNG POOLS

Fig. 5-2 shows the burning rate of liquid methane compared with liquid hydrogen as were measured in tests with a 6-inch (152 mm) dewar. The regression rate of the methane level corresponds to 2.3 mm/min [Zabetakis 1960].

In an experimental program within the US Bureau of Mines, two series of LNG spills on water have been conducted in 1970. The first consisted of small-scale tests to measure vaporization rates by spilling a weighed amount of LNG into a water-filled aquarium. In the second series, liquid quantities up to 0.5 m^3 were spilled on an artificial pond. The initial vaporization rate was found to be 0.18 kg s^{-1} m^{-2}. The maximum diameter of the LNG pool formed on the water surface was found to be given by $4.80 * M^{1/3}$ with M as the weight of LNG in kg. The stratification effect of the cold dense gas was observed to be similar to the effect of a temperature inversion. For small releases, the gravitational effects were insignificant. Peak

concentrations of methane in the ambient air were measured to be as much as twenty-fold higher than average values [Burgess 1970].

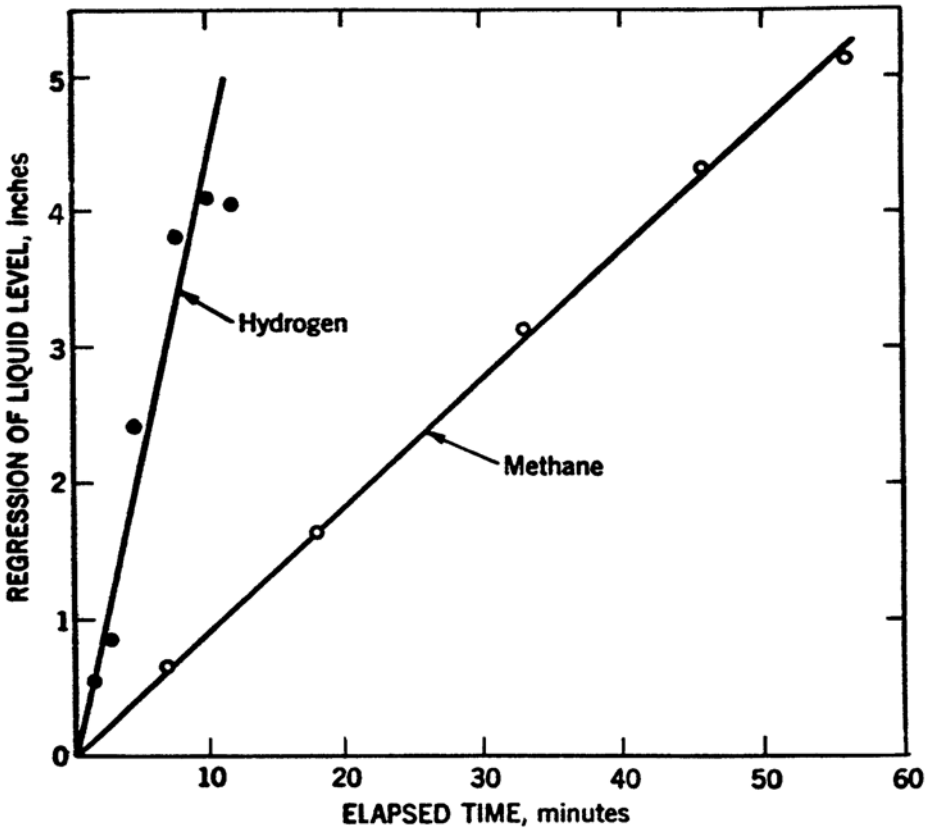

Fig. 5-2: Measured burning rates of liquid hydrogen and liquid methane in a 6-inch (15.2 cm) dewar

At Matagorda Bay, 17 tests have been conducted in 1971, organized by Esso and the American Petroleum Institute [Feldbauer 1972]. LNG was spilled on water in quantities between 0.8 and 10.2 m^3 at a rate of about 0.3 m^3/s. The goal was to derive parameters required to predict downwind concentrations with a continuous Gauss point source dispersion model. At low wind speeds, the gravitation effect resulted in very broad, horizontally extended vapor clouds with small vertical extension.

In 1972, Gaz de France has conducted an experimental study to investigate LNP vaporization rates on various solid grounds and the atmospheric dispersion of LNG vapor clouds evolving after spillage into square dike areas of 9 and 200 m² surface. Spill volumes in the 40 tests were up to 3 m^3 of LNG. The vaporization rate was observed to be 0.5 mm/min at the beginning and decreasing afterwards. Concerning the developing LNG vapor cloud, the flammable zone was always found to be inside the visible cloud. The maximum volume of the flammable region was found to be reached early after the release because of the high vaporization rate at the beginning, which rapidly decreased afterwards. Gaz de France has also carried out tests on different devices to extinguish large LNG fires such as emulsifiers, foam, powders, and also on different soil design for the impoundment area using armored soil technique or light colloid concrete as dike lining with minimum boiloff rates [Humbert-Basset 1972].

Within the experimental LNG Safety Program of the American Gas Association (AGA), Phase II in 1973, a total of 42 LNG spill experiments were conducted to investigate the consequences of LNG spills on land and to develop respective simulation models. Quantities between 0.4 and 51 m^3 were spilled within 20 - 30 s into a circular dike of 1.8, 6.1, and 24.4 m diameter, respectively. Observed vaporization rates remained for about 60 - 90 s near the initial high value of about 25 mm/min, before it diminished. The 14 tests with pool fire have been used to measure mass burning rates in order to derive an empirical model equation for the respective regression rate. The LNG was spilled into the different dikes to an initial depth of 1 - 1.5 m and the fires lasted roughly 10 minutes. The AGA LNG program was completed by experiments on fire control and vapor suppression to evaluate the effectiveness of different vapor suppression or fire extinguishing devices [Battelle 1973].

LNG burning rate measurements by the Tokyo Gas Company resulted in values of 6.6 - 7.6 mm/min, the portion of evaporation due to flame radiation was 0.36 mm/min. The Osaka Gas Company conducted similar experiments in a steel container and yielding unusually high values of 19 mm/min [Battelle 1973].

The “Dow Fire and Explosion Index”, which is a recognized procedure for identifying the hazards in a chemical plant due to the presence of flammable materials, quotes for the LNG burning rate a range of 7.5 - 10 mm/min.

Within the US Coast Guard Vapor Cloud Explosion Study in 1978 [Lind 1979, Parnarouskis 1980], 5 m^3 LNG spill trials on water have been conducted at China Lake. The tests included, apart from four pure dispersion tests, a pool fire, two delayed pool fire and three vapor fire tests. In the immediate-ignition pool fire test, 5.4 m^3 of LNG were spilled within 81 s under calm wind conditions. The flame observed was 8 m in diameter and 60 m high. In the delayed-ignition pool fire tests, a ring of flames around the pool was observed, whereas over the pool, the vapor mixture was too rich to burn until towards the spill end the vapor production rate decreased such that the flame could spread over the whole pool. The pool fire height was greater than for burning pools on land. In the vapor fire tests, no fireball-type burning was observed. The flame spreading was shown to increase with wind speed. Delayed fires were spreading back to the source, but halted at the pool edge. The emissive powers measured scattered considerably with an average of about 210 - 220 kW/m^2 for both pool and cloud fire.

In the Burro Series of the US-DOE at China Lake in 1980, eight LNG spill tests on water have been conducted to study the atmospheric dispersion of LNG vapor clouds. Spill rates were between 11.3 and 18.4 m^3/min and total volumes from 24 to 39 m^3 and were therefore considered continuous spills. Under various atmospheric conditions, gas concentrations were measured at different locations. At very low wind speeds, a displacement of the atmospheric flow by the cold gas was observed. Due to unexpected RPT in two tests, which were large enough to damage the facility, a separate subseries of experiments was to examine particularly these phenomena [Koopman 1982, Ermak 1983]. In his corresponding study on gas dispersion model calculations, Ermak assumed a liquid regression rate of 0.42 mm/s for the unrestricted spreading of the LNG pool over water, however, connected with a fairly high uncertainty [Ermak 1982].

The 34 spill experiments with both instantaneous and continuous release of LPG and LNG conducted by Shell Research in Maplin Sands in 1980 [Blackmore 1982] included the investigation of LNG pool fires following the spillage. The LNG cloud fire was observed in a

continuous spill test to back-travel to the spill point. Flame length to pool diameter ratio was up to 2.7 for LNG. The LNG pool fire was observed to be clean and brightly emissive with a large flame height of tilted cylindrical shape.

The British Gas company has conducted a series of tests to examine LNG vaporization and spreading rates on different types of grounds. The liquid was continuously discharged onto a 45 degree sector over a certain period of time, and its spreading was monitored. In agreement with other authors, a limiting value for the LNG vaporization rate of approximately 0.5 kg/(m^2 s) was found. This holds for impervious grounds. For grounds which allow percolation, peak boiloff rates were higher due to the increased surface area. For dry solid grounds, the boiloff rate is a function of $t^{-1/2}$, however, variation is given depending on the parameters of density, water content, and ground porosity [Moorhouse 1986].

In the Falcon field trial series in 1987 at Frenchman Flat, five dispersion experiments with vaporized LNG in an obstructed environment (fences) have been conducted. Total volumes of 21 - 66 m^3 were spilled onto a 40 x 60 m^2 lake at rates between 0.15 and 0.5 m^3/s [Chan 1992].

5.2.2. EXPERIMENTS WITH THE COMBUSTION AND EXPLOSION OF FLAMMABLE VAPOR CLOUDS

5.5.2.1. Gas Clouds in Unconfined or Congested Areas

In a detonation test series in 1972 to study blast effects, methane-oxygen mixtures have been applied as detonable gas. Spherical balloons with 33.5 m diameter and hemispherical balloons of 38.1 m diameter were used, where the latter successfully detonated corresponding to a TNT equivalent of about 20 t [Baker 1983].

Tests conducted by the US Coast Guard within the frame of their “Vapor Cloud Explosion Study” of 1973 [Parnarouskis 1980] included 15 field tests with hemispherically shaped premixed fuel-air vapor clouds of 5 and 10 m radius. Neither fuel has shown any potential of a DDT upon spark ignition. Methane of 10 % concentration was involved in three tests. A flame speed of < 10 m/s was observed which did not allow to detect a pressure wave. Efforts were also not successful to initiate a detonation in a methane-air cloud by using 1.35 and 2.05 kg of explosive. Detonation was achieved only when a stoichiometric methane-propane mixture with a minimum of 15 % of propane in the fuel and 1 kg of explosive was employed. In a later phase of the program, it was also tried with larger amounts of explosive to get a methane-air cloud detonation. But quantities as much as 22 kg, the “detonation” limit as predicted in [Bull 1976] (see next paragraph), and even 37 kg did not result in a detonation. Both flame speed and pressure decreased after ignition.

Bull et al. [Bull 1976] have tried to measure the critical conditions to establishing a self-sustaining spherical detonation in stoichiometric mixtures of methane, oxygen, and nitrogen. Combustion tests with explosives ranging between 2.5 and 520 g of tetryl were conducted in a cubical bomb chamber of 3.7 m side length, where the fuel mixture was initially kept in a balloon. The measured detonation velocities were in reasonable agreement with the calculated Chapman-Jouguet values over a wide range of N_2 fractions (Fig. 5-3). Extrapolating the resulting curve towards an N_2 fraction that is equivalent to a stoichiometric methane-air mixture leads to a maximum explosive charge of 22 kg, which was beyond the safe limit of the apparatus in order to be verified.

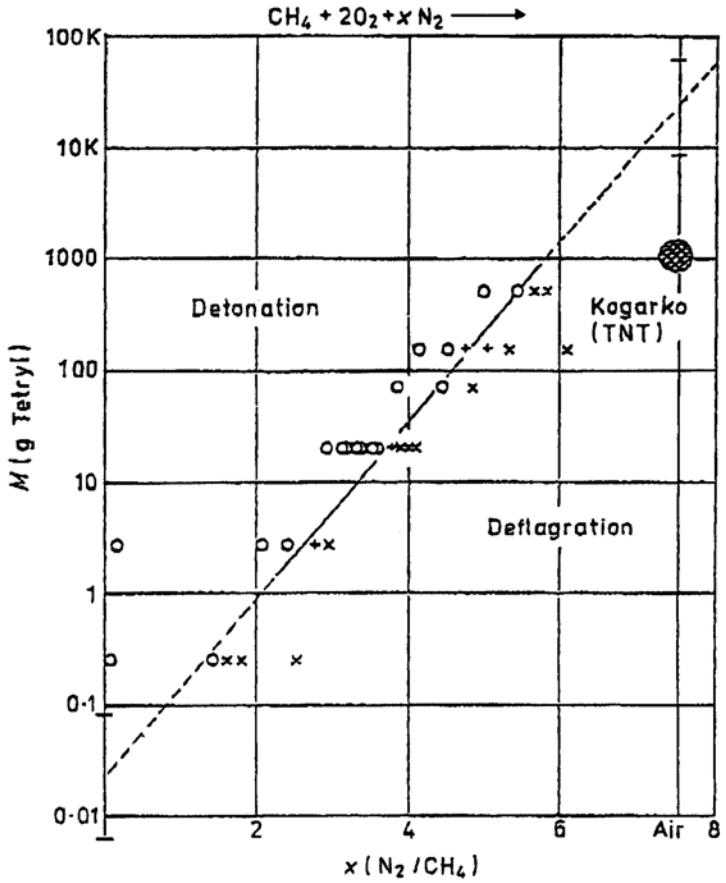

Fig. 5-3: Detonation experiments with methane-oxygen-nitrogen mixtures (circles = detonation, crosses = no detonation; vertical solid line on the right represents composition of air)

Within the frame of the "German Reactor Safety Program", research has been focusing on pressure-time and impulse history of chemical explosions. Pförtner has conducted combustion tests with ethylene-air mixtures in balloons of 1.5 and 15 m^3, respectively, as well as tubes with 0.8 m diameter and 25 m length. By using 200 J igniters, even under boundary conditions more severe compared to a real, unconfined gas cloud, no detonation was observed. Flame speeds measured were up to 30 m/s in turbulent areas with overpressures not exceeding 10 kPa [Pförtner 1977].

As part of the experimental program of the PNP Safety Program, Schneider and Pförtner from the Institute for Chemical Technology of the Fraunhofer Gesellschaft [Schneider 1978] have conducted in 1978 explosion experiments with unconfined, premixed stoichiometric H_2-air mixtures in hemispherical balloons of 3 m (five tests) and 6 m (three tests) diameter, respectively, which were spark-ignited at the center. Maximum overpressures resulting from flame acceleration were observed to range between 1.3 and 2.3 kPa for the small balloons and 2.9 - 4.5 kPa for the large balloons, decreasing outside the cloud with a 1/r dependence. Flame velocities ranged between 49 and 58 m/s at the cloud edge showing a certain dependence on cloud size and state of turbulence in the cloud. In additional tests with balloon diameters of 10 m (two tests) and 20 m (one test), respectively, measured overpressures went up to 6.3 kPa corresponding to a flame speed in the hydrogen-air mixture of 84 m/s [Pförtner 1985].

Shell Research has conducted in 1980 in Maplin Sands experiments with a spill of LNG and LPG in quantities up to 20 m^3 on water to investigate the dispersion and combustion behavior of the evolving vapor clouds [Blackmore 1982, Hirst 1982]. The tests were not performed in an industrial environment, but rather simulating maritime transportation accidents. Of the 21 tests, 11 were with combustion. Out of these 11, seven were with natural gas, from which two failed due to flame extinction soon after ignition. From the five tests left over, three were conducted with continuous release (20 - 40 kg/s) and two with instantaneous release (3500 - 5000 kg). The fuel-air concentrations across the cloud were obviously far from homogeneous. The vapor clouds burnt in a steady, non-explosive manner with a bright yellow flame in the fuel-rich portions. Maximum flame speeds of 28 m/s for propane and 10 m/s for natural gas have been observed, however, no sustained flame acceleration was achieved. Flame-generated overpressures were detected, but always on a very low level; the maximum value in any of the tests was approx. 100 Pa in consistence with a slow flame speed expected for a flat cloud. Flame extensions reached 130 m for both fuels; natural gas flames appeared more segmented than the propane flames. In one continuous case at a lower wind speed, the flame was even held stationary until the spill rate was reduced. Flame height during rich cloud fires was low compared to its width; ratios were between 0.15 and 0.4. Thermal emissive powers were ranging from 137 - 225 kW/m^2, suggesting that a value of 200 kW/m^2 may be representative for a large LNG pool fire on water.

The Coyote series at China Lake in 1981 was primarily focusing on the examination of the processes during rapid phase transitions under water. Both early and delayed RPT were observed in six of 18 tests. The RPT seem to be enhanced the higher the water temperature and the deeper the penetration into the water. Influence is also given by the LNG composition and presumably other still unknown mechanisms. With respect to the vapor burn experiments within the Coyote series, four tests with release rates of 100 - 120 kg/s and up to 12,000 kg of LNG mass released and one test with liquid methane released at 100 kg/s over 110 s were done. Flame speeds in the range of 7 - 13 m/s have been measured with a maximum at 30 m/s. The maximum overpressure was 250 Pa [Ermak 1983].

Key experiments on field scale with quiescent fuel mixtures in congested areas were conducted by Harrison and Eyre [Harrison 1987] using pipe grids as obstacle arrays with low-energy igniters. Flame speeds and overpressures under all conditions examined were greater for propane than for natural gas. The pipe grids caused progressive flame acceleration; the closer the intergrid spacing, the more rapid was the acceleration. Flame speeds, e.g., of more than 100 m/s could be achieved with natural gas at a blockage ratio of 40 %. Ignition with a flame jet produce even larger flame speeds with an overpressure of more than 70 kPa in one test.

In the Netherlands, large-scale tests with unconfined propane gas clouds have been conducted by TNO [Zeuuwen 1983] with and without congestion by repeated obstacles and also using vertical confinement. The vapor clouds consisting of up to 1000 kg of propane in the flammable range evolved from a vaporizing pool, dispersed freely, thus having a cigar or pancake shape before weakly ignited. For the arrangement with no obstacles, the observed flame speeds were normally in the range of 3 - 10 m/s, the maximum value measured was an unusual high of 32 m/s, presumably due to enhanced initial turbulence. In the arrangement with vertical obstacles and a partially confined top, flame acceleration was observed in the covered parts and a deceleration in the open parts. Maximum flame speeds measured were 50 - 66 m/s. The comparison with small-scale experiments showed that scaling is possible as long as flame

speeds are relatively low.

Maurer and Giesbrecht used liquid propylene in differently sized tanks (diameter of 40 - 700 mm) to investigate the instantaneous release after the catastrophic failure of a pressure vessel [Giesbrecht 1980, Giesbrecht 1981]. The propylene was stored under pressures of 4 - 7 MPa at temperatures of 50 - 80 °C. The vessels were made to fail by an explosive. The mechanical energy released during the flash vaporization was found to be not more than 0.1 % of the reaction enthalpy of the propylene. Spreading velocity of the gas cloud was initially 300 m/s and decayed rapidly as well as the respective pressures. A maximum fraction of the mixed vapor cloud was for a short time within the flammability limits. Maximum flame speed observed during the deflagration was 48 m/s and pressure of 7 kPa. There was no sign for a detonative reaction.

The Pförtner/Schneider [Pförtner 1988] experimental series of 17 tests with methane-air, methane-ethane-air, methane-oxygen enriched-air, propane-air mixtures in 1988 was investigating the effect of an unconfined flat cloud geometry of rectangular (40 m long, 40/20 m wide, 8 m high) or cylindrical (40 m diameter, 8 m high) shape. Initial turbulence was created by obstacles and fans. Weak point ignition resulted in hemispherical flame propagation which ended at the cloud boundary, where also the maximum overpressures were measured. The test with 100 equally distributed ignition points showed lowest overpressures, since combustion products could spread in all directions. Flame speeds were 6 - 8 m/s in the undisturbed case (100 - 200 Pa overpressure), increasing considerably (86 m/s, 10 kPa) in a CH_4-O_2-N_2 cloud atmosphere enriched to 30 % of O_2. Obstacle configurations increased flame speeds by a factor of 2 - 3. Fig. 5-4 shows a diagram of peak overpressures versus flame speed; curves must not be extrapolated beyond the measured range.

More tests were conducted by Pförtner in an arrangement with two parallel walls forming a 10 x 3 x 3 m^3 lane and with rich H_2-air mixtures as fuel. After generating fan-induced turbulence, flame acceleration to a detonation was observed. Fig. 5-5 shows clearly the transition to detonation after the flame front passed the fan [Diepold 1970, Berman 1986].

Explosive-initiated detonations have been observed in ethylene, propylene and propane mixtures with air by using 8 g, 30 g, and 80 g, respectively of high explosives. It was, however, not possible by using 2.5 kg explosive for a premixed methane-air mixture to initiate a detonation. There were only combustion-supported blast waves recognized which, after a certain distance, slowed down to a deflagration [Pförtner 1979, Pförtner 1985].

The first experiments to demonstrate the yield of a detonation by a turbulent jet of combustion products were conducted by Knystautas. The initial flame jet diameter was 40 mm, leading into an acetylene-oxygen mixture in a 2 m diameter detonation chamber [Moen 1993].

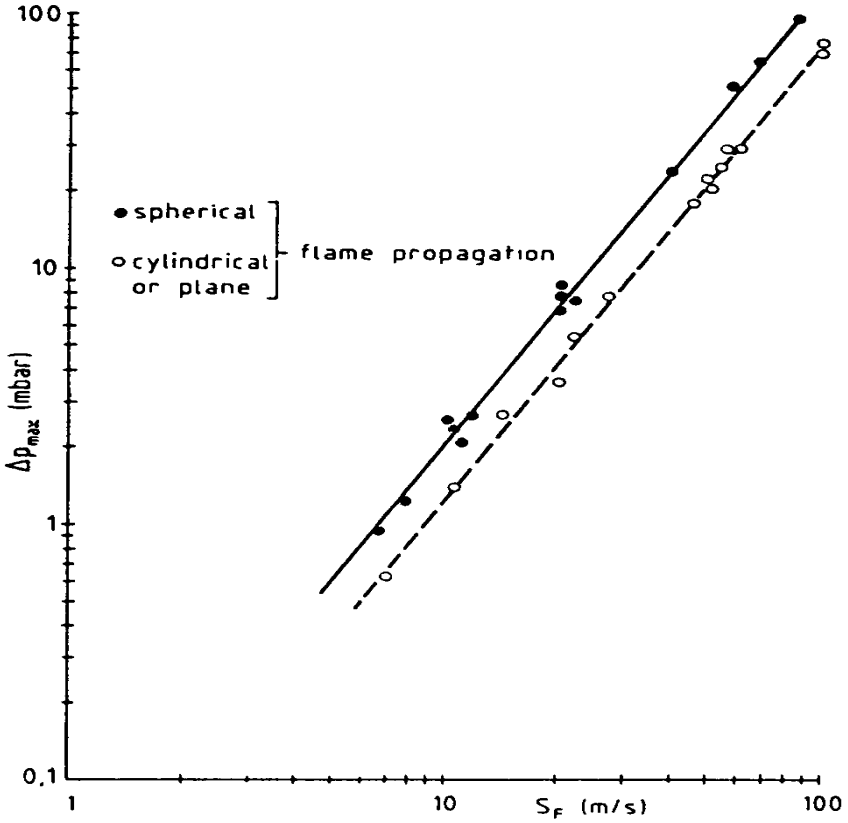

Fig. 5-4: Peak overpressure vs. flame speed from combustion tests with methane-oxygen-nitrogen mixtures

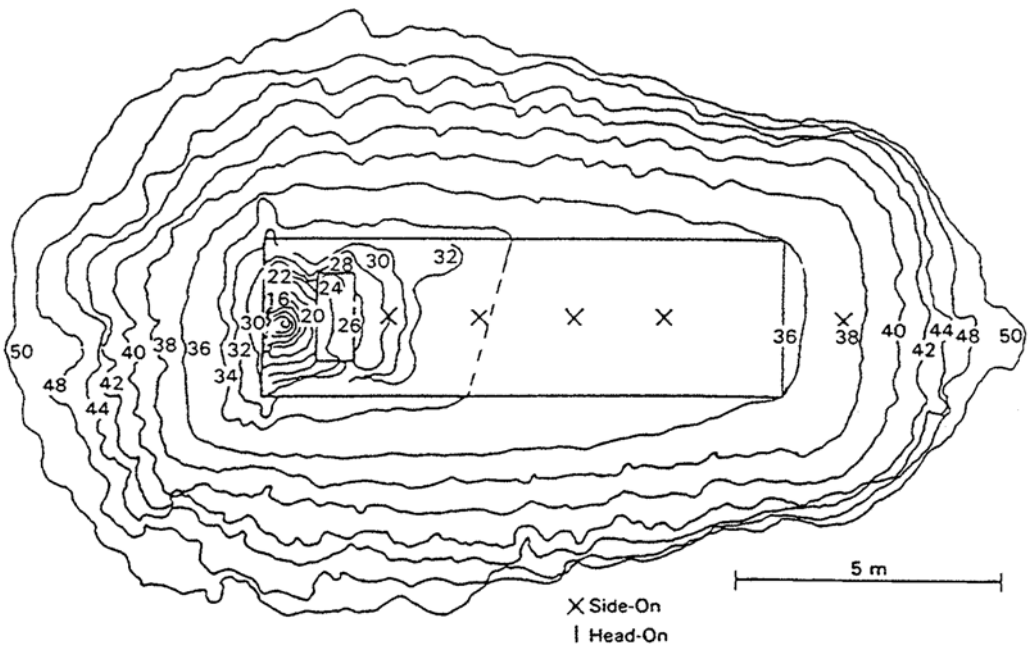

Fig. 5-5: Measured flame front profiles in the ICT detonation experiment within the PNP gas cloud program, „GHT 41“, with fan-induced turbulence

A similar series of jet ignition tests was conducted at the Defense Research Establishment Fuel-Air Explosive Facility, Canada, in a larger rig consisting of a 7.8 m long and 0.9 diameter tube with an 8 m long and 2.4 m diameter plastic bag attached. Test data with acetylene fuel indicated that a minimum jet speed of about 600 m/s for a detonation initiation in the most sensitive mixtures for a d_c/d ratio of 0.1, where d is the tube diameter and d_c the critical tube diameter (i.e., the minimum dimension of an unconfined detonable cloud, = 0.15 m for acetylene). Transferred to other fuels, it would mean a requirement of a 2 m, 3 m, 9 m, and 40 m diameter jet stream for hydrogen, ethylene, propane, and methane mixtures, respectively. These figures would be reduced by a factor of 5, if the jet velocity were increased from 600 to 700 m/s [Moen 1993].

There are three tests that reported the occurrence of DDT in not-confined fuel-air mixtures:

- DDT in a large-scale, partially confined (rectangular channel of 3 m height and 10 m length, closed at one end) hydrogen-air mixture was observed by Pförtner. A turbulent mixing region was created by a fan, sufficient to accelerate the arriving flame to detonation speed [Pförtner 1985].
- Geiger from the Battelle Institute Frankfurt used a rectangular box (0.5 x 0.5 x 1 m^3) connected through a small orifice to a larger volume of the same fuel mixture. The turbulent jet discharged from the box initiated a very fast deflagration eventually ending up in a detonation wave.
- In a similar (unintended) experiment by Moen with a C_2H_2-air mixture, a detonation was onset by a hot gas jet leading into a larger volume (2 m diameter, 3 m long). The detonation, however, did again not occur immediately, but only after being reflected from the plastic bag wall, which generated a recirculation zone.

It is even more difficult in a real, non-premixed mixture cloud to produce a detonation. Pförtner has used 300 g of an explosive and was not successful in obtaining a detonation in a non-premixed propylene mixture, which was achieved with only 20 g in a respective premixed cloud [Pförtner 1979]. The author concludes an estimated 17 % portion of a real gas cloud that reacted as if it were a premixed stoichiometric mixture.

The turbulence level is also depending on the strength of the ignition source. For a stoichiometric methane-air mixture, Pförtner has measured in a 15 m^3 balloon a flame speed of 11 m/s using a 100 J ignition source. US tests in a 262 m^3 balloon with a 10 J source yielded a flame speed of only 7 m/s [Pförtner 1979].

Large number of lab-scale experiments with ignition by frictional heating or frictional sparks showing that hot surface temperatures of at least 1000 °C are required to ignite a methane-air mixture [Laurendeau 1982].

Experiments using a small detonation tube, were conducted by Wagner in Göttingen, Germany. Flame speeds in stoichiometric methane-air mixtures in repeated obstacle environment were beyond 400 m/s with overpressures of about 65 kPa.

5.2.2.2. Gas Clouds in Confined Areas

Numerous partially confined vapor cloud explosion experiments have been carried out to quantify parameters such as obstacle parameters, degree of confinement, reactivity of fuels, ignition point, and many others.

Within the US Coast Guard Vapor Cloud Explosion Study [Parnarouskis 1980], detonation tube tests in a 0.6 m diameter steel pipe have been conducted with methane, propane, and ethylene oxide using explosives of 90 g (methane, propane) and 5 g, respectively. Except for methane, all tests resulted in detonation with pressures and velocities in agreement with the predictions. Maximum flame speed in methane was 1050 m/s at stoichiometric mixture and a pressure of 0.8 MPa. Spark-ignited (10 J) combustion yielded lower figures.

The TNO experimental series known under the name "Discoe" used a small-scale configuration of typically 4 m x 4 m with 0.1 m diameter obstacles and ethylene as fuel. The experimental program of the so-called "Spadeadam" trials employed a larger-scale configuration to study the effect of scaling using a test rig of 25.4 m x 12.7 m with a height of 1.0 m and obstacles of the same height and 0.5 m diameter. Fuels used in the seven tests were methane, propane, and ethylene. Tendencies observed at the small scale were also observed on the larger scale. Flame speeds and overpressures were generally found to be larger than at small scale. Flame speeds increase with larger blockage ratios. Also overpressures doubled when increasing the BR from 20 to 30 %. Venting opportunities decreased the flame speed significantly. Comparing flame speeds of different fuels, methane was found to be somewhat slower than propane [Mercx 1992].

In 1992/93, a series of 30 medium-scale fire tests has been conducted to investigate the BLEVE phenomena by using 0.4 m^3 cylindrical propane fuel tanks. The tests showed that the tank failure started with the development of a crack, when the thermal load had locally reduced the material strength by more than 80 %. From that moment, vapor was vented from the container. Subsequent events were either a crack growth termination with only jet release or a crack growth continuation to BLEVE with a crack-propagation velocity up to 200 m/s [Birk 1994].

In the FLAME apparatus at Sandia National Laboratories with dimensions of 30.5 m length, 1.8 m width, and 2.4 m height, flame acceleration and DDT were investigated in H_2-air mixtures. For absence of obstacles and 13 % top venting, DDT was observed. Increasing the top venting to 50 %, however, did no longer result in DDT. It confirmed also other observations that flame speeds are significantly reduced, if top venting is active [Moen 1993].

An open-sided, 3 x 3 x 18 m^3 long test section with repeated obstacles was used by Harris and Wickens [Harris 1989]. Maximum flame speeds obtained of 50 m/s in natural gas-air mixtures and 3 kPa pressure. Extending the channel length to 45 m, the corresponding figures were 80 m/s flame speed and 10 kPa overpressure, still less dramatic compared to H_2 or acetylene. Transition to detonation was not observed even with flame speeds of 1000 m/s in the confined region [Moen 1993].

Experiments described in [Urtiew 1983] were conducted in a channel (0.3 m high, 0.15 m wide, 0.9 m long), open on top and at the far end, using premixed propane-air mixtures as fuel. With no obstacles present, flame speeds of 2.3 - 3.2 m/s have been observed. Under conditions with obstacles, flame speeds of 4 - 15 m/s were measured. A major influence was found to be given by the position of the ignition source; an ignition at the bottom resulted in a higher initial

acceleration. Most tests did not show a continuous flame acceleration. Those tests with acceleration reaching speeds of 15 m/s had gaps under the obstacles, which allowed the flames to penetrate the neighbor cell, thus increasing the flame surface area.

In Pförtner experiments with hydrogen-air mixtures under partially confined conditions, i.e., in a 3 m high and 10 m long channel, flame speeds of 49 - 54 m/s have been measured at quiescent conditions. If fan-induced turbulence was present, flame velocities increased up to 222 m/s measured at the channel end. The flame, however, was still accelerating, so that a transition to detonation is likely to occur under these conditions [Pförtner 1985].

A key experiment was made by Harrison/Eyre, in which the explosion in a vented chamber resulted in the initiation of an external explosion. The pressure generated was temporarily higher than the internal pressure which could thus be increased by more than a factor of two.

Hjertager tests [Hjertager 1984] were done in a tube with 2.5 m diameter and 10 m long with internal obstruction and using methane and propane as fuel. He also investigated realistic structures in 1:33 and 1:5 scale models of offshore installations.

Combustion tubes of 12 m length and with diameters of 50, 150, and 300 mm, respectively, have been used by Lee et al. [Lee 1983] to investigate turbulent flame acceleration in various premixed fuel-air mixtures. Employing a spiral obstacle with 0.44 blockage ratio in the 50 mm tube, detonation velocities were reached for hydrogen and propane, whereas the flame speed in methane was in general less than 400 m/s, showing, however, a large fluctuation up to 800 m/s at stoichiometric mixture. Tests in the 15 cm tube with a BR of 0.39 revealed a maximum speed of 750 m/s in methane and of 850 m/s in propane, in both cases no detonation.

The Russian facility RUT with a length of 69.5 m and a total volume of 480 m^3 is presently the world's largest facility, in which H_2-air detonation processes have been investigated. One of the key results was the observation of a 12.5 % lower detonability limit for hydrogen showing that the detonation range expands with increasing size of the facility [Breitung 1995].

The Research Center Karlsruhe has been conducting numerous experiments in a 12 m detonation tube to investigate the combustion behavior of H_2-air mixtures [Bielert 1999]. In the most recent tests, the influence of carbon monoxide on the combustion process was examined [Breitung 2000]. The results were described in more detail in chapter 4.4.2.

5.2.2.3. Flammable Gas Mixtures in Nuclear Containments

In the Three Mile Island accident in 1979, the partial core melting process and reflooding of the core have resulted in the liberation of approximately 400 kg of hydrogen creating a flammable gas cloud, which eventually ignited after about 10 h. The deflagration in the containment took place at an estimated 8 vol% of H_2 concentration accompanied by a peak overpressure of 190 kPa, still below the design limit of 414 kPa.

This accident has initiated numerous experimental activities with respect to flammable gas mixtures for the simulation of deflagration/detonation processes in a nuclear containment. Experiments have been conducted, e.g., in Germany and the USA with a focus laid upon H_2-air-steam mixtures typical for LWR accident scenarios. They provided a better understanding of the H_2 distribution processes in confined structures and helping improve simulation tools, which appear to be applicable also to other gases or gas mixtures.

Several computer codes exist for modeling fire growth and spreading, toxic emissions and dispersion and fire/water spray interaction. They require further efforts in refined modeling of certain phenomena such as heat release or flame spreading in cables and equipment. Also fire data bases need to be improved. An IAEA fire safety project assembles fire experience and produces guidelines for fire hazard analysis and inspection of fire protection and fire fighting techniques; there is also an OECD-NEA group for fire PSA [OECD-NEA 2001].

Ongoing efforts are the research on new mitigation measures and accident management procedures to remove hydrogen from the containment, and on the improvement and validation of 3D analytical tools to simulate H_2 mixing and combustion phenomena including condensation processes effects of igniters and recombiners.

For the new generation of nuclear reactors, the hydrogen issue will be incorporated already during the design stage. Passive safety systems will be considered for containment cooling. Further experimental efforts, however, are hindered by the fact that the large-scale facilities HDR containment and the Battelle model containment have been taken out of service in the meantime. Therefore discussion has started on the establishment of a large European facility for containment-related studies.

5.3. Research Studies on Explosion Hazards for Nuclear Reactors

A variety of external impacts on a nuclear reactor containment have to be considered with respect to their potential damage of reactor components. Among them are fires and chemical explosions of hydrocarbons.

5.3.1. LOAD IMPACT FROM EXTERNAL DEFLAGRATION ON NPP

In an assessment for the German NPP Brunsbüttel, where at that time a chemical factory in the vicinity was under construction, the deflagration of a 50 m diameter flammable vapor cloud at the containment was assumed. The incident overpressure wave was estimated to be 30 kPa and the reflected overpressure wave 45 kPa, i.e., a reflection coefficient of 1.5.

Resulting from that discussion, the German RSK has specified the following load assumptions to be applied as minimum requirements to future NPP structural designs for pressure waves from the deflagration of saturated hydrocarbons [Jungclaus 1975]:

(1) pressure in incident wave	130 kPa
(2) reflected pressure	145 kPa
(3) time for pressure rise to peak pressure	0.1 s
(4) duration of pulse-effective triangle	0.2 s
(5) allround quasi-static load for > 1 s	130 kPa
(6) pressure wave may come from any direction	

The above requirements correspond to the (later) formulated BMI of 1976.

5.3.2. GERMAN RISK STUDY, PHASE A

On behalf of the German Federal Government, a risk study was conducted for a German PWR. The study was not part of a licensing procedure. Phase A (1976-79) basically applied the methodology as was used in the American WASH-1400 study. Phase A results were published in 1979. The methodology in terms of basic assumptions and methods was similar to WASH-1400, but a broader spectrum of events was considered. WASH-1400 does not include a more detailed quantitative event sequence analysis resulting from chemical explosion. In Phase B (1985-89), advanced methodologies were applied.

The risk study applies to the reference plant Biblis-B, a 3750 MW(th) PWR which started commercial operation in 1976. Results are not necessarily transferable to other plants and sites. A particular aspect, which led to an extension of the safety philosophy was the event sequence typical for impact from outside, namely possible "common cause" failures due to the effect on the total plant which carries a higher risk, if the plant is not designed against it. The question was whether and to what extent impacts from outside, such as earth quakes, airplane crash, shock waves, and others may contribute to the overall risk [GRS 1980]. The particular event of pressure waves following a vapor cloud explosion is described in the following in more detail:

The Biblis B reactor (as of the time of the study) is situated in a rural area with another nuclear reactor (Block A) in the immediate vicinity and a few chemical process industry facilities within a 10 km radius with shortest distance of 4 km to the nuclear site. Roads with potential tank truck transportation are in a distance of more than 2 km; the nearest railway is about 3.5 km away. As a waterway, the river Rhine is directly at the site boundary. The river transportation of hazardous goods, in particular liquefied gas, was thus considered the dominant risk of an explosion hazard to the Biblis NPP. From the information available, it was tried to derive the event frequency by assessing the single probabilities as given in Table 5-1.

Table 5-1: Single probabilities as assumed in the risk study for the Biblis B nuclear reactor

Probability of	Assumed frequency [yr^{-1}]
Severe accident of LFL tank ship	$2*10^{-3}$ - $3.2*10^{-4}$
Formation of flammable gas-air mixture	0.32
Drift of the cloud to the NPP	$7.8*10^{-2}$
Ignition of the cloud at the NPP	0.03 - 0.3
Deflagration of the cloud	1
Total	$1.5*10^{-5}$ - $2.4*10^{-7}$

The single probability of "1" for a deflagration as mentioned in the table means that a detonation is considered extremely unlikely. The total frequency should be considered as ballpark value only, since all single frequencies have a more or less large uncertainty range. The design assumption for the event frequency was fixed at the range $1*10^{-5}$ - $5*10^{-7}$. A subsequent core melting was considered very unlikely, such that a contribution to the overall risk was deemed insignificant. The same holds for explosions with pressure waves against which the NPP is not designed due to the extremely low frequency of such events.

Load assumption is the design basis pressure wave as prescribed in the RSK Guidelines. Safety distances were estimated according to the relation also given in the Guidelines are based on a mass of 50 % (pressurized liquefied gas) of the total mass of a single ship tank. The result is a safety distance of at least 338 m, which is realized for all relevant buildings except for one which, however, is basically an underground construction and thus not jeopardized.

Protection measures taken are, e.g., the realization of all entrances as air-locks to prevent the penetration of hazardous gases from outside, of blast-protected venting openings which can close automatically, and of gas warning systems. It is not a protection goal to continue reactor operation after the event, it is sufficient to protect the plant such that on the long term, no radioactivity be released that would lead to inadmittable doses. A consequence from external events to be assumed is a blackout of the NPP and the demand for emergency electricity supply systems. How to achieve the protection goals on which the safety philosophy is based for an accident due to impact from outside:

- Proper design of the systems necessary to control accidents: Safety systems must be designed such that they work properly also in the case of the accident in combination with a single fault in the safety system.
- Ensure emergency electricity supply: For almost all impacts from outside, it is assumed that the plant will be disconnected from the electricity grid with the consequence of a loss of all cooling systems.
- Keep integrity of primary system: The plant design has to be such that a loss of coolant accident can be excluded.
- Provide necessary degree of automation to control impacts from outside: If operability of the control room is not ensured, the plant must be transferred in a secure state automatically by means of an emergency control system and remain there for at least 10 hours.
- Ensure adequate component design: All components whose functioning cannot be guaranteed, are assumed to fail during the accident.

Considerations of the various impacts from outside leads to specific requirements to the constructive design and system technology. In particular, a comprehensive constructive protection of the reactor building and corresponding layout of the cooling system. The protection of other safety-relevant systems can be realized by respective sizing or segregation. However, rather than establishing a full protection of all buildings to be protected, the trend is towards an independent additional emergency system that is able to take over the safe shutdown of the reactor and the decay heat removal [GRS 1980].

5.3.3. GERMAN REACTOR SAFETY PROGRAM

The program “Research on the Safety of Light-Water Reactors” funded by the German Federal Government was conducted between 1979 and 1983 investigating the areas

- Conceivable mechanisms and configurations necessary for the evolution of detonation-like explosions;
- Relationship between the characteristic features of incoming blast waves and the

response of building structures;

- Strength of blast waves assuming the detonation of a realistic gas cloud.

The overall goal was the development of the methodology for a safety evaluation of accidents with gases transported in the vicinity of nuclear power plants. Results of this research program can be summarized as follows:

(1) The release of liquefied gases results in the formation of a flat gas cloud. A reliable prediction of cloud size, gas concentrations, and the flammable portion is not possible. There are indications that the BMI guideline provides conservative results.

(2) Only a strong ignition source has a significant influence on the flame spreading. The state of turbulence prior to and during the explosion is a decisive parameter for flame speed and overpressure. No fast deflagration with overpressures > 10 kPa are expected after explosions in open terrain; an exception may be the catastrophic failure of the pressure vessel. Partial confinement or obstruction is necessary to cause overpressures > 10 kPa with significant impact on building structures.

(3) Prerequisite for a DDT is the generation of very high flame speeds. A characteristic parameter is the detonation cell size with a higher reactivity of the fuel the smaller the cell size is. The direct initiation of a detonation is only feasible with strong igniters.

(4) The blast wave of a deflagration may exhibit a steep pressure rise, multiple peaks or a below-atmospheric pressure phase creating a complex load function enhanced by reflection or convergence of the wave.

(5) A stronger impact on the containment and components is expected for load functions characterized by multiple peaks or detonation or below-atmospheric pressure. The absolute impact, however, is in the range of elasticity and thus is in accordance with the design.

5.3.4. PNP GAS CLOUD PROGRAM

The main goals of the PNP gas cloud explosion program [Schildknecht 1987] were the improved understanding of the complex process of chemical explosions and its effect on the environment and, in particular, to demonstrate that a power station for nuclear coal gasification or process steam production is safely designed against explosions from outside, if the BMI guideline is applied.

A major section within the PNP safety program was dealing with the potential explosion of flammable gas clouds in the gas generation factory of the nuclear process heat plant and its consequences. The aim of this task was to acquire the necessary knowledge in terms of safety for the construction of process heat plants, and in particular to examine the course of a deflagration of a gas cloud, its pressure-time behavior, and to find an answer on the question, whether detonation of a free gas cloud is possible or not. The respective research works conducted within the so-called “PNP Gas Cloud Program” were dealing with

(1) Investigation of single mechanisms leading to a deflagration pressure buildup such as gas cloud formation, laminar and turbulent combustion, deflagration overpressures,

large-scale combustion, obstruction and vortex combustion, pressure wave reflecting and focusing effects;

(2) Analysis of damage of a deflagration pressure wave, conclusion from external load to internal load and compare with material characteristics, derivation of damage criteria;

(3) Analysis of severe accidents in terms of correlation between pressure-time history and damage by review and re-analysis of selected severe accidents based on the results gained under (2);

(4) Derivation of safety concept and damage limits from all results, pressure wave to form the basis for the design of safety-related components, guideline which ensures protection against pressure waves from chemical explosion.

The scenario of a process gas ingress into the nuclear containment has been studied in the past as part of the PNP safety program. The formation of flammable gas mixtures in the containment was investigated with focus on spreading and mixing processes, flammability limits of relevant mixtures, combustion processes, and pressure buildup. The aim was the experimental determination of flammability limits and laminar flame front velocities of multi-components gas mixtures with air as a function of pressure, temperature, ignition energy, mixture composition, and mixture concentration.

Experimental studies within the PNP gas cloud program were conducted and evaluated by the Fraunhofer Institute (Pförtner and co-workers). Flammable mixtures of hydrogen, methane, propane, or ethylene with air have been used to examine their explosion behavior with different concentrations, in different geometries (sphere, hemisphere, tube), in confined or unconfined arrangements. Various of those tests are described in more detail in chapter 5.2. Major findings can be summarized as follows [PNP 1981]:

(1) In a deflagration, the measured burning velocities were less than 10 m/s. If the combustion products, whose volume has become larger by a factor of 7 - 8, cannot escape to the sides, the flame front velocity will increase to about 70 m/s. The resulting overpressure will be then 0.74 kPa for a spherical flame front or 2.6 kPa for a linear flame front.

(2) The probability for a severe impact on the reactor will be comparably low, because the process gases are mainly light and hot, which due to buoyancy hardly can accumulate to explosible gas clouds. The hot temperatures will lead to autoignition, before a large-scale gas cloud can develop. In addition, in many parts of the gas factory, the ignition of process gases is rendered more difficult or even inhibited due to the presence of inert gas components (H_2O, CO_2).

(3) The experimental program could confirm the experts' opinion that gas mixtures typical for the gas factory cannot, independent of the distance, generate pressures beyond the design curve given in the BMI guideline.

5.4. Safety Studies for Similar Facilities

5.4.1. PROTOTYPE NUCLEAR PROCESS HEAT (PNP) PROJECT

The development of a system for nuclear coal gasification within the project "Prototype Nuclear Process Heat Plant" was conducted by five companies: Bergbauforschung GmbH, Hochtemperatur-Reaktorbau GmbH, Kernforschungsanlage Jülich GmbH, Rheinische Braunkohlenwerke AG, and acting as head the Gesellschaft für Hochtemperaturreaktor-Technik mbH. The project was sponsored by the German Federal Government and the State's Government of Northrhine Westphalia.

The concept of the PNP plant was reviewed by an advising committee in 1979/80 [RSK 1980], which identified several areas to be of relevance to safety:

- Integrated construction of primary circuit;
- Control of process gas and flammable gases inside and outside the reactor building;
- Tritium activity in process gas;
- Decay heat removal concept;
- Material research program;
- Status of component development and fabrication;
- Operational concept of the system;
- Radiation exposition of the personnel;
- Siting.

The integrated concept has the advantages that no primary circuit ducts would lead outside the prestressed concrete vessel, and that in case of a heat exchanger failure, process gas would penetrate into the primary circuit rather than liberated into the reactor containment.

5.4.1.1. Operation

Operation of the total system consisting of five major units requires a complex operation and control concept. The duration time to start the total system takes approx. 145 h, the shut-down procedure time is about 15 h. The concept is such that load changes in the gas factories do not have an influence on the nuclear primary circuit. Protective systems must work properly and effectively in the case of malfunctions. Thermal problems may arise, if only one of the two coal gasification units is being operated due to an unsymmetrical load in the core, or in case of an emergency reactor shut-down.

The process gas composition in a hydro gasification of lignite depends on the plant component. Some examples are given in the following Table 5-2 [Uni.Erlangen 1981].

The composition at the heat exchanger has a stoichiometric concentration of 20.9 % of process gas in air.

Table 5-2: Process gas composition in different components of the PNP plant for the gasification of lignite [Uni.Erlangen 1981]

Component	Concentration						Temp.
	CH_4	H_2	CO	CO_2	H_2O	N_2	
Splitting furnace, entrance	20	-	-	-	80	-	90 - 120
Splitting furnace, exit	5.1	38.0	4.7	6.0	46.3	-	75 - 112
Gas generator	28.2	56.3	3.9	-	10.5	-	40
Heat exchanger	22.9	68.1	4.0	-	-	5.0	23
Gas decomposition	6.7	61.2	2.6	19.3	-	10.2	23
Conversion	5.1	38.0	4.7	6.0	46.3	-	75 - 112

5.4.1.2. Flammable Gas Explosion Hazards inside the Reactor Building

There are several possibilities for a transition of flammable gases into the containment, where local explosions may occur [PNP 1981]:

(1) Penetration of flammable gases from outside through the venting system into the containment;

(2) Depressurization and water ingress in the primary system;

(3) Depressurization and air ingress in the primary system;

(4) Rupture of process gas line in the reactor building;

(5) Rupture of intermediate loop line plus leak in the gas generating system;

(6) Depressurization and process gas ingress in the primary system.

Case 1 must be controlled in any type of NPP, but it is of utmost importance in a nuclear process plant, since process gases are permanently present in the vicinity. The cases 2 and 3 are scenarios typical for HTGR. The cases 4, 5, and 6 are scenarios typical for a process heat plant. The cases 2 and 6 are similar in their accident sequence and the consequences.

The rupture of a process gas line (case 4) would result in the release of the gases into the reactor building. Therefore all process gas lines are enclosed in a second pipe, which is designed to sustain the pressure load in case of a rupture of the primary line. The space between the two tubes is inerted by helium and supervised by gas detection systems. Applying the leak-before-rupture criterion should exclude a complete failure of a process gas line and rather allow countermeasures, after a leakage has been detected. The same protection measures hold for the splitting tube reactor, which is equipped with a second pressure-resistant top.

The rupture of a line in the intermediate circuit combined with a failure of the gas generation system (case 5) results in the release of secondary helium and process gas into the reactor building. The tube dimensions in the intermediate circuit are much larger and are insulated at the inside, which precludes repeated inspection. The safety concept here is such that a removable, not pressure-resistant (for inspection) outer tube is applied together with a design of

the inner tube according to the leak-before-rupture criterion to detect leakages and initiate counteractions (e.g., disconnection) right in time. This scenario is considered the most critical, since the gas volume within the flammability range is largest and ignition must be assumed at high containment pressure level, thus resulting in a higher explosion pressure.

In case of a depressurization and a failure of the splitting tube furnace (case 6), locally flammable mixtures of process gases and helium cannot be excluded. Measures to minimize the risk are a design of the furnace to withstand the accident pressure in the reactor building after depressurization, which makes the assumed event combination very unlikely, and the limitation of the introduction of process gases due to line disconnection and depressurization on the secondary side.

Also in the case of a depressurization and the presence of an oxidizing atmosphere (water/air, cases 2 and 3), chemical reactions with the graphitic core structures (reflectors, fuel elements) may result in gas mixtures, which are locally flammable. Flow conditions and gas exchange processes between reactor pressure vessel and the containment building as well as the flammability ranges of the conceivable gas mixtures and their way of combustion are not completely clear yet and are subjected to further research.

It should be noted that the application of the "leakage-before-rupture" criterion, which was suggested as a solution of the safety problems in the above cases 4 and 5, is questionable under the conditions given. This criterion must not be applied in accident scenarios, which may result in unacceptable impacts on the environment. Alternative safety concepts would be, e.g., (partial) inerting of the reactor containment or an additional intermediate circuit.

The control of an accident scenario with the release of process gas into the neighborhood is not everywhere in compliance with the BMI guideline of 1976. However, it is only a limited number of components containing flammable gases, which do not meet the safety distance guideline.

If the reactor building is sufficiently designed to withstand the pressure waves resulting from an explosion outside, the impact on components inside the building due to induced shaking is expected to be covered by the respective design against air crash and earth quake [PNP 1981].

5.4.1.3. Tritium Transport

Before the product gas can be delivered to the consumer, the tritium contents in the gas must be measured. The upper limit allowed is 0.37 Bq/g (10 pCi/g) (today: 0.5 Bq/g) for any fabricated products, as defined in the (former version of the) German Preventive Radiation Protection Ordinance, which can only be met under conditions of significant improvements. The above given limit for the products corresponds to about 266 Bq/m^3 of SNG.

Measures to comply with the stringent limits imposed by German law include the employment of an intermediate circuit (considered for the hydro gasification process) and further efforts to reduce the tritium permeation into the product gas. Self-grown oxide layers on the heat transferring tube wall surfaces are able to reduce significantly tritium permeation rates. On the basis of PNP specific experiments, an average reduction factor of 100 was assumed with respect to the permeation rate through austenitic steel plus oxide layer.

Inhibiting or reducing effects on the permeation are also given with the addition of other

substances. A high doping of the intermediate circuit with hydrogen can reduce the permeation rate by a factor of 5. A drawback is the enhanced potential for graphite corrosion due to the H_2 permeating into the primary helium. If a maximum allowable level of 30 vpm of H_2 in the primary helium is assumed, the reduction factor is estimated to be 2 - 3. A doping with oxygen will enable a faster growth of the oxide layer. A doping with water vapor takes advantage of the tritium binding in water molecules ("HTO"), which can be broken up by oxidation processes only.

Taking account of above given effects, for the PNP-500 plant design considered, the estimated tritium activity in the product gas, SNG, is approximately 3.7 Bq/g (100 pCi/g) corresponding to a potential radiation impact on the consumer of about 0.0025 mSv/yr (0.25 mrem/yr). In more detail, it is in the range of 2.2 - 8.1 Bq/g (60 - 220 pCi/g), representing the upper limits assessed for steam-coal gasification (with IHX) and the hydro-gasification of coal (no IHX), respectively.

5.4.2. MCNAB CREEK LNG FACILITY

As an example for an hazard analysis of an LNG storage facility, some information is presented in the following taken from a project report prepared for the Westcoast Gas Services Inc. (WGSI) to operate the McNab Creek LNG Facility [CDS 1998].

5.4.2.1. Project

WGSI applied for the construction and operation of an LNG facility at McNab Creek, British Columbia, Canada to be used as a peak-shaving plant. It means that during low-demand months, natural gas is drawn from the pipeline, then liquefied, stored, and eventually re-gasified in the winter months, when the demand is high. The LNG facility is designed to have a liquefaction capacity of 450,000 m^3 of gas per day and a re-gasification capacity of 8,500,000 m^3 of gas per day to return into the grid.

The double-walled, single integrity, above-ground LNG storage tank is designed to contain a total of 145,000 m^3 of LNG at a pressure of 11 kPa (above atmospheric pressure) and a temperature of 113 °C. The tank dimensions are 74 - 82 m in diameter and 47 - 52 m in height. A compacted-earth dike serving as secondary containment impounding area is able to take up 110 % of the entire tank volume in case of an accidental spillage. In case of a major fire event, a water reservoir to hold > 5000 m^3 of water will be used.

The McNab Creek LNG facility has been designed based on proven technology in order to meet the required specifications in the respective codes including the Canadian code CSA Z-276-94, which is very much the same as the USA code NFPA-59A (1996).

5.4.2.2. Safety Concept

For the McNab Creek LNG storage tank, the potential hazard of "rollover" is taken into consideration. The LNG input which will be always of a high level of uniform homogeneous liquid, will be injected into the tank at either bottom or top to promote natural mixing. At longer storage periods, in-tank pumps can be activated to prevent stratification. Furthermore boiloff

compressors are available to maintain the tank pressure level. The tank is also fitted with three overpressure relief valves with either one being able to handle the full natural gas amount resulting from a fire-induced heat leakage into the tank. Finally there is a vent valve, which is controlled by the operator.

With respect to fire suppression, a protection system will be installed, which consists of a fire water storage reservoir, electric and diesel pumps, underground pipework, everything kept under pressure at all times. Firewater coverage is such that each process area is reached by at least two water sources with a supply duration of minimum five hours.

As a mitigation measure, an emergency response plan was established for the McNab Creek facility to effectively react on any kind in incident concerning operation and personnel/equipment. Three levels of alert have been defined with "3" marking the most serious ones. In case of a emergency, two groups become active:

1. Field Emergency Response Team: It is directed by an Incident Commander, who also declares the level of alert and who is responsible for the overall management of the response to the incident. An On-Site Supervisor takes care of control, containment, cleanup, and worker safety procedures at the site. If necessary, a Public Protection Supervisor is nominated to manage off-site activities like sheltering, evacuation, environment monitoring, or assistance to the public.
2. Crisis Management Team: It provides authoritative support mainly at alert levels "2" or "3" incidents dealing with legal issues, insurance issues, alternative gas supply or media relations support.

5.4.2.3. Design Spill Fire

The LNG released in a design spill will be collected in a 8.5 x 8.5 m^2 sub-dike, located at the lowest point of the main dike impounding area. The distance to the closest trees is 189 m and to the shell of the storage tank 181 m. The estimated time to burn the design spill is 1.6 hours. For this time, a radiant heat flux of 15 kW/m^2 is considered a representative threshold for piloted ignition of trees.

The reverse case, i.e., a forest fire impacting the LNG tank, was also calculated. Here the LNGFIRE model was taken to simulate burning trees as an LNG fire and deriving the heat flux at the tank. This case was also found to not present any hazard to the tank.

For the proposed McNab Creel LNG facility, worst-case accident scenarios have been identified and analyzed in terms of vapor dispersion, fire radiation, BLEVE, and/or vapor explosion hazards. The scenarios considered were:

(A) Failure of gas inlet line: Release of gas at 11.1 MPa and 297 K through 0.254 m diameter pipe for 10 min;

(B) Failure of LNG transfer line: Release of liquid at 7.5 MPa and 114 K through 0.076 m diameter pipe for 10 min;

(C) Failure of LNG storage tank: Release of entire tank contents at 0.1124 MPa and 112 K within 10 s into secondary containment impounding system;

(D) Failure of LNG send-out line: Release of slightly superheated LNG at 5.4 MPa and

116 K through 0.203 m diameter pipe for 10 min;

(E) Failure of gas send-out line: Release of gas at 15.3 MPa and 289 K through 0.254 m diameter pipe for 10 min;

(F) Failure of refrigeration separator outlet line: Release of superheated refrigerant liquid at 2.28 MPa and 304 K through 0.154 m diameter pipe for 10 min;

(G) Failure of refrigeration separator inlet line: Release of refrigerant vapor at 2.3 MPa and 304 K through 0.305 m diameter pipe for 10 min;

(H) Failure of refrigeration suction drum outlet line: Release of refrigerant vapor at 0.248 MPa and 295 K through 0.575 m diameter pipe for 10 min;

(I) BLEVE of refrigeration suction drum: Instantaneous release of the full 4500 kg of LNG content;

(J) Failure of odorant drum: Release of 200 l of mixed odorant within 5 s onto unconfined flat surface.

Basic assumptions in the calculations for the atmospheric boundary conditions are an ambient temperature of 289 K, a relative humidity of 30 %, a Pasquill atmospheric stability class of F ("moderately stable"), and a wind speed of 2 m/s. The dispersion calculations were performed with the DEGADIS code, a heavy gas dispersion model developed at the University of Arkansas [Havens 1985] and generally acknowledged in the USA to be used for siting LNG facilities. Radiation calculations were conducted with the LNGFIRE model, also a generally acknowledged tool for LNG hazard assessment. The calculation results are summarized in Table 5-3.

5.4.2.4. Hypothetical Accident of Catastrophic Storage Tank Failure

From all release scenarios considered, the almost instantaneous failure of the LNG storage tank would have the greatest impact. The evolving vapor cloud would cover an area up to 2.5 km downwind distance from the spill point and a width of 1.6 km, until it has diluted to half of the LFL. Neutral buoyancy would be reached after approx. 800 m. However, no LNG regulatory code requires the consideration of this kind of total tank failure; it rather defines design spills. The only event conceivable to cause a tank rupture, could be an earthquake. According to the (USA) code, the tank structure must be designed to allow a safe shutdown after a "10,000-yr-occurrence" earthquake.

The risks of asphyxiation or freeze burn injuries are given only in the immediate neighborhood of the spill point. A risk to the public would be given by the ignition of the flammable cloud. A flame in the leading edge of the cloud could burn back to the source and start a long-lasting pool fire. Trees within the zone (i.e., < 366 m distance) exceeding a heat flux of 21.1 kW/m^2 could ignite during a prolonged radiation exposure.

Table 5-3: Results of risk analysis calculations for the McNab Creek LNG facility

Case	Distance from center of impoundment [m]		
	1/2 LFL [1)]	**21.1 [kW/m^2] [2)]**	**6.85 kPa[3)]**
A	257	194	
B	185	24	
C	2540	366	
D	492	78	
E	123	109	
F	218	55	257
G	258	62	328
H	261	33	298
I		59 [4)]	
J	632 [5)]		

1) 2.5 vol% of methane in air;
2) 21.1 kW/m^2: level below which radiation heating is very unlikely to ignite wood;
3) 6.85 kPa: level beyond which severe damage to residences is expected;
4) Distance to the absorbed radiation level that could cause 1 % mortality level;
5) Distance to the "Immediate dangerous to life and health" concentration level.

5.4.3. LH_2 FUEL CELL POWER PLANT FOR DISTRICT HEATING

A safety audit has been conducted by the German Federal Institute for Materials Research and Testing, BAM, for an LH_2 storage and vaporization facility, to be installed within a residential area of the German city of Hamburg [BAM 1994].

Fig. 5-6: Fuel cell power plant in a residential area in Hamburg, Germany

5.4.3.1. Project

A pilot project of demonstrating the operation of a fuel cell power plant for the cogeneration of heat and electricity in a residential area has been realized in Hamburg, Germany (see Fig. 5-6). The power plant consists of two Phosphoric Acid Fuel Cell (PAFC) units based on the ONSI PC 25C type generating 220 kW(th) and 200 kW(e), respectively. The first PAFC unit fueled with natural gas is being operated since 1995 to meet district heat demand. The second PAFC unit, which is fueled with hydrogen, was set into operation in 1997 being the first-in-the-world H_2-based energy system in a municipal housing area. The efficiency of the H_2 unit is 40 % at an operation temperature of 180 °C. The hydrogen is stored as LH_2 in a cryogen storage tank located adjacent to the power unit. The demonstration project for the H_2-fueled unit was terminated in May 2000 after a comparably reliable operation and will be transferred for further operation to an industrial company, which produces hydrogen as a by-product.

Due to the pilot character of this project, a licensing procedure according to the German Federal Immission Control Act, BImSchG including the participation of the public, was conducted. In this context, the BAM was requested to provide a safety audit for the operation of the LH_2 storage vessel and the vaporization facility.

5.4.3.2. Tank Design and Operation

Legislation

With a storage capacity of more than 3 t, but less than 50 t of hydrogen, the simplified licensing procedure according to the Federal Immission Control Act (BImSchG) without a safety analysis is required. Also the Pressure Vessel Ordinance (DruckbehV) plus the respective technical rules for pressure vessels (TRB), for pressurized gases (TRG), and for piping (TRR) as well as the corresponding instruction sheets (AD-Merkblätter) apply. The presence of a flammable gas requires the consideration of the Explosion Protection Ordinance (Explosionsschutzverordnung) and the Hazardous Materials Ordinance (Gefahrenstoffverordnung) and related rules. Finally the Working Place Ordinance (Arbeitsstättenverordnung) also containing safety-related rules, and the Accident Protection Prescriptions (Unfallverhütungsvorschriften) of the Professional Associations apply, since the tank system is part of a commercial facility.

Tank Construction

The LH_2 storage vessel is a cylindrical, standing tank with a net capacity of 60 m^3. Because of the large temperature difference between the cryogenic liquid at 20 K and the ambient temperature, the pressure vessel is placed into an outer container with a highly effective thermal insulation in between to minimize the heat transport from the outside.

The tank is designed to sustain a maximum pressure of 1.2 MPa; the operating pressure is ranging between 0.6 and 1.05 MPa with a nominal value of 0.75 MPa. The typical boiloff rate of a 75 m^3 tank is 0.7 %/day, which translates into 22 kg/day or 0.35 m^3 of LH_2 per day or 300 N m^3 of gaseous H_2 per day. Both storage tank and vaporizer are designed to withstand a (wind) pressure of 5 kPa corresponding to a wind speed of 150 km/h.

The operation of a 200 kW PAFC plant with hydrogen requires approximately 6 kg/h, thus consuming the tank contents within about 700 days or one month. The refueling is done from a tank truck. Fig. 5-6 shows a diagram of the arrangement of the tank facility and its connections to the refueling truck (left-hand side) and to the fuel cell unit (right-hand side). Pneumatic valves are being operated by pressurized helium or air. In case of a loss of external electricity supply, the system is switched to a pressure bottles backup system. The main refueling valve is controlled from the tank truck. The truck driver stops the refueling process, when a filling level of 95 % is reached. The hydrogen is withdrawn from the liquid phase inside the tank and routed to the vaporizer.

Safety Measures

Since the facility is mainly automatically operated, measures have to be taken to provide automatic alarm in case of emergencies.

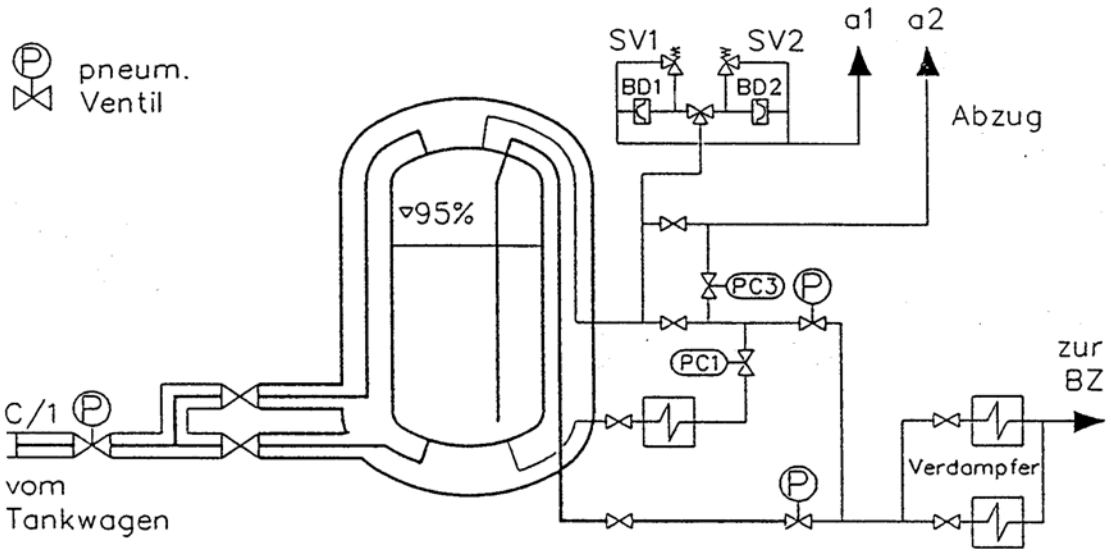

Fig. 5-7: Schematic of the LH_2 storage tank system

The storage tank is protected against overpressure by a consecutive series of relief arrangements (see Fig. 5-7). If the pressure exceeds 0.8 MPa, hydrogen from the vapor phase will be discharged to the vaporizer. At a pressure of 1.0 MPa, the H_2 will be vented via PC3 to the stack a2. Upon further increase of the pressure to 1.2 MPa, the safety valves SV1 and SV2 will open and release gaseous H_2 through stack a1. At still increasing pressure, rupture disks BD1 and BD2 will be activated at 1.69 MPa. Safety valves and rupture disks, however, are expected to be required only in case of a severe accident with a failure of the outer container. For an intact tank in a closed state, it needs in the order of several days until the pressure has reached a level where the first safety measure would be initiated.

In order to avoid a too low pressure in the storage tank, it is equipped with an own vaporizer connected via PC1 to the vapor phase inside the tank.

Measures in connection with the refueling procedure are such that the process is automatically interrupted, if

- the tank driver continues to fill the tank beyond 95 %;
- the grounding of the tank truck in insufficient;
- the storage tank pressure is too high;
- the storage tank pressure is too low;
- the helium pressure for valve control is too low.

According to the Technical Rule TRB, the double-walled storage tank is treated the same as an earth-covered tank with respect to the safety distance. The minimum distance from the outer tank to adjacent buildings or facilities is 5 m. The IGC recommendations, which are partly stricter than the TRB rules, mention safety distances of 10 m to roads and technical (non-residential) buildings and 20 m to residential buildings. The TRB rule for "normal" pressure vessels with flammable gases (which does not apply here) requires a minimum distance of 40 m. But even this criterion would be met, since the minimum distance to the next residence is 41 m.

The protection area, i.e., the zone in which the formation of flammable gas clouds is possible, is 5 m horizontally and 2 m in height. For the storage tank here with a height of 14 m and venting lines ending 4 m above the vessel, the protection area thus reaches a total height of 20 m.

5.4.3.3. Potential Consequences of Accidents

Storage tank and piping are designed according to the principle leak-before-rupture meaning that a relief through a smaller opening is expected after a failure rather than an immediate rupture. Therefore it is unlikely to expect any flying debris after a failure of the pressurized tank, at least it would not fly a long distance.

The failure of piping usually will soon be detected due to a significant change in the operational parameters such that the withdrawal of LH_2 from the tank will be disconnected immediately. Furthermore H_2 detection devices and warning systems are installed in areas where hydrogen can leak and accumulate.

In case of a failure of the insulation between the inner and outer container of the tank, hydrogen is estimated to vaporize at a rate of 55 kg/h and to be released through the two symmetrically arranged venting stacks. The worst case would be a release in wind direction, when a widely extended plume develops. In a no-wind situation, two symmetrical plumes spreading in opposite directions will be created. Because of its lighter-than-air property, hydrogen will always have the tendency to rise and thus will remain far away from the ground.

The WHAZAN model [Technica 1988] was used to assess the explosion hazards of a released H_2-air mixture cloud. Since the cloud will most certainly be a free vapor cloud, no severe blast wave is expected. Uncertainties in the boundary conditions are given with respect to the H_2 quantity involved in the explosion reaction, which might be in the range between 0.1 and 10 kg of hydrogen. Damage distances from the point of ignition as have been derived from the calculations, are 7 m for severe building damage, 14 m for minor building damage, 34 m for severe glass damage, and 92 m for a 10 % glass damage.

The development of a jet flame at the venting orifice was found to be very unlikely because of the small release rate of less than 10 g/s per stack. The assumption of an unrealistically high release rate of 100 g/s would result in a heat radiation of 37.5 kW/m^2 in a distance of 8.7 m, of 12.5 kW/m^2 in a distance of 9.5 m, and 1.6 kW/m^2 in a distance of 14.7 m, showing that no severe radiation hazard is given to the public.

A spill of LH_2 is conceivable during the refueling procedure, which usually takes about 1 - 2 h, e.g., by a moving tank truck while still connected to the tank. In such a case, the helium line and the grounding connection would fail first and disconnect the LH_2 line. The maximum quantity of LH_2 spilled is estimated to be not more than 0.2 l, too small to cause an explosion hazard.

6. CONCLUSIONS

The present report was subjected to safety aspects of the combined nuclear/chemical HTTR/SR system and the pertinent question of the probability of a methane-air vapor cloud detonation in the open atmosphere which may have a serious impact on the HTTR reactor building.

The evaluation of the characteristics of the fuel methane and its combustion behavior under various conditions allows the following conclusions:

(1) Methane is by chemical nature a relatively slow and less violently burning gas compared with other hydrocarbons.

(2) The combustion of an unconfined LNG vapor cloud in the atmosphere will normally result in a flash fire. Various experimental studies have led to the belief that the combustion of a methane-air mixture is very unlikely to produce damaging pressure waves. The effect of turbulence generation just ahead of the flame front as the most pertinent parameter for a possible transition to detonative combustion has not been observed so far to have resulted in significant flame acceleration. The only evidence for a DDT in connection with methane was observed in shock tube tests in mixtures with pure oxygen after comparably long run-up times.

(3) No data exist on the detonation of pure methane-air mixtures neither from field experiments nor from accidents. The conclusion that in partially or totally unconfined areas or in the absence of a sufficiently long travel distance, DDT is a highly improbable event, is based on the lack of a viable mechanism for flame acceleration. The only conceivable way to obtain the critical conditions to onset a detonation would be to directly generate the required conditions locally, e.g., by a sufficiently large explosive or an intense turbulent jet of hot combustion products.

(4) It seems to be reasonable to believe that a sufficiently large amount of explosive should be able to generate a detonation wave in an unconfined stoichiometric methane-air mixture. However, the extrapolation of experimental data by Bull resulting in a minimum of 22 kg of TNT to be necessary for a methane-air detonation could not be verified in later tests, where even the amount of 37 kg of TNT did not initiate a detonative combustion. Presumably only detonation-like processes with blast waves take place which decay after a while to a deflagration. Detonative quantities in this order would be rarely available in realistic accident scenarios.

(5) Even for other flammable hydrocarbon-air mixtures, there is no experimental evidence of a pure detonation initiated by a typically weak ignition in the open atmosphere. However, in reality there will hardly be a free gas cloud. Release-induced turbulence or any kind of turbulence-generating obstruction in industrial surroundings will to some extent always be present. The analysis of accidents has shown that in gas cloud explosions, overpressures higher than 30 kPa have been observed, which presumably have developed during the course of the explosion due to turbulence or partial confinement. According to an IAEA statement, the possibility of at least partial detonations within a cloud with overpressure higher than 30 kPa cannot be excluded. Detonable portions of the gas cloud, however, would be limited to relatively small areas.

(6) With respect to the BLEVE type of combustion relevant to storage vessels, there is no report in the literature known that any BLEVE has occurred with LNG.

(7) Concerning the predictability of the transition of a deflagrative combustion into a detonation, an overall statement was made within the frame of the PNP gas cloud program saying that the mechanisms for flame acceleration be qualitatively well understood. However, they cannot be described up to now on a quantitative basis for predictive purposes. This statement is, in principle, still valid today.

With respect to the HTTR hydrogen production plant, specific conclusions are:

(1) The planned distance of "more than 300 m" between the anticipated site of the 400 m^3 LNG storage tank and the HTTR building would meet the German BMI guideline. It would, however, not meet the much more conservative US Regulatory Guide 1.91.

(2) The PNP gas cloud explosion experimental program could confirm the experts' opinion that gas mixtures typical for the gas factory cannot, independent of the distance, generate pressures beyond the design curve given in the BMI guideline.

(3) If the reactor building is sufficiently designed to withstand the pressure waves resulting from an explosion outside, the impact on components inside the building due to induced shaking is expected to be covered by the respective design against air crash and earth quake.

(4) JAERI calculations using the P2A code system to simulate the impact of methane vapor cloud explosions on the HTTR have shown, under certain boundary conditions for the release rate, that no significant influence on the building be expected.

7. LITERATURE

[Baker 1983] Baker, W. E., Cox, P. A., Westine, P. S., Kulesz, J. J., Strehlow, R. A., Explosion Hazards and Evaluation, Fundamental Studies in Engineering Vol. 5, Elsevier Scientific Publishing Company, Amsterdam (1983).

[BAM 1994] Bundesanstalt für Materialforschung und –prüfung, Sicherheitsgutachten zur Vorprüfung einer Tank- und Verdampferanlage für verflüssigten Wasserstoff (LH_2) im Rahmen eines öffentlichen Zulassungsverfahrens nach Bundes-Immissionsschutz-gesetz (BImSchG), Federal Institute for Materials Testing and Research, Berlin, Germany (1994).

[Battelle 1973] Battelle Columbus Laboratories, LNG Safety Program Phase II (1973).

[Berman 1986] Berman, M., A Critical Review of Recent Large-Scale Experiments on Hydrogen-Air Detonations, Nucl. Sci. Tech. 93 (1986) 321-347.

[Bielert 1999] Bielert, U., et al., Multi-Dimensional Simulation of Hydrogen Distribution and Combustion in Severe Accidents, Report within EU Project FI4S-CT-95-0001, Research Center Karlsruhe, Germany (1999).

[Birk 1994] Birk, A. M., Cunningham, M. H., The Boiling Liquid Expanding Vapour Explosion, J. Loss Prev. Process Ind. 7 (1994) No. 6 474-480.

[Blackmore 1982] Blackmore, D. R., Eyre, J. A., Summers, G. G., Dispersion and Combustion Behaviour of Gas Clouds Resulting from Large Spillages of LNG and LPG on the Sea, Trans. I. Marine Eng. 94 (1982) Paper 29.

[BMI 1976] Bundesministerium des Innern, Bekanntmachung der Richtlinie für den Schutz von Kernkraftwerken gegen Druckwellen aus chemischen Reaktionen durch Auslegung der Kernkraftwerke hinsichtlich ihrer Festigkeit und induzierter Schwingungen sowie durch Sicherheitsabstände, September 13, 1976.

[Böke 1995] Böke, J., Vorhersagemöglichkeiten von Störfallauswirkungen, vfdb 44 (1995) 51-58, Verein zur Förderung des deutschen Brandschutzes.

[Boltendahl 1980] Boltendahl, U., Harth, R., Wärmetransport auf kaltem Wege, Bild der Wissenschaft, 17 (1980) April 44-55.

[Boni 1977] Boni, A. A., Chapman, M., Cook, J. L., Schneyder, G. P., Transition to Detonation in an Unconfined Turbulent Medium, Proc. AIAA 15th Aerospace Sciences Meeting, held at Los Angeles, USA (1977) 379-405.

[Breitung 1995] Breitung, W., Redlinger, R., A Model for Structural Response to Hydrogen Combustion Loads in Severe Accidents, Nucl. Tech. 111 (1995) 420-425.

[Breitung 2000] Verfondern, K., Moormann, R., Breitung, W., Veser, A., Contributions to a Safety Analysis for a Hydrogen Production System with HTGR, 1st Information Exchange Meeting on Nuclear Hydrogen Production, October 2000, Paris, France (2000).

[Bull 1976] Bull, D. C., Elsworth, J. E., Hooper, G., Quinn, C. P., A Study of Spherical Detonation in Mixtures of Methane and Oxygen Diluted by Nitrogen, J. Phys. D: Appl.

Phys. 9 (1976) 1991-2000.

[Burgess 1970] Burgess, D. S., Murphy, J. N., Zabetakis, M. G., Hazards Associated with the Spillage of Liquefied Natural Gas on Water, Report of Investigations 7448, US Department of the Interior, Washington D.C., USA (1970).

[Canvey 1978] Canvey : An Investigation of Potential Hazards from Operations in the Canvey Island-Thurrock Area, London, UK (1978).

[CDS 1998] CDS Research Ltd, LNG Storage Facility, Project Report for Westcoast Gas Services Inc., (1998), http://www.eao.gov.bc.ca/PROJECT/ENERGY/Wgsi/ Stage_ two/p_report/appd.htm, (1998).

[Chan 1991] Chan, C. K., Tennankore, K. N., A State-of-the-Art Report on Flame Acceleration and Transition to Detonation in Hydrogen/Air/Diluent Mixtures, Draft Report, OECD-Nuclear Energy Agency (1991).

[Chan 1992] Chan, S. T., Numerical Simulations of LNG Vapor Dispersion from a Fenced Storage Area, J. Haz. Mat. 30 (1992) 195-224.

[Dienhart 1995] Dienhart, B., Ausbreitung und Verdampfung von flüssigem Wasserstoff auf Wasser und festem Untergrund, Report Jül-3155, Research Center Jülich (1995).

[Diepold 1970] Diephold, W., Pförtner, H., Hommel, H., Sicherheitsabstände bei der Lagerung und Handhabung explosionsfähiger Stoffe, Explosivstoffe 18 (1970) 25-39.

[Droste 1990] Droste, B., Die Bewertung der Sicherheit von Umschließungen zur Lagerung von Flüssiggas, 5th Colloquium on Questions of the Chemical Safety Technology, Berlin, May 14-15, 1990, Proc. BAM, ISBN 389 429-070-6, 83-101.

[Edeskuty 1996] Edeskuty, F. J., Stewart, W. F., Safety in the Handling of Cryogenic Fluids, The International Cryogenics Monograph Series, Plenum Press (1996).

[Ermak 1982] Ermak, D. L., Chan, S. T., Morgan, D. L., Morris, L. K., A Comparison of Dense Gas Dispersion Model Simulations with Burro Series LNG Spill Test Results, J. Haz. Mat. 6 (1982) 129-160.

[Ermak 1983] Ermak, D. L., Goldwire, H. C., Hogan, W. J., Koopman, R. P., McRae, T. G., Results of 40 M³ LNG Spills onto Water, Proc. 2nd Syposium on Heavy Gases and Risk Assessment, May 25-26, 1982, Frankfurt, Germany (1983).

[Feldbauer 1972] Feldbauer, G. F., et al., Spills of LNG on Water – Vaporization & Downdrift of Combustible Mixtures, Report No. EE61E-72, Esso Research & Engineering Company, Washington D.C., USA (1972).

[Geiger 1980] Geiger, W., Synofzik, R., Influence of Dispersion Behavior of Dense Explosive Gases on the Possible Strength of Explosion, in: Hartwig, S. (Ed.), Heavy Gas and Risk Assessment, D. Reidel, Frankfurt (1980).

[Geiger 1982] Geiger, W., Present Understanding of the Explosion Properties of Flat Vapour Clouds, Proc. 2nd Symposium on Heavy Gases and Risk Assessment, Frankfurt, Germany (1982), 225-236.

[Giesbrecht 1980] Giesbrecht, H., Hess, K., Leuckel, W., Maurer, B., Analyse der potentiellen Explosionswirkung von kurzzeitig in die Atmosphäre freigesetzten Brenngasmengen,

Teil 1: Gesetze der Wolkenausbreitung und –deflagration aus Berstversuchen an Metallbehältern, Chem.-Ing.-Tech. 52 (1980) 114-122.

[Giesbrecht 1981] Giesbrecht, H., Hess, K., Leuckel, W., Maurer, B., Analyse der potentiellen Explosionswirkung von kurzzeitig in die Atmosphäre freigesetzten Brenngasmengen, Teil 2: Überprüfung der Modellgesetze anhand der Analyse von Schadensfällen, Chem.-Ing.-Tech. 53 (1981) 1-10.

[GRS 1980] GRS, Deutsche Risikostudie Kernkraftwerke, Fachband 4: Einwirkungen von außen (einschließlich anlageninterner Brände), Verlag TÜV Rheinland, Cologne (1980).

[Gugan 1978] Gugan, K., Unconfined Vapour Cloud Explosions, The Institution of Chemical Engineers, Rugby, UK (1978).

[Gwehenberger 1999] Gwehenberger, J., Mayer, H., Matzarakis, A., Schadenpotential über den Ausbreitungspfad Atmosphäre bei Unfällen von Gefahrguttankfahrzeugen, TÜ 40 (1999) No. 11 52-57.

[Hada 1994] Hada, K., Fujimoto, N., Sudo, Y., Design of Steam Reforming Hydrogen and Methanol Co-Production System to be Connected to the HTTR, Proc. IAEA-TCM on High Temperature Applications of Nuclear Energy, Oarai, Japan (1992), IAEA-TECDOC-761, Vienna Austria (1994)124-134.

[Harris 1989] Harris, R. J., Wickens, M. J., Understanding Vapour Cloud Explosions – An Experimental Study, 55th Meeting of the Institution of the Gas Engineers, Kensington, UK (1989).

[Harrison 1987] Harrison, A. J., Eyre, J. A., The Effect of Obstacle Arrays on the Combustion of Large Premixed Gas/Air Clouds, Comb. Sci. Techn. 52 (1987) 121-137.

[Havens 1985] Havens, J. A., Spicer, T. O., Development of an Atmospheric Dispersion Model for Heavier-than-Air Gas Mixtures, Final Report to US Coast Guard CG-D-23-85, Washington D.C., USA (1985).

[Hirst 1982] Hirst, W. J. S., Eyre, J. A., Maplin Sands Experiments 1980: Combustion of Large LNG and Refrigerated Liquid Propane Spills on the Sea, Proc. 2nd Symp. On Heavy Gases and Risk Assessment, Frankfurt (1982).

[Hjertager 1984] Hjertager, B. H., Influence of Turbulence on Gas Explosions, J. Haz. Mat. 9 (1984) 315-346.

[Holzmann 1986] Flüssiggasbehälter Kaarstoe/Norwegen, Philipp Holzmann AG, Frankfurt, Company's Pamphlet (1986).

[Hord 1978] Hord, J., How Safe is Hydrogen, Symp. on Hydrogen for Energy Distribution, Chicago (1978).

[Humbert-Basset 1972] Humbert-Basset, R., Montet, A., Dispersion dans l'Atmosphere d'un Nuage Gaseux Forme par Epandage de G.N.L. sur le Sol, Proc. 3rd Int. Conf. on Liquefied Natural Gas (1972), Washington D.C., USA.

[IAEA 1981] IAEA, External Man-Induced Events in Relation to Nuclear Power Plant Siting, A Safety Guide, Safety Series No. 50-SG-S5, International Atomic Energy Agency,

Vienna (1981).

[IAEA 1984] IAEA, Status of and Prospects for Gas-Cooled Reactors, Technical Reports Series No. 235, International Atomic Energy Agency, Vienna (1984).

[Inaba 2002] Inaba, Y., Nishihara, T., Inagaki, Y., Analytical Study on Fire and Explosion Phenomena in HTTR Hydrogen Production System, 14th World Hydrogen Energy Conference, Montreal, Canada (2002).

[INSC 1998] International Nuclear Societies Council, Action Plan 1997-98, http://www2s.biglobe.ne.jp/~INSC/INSCAP/Risk.html (1998).

[Jenkins 1983] Jenkins, D. R., Timmers, A. C., LNG Plant Safety in the Light of Recent Experimental Trials and Theories, 7th Int. Congress on Liquefied Natural Gas, held at Jakarta, Indonesia, May 15, 1983, Session III, Paper 13, Proc. Chicago, Institute of Gas Technology (1983).

[Jungclaus 1975] Jungclaus, D., Basic Ideas of a Philosophy to Protect Nuclaer Plants against Shock Waves Related to Chemical Reactions, Int. Seminar on Extreme Load Conditions and Limit Analysis Procedures for Structural Reactor Safeguards and Containment Structures (1975), Berlin, Germany.

[Koch 1975] Koch, C., Phenomenology of Explosions of Hydrocarbon Gas-Air-Mixtures in the Atmosphere, Int. Seminar on Extreme Load Conditions and Limit Analysis Procedures for Structural Reactor Safeguards and Containment Structures (in SMIRT 3), Berlin, Germany (1975).

[Koopman 1982] Koopman, R. P., et al., Analysis of Burro Series 40 M³ LNG Spill Experiments, J. Haz. Mat. 6 (1982) 43-83.

[Kumar 2000] Kumar, R. K., et.al., Carbon Monoxide - Hydrogen Combustion Characteristics in Severe Accident Containment Conditions, Final Report NEA/CSNI/R(2000)10, OECD-Nuclear Energy Agency, Paris, France (2000).

[Laurendeau 1982] Laurendeau, N. M., Thermal Ignition of Methane-Air Mixtures by Hot Surfaces: A Critical Examination, Combustion and Flame 46 (1982) 29-49.

[Lee 1983] Lee, J. H. S., Overview of Gas Explosions and Recent Results in the Study of Turbulent Deflagrations and Detonations, Proc. Conf. On the Control & Prevention of Gas Explosions, London, UK (1983) 3-36.

[Lind 1979] Lind, C. D., Whitson, J. C., China Lake Spill Tests, Report L, in: Liquefied Gaseous Fuels Safety and Environmental Control Assessment program: A Status Report, DOE/EV-0036, US Department of Energy, Washington D.C., USA (1979).

[Mercx 1992] Mercx, W. P. M., Large-Scale Experimental Investigation into Vapour Cloud Explosions: Comparison with the Small-Scale Discoe Trials, Trans. I. Chem. E. Part B: Process Safety and Environmental Protection, 70 (1992) 4 197-204.

[Mercx 2000] Mercx, W.P.M., van den Berg, C.J., Hayhurst, C.J., Robertson, N.J., Moran, K.C., Developments in Vapor Cloud Explosion Blast Modeling, J. Haz. Mat. 71 (2000) 301-319.

[Miyamoto 1998] Miyamoto, Y., Shiozawa, S., Ogawa, M., Hada, K., Inagaki, Y., Takeda, T.,

Nishihara, T., Overview of Hydrogen Production Program in HTTR, ECN-R-98-004 (1998).

[Moen 1993] Moen, I. O., Transition to Detonation in Fuel-Air Explosive Clouds, J. Haz. Mat. 33 (1993) 159-192.

[Moorhouse 1988] Moorhouse, J., Carpenter, R. J., Factors Affecting Vapour Evolution Rates from Liquefied Gas Spills, Report MRS E 460, British Gas, Midlands Research Station, Solihull, UK (1986).

[Moorhouse 1986] Moorhouse, J., Roberts, P., Cryogenic Spill Protection and Mitigation, Cryogenics 28 (1988) 838-846.

[OECD-NEA 2001] Nuclear Safety Research in OECD Countries – Major Facilities and Programmes at Risk, OECD-Nuclear Energy Agency, Paris, France (2001).

[Ogawa 2003] Ogawa, M., Shiozawa, S., Evaluation of Hydrogen Production System with High Temperature Gas-Cooled Reactor, GENES4/ANP Conference, held in Kyoto, Japan, Sept. 15-19, 2003, paper 1055.

[Ohashi 2004] Ohashi, H., et.al., Experimental and Analytical Study on Chemical Reaction Loss Accident with a Mock-up Model of HTTR Hydrogen Production System, ICONE 12 Conference, held in Arlington, USA, April 25-29, 2004.

[Parnarouskis 1980] Parnarouskis, M. C., Lind, C. D., Raj, P. P. K., Cece, J. M., Vapor Cloud Explosion Study, 6th Int. Conf. On Liquefied Natural Gas, Session III, Paper 12, Proc. Vol. II (1980).

[Pförtner 1975] Pförtner, H., Gas Cloud Explosions and Resulting Blast Effects, Int. Seminar on Extreme Load Conditions and Limit Analysis Procedures for Structural Reactor Safeguards and Containment Structures (1975), Berlin, Germany.

[Pförtner 1977] Pförtner, H., Gas Cloud Explosions and Resulting Blast Effects, Nucl. Eng. Des. 41 (1977) 59-67.

[Pförtner 1979] Pförtner, H., Zündverhalten von Erdgas/Luft-Gemischen in freien Wolken, gwf-gas/erdgas 120 (1979) 1 19-24.

[Pförtner 1985] Pförtner, H., The Effects of Gas Explosions in Free and Partially Confined Fuel/Air Mixtures, Propellants, Explosives, Pyrotechnics 10 (1985) 151-155.

[Pförtner 1988] Pförtner, H., Schneider, H., Experimental Investigations into the Deflagration of Flat, Premixed Hydrocarbon/Air Gas Clouds, Progress in Astronautics and Aeronautics 114 (1988) 488-498.

[PNP 1981] PNP, Referenzkonzept der Prototypanlage Nukleare Prozesswärme PNP, Gesamtanlage und Kraftwerk, Bergbau-Forschung GmbH, GHT Gesellschaft für Hochtemperatur-Technik mbH, Hochtemperatur-Reaktorbau GmbH, Kernforschungs-anlage Jülich GmbH, Rheinische Braunkohlenwerke AG, (1981).

[Puttock 1995] Puttock, J. S., Fuel Gas Explosion Guidelines – the Congestion Assessment Method, Proc. Major Hazards Onshore and Offshore II, ICHEME Symp. Ser. No. 139, Rugby (1995) 267-284.

[Rijnmond 1982] Risk Analysis of Six Potentially Hazardous Industrial Objects in the

Rijnmond Area : A Pilot Study, Dordrecht, The Netherlands, Reidel (1982).

[RSK 1980] RSK, Bewertung der sicherheitstechnischen Realisierbarkeit der Prototypanlage Nukleare Prozesswärme, Stellungnahme des Beratungsgremiums PNP/HHT-Sicherheit, Reactor Safety Commission, Technical Note (1980).

[Saito 1994] Saito, S., et al., Design of High Temperature Engineering test Reactor (HTTR), Report JAERI 1332, Japan Atomic Energy Research Institute, Oarai, Japan (1994).

[Schildknecht 1987] Schildknecht, M., Stock, M., Statusbericht zum Kenntnisstand des Übergangs Deflagration/Detonation unter besonderer Berücksichtigung der Zielsetzung des PNP-Gaswolkenprogramms, Final Report BF-R-66.459-2, Battelle Institute, Frankfurt (1987).

[Schneider 1978] Schneider, H., Pförtner, H., Flammen- und Druckwellen- ausbreitung bei der Deflagration von Wasserstoff/Luft-Gemischen, Technical Note, Institute for the Chemistry of Fuels and Explosives of the Fraunhofer Gesellschaft, Pfinztal (1978).

[Stamps 1991] Stamps, D. W., Benedick, W. B., Tieszen, S. R., Hydrogen-Air-Diluent Detonation Study for Nuclear Reactor Safety Analysis, Report NUREG/CR-5525, SAND89-2398, Sandia National Laboratories (1991).

[Takeda 1999] Takeda, T., et.al., Study on Tritium/Hydrogen Permeation in the HTTR Hydrogen Production System, ICONE 7 Conference, held in Tokyo, Japan, April 19-23, 1999.

[Takeda 2004] Takeda, T., Iwatsuki, J., Couter-Permeation of Deuterium and Hydrogen through Inconel 600, Nucl. Tech. 146 (2004) 83-95.

[Technica 1988] Technica Ltd., Techniques for Assessing Industrial Hazards – A Manual, World Bank Technical Paper Number 55, Washington D.C., USA (1988).

[TNO 1980] TNO Yellow Book, Methods for the Calculation of the Physical Effects of the Escape of Dangerous Material (Liquids and Gases), Order No. 9092, Rijswijk, The Netherlands (1980).

[TNO 1992] TNO Green Book, Methods for the Determination of Possible Damage to People and Objects Resulting from Releases of Hazardous Materials, Report CPR 16E, Voorburg, The Netherlands (1992).

[Uni.Erlangen 1981] University of Erlangen, Prozessgasfreisetzung – Explosionen in der Gasfabrik und Auswirkungen von Druckwellen auf das Containment, PNP-Sicherheitssofortprogramm – Vorhaben 3.3, Technical Note, Institut für Technische Chemie I (1981).

[Urtiew 1983] Urtiew, P. A., Brandeis, J., Hogan, W. J., Experimental Study of Flame Propagation in Semiconfined Geometries with Obstacles, Combustion, Science and Technology 30 (1983) 105-119.

[Westfalen-Gas 2001] Aufstellen oder Einlagern von Flüssiggas-Behältern, Westfalen-Gas, Münster, Germany, Company's Pamphlet (2001).

[Wischnewski 1971] Wischnewski, R., Zündversuche an einem Wassergas-Helium-Luft-gemisch bei verschiedenen Konzentrationen, Arbeitsgemeinschaft Versuchsreaktor

(AVR) Experimental Report (1971).

[Zabetakis 1960] Zabetakis, M. G., Burgess, D. S., Research on the Hazards Associated with the Production and Handling of Liquid Hydrogen, Report WADD TR 60-141, Wright Air Development Division, Ohio, USA (1969).

[Zabetakis 1967] Zabetakis, M. G., Safety with Cryogenic Fluids, The International Cryogenics Monograph Series, Heywood Books, London, UK (1967).

[Zeuuwen 1983] Zeeuwen, J. P., Van Wingerden, C. J. M., Dauwe, R. M., Experimental Investigation into the Blast Effect Produced by Unconfined Vapour Cloud Explosions, 4th Int. Symp. on Loss Prevention and Safety Promotion in the Process Industries, Harrogate (1983) D20-D29.

ACKNOWLEDGEMENTS

K. Verfondern from the Research Center Jülich in Germany stayed at the Department of HTTR Project as a foreign researcher from beginning of March to end of May 2001. The authors wish to express their gratitude to Mr. T. Tanaka, Director General of the Oarai Research Establishment, Mr. O. Baba, Deputy Director of the Department of HTTR Project, Mr. Y. Inagaki, head of the HTTR Nuclear Heat Application Laboratory, and the members of the HTTR Nuclear Heat Application Laboratory, furthermore to M. Ogawa, Deputy Director and Head of the Department of Advanced Nuclear Heat Technology, for their encouragement of this study.

A part of the work was also conducted under the MICHELANGELO network funded by the European Commission (FIKW-CT-2001-20180).

Forschungszentrum Jülich
in der Helmholtz-Gemeinschaft

Jül-4135
Juni 2004
ISSN 0944-2952